Development of a crop model to examine crop management and climate change in Senegal

Paul Edward Dodds

University of Leeds

School of Earth and Environment

Submitted in accordance with the requirements for the degree of

Doctor of Philosophy

March 2010

The candidate confirms that the work submitted is his own and that appropriate credit has been given where reference has been made to the work of others.

This thesis is dedicated to my parents, whose steadfast support and encouragement will always be appreciated and remembered, and could never be sufficiently repaid.

Acknowledgements

I must first thank my supervisors, Andy Dougill, Doug Parker and Klaus Hubacek, who have supported me throughout. They have always found time when I have needed to talk to them and have introduced me to a number of useful contacts. They provided me with much useful feedback on the drafts of this thesis.

This thesis would not have been possible without the guidance and generosity of François Affholder at CIRAD in Montpellier, France. I was a guest of François for more than 6 months and was given access to databases and literature from agricultural studies that have been performed by CIRAD in West Africa. François's patience and encouragement with my French language skills were also much appreciated! Also within CIRAD, Bertrand Muller provided some very valuable data, ideas and contacts. Christian Baron introduced me to the work of AGRHYMET and the climatological atlas of Robert Morel, which underpinned the creation of the meteorological dataset for Senegal. Finally, Bruno Barbier was very helpful and supportive with ideas for my PhD.

I also received much help from members of the AMMA EU project. Inge Sandholt welcomed me to Copenhagen on several occasions, introduced me to other members of the AMMA impacts group and provided some useful meteorological measurements. The SVS project on the vulnerability to food insecurity, led by IBIMET, provided much useful information which allowed me to investigate the broad agricultural trends in Senegal. AMMA funded my attendance at two international conferences which were vital for making the contacts that led to this thesis.

The UK Met Office provided the MIDAS synoptic weather station database through the British Atmospheric Data Centre. The NCEP/NCAR reanalysis model data was supplied by the Physical Sciences Division of NOAA in the United States. The climate change model data was supplied by the IPCC Data Distribution Centre.

Finally, I would like to thank my partner, Say Ayala Soriano, who has consistently supported me throughout the latter stages of this study.

Abstract

Frequent droughts and sub-optimal crop management have been identified as the principal constraints on agricultural intensification in the Sahel. A new model, the Crop Model for Sahelian Adaptation Studies (CROMSAS), was developed to examine the influence of climatic variability, climate change and crop management strategies on millet yields. To improve the simulation of environmental stresses, several original features were implemented including a new leaf expansion methodology, semi-independent tillers, stress-dependent partitioning, and intercropping. CROMSAS was designed in a structured, accessible way to facilitate the use of the model by other researchers who want to examine climate change impacts in Africa.

The influences of rainfall and crop management decisions over the period 1950–2009 were assessed for six locations in Senegal with average rainfall from 200 mm to 1200 mm. Poor rainfall severely restricted yields in the north of the country in most years while having little impact in the more humid south. In the highly-populated groundnut basin, rainfall variability reduced the effectiveness and hence the profitability of fertiliser application. Current planting densities were found to lie within the optimal range but higher grain yields could have been produced, with lower risk of crop failure, by delaying planting by 2–3 weeks.

The benefits of adapting crop management strategies according to the conditions in previous years were assessed. Using a fixed long-term strategy produced higher long-term yields and profits, at lower risk of crop failure, than frequently changing strategies.

Projections from three GCMs for the period 2000–2100 were converted to daily weather data using a novel methodology and used to examine the impact of climate change on millet cultivation across Senegal. Grain yields were projected to be relatively unchanged for the SRES A2 and B1 scenarios, with losses due to temperature increases and higher vapour pressure deficits being balanced by CO_2 fertilisation.

Contents

List of Figures

List of Tables

Chapter 1

Introduction

Food security has been a concern in the Sahel region of West Africa since a series of great droughts began to afflict the region in the early 1970s. Rapid population growth over recent decades has not been accompanied by a commensurate increase in food production and a large minority of the rural population are at risk of food insecurity.

Variable rainfall during the short summer growing season is often identified as the most important reason for the loss of food self-sufficiency in the Sahel, but no studies have systematically examined the long-term influence of rainfall variability on agricultural systems in the Sahel. The aim of this study was to examine how long-term rainfall variations affect agricultural systems, for several locations covering a range of Sahelian rainfall regimes, to gain a better understanding of why crop yields are so low in the region.

A second factor that many studies identify as an inhibitor of higher crop yields is poor soil fertility and poor crop management strategies. A second aim of this study was to examine fertilisation strategies and other management decisions of farmers, to assess how they are influenced by rainfall variability and to determine whether they are optimised for the region.

Climate change has been identified as a threat to farming in the Sahel, with some studies even forecasting the demise of rainfed Sahelian agriculture. The final aim of this study was to examine how Sahelian agriculture is likely to be affected by climate change in the future.

The study focused on a single crop, millet, and a single country, Senegal. Millet was chosen because it is the most widespread grain crop in the Sahel and the best-suited crop to hot, dry climates. Senegal was chosen because the climate is representative of the Sahel, with the average annual rainfall ranging from 1200 mm in the south to 200 mm in the north. In addition, good-quality long-term meteorological datasets were available for locations throughout the country and a large database containing Senegalese agricultural field data was made available for the study.

1.1 Thesis outline

This chapter provides a background to the study by examining the influence of rainfall and crop management strategies on crop cultivation in Senegal. Chapter 2 critically reviews the literature to compare and contrast existing crop models, to examine how models have been used to examine crop management strategies and climate change in dryland regions and to identify the strengths and weaknesses of climate models.

A dynamic crop model, CROMSAS, was developed by this study to estimate crop yields for a variety of environmental conditions and crop management strategies. Chapter 3 describes the design of the model and Chapter 4 describes the calibration and evaluation. A meteorological data record was created using data from several sources for the period 1950–2009 at twelve locations in Senegal for use in the crop model. Chapter 5 describes how the dataset was produced and the validation techniques that were used to confirm the accuracy of the data.

Crop model simulations were performed to characterise the impacts of long-term rainfall variability and crop management strategies on crop yields at several locations across Senegal, and these are presented in Chapter 6. The analysis included a simple financial analysis which examined the economic constraints on intensification, and an appraisal of the benefits of adapting crop management practices according to the conditions in previous years.

The final part of the study looked to the future using climate data from three IPCC climate models, for two potential future scenarios. Chapter 7 describes how meteorological datasets were created from climate model data and assesses the impacts of climate change on millet cultivation in Senegal in the twenty-first century.

The thesis concludes with a general summary in Chapter 8. Several potential studies for the future are also identified in this chapter.

1.2 Population growth and food production in West Africa

West Africa is one of the poorest and least developed regions of the World. The United Nations Human Development Index (UNHDI), which ranks countries according to income, life expectancy and education, places most West African countries near the bottom of the league table (UNDP, 2005). The “Global Hunger Index” (von Grebmer *et al.*, 2008) identifies sub-Saharan Africa as the region with the most widespread food insecurity, with the semi-arid Sahel region of West Africa being of particular concern. Most farmers in the Sahel rely on the summer monsoon rains to provide water for their crops. Food security in the region became an international concern during a series of droughts that commenced in the early 1970s (Batterbury and Warren, 2001). Population growth and land degradation caused by poor farming practices have been identified as drivers that are further deteriorating the already fragile position.

This thesis examines smallholder farming practices in Senegal, a small country on the western edge of the Sahel. Senegal is a low-income country: the per capita gross domestic product (GDP) was US$710 in 2005 (World Bank, 2006). Although agriculture contributed only 18 % of the total GDP in 2005 (World Bank, 2006), it was the main source of income, directly or indirectly, for 81 % of the rural population. Yet food insecurity is an ongoing concern. Food security is defined as having access to sufficient, safe, nutritious food, whether grown or purchased (World Food Summit, 1996). A vulnerability and mapping survey in 2005 (WFP, 2005) showed that 20 % of Senegalese households suffered from severe food insecurity and 26 % from moderate food insecurity, while a further 36 % were at risk of food insecurity in the future.

1. INTRODUCTION

Senegal became a French colony towards the end of the nineteenth century and achieved full independence in 1960. Figure 1.1 shows the population density distribution in Senegal in 1988. The majority of the population live in regions close to Dakar. This distribution reflects two historical trends. The first was the establishment of Dakar as the capital and major port of French West Africa in 1902. The city has continued to grow strongly in recent decades, with the civil service and much of the industry in Senegal located nearby. The second trend was the establishment and subsequent growth of the *bassin arichidier* (groundnut basin) over the last century (marked on Figure 1.1), to produce groundnuts for export. The basin is a large semi-arid region of sandy soils in the west of the country. The greatest rural population densities in Senegal, of more that 100 peoplekm^{-1}, are found there.

Groundnut production reduced by 41 % between 1961 and 2007 as a result of the long drought after 1970, fluctuations in the world market price and the removal of much state support in the 1990s when the state marketing parastatal was disassembled as part of a structural adjustment programme (Kelly *et al.*, 1996). Production has diversified with sugar cane and many different vegetables now being produced for export (FAO, 2009a). The production of rice and maize has increased in the more humid southerly regions but much of the population continues to rely on millet cultivation in the semi-arid groundnut basin.

Senegal is a good proxy for the Sahel because it contains the full range of climatic zones, from sub-humid to arid, that are found in the Sahel. The total population of Senegal has grown from 3.3 million in 1960 to 13 million in 2008, and is forecast to continue growing to 31.6 million in 2050 (Figure 1.2). Poverty is particularly prevalent in rural areas where half the population lives; 65 % of the rural population are classed as living in poverty with a third of these in extreme poverty (World Bank, 2004).

Total cereal production in Senegal has increased since 1961 but at a lower rate than the population (Figure 1.3). The total area cultivated for cereals has increased slightly but the overall increase and variability in the total production is primarily driven by fluctuating grain yields. Production has lagged population growth despite a significant fraction of the rural population suffering food insecurity, and Senegal currently imports more than 50 % of its food requirements

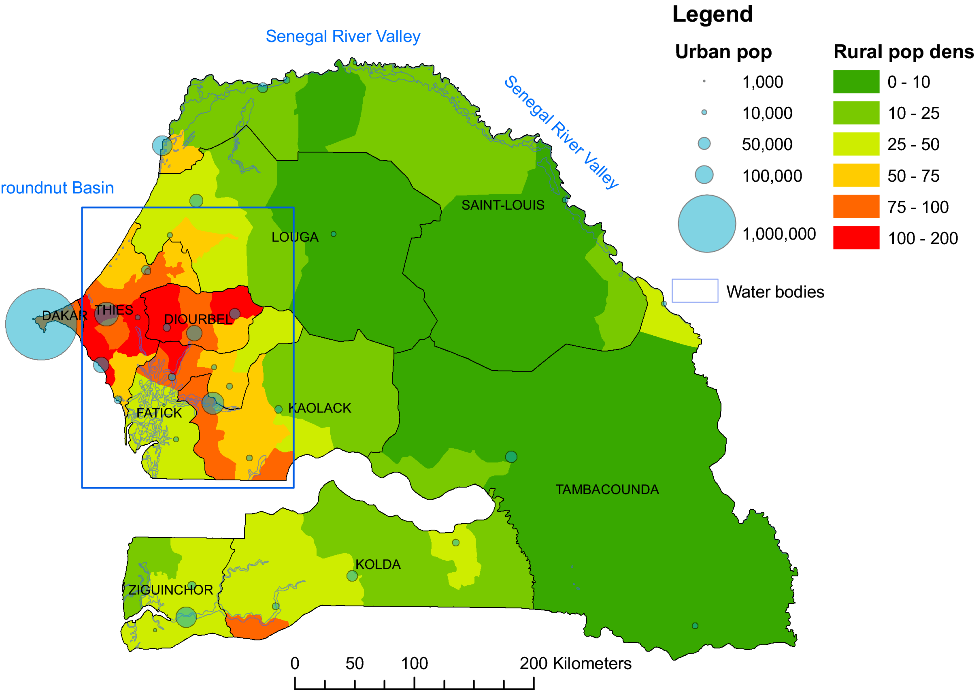

Figure 1.1: Rural population density and urban zones of Senegal. The 11 administrative regions are named. Rural population densities are averages in each *arrondissement* from the national census in 1988. It is estimated that the total rural population increased by 50 % between 1988 and 2009. The original data are presented in this map because the rate of population growth varies substantially between *arrondissements* (Raynaut, 2001). The map was constructed using data from the SVS project (2009).

(FAO, 2009b). Reliance on imports from the world market increases the vulnerability of the inhabitants to price fluctuations, as occurred in early 2008 when there were several protests in the capital, Dakar, about high food prices (IRIN News, 2009). In response, the government plans to greatly increase paddy rice production in the Senegal river valley.

Millet is the most important subsistence cereal in Senegal, comprising more than 50 % of the total cereal production over the last 50 years. Millet yields have increased over the period, despite the droughts, but only average 650 kg ha^{-1} at present (Figure 1.4), which is much lower than the potential yield of 4000 kg ha^{-1} in optimal conditions (Baron *et al.*, 2005). One of the aims of this study was to

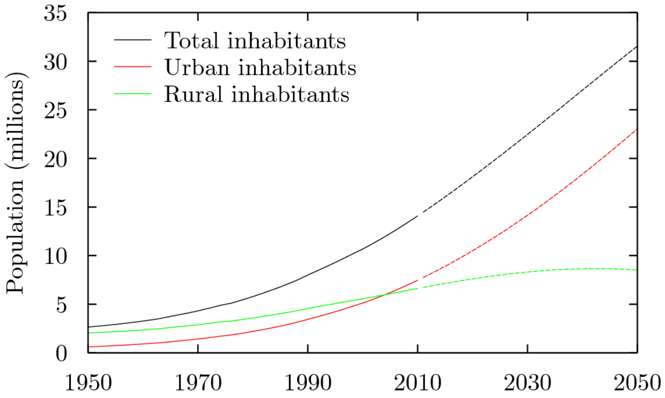

Figure 1.2: Senegal population time series for the period 1950–2050. The population data, including the forecast to 2050, were taken from the U.S. Census Bureau (2009). The urban and rural population split was calculated using data from Cour and Snrech (1998).

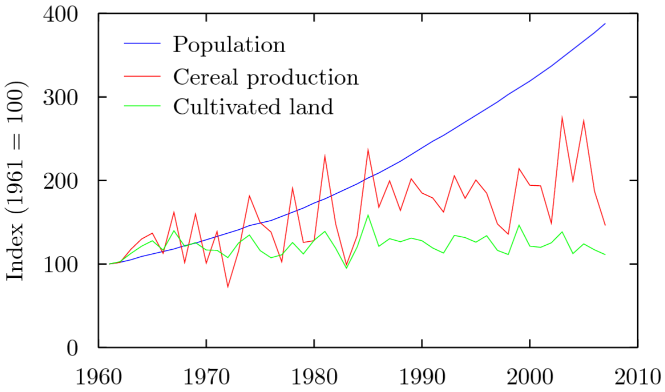

Figure 1.3: Long-term changes in the population and production of grain in Senegal. All changes are relative to 1961 = 100. The population data were obtained from the U.S. Census Bureau (2009) and the agricultural data from FAO (2009a).

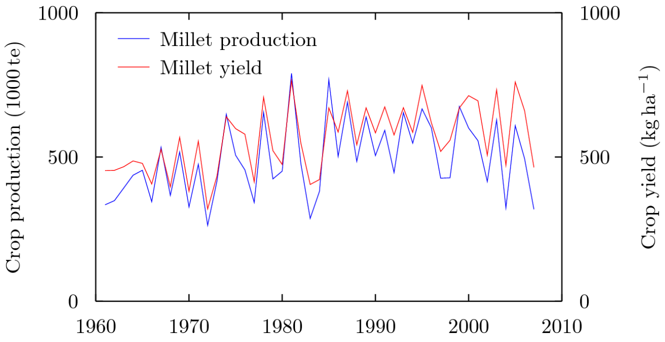

Figure 1.4: Total grain production and crop yield time series for pearl millet in Senegal. The data were obtained from FAO (2009a).

examine why millet yields are so low and to find out whether the current millet crop management practices are optimised to the environment across the country.

1.3 Factors constraining agricultural development in Senegal

Annual yields of the major crops in each *departement* of Senegal were obtained from the “Suivi de la Vulnérabilité au Sahel” (SVS) project (2009) for the period 1986 to 2000. Figure 1.5 shows the millet yield in each *departement* where millet is widely cultivated (defined here as using more than 20 % of the total cropped area). Yields are highest in the south of the country and lowest in the north. Millet is not widely grown in most of the humid south where maize and rice are more important. The northern *departements* have little cultivation because they are too dry for rainfed agriculture and are instead dominated by extensive irrigation schemes in the Senegal river valley.

The percentages in Figure 1.5 show the area of each *departement* that is cultivated with millet. The highest land use occurs in the groundnut basin where more than 20 % of the total land is devoted to millet; between 30 % and 75 % of the land in this region is regularly cultivated. Little land is used for millet, or any other crops, elsewhere. In the north, west and south of the country, less than 15 % of the land is cultivated. This pattern results from a range of environmental and socio-economic factors (Raynaut *et al.*, 1997).

The first environment factor is the distribution of soil types in the country. Figure 1.6 summarises the agricultural quality of the soil across the country. The light sandy soils in the west drain quickly and are easy to manage, but sometimes suffer from crusting, wind and water erosion, and high soil temperatures, and have low fertility due to the low levels of organic matter which lead to low cation exchange capacities (Sivakumar and Glinni, 2002). The best soils are found in depressions and in large valleys; these young alluvial and tropical black soils (vertisols) are highly fertile and used for irrigated agriculture. Salination is a problem in some coastal regions and is difficult to reverse. Eastern Senegal is

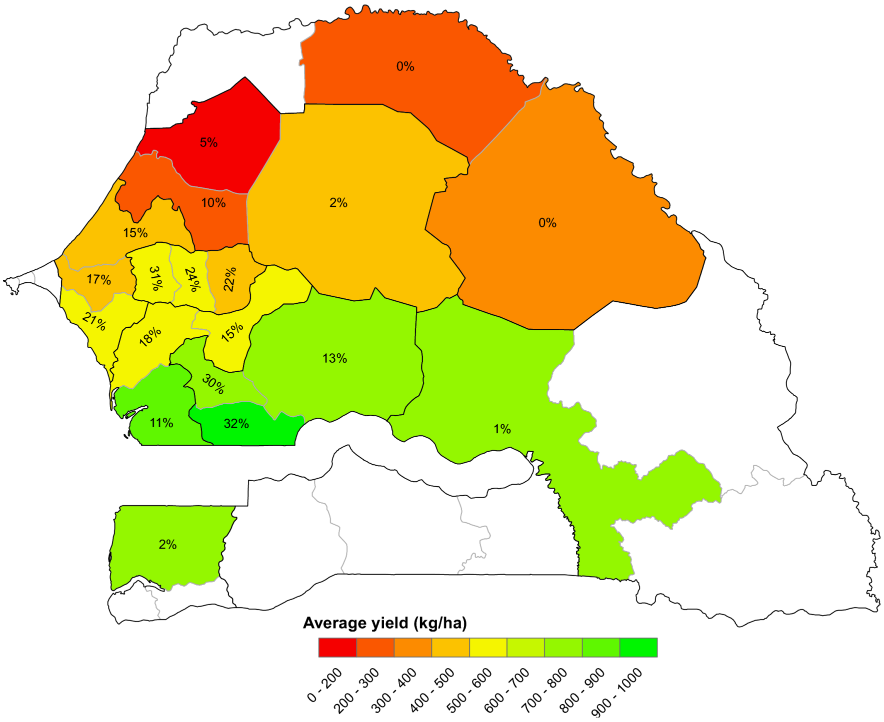

Figure 1.5: Average millet yields in the period 1986–2000 in Senegal. Only regions where more than 20 % of the planted area were devoted to millet were included. The shading shows the average millet yield in each *departement*. The percentages denote the fractional area of the whole region that is used for millet cultivation (averaged over the time period). The map was constructed using data from the SVS project (2009).

dominated by unproductive hardpans and gravelly soils that are unsuitable for agriculture.

The second important environmental factor is the rainfall pattern across the country, which is shown in Figure 1.7. The south of the country is sub-humid, with more than 1200 mm rainfall recorded in an average year. The rainfall steadily reduces towards the north and sub-humid vegetation gives way to semi-arid and then arid regions where rainfed crop cultivation is rarely possible. The influence of the climate on crops is discussed further in the next section.

The droughts and famines that started in the early 1970s were described as ‘environmental emergencies’ and prompted extensive international assistance

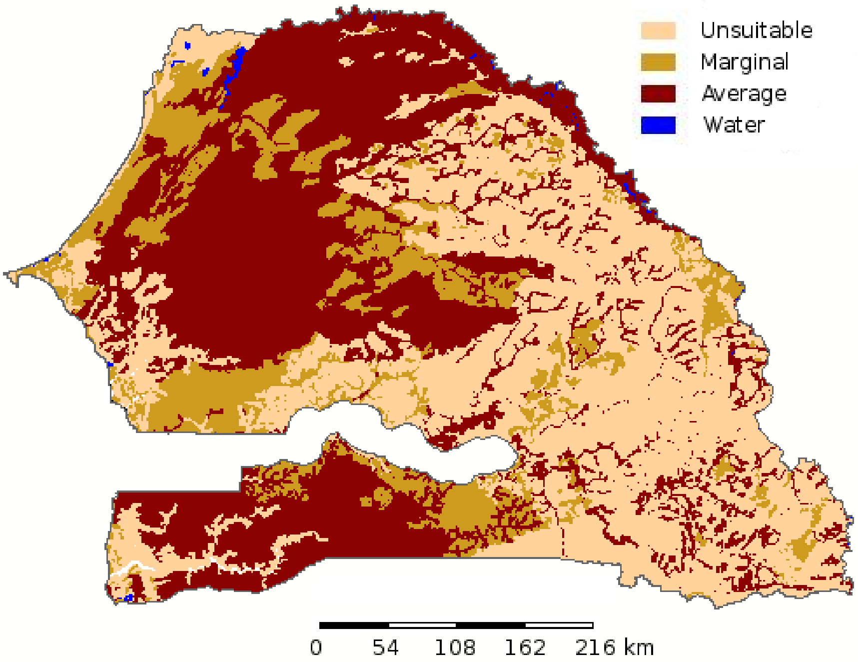

Figure 1.6: Soil constraints on agriculture in Senegal. The image was taken from the “Caractérisation de la Vulnérabilité” project of the SVS project (2009).

(Batterbury and Warren, 2001). The change in the rainfall across the region can be visualised using a standardised rainfall index, which is calculated over a period of years using:

$$sr_i = \frac{r_i - \overline{r}}{\sigma\left(r\right)} \tag{1.1}$$

where sr_i is the standardised index for year i, r_i is the rainfall in year i, $\overline{r}$ is the mean rainfall over the period and $\sigma\left(r\right)$ is the standard deviation over the period. Figure 1.8 shows the standardised rainfall index for Senegal in the period 1950–2009. The reduction in the rainfall across the region after 1970 can be clearly observed. The drought followed two decades with plentiful rainfall but lasted for more than 30 years. The Sahelian climate has been described as “the most dramatic example of climate variability that we have quantitatively measured anywhere in the world” (Hulme, 2001).

If there is insufficient soil water then crop growth will at best be stunted (Affholder, 1995); if there is persistent water stress or if the stress falls during

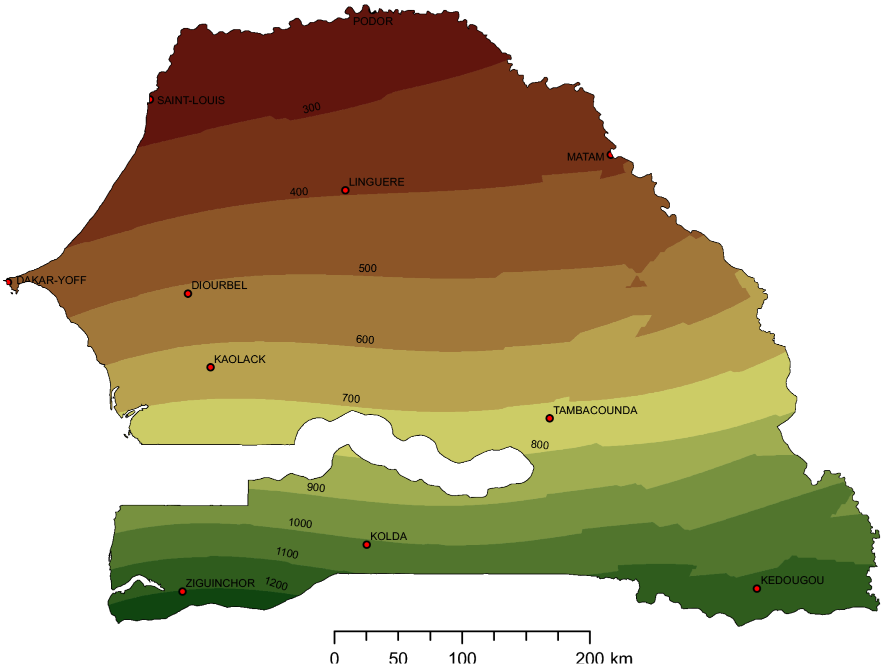

Figure 1.7: Annual rainfall isohyts in Senegal. The isohyts were identified using a kriging calculation driven by rainfall observations for the period 1950–2008 at eleven synoptic weather stations around the country (marked the map). The origin and processing of the rainfall data are described in Chapter 5.

a critical period such as flowering then the grain yield can be severely affected (Challinor *et al.*, 2005). The distribution of rainfall through the rainy season and the date of the first rains can be just as influential as the total amount of rain on the achieved crop yield (Sultan *et al.*, 2005). An alternative viewpoint has been expounded by Dietz *et al.* (2004), who examined correlations between regional agricultural yields and rainfall and concluded that yields were higher in drier years. The factors underlying this correlation were not identified.

Flooding is less frequent than drought but can destroy crops, property and infrastructure (Tarhule, 2005). For example, Dakar, the capital of Senegal, was affected by flooding in 2008 and 2009 (USAID, 2010). Unfortunately, little information is available about the impact of flooding in rural areas of the Sahel.

As well as growing grain crops for food, the straw that remains is used to feed livestock. The total straw biomass that can be produced each year, and hence

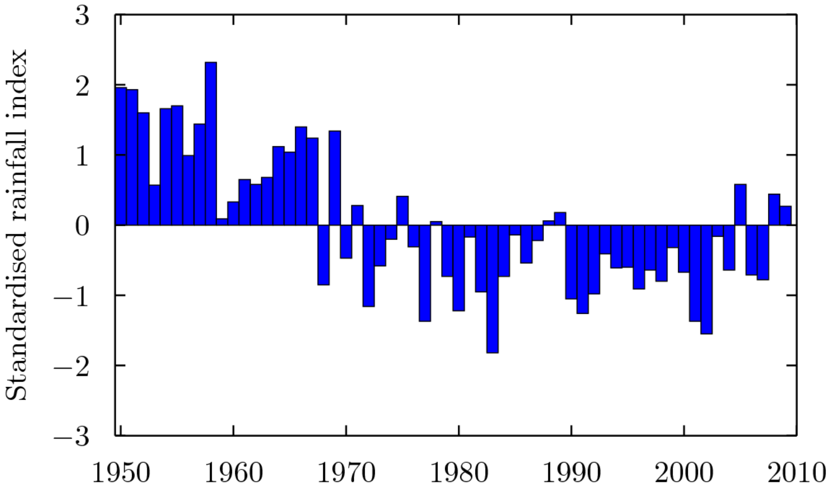

Figure 1.8: Standardised rainfall index for Senegal in the period 1950–2009. Each value represents an average of the 11 synoptic weather stations in Senegal.

the total number of animals that can be supported, depends on the total areal rainfall. Manure production is limited in low-rainfall regions, with the interannual rainfall variability creating a non-equilibrium pattern of livestock stocking levels.

In summary, poor soils limit agricultural development in the west of the country and low rainfall restricts development in the north. However, neither of these factors explains why agricultural development has been limited in the large areas of the southern Casamance region (lying south of The Gambia) that have not been affected by salination. Socio-economic factors are significant here. There was widespread warfare between local families from 1880 with a clash of Islam and Animist religions as a backdrop, leaving the area relatively unpopulated (Nugent, 2007). In view of the low population, local unrest and the distance from Dakar, the region was given little attention by the colonial authorities. In more recent times, the region has suffered from a low-level separatist war with the Senegalese government, lasting several decades, which has led to widespread insecurity and the use of landmines across the territory.

In contrast to the Casamance, the population of the groundnut basin has increased rapidly with sustained support being supplied by the colonial and then the Senegalese governments. The large density of towns that have developed in the region (Figure 1.1) provide many opportunities to earn off-farm income and to sell crops. Opportunities are more limited elsewhere in the country.

1.4 The influence of climate on crop cultivation

The climate of the Sahel is dominated by two weather systems. In the northern hemisphere winter, the climate of Senegal is under the influence of hot, dry north-easterly trade winds from the Sahara desert which are locally called the “harmattan” winds. The harmatten winds meet the cool oceanic winds at the Intertropical Convergence Zone (ITCZ) over the southern Guinea Coast (McGregor and Nieuwolt, 1988). Areas north of the Guinea coast, including all of Senegal, have no rainfall for 6–9 months of the year and the relative humidity of the air is very low.

In the northern hemisphere summer, the moist monsoonal winds move north and the rainy season commences. The penetration of the monsoonal winds depends on the intensity of the Saharan thermal low pressure area and the overall progress is characterised by stuttering advances and retreats, with an abrupt move north during June or July (Gu and Adler, 2004; Sultan and Janicot, 2000, 2003). The retreat of the monsoonal winds at the end of summer, which follows the peak solar radiation towards the south, is smooth and more rapid by comparison. In Senegal, which lies between 12.5°N and 16.5°N, the duration of the monsoon ranges from six months in the south to three months in the north (Sultan and Janicot, 2000). The average annual rainfall reduces by $2\,\mathrm{mm\,km^{-1}}$ as one moves north through the country (Figure 1.7). This sharp gradient occurs because the southerly regions of the country have more intense rainfall for a longer period.

Most smallholders in the Sahel rely on rainfall to provide soil water for their crops so the choice of crop species across Senegal is primarily influenced by the length of the monsoon season and the total rainfall during the season (Brooks, 2004; Raynaut *et al.*, 1997). Millet, groundnut and to a lesser extent sorghum are well suited to hot, dry conditions with intense sunlight. Maize and rice are better suited to hot, humid conditions. The response to water and nutrient stress varies between species; for example, maize will produce very high yields under optimum conditions but will fail under severe water stress, while millet is hardier but has lower maximum yields. In the south of Senegal, farmers have a choice of several crops that are suitable for the climate of the region. Further north, millet is the most appropriate cereal for coping with rainfall variability because it is the hardiest of the cereals. Smallholders in the north can adapt their farming systems to climate change by adopting alternative varieties of millet, but their options are limited in comparison with their brethren further south.

1.4.1 Rainfall variability

Most monsoonal rainfall is produced by westward-moving squall lines which typically persist for 3–15 hours. Most rainfall tends to occur between late afternoon and early morning (Taylor *et al.*, 1997). There is often substantial variability in the distribution of rainfall from storms. More northerly regions in particular can receive most of their annual rainfall from a small number of very large storms and there can be significant local variations. For example, in a study of rainfall variability in Niger, one measuring site received only half the rainfall of another site that lay 9 km to the north (Taylor and Lebel, 1998). For smallholders, this translates into potentially wide rainfall disparities even on fields scattered around the same village. In more southerly regions, the disparities between the storms tend to average out over the rainy season because there are so many storms. The interannual variability increases towards the north of the country because there are fewer storms and hence fewer opportunities for disparities between storms to average out. It is difficult to consistently cultivate rainfed crops in regions where the average annual rainfall is below 400 mm because of the wide spatial and interannual variability.

1.4.2 Solar radiation, temperature and humidity

Variations in the solar radiation, temperature and relative humidity affect the crop development and crop growth rates.

The solar radiation peaks across the country in the summer as the solar maximum passes overhead. There is little spatial variation: in the period 1950–2008, the annual mean across the north and centre of Senegal was approximately $20\,\mathrm{MJ\,m^{-2}\,d^{-1}}$, only $1.5\,\mathrm{MJ\,m^{-2}\,d^{-1}}$ higher than the cloudier south.

Temperatures are high year-round and, in common with many tropical countries, the diurnal temperature range exceeds the seasonal variation (Parker *et al.*, 2005). There is little spatial variability across the country, with annual mean temperatures ranging from 26 °C at the coast to 29 °C inland in the period 1950–2008.

Crops grow more slowly and use more water in regions with lower relative humidity. The relative humidity is higher towards the south and the west of Senegal, because of the longer duration of the monsoonal winds in the south and the influence of the Atlantic Ocean in the west.

Chapter 5 examines in more detail how each of these climatic characteristics varies throughout the year at several synoptic weather stations.

1.4.3 Climate change

The impact of anthropogenic climate change has recently received much attention. The IPCC Fourth Assessment Report notes that “Observational evidence from all continents and most oceans shows that many natural systems are being affected by regional climate changes, particularly temperature increases” (IPCC, 2007).

The impacts of climate change are forecast to be much more pronounced in the twenty-first century (Meehl *et al.*, 2007) and it is very likely that the temperature in Africa will rise faster than the global mean, particularly in dryland regions such as the Sahel (Christensen *et al.*, 2007). There is much uncertainty about how rainfall in the Sahel will be affected. The rising atmospheric CO_2 concentration will reduce crop water requirements and could boost crop growth.

The daily maximum and minimum temperatures have already increased across Senegal both annually and during the growing season. Since 1950, the diurnal temperature range has narrowed with minimum temperatures increasing by almost 3.8 °C while maximum temperatures have increased by only 0.7 °C. However, the trend is different during the growing season (July–September) with maximum temperatures increasing by 1.6 °C and minimum temperatures by only 1.4 °C. Increasing temperatures could adversely affect grain yields in the future. The impact of climate change on agriculture is explored in Chapter 7.

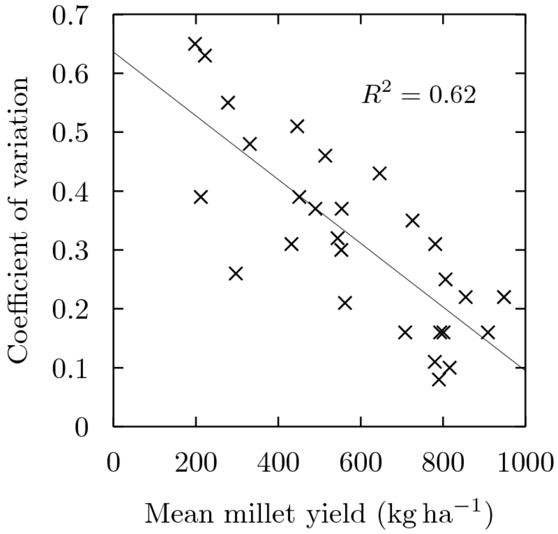

Figure 1.9: Millet yield variability in Senegal. The yield variability is represented by the normalised standard deviation. Each point represents one *departement* of Senegal. Annual millet yield data for the period 1986–2000 were obtained from the SVS project (2009).

1.4.4 The impact of rainfall variability on millet cultivation

It was previously shown that millet yields are higher towards the south where the rainfall is higher (Figure 1.5). Yields towards the north are also more variable as a result of the increased rainfall variability explained above. Figure 1.9 demonstrates this trend by showing the coefficient of variation reducing as the average yield increases.

It would be premature, however, to conclude that rainfall variability is the only factor that affects millet yields. Table 1.1 shows the average grain yields in nine Senegalese villages (Affholder, 1992). There were wide variations both between villages and within each village. Yields exceeding 2000 kg ha^{-1} were achieved in two villages. The high yields at Bambey are particularly interesting because the rainfall was lower than elsewhere. It is possible that the distribution of rain was favourable at Bambey despite the low overall total, or perhaps that better crop management practices were used (there is a nearby agricultural research station). M'Bediene had particularly low yields, despite having receiving 90 mm

	Rainfall (mm)	Mean yield	Minimum	Maximum
N'Diefoune Pal	718	535	185	1278
N'Dimb Taba	614	981	452	2268
Darou Khoudos	579	820	324	2114
Dialacouna	531	760	293	1248
Keur Lamine	437	1015	317	2326
M'Bediene	433	137	44	352
Sob	352	757	249	1937
Bambey	345	1012	464	1857
Keur Boumi	218	349	250	477

Table 1.1: Millet grain yields in nine villages in Senegal. The rainfall figures are means of the years when field observations were performed. Grain yields have units $\mathrm{kg\,ha^{-1}}$. The data were collected by the ESPACE project (Affholder, 1992) during the period 1989–1991 (only one village had observations in all three years).

more rainfall than Bambey. Rainfall is clearly not the only limitation on the grain yield in Senegal and it is necessary to examine crop management practices to understand why some farmers achieved higher yields than others.

Affholder (1994) identified a subset of higher quality records from six of these villages and, using a water balance model, identified a relationship between the plant water stress and the grain yield. There was also a relationship between the field fertilisation and the crop yield, particularly in fields receiving higher rainfall, and a weaker relationship between the weed management and the yield. The long-term relationships between the crop management, rainfall variability and grain yields were the subjects of this study.

1.5 Crop management strategies

Most farmers in the Sahel are smallholders who live in households of up to 20 people in rural villages (Mortimore and Adams, 1999). They grow crops, keep livestock (normally cattle or goats) and have a variety of other occupations that provide alternative income streams. Their farms are normally composed of several small widely-spaced fields surrounding the village (Netting, 1993). They grow both subsistence and cash crops (e.g. millet and groundnut in the groundnut basin). Manure from their livestock is primarily used to fertilise the fields, reflecting the fact that they have few assets to invest in the farm other than their household labour. Every village has a range of richer to poorer households which are characterised by varying manpower, land, assets and knowledge (Amerena, 1982; Scoones, 2001). Fathers normally split their farms equally between their sons (Mortimore and Adams, 1999) so the average farm size tends to reduce over time as the population density rises.

This section examines the factors that influence whether smallholders try to improve the crop yields from their farms through agricultural intensification.

1.5.1 Theory of agricultural intensification

If the environmental conditions are favourable then crop yields can be increased by agricultural intensification. The first holistic description of agricultural intensification was produced by Boserup (1965), who concluded that the level of agricultural intensification in a region depended on the population density. Crop yields are increased by carefully clearing land, producing and applying fertiliser, and eventually by building irrigation systems. Intensification increases the overall crop yield but decreases the yield per hour of labour (and hence the economic return), so will not occur unless driven by population pressure or some other external factor. Pingali *et al.* (1987) characterised farming systems in nine African countries according to their population density and found a clear pattern of farming intensification with increased population caused by land scarcity. Netting (1993, p267) presents an example of Nigerian farmers altering their farming systems as the population density varies.

Intensification has occurred in isolated parts of the Sahel, particularly near Kano (Mortimore and Adams, 1999), but these areas have mostly been highly populated for a long time, often as a result of pre-colonial period warfare or colonial development policies (Raynaut *et al.*, 1997). In Senegal, crop yields have not increased at the same rate as the population density over the last few decades. Rainfall variability, soil nutrient mining and desertification have been identified as environmental constraints on intensification (Breman *et al.*, 2001), although there are strong disagreements in the literature about the extent of nutrient mining (e.g. Batterbury and Warren, 2001; Kandji *et al.*, 2006; Shapiro and Sanders, 1998; Tiffen *et al.*, 1994) and desertification (Warren *et al.*, 2001). Socio-economic constraints include reduced economic returns with intensification, a lack of household assets for purchasing fertiliser and other inputs, and low market prices for selling produce which are a consequence of cheap food imports (Brown *et al.*, 2009; Gray, 2002).

1.5.2 Intensifying millet cultivation through fertilisation

Africa is dominated by very old rocks topped by old, heavily leached or sandy soils which have low concentrations of soil organic carbon and are typically deficient in the major plant nutrients (Breman *et al.*, 2001). If fertiliser is not applied by the smallholder, yields decline rapidly over 3–4 years towards a low equilibrium (Syers, 1997). The land then requires extensive fallowing to increase the productivity again, which is not possible in much of Senegal because the land per capita is too low. Perennial species are the main source of soil organic matter in soils but the long, hot dry season of the Sahel is very inhospitable for such plants, so the soils in the region have the lowest organic matter of any known agricultural land (Breman *et al.*, 2001).

The soil fertility can be increased by applying mineral fertilisers. Fertilisers are expensive to buy and are often relatively ineffective in sandy soils because most of the cation exchange capacity depends on the concentration of organic matter in the soil, which is very low. For example, Lal (1995) concludes that fertiliser utilisation drops significantly if the organic matter is reduced to 1 %, yet Affholder (1995) measured concentrations of only 0.35 % in sandy soils in a Senegalese village. Poor management of mineral fertiliser can also lead to soil degradation and acidification of sandy soils (Dougill *et al.*, 2002).

The soil fertility can also be increased by applying manure. Manure is time-consuming to produce and difficult to transport. The total potential production depends on receiving enough rainfall to produce the required amount of animal feed, unless passing herders can be persuaded to rest their livestock on the fields in the dry season. Furthermore, using crop residues for animal feed reduces the soil organic carbon concentration and hence the effectiveness of any mineral fertiliser that is applied.

Fields in the groundnut basin have been categorised according to their distance from the household compound (Pelissier, 1966, cited by Affholder (1995)). House fields (*champs de case*) are closest to the compound, often undergo annual cultivation, receive much of the household manure, and are relied on to produce the highest crop yields. Bush fields (*champs de brousse*) lie further from the compound which increases the labour costs of applying manure. They receive less manure and often undergo short fallowing. Finally, distant fields (*champs de loin*) are furthest from the compound. They receive even less attention unless there is an outpost of the compound nearby.

Observations of the use of mineral fertiliser and manure on smallholder fields in Senegal are summarised in Table 1.2. Manure was applied predominantly to house fields while mineral fertiliser was applied most often to distant fields, reflecting the labour required to transport large quantities of manure over long distances by cart or on foot. Few fields received both manure and mineral fertiliser. It was rare that house fields received no fertiliser over a three-year period; since manure decays over a period of around three years, most unfertilised fields would have benefited from fertilisation in previous years. House fields were more likely to be fertilised than bush fields; distant fields were rarely fertilised over consecutive years.

In summary, the soils are naturally very nutrient-poor. Smallholders can improve soil fertility by fallowing or by applying mineral fertiliser or manure, but there are substantial costs associated with all three methods so fertiliser use is normally limited. The costs are particularly high if poor rainfall leads to poor yields despite high soil fertility, so a balance must be found to maximise the long-term economic return from intensification. This study examines intensification in terms of both the achieved yields and the economic value to the farmers (Chapter 6).

	House fields	Bush fields	Distant fields
Fertiliser type			
None	32%	43%	54%
Manure	53%	38%	21%
Mineral	3%	11%	17%
Manure+mineral	12%	8%	8%
Frequency			
3 out of 3 years	6%	4%	4%
2 out of 3 years	46%	35%	12%
1 out of 3 years	40%	45%	55%
0 out of 3 years	8%	16%	29%

Table 1.2: Field fertilisation strategies in Senegal. Organic fertiliser was applied through animals grazing on the fields during the dry season or by the manual application of manure. The application of fertiliser (organic or mineral) on each field was recorded for the year of observation and for the two preceding years. The data were collected by the ESPACE project (Affholder, 1992) in several villages during the period 1989–1992.

1.5.3 Planting strategies in Senegal

In the Sahel, fields are cleared and manured during the dry season and seed is normally planted prior to the rainy season or straight after the first rains. The early rains are often particularly variable (Sultan and Janicot, 2000) and long dry periods in the early stages of crop growth cause severe water stress that can often lead to crop damage or death (Affholder, 1995). Dead crops are replaced if enough time remains before the end of the rainy season. There is little flexibility over the planting date because of the short length of the dry season, but Sultan *et al.* (2005) concluded that the yields would increase if crop planting were delayed until the date of monsoon onset. The optimum planting date in Senegal is examined in Chapter 6.

One cause of low grain yields in the Sahel has been identified as the use of unnecessarily low planting densities by smallholders (Payne, 1997, 2000; Shapiro and Sanders, 1998). Planting densities are normally varied by farmers to adapt to the expected rainfall and the soil fertility (Mortimore and Adams, 1999).

The planting density is difficult to measure because farmers tend to plant rows of 'stands' or 'hills'. Initially, around ten seeds are planted in each stand, but these are thinned to two or three plants around two weeks after germination. A second complication is the tendency of millet plants, in common with other grasses, to produce tillers. These are semi-independent stems which sprout from the base of the plants and develop leaves and, occasionally, a head of grain. The number of tillers depends on the variety of millet being grown and the availability of water and nutrients; Souna millet, the dominant variety in Senegal, normally has one productive basal tiller on average. Since there are several plants per stand and since each plant can produce several ears of grain, it is difficult to accurately count the number of plants. Instead, the stand density and the number of productive stems per stand (including tillers) are measured.

A survey in Senegal found higher stem densities in fertilised fields than unfertilised fields of the same type (Table 1.3). Both the stand density and the stems per stand were higher in the fertilised than the unfertilised fields. The stem densities in the fertilised house fields were higher than in the other fields, but there was little difference between the unfertilised fields. Smallholders appear to vary the planting density of millet to take account of both their fertilisation strategy and the natural fertility of the field. However, this conclusion does not adequately convey the great diversity between fields within each category. The standard deviations in Table 1.3 demonstrate the wide variations; the stem densities across all of the fields ranged from 0.2–16.3 stems m^{-2}.

At planting, when the planting density is decided, farmers are aware of the soil fertility but do not know how much rainfall will be received during the rainy season. The stand density is chosen to reflect the expectations of the farmer, which are based on the long-term climate, so the stand density reduces towards the north of Senegal where rainfall has historically been lower (Figure 1.10a). The number of stems per stand is sensitive to the actual amount of rainfall as plants produce more productive tillers in favourable years and are more likely to die in poor years, so the stem density is less correlated to the latitude than the stand density (Figure 1.10b).

	House fields	Bush fields	Distant fields
Fertilised fields			
Number of fields	44	88	44
Mean stem density	7.0	5.2	6.2
Standard deviation	3.1	2.5	2.2
Unfertilised fields			
Number of fields	22	68	48
Mean stem density	4.4	4.2	4.9
Standard deviation	2.7	2.4	2.0

Table 1.3: Millet stem harvest densities from a survey of smallholder fields in Senegal. The data were collected by the ESPACE project (Affholder, 1992) in several villages during the period 1989–1992. Fertilised fields received manure or mineral fertiliser during the year of observation. The stem density has units stems m^{-2}.

Payne (1997) notes that the millet stand density in Niger is often as low as 0.5 stands m^{-2} and suggests that yields could be increased by raising this to 2 stands m^{-2}. In the ESPACE study, the mean stand density ranged from 0.6 stands m^{-2} in the north to 2 stands m^{-2} further south. The minimum density was 0.15 stands m^{-2} while the maximum exceeded 3 stands m^{-2} in one field. The relationship between the planting density, the nitrogen application and the grain yield is examined in Chapter 6.

In the western Sahel, grain and leguminous crops are often intercropped in the same field (Craufurd, 2000; Gilbert *et al.*, 2003; Mortimore and Adams, 1999). By growing an early-maturing species with a late-maturing species, the farmer can sometimes utilise the available light and water more fully than if only one crop is planted in the field (Reddy and Willey, 1981). However, intercropping is not well-suited to mechanical agriculture. Intercropping is rarely practised in Senegal but is a potential option for smallholders. The potential long-term benefits of intercropping in Senegal have not previously been examined.

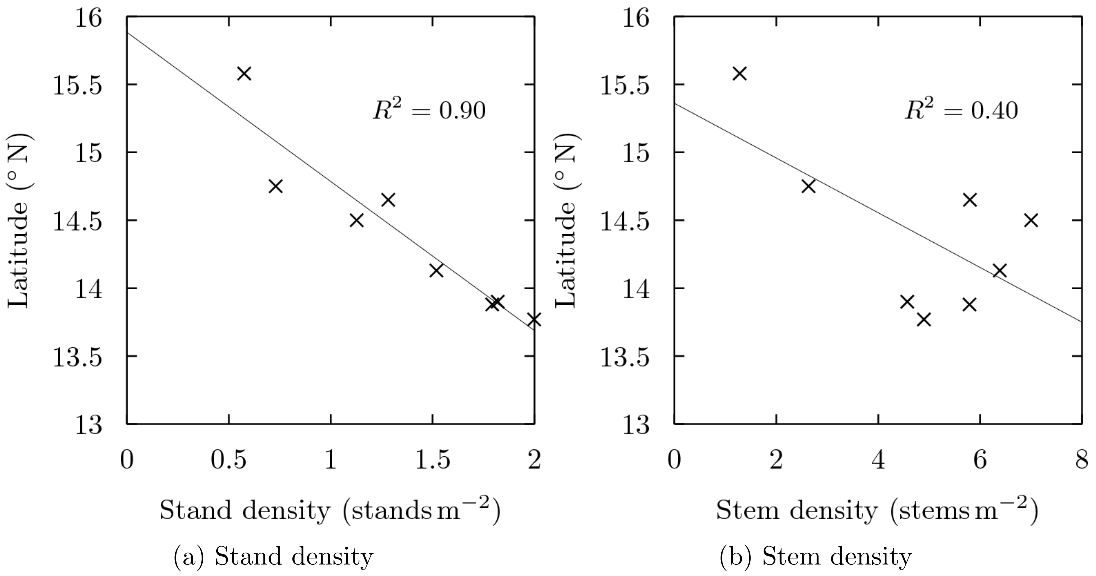

(a) Stand density

(b) Stem density

Figure 1.10: Millet stem and stand densities in eight villages in Senegal. The data were collected by the ESPACE project (Affholder, 1992) during the period 1989–1992. Each point represents the mean of all fields in the village. For the stand density, $R^2 = 0.90$ (p < 0.001), and for the stem density, $R^2 = 0.40$ (p < 0.1).

1.5.4 Weeds, pests and disease

Weeds reduce crop yields, although smallholders can target labour towards weeding at the appropriate times. A survey in Senegal concluded that most fields were effectively weeded (Table 1.4).

An important constraint on agricultural intensification is the impact of pests and disease on crops. Few farmers in Senegal can afford to use chemical herbicides or pesticides so their farms are consequently at risk of damage. The parasitic plant Striga (*Striga hermonthica*) is a widespread problem for smallholders growing millet and sorghum in the Sahel (Aliyu and Emechebe, 2006). Pests can also cause significant damage, particularly if the climatic conditions are favourable for the development of large swarms. For example, locust swarms caused widespread local damage to crops across West Africa in 2004 (FAO, 2004).

Table 1.4 shows that a substantial proportion of crops observed by the ESPACE project were affected by pests or disease. Fertilised fields appear to be

		House fields	Bush fields	Distant fields
Weed prevalence	Fertilised	1.80	1.84	1.74
Weed prevalence	Unfertilised	2.14	1.94	2.04
Pest damage	Fertilised	48 %	34 %	64 %
Pest damage	Unfertilised	23 %	30 %	47 %

Table 1.4: Weed and pest prevalence in millet fields in Senegal. The weed prevalence in each field was scored on a scale of 1 (no weeds) to 5 (weeds dominate) by the observer, in surveys that took place approximately 60 days after crop germination. Lower values indicate fewer weeds. The pest damage shows the fraction of crops that were affected by pests or disease. The severity of the impact was not recorded. The data were collected by the ESPACE project (Affholder, 1992) in several villages during the period 1989–1992. Fertilised fields are those to which either manure or mineral fertiliser were applied.

particularly at risk of attack; perhaps the larger, healthier plants provide a better meal. The increasing prevalence of pests and disease as the farming system is intensified represents an additional risk to smallholder livelihoods that must be managed.

1.6 Overview of this study

This chapter has shown that rainfall variability has a strong influence on crop yields across the country. Agricultural experiments were originally used to characterise the impact of rainfall on crop yields but they are necessarily short-term and spatially-restricted, covering only a few years and a few locations at most. It is very unlikely that the weather during such an experiment will fully represent the long-term climate so such experiments alone cannot be reliably used to identify the most appropriate agricultural strategies for a location. Crop models, on the other hand, can simulate crop growth at large number of locations over many years so can be used to characterise the agro-meteorological characteristics of a region if the model simulations are accurate enough.

The wide range of crop yields recorded in the ESPACE database, both between and within villages, shows that rainfall variability cannot be the sole cause of low yields in Senegal. Four important crop management decisions have been identified in this chapter that also affect yields: *a*) crop species and variety; *b*) nutrient application; *c*) planting date; and, *d*) planting density. Studies such as ESPACE produce valuable information about how crop management strategies vary across the country, but are also limited by the short time frame. It would be too expensive to perform field experiments to test combinations of all of these crop management decisions, but a crop model can rapidly examine their consequences over the long-term in many locations.

The aim of this study was to use a crop model to characterise the influence of climate and crop management decisions on crop yields across the climatic zones of Senegal over the long term (1950–2009). Following a review of existing crop models, it was decided that a new model should be created and evaluated for the study. Numerous combinations of the nutrient application, planting date and planting density were examined for six locations in Senegal. The financial benefits of nitrogen application and the potential benefits of adapting strategies according to the climate in previous years were assessed. The choice of crop species and variety was not examined but could be looked at in an extension to this study.

Climate change is expected to cause higher temperatures in the Sahel which could adversely affect crop growth. Rainfall patterns are also expected to be affected but there is much variation between climate model projections. The long-term impacts of climate change on crop yields can only be projected using a crop model. In this study, climate projections from three climate models were used to construct long-term daily weather data for two scenarios in the twenty-first century. This data were used in the crop model to assess the likely impacts of climate change on millet cultivation in Senegal, and to examine how the impacts might be reduced by adapting crop management practices.

1.6.1 Aims and objectives

The aims of this study were to:

1. assess the extent to which rainfall variability causes low crop yields in the Sahel;

2. understand how rainfall variability influences soil nutrient strategies and other crop management decisions of smallholders; and,

3. consider how climate change might affect rainfed farming in the Sahel in the twenty-first century and how crop management practices can be adapted to reduce any impacts.

The objectives of the study reflected the work required to achieve the aims. The primary objectives were to:

1. develop a crop model that could simulate the impact of water and nutrient stress, changing temperatures, and the influence of crop management decisions (the planting density, planting date and nitrogen management) on the final grain yields (Chapter 3);

2. calibrate and evaluate the crop model using field data from Senegal (Chapter 4);

3. produce a long-term meteorological dataset for Senegal to drive the crop model (Chapter 5);

4. characterise the relative influences of rainfall variability and crop management strategies on crop yields (Chapter 6);

5. develop a simple analysis to evaluate the financial constraints on agricultural intensification (Chapter 6); and,

6. produce representative weather data projections for the twenty-first century and analyse the potential impacts of climate change on smallholder farms (Chapter 7).

1.6.2 Academic contribution

A review of existing crop models concluded that none fulfilled the required criteria for this project. A new model, CROMSAS, has been developed which simulates the impacts of changing the planting date, planting density and fertiliser application on crop yields. The influences of temperature, water and nitrogen stress are simulated, as is the effects of rising atmospheric CO_2 concentration on crop growth. The model has been designed to address some of the deficiencies that were identified in existing models.

The new model has two further features that are not used in this study but which could be used in the future. Firstly, the model has been designed to simulate intercropping with cereals and legumes as an additional adaptation option; early tests have produced promising results. Secondly, the model has been designed to be used within a broader farming system model so that interactions between crop cultivation and other aspects of smallholder livelihoods can be simulated in the future.

Meteorological data for twelve locations in Senegal have been obtained from multiple sources for the period 1950–2009 and gaps in the data have been filled using data from the NCEP/NCAR reanalysis model. The dataset has undergone a series of quality checks and represents the most complete dataset that is available for a region of the Sahel. The accuracy of the reanalysis model predictions has been characterised for a range of Sahelian climates. Long-term evaporation pan measurements have been used to assess the accuracy of several evapotranspiration methodologies in the region for the first time.

CROMSAS has been used to identify the long-term (60-year) impact of rainfall variability on millet yields in several locations across Senegal. The optimal planting dates, planting densities and nitrogen management strategies have been assessed. This is the first study to examine all three of these factors in a holistic way for millet cultivation in West Africa. The analysis has been augmented by an appraisal of the benefits of changing crop management strategies in response to the rainfall in previous years.

Climate change is likely to lead to longer-term changes to the temperature and rainfall but the impact on smallholders, and the extent to which smallholders can adapt their farms to mitigate the impact, are not well understood. Daily meteorological data has been produced for the period 1950–2100 using historical meteorological observations and the projections of three climate models for two scenarios. The crop model has used these datasets to examine the potential impact of climate change on millet cultivation in the twenty-first century and to assess whether crop management practices can be adapted to mitigate these impacts. This is the first long-term holistic study that has examined how millet cultivation in West Africa might be affected by climate change and how the impacts might be reduced through adaptation.

Chapter 2

Literature Review

Chapter 1 introduced some of the challenges facing smallholders in Senegal and explained why a crop model study could aid our understanding of optimal long-term crop management strategies for pearl millet. No previous crop modelling studies have investigated agriculture over the long-term in Senegal but comparable studies have examined other dryland regions in West Africa, East Africa, India and Australia, to characterise the influence of rainfall and to understand the consequences of a range of crop management strategies.

This chapter critically analyses the crop modelling literature with the aim of: *a*) characterising the strengths and weaknesses of current crop models that are used to simulate millet (Section 2.1); *b*) deciding whether to use an existing model or to create a new crop model for this study; *c*) examining how crop models have been used to examine the crop management of millet and other cereals in dryland farming systems (Section 2.2); and, *d*) reviewing the use of crop models to forecast the impact of climate change on cereals in dryland farming systems (Section 2.3).

Farming is fundamentally an economic activity and most smallholders also keep livestock and have non-farm business interests. To fully understand the impact of crop management strategies on smallholder livelihoods, it is necessary to take a holistic view which encompasses the farm and all of the other household activities. Section 2.4 briefly reviews models that have been designed for livelihood studies.

Much of the climate data that was used by this study was indirectly sourced from climate models. This chapter concludes with a brief overview of climate models in Section 2.5 which highlights some of the strengths and weaknesses of data from this source.

2.1 Crop models

The simplest types of crop model are statistical in nature (Ritchie and Alagarswamy, 2002) and are used for large-scale seasonal yield predictions; for example, regression analysis can be used to find relationships between crop yields and climatic conditions using large-scale data for a particular region (e.g. Challinor *et al.*, 2003; Lobell and Burke, 2008). Statistical models are the simplest to use but are only valid for the environment in which the relationships are derived and are unable to simulate non-linear relationships during the growing season (e.g. variations in the rainfall distribution). More complex models are required to understand how crop growth is affected by management decisions and environmental conditions. These models combine research on plant physiology, agronomy, soil science and agro-meteorology to predict how a crop will grow under specific environmental conditions (White and Hoogenboom, 2010). They can be termed ‘ecophysiological’ models because mathematical descriptions of physiological, physical and chemical processes are combined to simulate crop development and growth within the crop—soil system.

The development of a plant refers to the phenological development of the crop from germination to harvest and includes the timing of vegetative growth, flowering and grain-filling. Different plant organs tend to grow at different stages of development. The growth of a plant refers to the actual growth rate of the organs, so the plant growth rate determines the final size of the organs. The final grain yield depends on both the development characteristics and growth rate of the plant so all crop models simulate these two processes independently. The growth rate depends on the amount of solar radiation, soil water and nutrients that are available to the plant (McPherson and Slatyer, 1973) and is also sensitive to the temperature, atmospheric humidity and atmospheric carbon dioxide concentration (Bierhuizen and Slatyer, 1965). The development rate is very sensitive to the temperature and can also be sensitive to the daylength (Ong and Monteith, 1985). Most crop models simulate the development and growth of the crop independently. The final crop biomass is determined from the growth rate. The partitioning of the crop biomass to each plant organ, and hence the final grain yield, is determined by the crop development rate.

A key issue in the development of crop models has been the identification of an appropriate level of model complexity (Sinclair and Seligman, 1996). Attempts to include every possible plant×environment mechanism in models have largely failed to improve model performances because there are insufficient experimental data and knowledge for the processes to be properly represented. Over-calibration of models has led to poor performance outside of the calibrated environment (Passioura, 1996). It is therefore not possible to create a universal crop model that is adequate for all environments and problems (Spitters, 1990). Instead, crop models are created to address particular problems and the level of model complexity is set to the minimum required for the investigation.

Passioura (1996) identifies two types of crop model. The first is practical in nature, combining a few key relationships to predict crop behaviour, and is termed a 'functional' model. The second is more scientific in spirit, representing biological and physiological processes on short timescales, and is termed a 'mechanistic' model. Mechanistic models require high volumes of input data and the large number of relationships and assumptions that are involved in their development tends to limit the use of such models to academic purposes by the authors. Functional models are generally considered the most useful for practical problem solving and are the focus of this study.

2.1.1 Comparison of existing crop models of millet

A summary of existing functional crop models that can be used to simulate millet is presented in Table 2.1. The table contains the relevant references for each model. A comparison of the principle differences between the models is useful to inform the development of a new model.

Model	Description
GLAM	Estimates crop yields over large areas using a mechanistic soil water sub-model with an empirical leaf expansion function (Challinor *et al.*, 2004). Growth depends on TUE only. Yield depends on the HI.
RESCAP	Uses a mechanistic soil water sub-model (Monteith *et al.*, 1989). Leaf expansion depends on the plant growth rate. Growth depends on both RUE and TUE but assumes no nutrient stress. Yield depends on the HI.
PARCH	Developed from RESCAP with the addition of soil nitrogen and phosphorus sub-models (Stephens and Hess, 1999) but appears to have fallen out of use.
SARRA	Simulates millet in the Sahel using a mechanistic soil water sub-model with an empirical leaf expansion function that depends on a fertility index which is calculated from the field fertiliser application (Affholder, 1995). Growth is calculated from the maximum leaf area. Yield depends on the HI.
STICS	Generic crop growth model with mechanistic soil water and nitrogen sub-models (Brisson *et al.*, 1998). Uses an empirical leaf expansion function which is a function of the planting density. Growth depends on RUE only. Yield depends on individual grain sinks. Simulates intercropping.
EPIC	Designed to assess the effect of soil erosion on crop productivity in the USA (Easterling *et al.*, 1992; Williams *et al.*, 1989). Contains a comprehensive mechanistic soil sub-model but growth of all crops is simulated using a single sub-model based on RUE only with an empirical leaf expansion function. Yield depends on the HI.
CropSyst	Similar design to EPIC but with a more process-orientated approach to crop growth, which depends on both RUE and TUE. Leaf growth depends on the plant growth rate. Yield depends on the HI. (Stöckle *et al.*, 2003, 1994).
CERES	Widely-used model with mechanistic soil water and nitrogen sub-models. Simulates several cereals, including millet, in different versions of the model (Ritchie and Alagarswamy, 1989a,b,c). Leaf expansion is calculated as a function of the number of leaves but is constrained by the growth rate. Growth depends on RUE only. Yield is calculated as the assimilate partitioned to the panicle.
APSIM	Designed as a modular system with crop and soil modules that can be plugged into a central interface (Keating *et al.*, 2003; McCown *et al.*, 2002). Uses mechanistic soil water, nitrogen and phosphorus sub-models. In the millet module, growth depends on both RUE and TUE (van Oosterom *et al.*, 2001a). Leaf expansion is calculated using a complex empirical function of the number of leaves but is constrained by the growth rate. Independent tillers are simulated. Yield is calculated from the growth of individual grain sinks.

Table 2.1: List of existing crop models for simulating millet. RUE is the radiation use efficiency and TUE is the transpiration use efficiency. HI is the harvest index. See the main text for definitions.

The rate of crop development is simulated as a fixed number of days in SARRA. All of the other models simulate development as a function of the temperature, with all but GLAM simulating photoperiodic sensitivity as well.

All of the models simulate the soil water balance using mechanistic sub-models, which is crucial for rainfed crops in dryland regions. However, different approaches are taken to nutrient stress with RESCAP assuming no stress while GLAM and SARRA calculate the impact of nutrient stress using a calibrated function. All of the other models have mechanistic soil nitrogen sub-models. PARCH, EPIC and APSIM also have soil phosphorus sub-models. The main difficulty with the mechanistic nitrogen and phosphorus models is obtaining the large amount of good-quality experimental data that are required to drive the many parameterisations. If the data are not available then the sub-models will perform poorly and simpler approaches will be more appropriate; for example, two field studies in California identified a number of deficiencies in the soil nitrogen sub-model of CERES which adversely affected simulations (Hasegawa *et al.*, 2000, 1999).

The rate of leaf expansion is a crucial part of a crop model because it determines the radiation interception and hence the growth rate. It is also one of the most difficult processes to simulate, a factor which is reflected by the different approaches taken by each model. GLAM, STICS and EPIC all use different empirical leaf area curves that are independent of the growth rate (although the leaf area is reduced by water and nutrient stress). CERES and APSIM also use empirical leaf area functions to calculate the demand from the leaves for assimilate but leaf expansion in these models is constrained to the growth rate by applying a constant called the specific leaf area (SLA), which is the ratio of leaf area to leaf mass. RESCAP, PARCH and EPIC calculate the leaf area from the partitioned leaf mass using a constant SLA. Calculating the leaf area as a function of the leaf mass ensures that the plant dimensions are consistent and that the plant growth rate is constrained by the laws of physics. Nevertheless, there are drawbacks with the SLA approach, the most important being that the SLA is not constant (Brisson *et al.*, 1998). Payne *et al.* (1991) measured the SLA for a large number of millet leaves and concluded that it decreases from a maximum of $85\,\mathrm{m^2\,kg^{-1}}$ for newly-emerged leaves to $15\,\mathrm{m^2\,kg^{-1}}$ for large leaves. Models which use a constant SLA (e.g. RESCAP, which uses $33\,\mathrm{m^2\,kg^{-1}}$) are likely to underestimate leaf expansion in the early growth stages but overestimate it later. CERES and APSIM both simulate the SLA reducing as the canopy develops using empirical functions, with final SLAs of $\sim 55\,\mathrm{m^2\,kg^{-1}}$ (Birch *et al.*, 1990) and $\sim 45\,\mathrm{m^2\,kg^{-1}}$ (van Oosterom *et al.*, 2001a) respectively. It is interesting that the SLA varies so substantially between these three models and that the final values are so much higher than those measured by Payne *et al.* (1991). Simulating leaf expansion independently of the mass requires a number of empirical parameters that are not generally measured in field experiments. On the other hand, simulating a SLA as a function of the total leaf area rather than individual leaf sizes also introduces assumptions into the model that might not be valid under certain circumstances (for example, a crop with a large number of small leaves would be simulated with the same SLA as another crop with a small number of large leaves, but in reality the SLA of the two crops would be very different). Both approaches have drawbacks and could be improved by, for example, modelling the mass and area of individual leaves using a similar relationship to Payne *et al.* (1991) and summing these for the whole plant.

None of the crop models simulate plant growth as a function of the photosynthesis rate. Instead, plant growth is assumed to be proportional to either the solar radiation that is intercepted by the leaves or to the plant water use. The radiation use efficiency (RUE) constant links the plant growth to the solar radiation and is generally set to $4\,\mathrm{g\,MJ^{-1}}$ (some models reduce this value during grain filling). The transpiration use efficiency (TUE) similarly links the plant growth to the water that is transpired by the plant, but is modified by the vapour pressure deficit (VPD) to reflect the observation that water use increases as the VPD increases (Tanner and Sinclair, 1983). The TUE is set to a constant $9\,\mathrm{g\,kg^{-1}\,kPa}$ throughout growth in RESCAP and APSIM. Some models calculate the growth rate as the minimum of the RUE and TUE methods while others choose one or the other. The conclusions of experimental studies (e.g. Bierhuizen and Slatyer, 1965) suggest that growth should be constrained by both methods, for two reasons. Firstly, while solar radiation generally limits crop growth at mid to high latitudes, the regions for which many crop models were originally designed, it is likely that the transpiration rate will often limit growth in the semi-arid tropics where the peak planetary solar radiation occurs. Secondly, field experiments have shown that the TUE increases relatively more than the RUE for C_4 crops as the atmospheric CO_2 concentration increases (e.g. Triggs *et al.*, 2004) so the influence of climate change in Senegal will not be properly simulated if either mechanism is absent from a model.

The models simulate the mass partitioning to the plant roots in different ways. RESCAP, PARCH and CERES simulate the growth of the roots as a function of the assimilate that is partitioned to them. The other models only partition assimilate to the shoot and simply assume that root growth is not affected by the plant mass. This is particularly interesting in the case of APSIM since the same RUE and TUE coefficients are used as for RESCAP and CERES, respectively, but they are implicitly higher in APSIM since assimilate is not transferred to the roots as it is in the other two models. It is possible that the higher SLA in CERES mentioned above reflects the lower shoot growth rate caused by partitioning assimilate to the roots. These discrepancies show that care must be taken when interpreting experimental measurements of the RUE and TUE to understand whether partitioning to roots has been included in the mass balance.

Grain yields can be calculated by simulating individual grains (STICS, CERES and APSIM) or by applying a harvest index (HI) to the crop. The HI is the ratio of the grain yield to the total biomass and some models simulate this ratio increasing towards a maximum value during grain filling. The HI approach is simpler than simulating individual grain sinks but requires empirical parameters to set the maximum HI and the impact of water and nutrient stress. Simulations of individual grains can use readily-available parameters from field studies (e.g. Fussell *et al.*, 1980) and can improve the simulation of crops that are sink-limited (e.g. if there is plant stress during flowering), so this is the ideal approach.

In summary, the plant development and soil water balance are simulated with a similar level of complexity across the models but the treatment of plant growth, grain yields and particularly leaf expansion differ substantially. The differing treatment of partitioning to the roots in different models raises concerns about the accuracy of the RUE and TUE parameters. Most of the models were designed to simulate temperate crops in rich soils at mid to high latitudes. Proper evaluations should be performed before using the same models to simulate tropical crops in sandy soils at low latitudes.

2.1.2 Rational for developing a new crop model

The models were examined to assess their suitability for this study. The ideal model would: *a*) simulate varying planting dates; *b*) simulate varying planting densities; *c*) simulate the impact of manure and fertiliser application; *d*) simulate intercropping; *e*) simulate the impacts of climate change; *f*) have few unnecessary parameterisations; and, *g*) have a flexible design permitting alterations and ultimately coupling with other broader farming system models.

All of the models except SARRA are designed to simulate the impact of changing the planting date in the Sahel because they simulate the influence of temperature and photoperiod on crop development. However, as will be seen in Section 3.3.1, temperature and photoperiod can have very different influences on the phenological development of different varieties of millet so it is important to properly calibrate models for each variety that is being simulated.

Only CERES and APSIM can directly simulate varying planting densities because these are the only models that simulate the leaf area of individual plants. However, since APSIM simulates the reducing SLA as a function of the crop leaf area rather than the plant leaf area, it could be argued that the APSIM simulation of the planting density is flawed because different crops with plants of different sizes, but with the same overall crop leaf area, would have a different SLAs in reality but the same SLA in the model. STICS simulates planting density indirectly by altering the empirical crop leaf area function, and similar empirical fixes could be applied to the other models. However, the better approach in the absence of firm empirical data is to simulate individual plants.

It was necessary to quantify the impact of manure and fertiliser on crop growth in this study so models which use calibrated empirical functions were considered unsuitable. Several models have mechanistic soil nitrogen sub-models but there was concern that good-quality experimental data to drive the parameterisations were not available for Senegalese soils, and that the current data might not be appropriate for tropical mineral-poor sandy soils. For CERES in particular, it is not possible to change the nutrient model without changing the model code directly. In view of the very low natural fertility of the sandy soils, it was concluded that a simpler nitrogen sub-model than those commonly used would be adequate.

The only models that can directly simulate intercropping, where two or more crops compete above and below-ground for resources, are STICS (Brisson *et al.*, 2004) and APSIM. The other models would require broad changes and potentially coupling with other models.

There was particular concern about the simulation of climate change by all of the crop models. It has already been noted that some models do not simulate both RUE and TUE. Another concern was that important relationships between the crop and the environment (e.g. the impact of high temperatures on some plant processes) have not been firmly established. White and Hoogenboom (2010) note that: *a*) crop models differ greatly in their approaches to modelling the effect of temperature on leaf expansion and thickness; *b*) the effect of heat stress on reproductive growth is rarely explicitly modelled; *c*) the effects of rising CO_2 concentration on plant development are not well understood and are not modelled; and, *d*) the impact of low relative humidity on leaf development is not well understood. It is therefore useful to be able to alter a model to permit sensitivity studies to be performed and to allow changes in the future when new experiment work becomes available.

APSIM was the only model that could simulate all of the required crop management options, but there was concern about the simulation of the leaf expansion, planting density and root partitioning as described above. The APSIM millet module is reasonably compact and flexible but the overall system is far more complicated than was required for this study. As a result of the complexity, development of APSIM is very tightly controlled with a strict version control and distribution system (Keating *et al.*, 2003). The source code is only shared if there is an agreed program of joint development. Hence the APSIM system was considered too complex for use by this study and it was decided that a new crop model should be developed. Chapter 3 describes the new model.

2.1.3 Limitations of crop models

Each plant species, and to a lesser extent each variety, reacts differently to the environment in which it is grown. The response of crops to water and nutrient stress is particularly diverse (e.g. Bidinger *et al.*, 1982; Bieler *et al.*, 1993). This raises particular difficulties for crop models of the Sahel where widespread water and nutrient stress is the norm. Most crop models address these difficulties by simulating only one species or by simulating each species separately. Parameters are then used to simulate the behaviour of particular varieties of a species.

Crop parameterisation is not usually limited to just simulating different varieties. Crops models are normally parameterised for particular environments (climates and soils) as well and often perform poorly outside of these environments. For example, Fechter *et al.* (1991) compared the SWATRER soil water model and the CERES-Millet model with a field experiment performed in Niger. While SWATRER accurately simulated the soil water content throughout the season, CERES-Millet overestimated the soil water by 5 %, the leaf growth and dry matter by around 40 % and the grain yield by 100 %. Yet the study concluded that CERES-Millet would be a useful tool once fully calibrated for the local environment.

Crop models are necessarily limited in scope so important assumptions are often made, for example that weeds, pests and disease will have negligible impact on the crop and that the crop will be managed in the optimal way by the farmer. Such assumptions are reasonable for intensively-managed temperate crops but are less valid for low-input smallholder fields in tropical areas (Lobell *et al.*, 2009). There is often a substantial 'yield gap' between the model predictions of the expected grain yield and the actual yield that is achieved.

Rainfall in the Sahel has high spatial variability (Section 1.4) and is normally only measured at widely-dispersed weather stations so estimates for sites that lie far from the stations are likely to be poor. This is only one of difficulties with environmental data that affect crop model simulations. Section 1.3 described how some soils are more suitable for agriculture than others. Even within a single field, the soil will be composed of many layers with a range of materials and structures that affect the nutrient content, water percolation and retention, and root development. The topography of the field and the surrounding area will determine whether water is gained or lost from the field through runoff. Studies have recorded substantial yield variations in different parts of apparently uniform fields, both in the Sahel (Affholder, 1992) and elsewhere (e.g. Russell and van Gardingen, 1997). For example, Sadler *et al.* (1995) measured a mean maize yield of 2148 $\mathrm{kg\,ha^{-1}}$ in a uniformly-managed field in South Carolina, USA, but the yield varied between 185 $\mathrm{kg\,ha^{-1}}$ and 4198 $\mathrm{kg\,ha^{-1}}$ in different parts of the field. Crop models assume that crop growth is homogeneous across the field and hope that this method will produce the correct overall field mean yield.

The performance of all crop models is impaired by these limitations to some extent. Such limitations should be taken into consideration when interpreting the results of crop simulations and producing policy recommendations.

2.2 Crop modelling studies of crop management in dryland regions

Crop models are most often used to examine the management options for a single crop. The first analysis for dryland crops is often a yield gap analysis. Further analyses to identify optimum planting dates, planting densities and nutrient management strategies are then performed. Since rainfed dryland crop yields are often sensitive to variable climates, some studies have examined the potential for changing crop management on a season-to-season basis in response to environmental conditions early in the season, and farming decision support systems have been developed which can support this approach. All of these types of crop management analysis are current or potential future interests of this study so are reviewed below.

2.2.1 Yield gap analyses

Yield gap analyses are used to evaluate the difference between the attainable yield in a location and the actual yield (Matthews, 2002). The actual yield can be reduced by poor management practices, weather and soil conditions, stresses due to inadequate soil nutrients, pests and disease, or by using a sub-optimal crop variety. For example, van Keulen (1975) used a crop model to show that production in the Sahel was limited in most years by nutrient deficiency rather than drought. More recently, Dingkuhn and Sow (1997) examined why yields of irrigated rice in Mali were lower than expected in some years. They identified temperature as the primary driver of the yield variations, with crop duration varying according to the temperature of the flood water and leaf expansion and the number of grain sinks being affecting by high and low temperatures. Yield gap analyses can be used to identify locations where the natural resources are not being fully utilised so that further studies can be targeted to identify the cause of the yield gap.

2.2.2 Planting date

The planting date can have an important influence on the growth of a crop and the final yield, particularly in locations with strong seasonal climates. In the Sahel, planting too early can result in poor establishment of the crop, while planting too late can lead to drought stress during grain filling. Omer *et al.* (1988) used a crop model to determine the optimum planting date for sorghum in Sudan, identifying the period between 20 June and 10 July. Sultan *et al.* (2005) identified the optimum planting dates over 17 years at Niamey, Niger using the SARRA-H model then simulated the yield gap caused by using the traditional planting strategy and an alternative strategy related to the onset of the monsoon. The alternative strategy, in which the crops were usually planted later in the season, was found to lead to higher yields.

Soler *et al.* (2008) used 20 years of climate data to identify the optimum planting date for Kollo, Niger. 12 planting dates were simulated from 10 April until 29 July for three varieties of millet and the overall optimum planting window was identified as mid-May to early-June, although there was much variability between seasons. One of the varieties had a longer duration of development and it was beneficial to plant this variety earlier than the others. The optimum planting date was not influenced by the nutrient availability of the field. Only 20 years of climate data was used in the analysis, arguably too short a period to accurately appraise the agricultural potential of Kollo because the region had a long-term drought throughout.

A study of the potential for sorghum cultivation was performed by Muchow *et al.* (1994) for three sites in Australia. The influence of eight planting dates between August and March was assessed using 95 years of climate data, and used to assess the climatic risk of planting at different times (which were predominantly frost in winter and occasionally drought).

Some studies have concluded that the optimum planting date depends on the level of risk that is acceptable to the farmer. Studies in South Africa (Singels, 1992) and Kansas (Williams *et al.*, 1999) both concluded that risk-averse farmers should choose later sowing dates, which would reduce the interannual grain yield variability (but at the expense of a reduction in the long-term mean yield).

It is important to recognise the influence of factors that affect smallholders and crops but which are not represented in model simulations. For example, crops are often dry-planted in West Africa at times when household labour is not required for other off-farm tasks, which allows poorer smallholders to earn additional income as labourers on other farms at the start of the rainy season (Netting, 1993). Moreover, planting after the first rains can also lead to additional weeding for the household if the soil cannot be ploughed before sowing, and the ‘nutrient flush’ that occurs as manure decomposes rapidly after the first rains (Mortimore and Adams, 1999) is lost to weeds if a crop has not been planted. Biotic factors can also influence the planting strategy. In a study of groundnut production in India using the CROPGRO model, Hoogenboom *et al.* (2001) concluded that planting later in the season would improve yields, but this strategy was found to be unpopular with farmers because late-planted crops suffered disproportionately from pests and disease which were not simulated by the model.

The planting date clearly influences crop yields but the degree of influence appears to vary according to the local environmental conditions and the type of crop. To accurately assess the impact of varying the planting date, it is necessary for the new crop model to simulate the crop duration and the impact of temperature variations and water stress on the crop.

2.2.3 Planting density

Crop models have been used to examine the influence of the crop planting density on the final yield. For example, Keating *et al.* (1988) examined the how the planting density affected maize yields in Kenya using the CERES-Maize model and concluded that the density should be increased as the N supply increased. Singh *et al.* (1993) reached a similar conclusion for Malawi. In general, reducing the planting density causes sub-optimal yields in good growing conditions but produces higher yields if the crop suffers water or nutrient stress. Mortimore and Adams (1999) observed that the planting density was lower in locations with lower rainfall where fewer nutrients were applied.

Models can be used to identify variations in the planting density—yield relationship for locations with variable environments like the Sahel. The optimal planting density in such locations is likely to vary from year to year. Wade *et al.* (1991) performed a planting density analysis for sorghum over a 30-year period in northern Australia and concluded that increasing the planting density would lead to higher yields in 5 years but would cause crop failure in 14 years, except at the wettest site where increasing the planting density increased the yield in all years. No similar studies were found for West Africa.

2.2.4 Nutrient management

Many experiments have been performed on agricultural field stations to identify appropriate nutrient management strategies for the local regions. But the results of such experiments can be misleading in environments with high climatic variability if the weather is not representative of the long-term regional average (Muchow *et al.*, 1991; Thornton *et al.*, 1995). Crop models offer the opportunity to test and refine the recommended strategies for such environments. For example, Thornton et al (1995) used the CERES-Maize model to determine optimal crop management strategies across Malawi and concluded that the optimum planting density and nitrogen fertiliser application depended on the variety, local rainfall and soil type. This review concentrates on studies of nitrogen (N) management as N is usually the most limiting nutrient and other nutrients are rarely examined.

An important constraint for smallholders in Africa is the cost of fertiliser. The price volatility of mineral fertiliser increased in many African countries when governmental subsidies were removed by structural adjustment programmes in the 1990s (Matthews, 2002). Crop models can be used to identify a range of strategies to optimise the returns from farms under a variety of situations.

The APSIM model has been used with 46 years of daily meteorological data for a site in Zimbabwe with the aim of identifying the most appropriate level of fertiliser application (Cooper *et al.*, 2008). It was concluded that the rates of return to the farmer from applying 17 kg N ha^{-1} would be substantially better over the long-term than applying the previously-recommended quantity of 52 kg N ha^{-1}, and led to a widespread campaign to persuade 170 000 farmers to adopt this ‘micro-dosing’ strategy with encouraging results.

The CERES-Maize model was used by Keating *et al.* (1991) to identify the response of maize crops to N in a semi-arid region of Kenya. In general, the response to N application was proportional to the rainfall, but in some years of very high rainfall (above 800 mm), large losses of N were predicted to occur through leaching. While the highest average yields were achieved at the highest level of fertilisation, 160 kg ha^{-1}, the variability at this level was very high, with large losses in some years, and the optimum strategy to maximise income while minimising risk was to use 40 kg ha^{-1}.

Irénikatché Akponikpè *et al.* (2010) reached similar conclusions using APSIM-Millet for a site near Niamey in Niger. Both the model simulations and the two-year experiment that was used to test the model suggested that the grain yield increased proportionally with N application in years of sufficient rainfall. Increasing the fertiliser application above 25 kg ha^{-1} steadily increased the risk of economic losses to the farmer.

The benefits of intercropping millet and legumes were investigated by McDonagh and Hillyer (2000) using a crop model. They concluded that there would be a minimal contribution of N from the legumes to the millet crop (4 kg N ha^{-1}), unless the legume residues could be incorporated into the field. Leguminous residues are normally used as forage in that region so it was concluded that mineral fertilisation would be a better strategy in areas with sufficient annual rainfall.

One of the difficulties of simulating smallholder fields is to quantify the nutrients available to the crop because the fertility of the soil and the amount of applied manure are often not known. Affholder (1994) describes a fertility index for smallholder fields in Senegal to estimate the available nutrients from the type of manure and the soil carbon content, and Affholder (1997) uses this with the SARRA-millet model to simulate the crop yields from 89 millet fields across the groundnut basin with reasonable accuracy. No other crop management simulations for millet in Senegal have been published.

Where N is limiting, these studies suggest that the grain yield will rise proportionally with N application. If there is water stress then high N applications will have less influence on plant growth and could even reduce the grain yield. Conversely, high rainfall can cause high losses of N from the soil. Despite these complex rainfall—nitrogen relationships, the most important limitation on N application in several studies is the cost of the fertiliser. The optimal economic quantity is often lower than the optimal quantity for maximising the crop yield as a result of large losses occurring in years with poor rainfall. Such losses can have a strong adverse impact on the livelihoods of smallholders so the level of fertiliser application also depends on the financial risk that smallholders are willing to accept. It is therefore necessary to include economic considerations in any comprehensive study of N management by smallholders.

2.2.5 Use of rainfall information

The previous sub-sections have described how models have been used to identify the optimal long-term crop planting date, planting density and nutrient inputs. Models can also provide useful information to farmers and national organisations both before and during particular cropping seasons.

Seasonal weather predictions have been developed to assess the amount of rainfall that is likely to occur during a growing season, and these can be integrated with crop models to assess the likely impacts on regional agriculture (Hansen, 2005). For example, Mishra *et al.* (2008) evaluated a sorghum yield prediction system for five locations in Burkina Faso using historic weather data and concluded that a functional crop model could produce better yield predictions using the rainfall forecast than a linear regression model.

Yield prediction systems can be used to identify the most appropriate choice of crop and planting density for a particular season. Keating *et al.* (1991) used CERES-Maize to examine the value of changing the application of N fertiliser for maize based on the seasonal weather forecast for Machakos, a semi-arid region of Kenya. The most useful predictor of the response to fertiliser inputs was found to be the rainfall onset date, when planting traditionally takes place. However, varying the fertiliser input according to the onset date produced only a small increase in the gross return, although the overall losses were lower in years with poor rainfall. Use of some fertiliser, irrespective of the seasonal forecast, was the highest priority.

Stewart (1991) identifies relationships between the monsoon onset and the magnitude of the seasonal rainfall in Kenya and Mali. A crop model study that incorporated this information could produce recommendations about the choice of crop for a season that was based on the monsoon onset date; perhaps maize would be sown in years with early rains but sorghum or millet in years when the rains were delayed. Stewart (1991) calls this approach ‘response farming’.

The principle difficulties with seasonal climate predictions are the accuracy of the predictions and the ability to pass them to farmers, in a suitable format at an appropriate time, to allow them to consider the consequences and alter their crop management strategies (Barrett and Nearing, 1998). It is necessary to quantify the accuracy of the crop prediction method by evaluating it against historical climate data (e.g. Cooper *et al.*, 2008; Mishra *et al.*, 2008). In the longer term, it might be necessary to take a more holistic view of how to adapt existing crop management strategies to allow farmers to benefit from the information. The information could be targeted at particular groups of farmers who would benefit the most.

Governments and aid organisations can use the forecasts of seasonal agriculture in conjunction with market prices and other socio-economic data to develop early warning systems to identify populations at risk of food insecurity. A pearl millet yield estimation system based on CERES-Millet was developed by Thornton *et al.* (1997) for 30 provinces in Burkina Faso. The system used remotelysensed estimates of rainfall embedded in a geographic information system (GIS) to create an early warning system for food shortages. In a 1-year trial, the final grain yield that was forecast in the middle of the growing season by the system differed from the achieved yield by 15%. A similar system was developed by Badini *et al.* (1997) which coupled the CropSyst model with GIS databases of soil types, long-term weather and crop management from Burkina Faso.

Decision support systems (DSSs) could be developed to assist smallholders with the short-term management decisions described in this section. DSSAT (IBSNAT, 1989), which contains the CERES and CROPGRO models, is perhaps the most well known system, but APSIM has also been developed into a DSS. DSSs were originally targeted at farmers in developed countries but there has been limited uptake, despite many farms purchasing computers for other business-related tasks like accounting (McCown *et al.*, 2002). Some large-scale outreach programmes have been performed to encourage adoption of the technology. Since this study is primarily concerning with long-term crop management strategies rather than short-term decision-making, DSSs are not considered further in this thesis.

The short-term use of rainfall information is a developing field. Systems are currently used by governments and aid organisations to aid large-scale planning but there is little evidence of adoption of these systems by farmers. While such systems might benefit farmers in the long-term, it seems that studies have yet to demonstrate clear benefits to farmers from using such systems. The development of such a system is outside the scope of this study but it could be considered in the longer-term using the crop model developed here.

2.3 Crop modelling studies of the climate change impacts on agriculture

Climate change is forecast to alter the distribution and productivity of agricultural land across the planet. Fischer *et al.* (2005) conclude that the agricultural land area will increase significantly in North America and the Russian Federation but that there will be a reduction in the cultivated area in sub-Saharan Africa.

Africa has been identified as one of the regions with the greatest challenge for food security in a climate-changed world, because grain yields could decrease substantially if periods of extreme temperatures occur more often or if the frequency of drought increases (Easterling *et al.*, 2007).

It is estimated that the agricultural sector accounts for approximately 60 % of total employment in Africa (Slingo *et al.*, 2005). The sector has a crucial role in rural food security. Studies of the impact of climate change on agriculture have tended to examine the broader issue of food security rather than focusing on food production, with the aim of understanding how agricultural impacts interact with other environmental and socio-economic factors that determine the vulnerability of populations (Brooks *et al.*, 2005). Early studies were split into several stages. First, the IBSNAT system was developed using the DSSAT and CROPGRO models (IBSNAT, 1989) and was used to analyse how climate change might affect the yields of important crops at 112 sites in 18 countries (Rosenzweig and Parry, 1994). Statistical relationships were derived to estimate yields for a range of temperatures and rainfall magnitudes at each location. These relationships were then combined with projections from climate models to calculate future yields. These yield data were used by a dynamic model of the world food system (the Basic Linked System, or BLS) to assess the impact of climate change on future food production, commodity prices and the number of people at risk from hunger (Fischer *et al.*, 2002). It was concluded that climate change would reduce global food production and would increase food insecurity in the most marginalised economies, particularly in Africa.

More recent studies have used similar methodologies and reached similar conclusions. Parry *et al.* (1999, 2005, 2004) repeated their earlier work with higher resolution data and for a range of future scenarios. They concluded that adaptation (changing crop varieties and using irrigation) would reduce the impacts of climate change. Fischer *et al.* (2005) also identified adaptation as the key to limiting the potential damages of climate change. Cline (2007) used a similar approach but with different economic models and crop yield functions, and disaggregated the results by country. He reached the disturbing conclusion that the net revenue from dryland agriculture in Senegal would reduce to a level that would cause the abandonment of dryland agriculture across the country.

These studies necessarily have limited scope and make simplifying assumptions. They concentrate on crops that are traded rather than subsistence crops, so minor grain crops including millet are assumed to grow in the same way as wheat or maize. The studies use statistical relationships between crop yield and total rainfall from past seasons which are assumed to accurately represent a changed climate in the future. The relationship between temperature and yield is also simulated using statistical functions so the impacts of periods of high temperatures at critical times in the growth cycle, which can substantially reduce the grain yield (e.g. Challinor *et al.*, 2005), are not represented. The IPCC Fourth Assessment Report concludes with high confidence that changes in the frequency and severity of extreme climatic events will have more serious consequences for food production than changes in the projected means of temperature and precipitation (Easterling *et al.*, 2007). Another widely-used assumption is that climate models can simulate current and future climates with reasonable accuracy. Using this assumption obviates the need for observed meteorological data and simplifies the climatic data handling, but few climate models produce skilful simulations of the Sahel; for example, Huntingford *et al.* (2005) tested four models and found that none captured the pattern of diminished Sahelian rainfall in the period 1971–1989.

Studies of the impact of climate change on millet in West Africa using crop models have recently been published for the first time. Adejuwon (2006) examined the impact of climate change on the cultivation of millet in Nigeria using the EPIC model and concluded that enhanced grain yields would be achieved in the first half of the century but that temperature-related losses would be experienced during the second half. This study used 30-year averaged climate data, from a single climate model for the SRES A2 scenario, and compared the resulting crop model projections with projections using averaged observed data for the period 1961–1990. Using averaged data in this way is likely to produce overly-high yield estimates because the averaging process removes any extreme climatic events that might have been simulated. This approach also does not allow the impact of long-term climate variability on yields to be quantified.

Liu *et al.* (2008) simulated the impact of climate change on millet across sub-Saharan Africa using a high-resolution GIS system linked to the EPIC model and concluded that millet yields would increase by 25 %–50 % in Senegal. This study also used long-term climatic data averages, with observed meteorological data from 1990–1999 and HADCM3 climate model projections for 2030–2039. Monthly data was obtained in each case and converted to daily data using a statistical down-scaling model. This study therefore has the same limitations as the study of Adejuwon (2006) with no long-term yield trend being simulated and the impact of climate variability being ignored.

The limitations of crop models for climate change assessments that were identified in Section 2.1.2 should be heeded when examining studies of crop yield projections. One method to produce more authoritative agricultural forecasts would be to use ensembles of crop models to produce future projections in the same way that climate model ensembles are currently used. The IPCC Fourth Assessment Report (Easterling *et al.*, 2007) notes that "calls by the Third Assessment Report (TAR) to enhance crop model inter-comparison studies have remained unheeded; in fact, such activity has been performed with much less frequency after the TAR than before." Part of the problem is the current necessity to calibrate a model for a particular region and even for the meteorological data that is being used to represent the region. All of the models must be calibrated so that a reasonable comparison can be performed. Several crops are normally grown in each region of the world so the number of region × crop combinations is very large.

In summary, few studies have examined the impacts of climate change on dryland agriculture using crop models. Most of these have examined large-scale global trends and have not considered pearl millet. More recently, two studies have examined the impact of climate change on millet cultivation in West Africa but have both probably overestimated the crop yields as a result of using averaged climate data. Neither have examined how the interannual grain yield variability is likely to change and neither have examined how the changes might have been mitigated through adaptation. There is a need for a study to properly quantify the long-term impact of climate change on millet in West Africa using more realistic climate data.

2.3.1 Adaptation by changing crop management practices

It has been suggested that the best strategy to manage climate change in Africa might be to focus on coping with climate variability rather than specifically targeting longer-term climate change (Washington *et al.*, 2004). This strategy has an implicit assumption that changes to the rainfall patterns will have the greatest impact on agriculture in the future. However, some studies have concluded that temperature changes will have greater impact than rainfall changes in West Africa (Adejuwon, 2006; Lobell and Burke, 2008).

Changes to the planting date, planting density and nutrient application through the century are expected to reduce the impacts of climate change. Another option for smallholders is to choose alternative crop species and varieties that are hardier to high temperatures and have more appropriate developmental durations for the changed climate. Few crop modelling studies have looked at this option (Soussana *et al.*, 2010) although Challinor *et al.* (2007) is a notable exception. Kurukulasuriya and Mendelsohn (2007) used a statistical model to examine crop selection as an adaptation strategy in Africa and found that the choice of species was very sensitive to the local climate; however, smallholders who live in the drier parts of the Sahel have no realistic alternative to millet, the best-adapted grain crop to hot, dry environments. The genetic diversity of millet in West Africa is unusually large (Haussmann *et al.*, 2006) so there should be opportunities to breed new well-adapted varieties. Crop models have recently been developed to identify desirable plant characteristics in different varieties in order to accelerate breeding programmes (e.g. Hammer *et al.*, 2010)

Even where climate change has relatively moderate large-scale impacts on agriculture, there is likely to be much more severe climatic and economic vulnerability at the local level. Research is required to identify vulnerable households and to develop coping strategies. Adaptation to climate change has so far been simulated in very simple ways and the extent to which smallholders will be able to adapt their crop management to cope is unclear (Boko *et al.*, 2007). For the Sahel region, climate change adaptation research has been principally qualitative and has concentrated on the concepts of building resilience and disseminating climate data for interpretation by farmers (e.g. Ziervogel *et al.*, 2008). Studies have not been performed for the Sahel with crop models to examine the benefits of adaptation in the future.

It seems likely that agricultural practices will have to change with climate change. But they will also be affected by technological developments, environmental regulation, market conditions and other factors (White and Hoogenboom, 2010). Climate change is only one of several factors that will affect agriculture in the future.

In summary, few studies have examined the potential for adapting crop management practices to reduce the impacts of climate change and the effectiveness of these adaptation options needs to be quantified before the full impact of climate change on West African agriculture can be understood.

2.4 Broader models of farming systems

In Senegal, rural smallholders generally aim to maximise the economic returns from their farms rather than the grain production. The farm is only one aspect of their livelihoods as most smallholders also own livestock and have non-farm business interests (Mortimore and Adams, 2001). It is therefore necessary to appraise the economic benefits of changing crop management systems before recommending changes (e.g. Cooper *et al.*, 2008). A number of models have been developed to examine livelihoods and farming systems which incorporate both crop models and economic appraisals. These models were not used in this study but a longer-term aim is to couple the new crop model into a broader farming system model to better understand the influence of climate and financial constraints on smallholders livelihoods, so the potential benefits of farming system models are briefly reviewed here.

2.4.1 Whole farm and livelihoods models

Some models have been developed to simulate the operations across whole farms. These models capture the operational constraints of a farm and the behaviour of farmers (Lal, 1998). They can be used to simulate the response of the farm to different management strategies for a range of soil and climatic conditions.

The simplest types of whole-farm model are algorithmic models. This approach simulates the system based on the processes involved in the system but is only meaningful if the algorithm that is developed can capture the farmer's priorities and preferences sufficiently accurately (Lal, 1998).

An alternative category of whole-farm models use an object-oriented approach. The system is defined as a collection of objects which communicate with each other by passing and receiving events (Blaha and Rumbaugh, 2005). For example, the GPFARM model of Shaffer *et al.* (2000) includes a crop model as an object which calculates the crop yield and passes the information to the other parts of the model.

Some of the difficulties of building and using whole-farm models have been identified by Edwards-Jones *et al.* (1998), who linked CERES-Maize to a family decision-making model to represent a subsistence farming system. The principle difficulties were: *a*) an inability to make farming decisions during the season due to an inflexible crop model structure; *b*) identifying an appropriate scale for the analysis; *c*) identifying the drivers of household behaviour from the available socio-economic data; and, *d*) validating the model.

Linked ecological and economic models were developed by Shepherd and Soule (1998) to study the soil management strategies of three households with a range of resource endowments in Kenya. The richest household had the most productive and profitable farm and achieved a long-term increase in the soil fertility. The other households (representing 90 % of the population) had low productivity, were less profitable and had declining soil fertility. Their study had two principle drawbacks: *a*) variations in the annual rainfall, which are particularly important in semi-arid farming systems, were not simulated; and, *b*) the farmers were assumed to not adapt their management practices in any way throughout the simulation. Nevertheless, a similar study could make a valuable contribution to our understanding of Sahelian households if these drawbacks could be addressed.

Agent-based Models (ABMs) have been developed to simulate the interactions between human 'actors', and their relationships with biophysical systems, in an attempt to avoid the problem of having to define and parameterise particular household behavioural trends (Parker *et al.*, 2003). The People and Landscape

Model (PALM) is a recent example that has been developed to simulate a number of interacting households which own arable fields and livestock (Matthews, 2006). Each household is an independent agent with stores of food, cash, fertiliser, fodder, seed, labour, manure, milk and meat. The DSSAT crop models are integrated into the model to simulate crop yields. The model has been used to examine the behaviour of rural households in Nepal.

ABMs are complex, heavily parameterised and limited by the rules set by the model designers. However, this type of model might be invaluable in the future to understand how households might adapt to changing environments caused by climate change.

2.4.2 Linear programming models

Linear programming is a modelling tool that can be used to select the best approach from a number of alternative courses of action. For example, linear programming has been used to find the optimum crop mix for a farmer with several fields of limited size who has a limited amount of water for irrigation (Sowell and Ward, 1998). A government might use a linear programming model to identify the optimum approach to maximising crop production within a region. Most investigations, however, are at the farm scale and aim to maximise the profit from the farm.

The output of a crop model can be used to produce relationships between the climate, inputs and achieved yields. These relationships can then be used more widely to examine the optimal agricultural practices within a region. For example, van Keulen and Veeneklaas (1993) used an interactive multiple goal linear programming (IMGLP) model to identify the optimal land use in the Fifth Region of Mali. A number of regional constraints were placed, including the maximum livestock level, the maximum regional grain deficit, the maximum monetary agricultural inputs and the potential emigration rate in times of drought. The model calculated the maximum regional gross revenue within these constraints. While it was generally possible for the region to be self-sufficient for food, it was concluded that arable farming was not an economically-attractive activity and that farming system intensification would not be economically viable under the prevailing socio-economic conditions. Pastoral activities coupled with food imports produced the highest income. If more conservative constraints were chosen to make the region more self-sufficient, then crop production was increased but income decreased substantially.

Barbier (1998) used a linear programming model of a rural village in Mali to examine the causes of agricultural land degradation. A similar model was later used to characterise five contrasting farming systems in the country (Barbier and Carpentier, 2000).

Linear programming models offer a less complex economic framework than ABMs for investigating the likely behaviour of smallholders. Integrating a crop model with a linear programming model could create a powerful tool for understanding adaptation to climate change in the future.

2.5 Climate models

Climate models simulate the interactions of the atmosphere, oceans and land surface. They were originally developed from weather prediction models to produce long-term climate projections. The most common type of climate model is the general circulation model (GCM), which is a four-dimensional model of the entire globe. In Africa, weather GCMs are used for weather prediction and to produce seasonal forecasts while lower-resolution climate models are used to better understand regional climatic variations and to assess the likely regional impacts of climate change. In this study, data from a weather hindcasting model were used to fill in gaps in the observed meteorological dataset and data from climate models were used to produce meteorological datasets for the twenty-first century. Both types of model are reviewed below.

2.5.1 GCMs for weather hindcasting

The NCEP/NCAR reanalysis model (Kalnay *et al.*, 1996) is a "hindcasting" GCM, meaning that it uses weather observations from each day, from around the world, to accurately simulate the state of the global weather system on that day using series of short initial-value simulations. An alternative reanalysis model called ERA-40 has been produced by the ECMWF (Uppala *et al.*, 2005). Hindcasting models assimilate a wide range of meteorological observations from across the planet and dynamically fill gaps in the dataset. Although model simulations are not accurate enough to replace observed data, they can be used to fill gaps in the observed record. The quality of the generated data is tested at source. Spatial trends are averaged over large regions so can be more representative than synoptic weather stations which show a snapshot of the local area.

GCMs tend to perform better at mid-latitudes than in the tropics because many of the model components were designed and calibrated for these latitudes (most models were originally designed for weather prediction at mid-latitudes). The relative scarcity of data and the low density of synoptic weather stations in Africa also reduces the quality of calculations on that continent (Tompkins *et al.*, 2005; Washington *et al.*, 2004). In general, hindcasting models produce reasonable estimates of the annual temperature, humidity, wind and radiation trends, but simulate rainfall poorly. Data from the NCEP/NCAR reanalysis model (Kalnay *et al.*, 1996) are compared with observations from Senegalese synoptic weather stations in Chapter 5.

2.5.2 GCMs for climate change

More than 20 GCMs have contributed simulations to the IPCC Fourth Assessment Report (IPCC, 2010) for the SRES range of scenarios (IPCC, 2000). The GCMs have good agreement in some areas of the globe, for example the Mediterranean basin, but poor agreement in others (Christensen *et al.*, 2007). There is little agreement about how climate change will affect Sahelian precipitation. d'Orgeval *et al.* (2006) identified the primary driver of the precipitation discrepancies to be differences in the pattern of sea surface temperature estimations between GCMs. Uncertainties arising from land surface schemes also contributed. Cook and Vizy (2006) examined the twentieth-century projections of 18 GCMs and, using their criteria, identified only four with moderately realistic rainfall variations in the Sahel region. It seems necessary to evaluate the quality of the climate data produced by GCMs before using it for modelling.

The ENSEMBLES project was set up to produce probabilistic estimates of climatic risk by integrating the results of GCMs (van der Linden, 2009). It has also developed impact models (for water, crops and health) and has integrated these into the climate projection system to produce probabilistic estimates of future climate change impacts. Nine crop and vegetation models have been involved in the study, including GLAM and CERES. The crop models in this project have limited geographical scope - there is no worldwide model for all crops that can be fully integrated with the climate models.

All GCMs now include SVAT (soil-vegetation-atmosphere) sub-models. These are conceptually similar to a crop model but simulate a wide variety of ecosystems and feedback ecosystem changes to the atmosphere. Osborne *et al.* (2007) has incorporated the GLAM crop model into the SVAT scheme of the HadAM3 climate model. The coupled model simulates the growth of a summer crop in an attempt to produce a more realistic surface energy balance and atmospheric projection in the model. It is likely that more comprehensive coupled crop—climate models will be developed in the future.

In summary, there are substantial discrepancies between climate model projections for the Sahelian area. The fact that only four out of 18 models simulate an accurate seasonal rainfall distribution for West Africa shows that technical improvements to the models are required and suggests that the climate projections from all models should be treated with caution. The impact of climate model data discrepancies can be better understood by performing crop model impact studies using climate data from several models.

2.6 Summary

A number of crop models have been developed that can simulate the cultivation of pearl millet. A review of these models concluded that plant development and the soil water balance are simulated with a similar level of complexity by all of the models but that the treatment of plant growth, grain yields and particularly leaf expansion differ substantially. Most of the models were designed to simulate temperate crops in rich soils at mid to high latitudes, and it is necessary to evaluate the models against field data before using them to simulate tropical crops in sandy soils at low latitudes.

The suitability of the crop models to be used in this study was assessed against the requirements of the study. Drawbacks were identified with all of the models and it was concluded that the best approach would be to create a new model that was specifically designed to fulfil the research aims of the study. The new model is described in Chapter 3.

The literature was reviewed to identify how crop models have been used to identify the most appropriate planting dates, planting densities and nutrient management strategies for millet and other crops in dryland regions. These analyses have been limited to a small number of sites in Africa, India and Australia. Few studies have examined all three of these aspects of crop management using a consistent model and climatic dataset and none have examined agriculture in Senegal.

Climate change is expected to adversely affect agriculture across Senegal and semi-arid dryland regions are considered to be at particular risk. Most climate change studies have been global in nature and have not examined pearl millet. Two recent studies have examined the prospects for growing millet in West Africa and have concluded that grain yields will increase initially before decreasing later in the century, but both studies are likely to have overestimated the crop yields and neither examined whether the yield variability is likely to change in the future. No studies have examined the potential for farming system adaptation to reduce the impact of climate change on millet cultivation in Africa.

There are a number of uncertainties about the response of crops to high temperatures and to an increased atmospheric CO_2 concentration. There is further uncertainty about the ability of current crop models to simulate the effects of climate change because the models would be operating outside of the environment used for their evaluation and because a number of the potential influences of climate change are not simulated in current crop models. Further experimental research in particular is required to resolve these uncertainties. In the meantime, it is necessary for crop modellers to use sensitivity studies to examine the range of alternatives that is created by the uncertainty.

There are further concerns about the quality of climate projections from climate models since few models simulate an accurate rainfall distribution for West Africa. The impact of the climate model data discrepancies can be characterised by performing crop model impact studies using climate data from several models. This approach was adopted by this study.

Chapter 3

The CROMSAS Model

This chapter describes the design of the new crop model. Section 3.1 describes the characteristics of pearl millet. An overview of the crop model design is presented in Section 3.2. The remaining sections describe the various parts of the model. The calibration and evaluation of the model are the subject of Chapter 4.

3.1 Pearl millet

Pearl millet is an annual crop that is cultivated predominantly in tropical environments (Pearson, 1984). Short-duration millets (*Pennisetum americanum*, also termed *P. glaucum* and *P. typhoides*) are not strongly sensitive to daylight. Long-duration millets (*Pennisetum maiwa*) are strongly daylength-sensitive and, in the Sahel, are grown at lower latitudes than short-duration millets where the wet season is relatively longer. Millets hybridise readily and form stable intermediaries so the classification is not straightforward; one survey in West and Central Africa found 269 different varieties in cultivation by farmers (Haussmann *et al.*, 2006). Figure 3.1 shows two crops of millet at different stages of development.

Millet is the best-adapted grain cereal to hot, dry environments. Bidinger *et al.* (1982) identify four particular features of millet that make it suitable for such environments:

1. the plant maximises soil water use by having short stages of development

(a) Young millet (b) Mature millet

Figure 3.1: Photographs of young and mature millet plants in Niger. The young plants are short-duration varieties growing at the ICRISAT agricultural research station at Sadoré, Niger, while the maturing plants are long-duration varieties growing on an irrigated plot beside the Niger river. The photographs are the property of the author.

and by having the capacity for high growth rates under favourable conditions;

2. a quick recovery following a period of stress allows the crop to thrive when growing conditions change intermittently;

3. by having effective control of water loss, the plant is more efficient than other crops in a high temperature, high radiation, low humidity environment; and,

4. plants are hardy and can survive periods of severe drought by suspending development and through an unusual tolerance for heat stress.

The most evident differences between varieties are the rate of development and the photoperiodic sensitivity (Carberry and Campbell, 1985; Craufurd and Bidinger, 1988b). Partitioning to the plant organs can also vary; for example, some varieties of millet partition more assimilate to the roots and less to the leaves than others (Bruck *et al.*, 2003b), which increases the drought tolerance by allowing plants to exploit deeper water reserves but at the expense of a slower growth rate and a lower yield (Gregory, 1982). Many modern cultivars of cereals have been bred to partition a greater proportion of the assimilate to the reproductive organs to boost the harvest index (Ritchie *et al.*, 1998). African varieties tend to produce fewer tillers but larger main stem panicles than Indian varieties (Craufurd and Bidinger, 1988a). Some varieties are particularly drought-tolerant (Bidinger *et al.*, 1982), although the underlying physiological differences between varieties are difficult to identify. At harvest, most smallholders select the plants whose characteristics best meet the household requirements and save the seed for planting in the following year (Mortimore and Adams, 1999).

A series of parameters are used in CROMSAS to represent the characteristics of different varieties of millet. There are parameters throughout the model to simulate variations in the phenological development, growth rate, leaf extension, tiller development and the response to water and temperature stress.

3.2 Overview of the CROMSAS model design

Reviews of crop modelling have recommended that models should be as simple as possible (e.g. Passioura, 1996), with authors striving to find an appropriate balance between model simplicity and the complexity of the crop—soil system being simulated (Monteith, 1996). Sinclair and Seligman (1996) suggest several guidelines for developing functional models: *a*) the objectives of the model need to be clearly defined; *b*) the criteria for judging the acceptability of the model should depend on the model objectives; *c*) the process is likely to be more successful if the approach is not prejudiced by relying on existing models; *d*) the model structure should be determined from the organisational level of the problem (for example, there is little benefit from modelling individual tissues when the aim is to simulate the overall crop yield because the extra simulations are not likely to improve the performance of the model); and, *e*) summary models of emergent properties (for example, exponential radiation interception or radiation use efficiency) should be used wherever appropriate. Similarly, Challinor *et al.* (2009) recommends that large-area crop models should have a basis in observed relationships, should have an appropriate level of complexity and should, where possible, use parameters based on observations.

The new model, called CROMSAS (Crop Model for Sahelian Adaptation Studies), has been designed using these guidelines. It is composed of a series of differential equations (model structures) that are solved using the Euler forward difference method (Wallach, 2006a) with a daily timestep. It has been designed with a similar overall structure to the models reviewed in Section 2.1.1 with the final yield calculated as a function of the growth and development of the crop.

The GLAM model (Challinor *et al.*, 2004) was used as a template for CROMSAS. Figure 3.2a is a diagram of the resource flows in CROMSAS. Nitrogen and water flows between the atmosphere, soil and plant are simulated. Figure 3.2b shows the daily calculation that is performed by CROMSAS. The production of assimilate is calculated from the radiation interception, temperature, humidity, water uptake and plant nitrogen content. Assimilate is partitioned to the roots, leaves, stem, reproductive organs and grain according to the plant development stage, demand from the organs and the influence of water and nitrogen stress. Using the approach of Monteith *et al.* (1989), the growth of each organ is simulated as a function of the partitioned assimilate so that resource flows are conserved through the model. The daily calculation is completed with simulations of leaf senescence and plant death.

3.2.1 Modelling varying planting densities, nitrogen application, and intercropping

An important requirement for CROMSAS was the capability to model the impact of varying plant densities. At low densities, the plant physiological indicators (e.g. leaf area, root density and stem height) are directly proportional to the plant density, but at high densities there is competition for resources between plants and the average plant size tends to reduce (Carberry and Campbell, 1985). Two

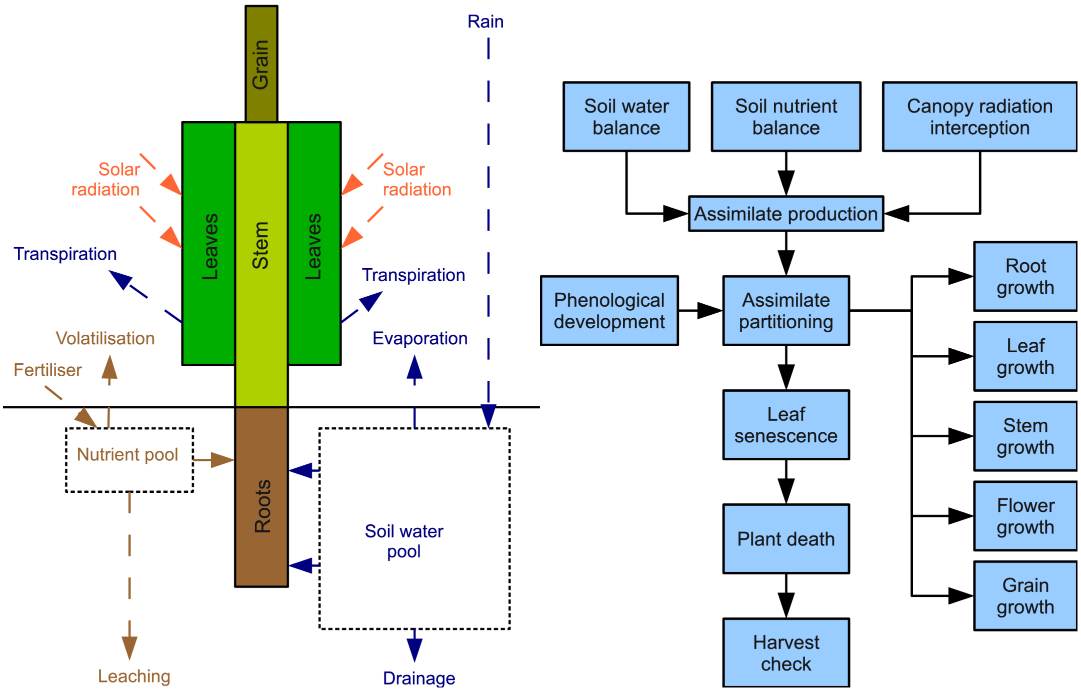

(a) Model resource flows (b) Calculation flowchart

Figure 3.2: Schematic diagrams of the CROMSAS model processes. The first diagram displays the flows of resources (solar radiation, water and nutrients) between the soil, plant and atmosphere. The second diagram shows the crop growth calculations for a single day.

approaches were considered to simulate the plant density in CROMSAS. The first, used by APSIM and DSSAT, simulates a typical individual plant in the field. Partitioning and organ growth are simulated for this typical plant and then up-scaled to the whole crop. The second approach, which is used by STICS, simulates an empirical leaf area function for the crop that is independent of the partitioning. The maximum leaf area is calculated as a function of the plant density and then reduced during crop growth if there is water or nitrogen stress (Brisson *et al.*, 1998). The typical plant method has the advantage that the crop growth depends on the physiological limits of the local environment rather than being set as a parameter by the modeller. The empirical method has the advantage of being less complicated. Since there were no experimental data to calculate the maximum leaf area as a function of the plant density, the typical plant method was adopted in CROMSAS.

Modelling both the overall crop and a typical plant of the crop required numerous changes to GLAM. The growth rate was calculated for the whole crop and the assimilate was then equally divided between the plants. The partitioning of biomass to the roots, leaves, stem and grain was simulated for the typical plant then aggregated for the whole crop.

It was assumed that the plant density was high enough and the field was large enough for any field boundary effects to be insignificant. In reality, crop canopies are not uniform and the radiation interception of lower leaves increases at low plant densities (Matthews, 2002). The canopy is also affected by the distribution of the plants in the field, otherwise known as the rectangularity (the ratio of inter-row to between-row spacing). As the planting density is increased, shading reduces both the photosynthetic energy available to each plant and the red/far-red (R/FR) ratio of the light reaching the lower canopy. Experiments under controlled conditions have shown that a reduction in either of these reduces tillering (Casal *et al.*, 1986). Tillering can therefore be promoted in a crop by altering the planting pattern to increase the R/FR ratio, for example by increasing the rectangularity. Another method that is particularly common in the Sahel is to decrease the hill density but to increase the number of plants in each hill.

In CROMSAS, the influence of rectangularity on tillering is not directly simulated because: *a*) the development of such a mechanism would exceed the complexity of the rest of the model; *b*) supporting experimental studies were not available; and, *c*) the Souna variety is low-tillering. Rectangularity is simulated in two other parts of the model. Firstly, the light extinction coefficient, k_c (see Section 3.4.5), can be varied with the row spacing. In APSIM, using data for an Indian variety, k_c is reduced from 0.79 to 0.37 as the row spacing is increased from 20 cm to 150 cm. In Africa, Azam-Ali *et al.* (1984b) cultivated millet at three planting densities in Niger but there was no clear relationship between the planting density and k_c, possibly because the narrow-spaced crop was water-stressed from an early stage. Secondly, the water and nitrogen uptake can be restricted in the early growth stages as the model can simulate the area around each stand that is tapped as a function of the plant root length, representing the observation that there can be large gaps between plants where resources are not tapped in the early stages (Azam-Ali *et al.*, 1984a). If this mechanism is used then crops with several plants on each stand will have access to fewer resources in the early stages than crops planted homogeneously across the field.

A second requirement, little explored in this study, was to model several crops co-existing in a single field. Smallholders, particularly in the western Sahel, often plant several species in a single field, at different times, with the aim of maximising the productivity of the field and reducing the risk of losing the entire crop. Cereals and leguminous crops are often planted together (Mortimore and Adams, 1999). In CROMSAS, intercropping is simulated by calculating the total field radiation interception, water and nitrogen use of all of the crops and then splitting these between each crop according to the individual leaf interception and the crop root densities. The intercropping routines are also used to simulate tillers with each stem being quasi-independent but sharing a common root system. The impact of weeds can be quantified by modelling the weeds as one or more co-existing crops.

The model was designed to allow several fields to be simulated concurrently, so that the management decisions of smallholders that own several fields could be simulated throughout the season. It is flexible enough to be used within a broad farming system framework such as those described in Section 2.4.

3.2.2 Parameterising the model

Parameters are required throughout the model. These were mostly obtained from the literature using the results of agricultural experiments that have been performed in glasshouses and at agricultural research stations. The wide range of experiments have aimed, for example, to better understand the response of crops to temperature (e.g. Ong, 1983a), radiation (e.g. Squire *et al.*, 1984) and water stress (e.g. Black and Ong, 2000), and to understand the impact of changing the crop management regime (e.g. Azam-Ali *et al.*, 1984b; Hafner *et al.*, 1993). During this study, it became clear that many of the agricultural studies that have been performed at the Bambey research station have only been reported in French ‘grey literature’ and are not available in international peer-reviewed journals. Boulier and Jouve (1990) summarise some of these studies.

A number of nutrient balance studies have been performed in farmers' fields away from research stations (e.g. Harris, 2002). Surprisingly few studies have examined the impact of rainfall variability on the crop yields of farmers' fields (the ESPACE project (Affholder, 1992) is a notable large-scale exception whose results were analysed in Chapter 1).

Some of the parameters that were taken from the literature are discussed in the appropriate sections of this chapter. Others were calibrated using the results of an experiment in Senegal and these are discussed in Chapter 4.

3.3 Plant development

The development of a plant refers to the phenological development of the crop from germination to flowering, grain-filling and harvest. Different plant organs tend to grow at different stages of development. The development of millet can be split into three broad growth stages (Ong and Monteith, 1985).

3.3.1 GS1: vegetative growth

Millet seeds germinate when there is sufficient soil moisture. The time between germination and plant emergence is temperature-dependent (Pearson, 1975).

Development of the plant during GS1 is relatively insensitive to temperatures between 20 °C and 30 °C but can be substantially longer outside of this range. There is substantial variability between varieties; for example, GS1 of the BK560 variety lasts for 17 days (Ong, 1983a) while the Serere 10 B variety reaches panicle initiation after 23 days (University of Nottingham, 1984). Millet is photoperiod-sensitive and the time to flowering is extended, sometimes substantially, if the daylength exceeds 12 hours (Ong and Everard, 1979). Photoperiodic behaviour can be a useful trait for a farmer; for example, in the variable Sahelian rainfall climate, photoperiodic strains will not flower until late in the season when the rainfall variability tends to reduce (Vaksmann *et al.*, 2008).

The cumulative temperature—photoperiod influence can be complex. For example, Table 3.1 shows how temperature and photoperiod affects the development of the Serere 10 B variety, which is an improved variety of Souna. Temperature

Daylength (h)	Temperature (°C)				
	20	23	26	29	32
10	23	23	23	22	23
12	23	23	23	23	23
14	26	26	26	26	41
16	34	27	26	26	41
18	34	34	30	30	42

Table 3.1: Number of days between germination and panicle initiation for millet variety Serere 10 B for a range of temperatures and daylengths (University of Nottingham, 1984).

only influenced development when the daylength exceeded 12 hours. Varying but similarly complex behaviour was found in several other varieties (University of Nottingham, 1984). No studies were found which examined the interaction of temperature and photoperiod at higher average temperatures than 32 °C.

Studies have shown that many plant processes are temperature-dependent and the concept of thermal time, which is the total number of degrees 'accumulated' by the plant above a base temperature since germination, has been developed to measure the development of plants and plant organs (Ong and Monteith, 1985). For millet, the base temperature for many processes is between 10 °C and 12 °C. The thermal time is measured in degree days (°C d). The optimum temperature for crop development generally lies in the range 25 °C to 30 °C for temperate crops and 30 °C to 35 °C for tropical crops.

In CROMSAS, GS1 is split into three stages. The first stage, from germination to emergence, lasts for a fixed period of thermal time. The second stage is the juvenile phase. In most models, including APSIM and CERES, it is also simulated using thermal time, despite the insensitivity of some varieties of juvenile millet to temperature such as that demonstrated in Table 3.1. Using a thermal time relationship would cause the simulated duration of GS1 of Serere 10 B to reach a minimum at 32 °C, which is clearly inconsistent with the findings of the experiment. In CROMSAS, this stage lasts for a fixed number of days instead.

The third stage in CROMSAS is a photoperiod-sensitive phase that, in common with other models, depends upon both thermal time and the daylength.

For the first and third stages, the amount of thermal time accrued each day, t_{tt}, is a maximum at an optimum temperature T_o and zero below a base temperature T_b or above a maximum temperature T_m:

$$t_{tt} = \begin{cases} 0 & T \leq T_b, \quad T \geq T_m \\ T - T_b & T_b < T \leq T_o \\ T_o - (T_o - T_b)\left(\dfrac{T - T_o}{T_m - T_o}\right) & T_o < T < T_m \end{cases} \tag{3.1}$$

The plant temperature, T, is estimated by averaging the daily air temperatures T_{max} and T_{min}. The base, optimum and maximum temperatures are set to 12 °C, 33 °C and 47 °C, respectively (e.g. Ong, 1983a,b; Squire, 1989; Squire *et al.*, 1984).

For the third stage, the sensitivity to photoperiod is simulated using the same method as the CropSyst model (Stöckle *et al.*, 2003) with the length of the stage being extended by a factor p_{sens}. For short-day crops, the calculation is:

$$p_{sens} = \frac{dl_{ins} - dl}{dl_{ins} - dl_{crit}} \tag{3.2}$$

$$tt_{boundary} = tt_{boundary} + t_{tt}\left(1 - p_{sens}\right) \tag{3.3}$$

dl is the daylength, dl_{crit} is the critical daylength below which the rate of development is maximised and dl_{ins} is the insensitive daylength above which development stalls. For long-day crops, when the critical daylength exceeds the insensitive daylength, p_{sens} is calculated using:

$$p_{sens} = \frac{dl - dl_{ins}}{dl_{crit} - dl_{ins}} \tag{3.4}$$

For the Souna variety, the thermal time to emergence is set to 50 °C d. The juvenile daylength is set to 17 days. For the third stage, the thermal time is set to 80 °C d, the critical daylength $dl_{crit} = 12$ h and the insensitive daylength $dl_{ins} = 14$ h. For the normal temperatures and daylength of the monsoon season in Senegal, these parameters cause GS1 to have a duration of 23 days, similar to the Serere 10 B variety (Table 3.1) and other improved 90-day Souna varieties.

3.3.2 GS2: reproductive initiation to flowering

GS2 commences at panicle initiation, the time when the plant begins to produce reproductive instead of vegetative primordia. The existing vegetative organs continue to grow during this period. The length of GS2 is strongly temperature-dependent with an optimum temperature of 33 ℃; Ong and Monteith (1985) observed crops at 19 ℃ spending twice as long in GS2 as crops at 31 ℃. In CROMSAS, GS2 is simulated using two stages. The first is from panicle initiation to the start of flowering and the second is from the start to the end of flowering. The duration of both stages is calculated using thermal time. Flowering and the production of grain sinks are simulated in the second stage. The total length of GS2 for Souna is 650 ℃ d.

3.3.3 GS3: grain filling

GS3 is dominated by grain filling and the grain yield of the plant depends on the duration of this period and the daily growth rate of the grains (Bieler *et al.*, 1993). The duration of the final stage is also strongly temperature-dependent (Ong, 1983b). In CROMSAS, GS3 is simulated using a single stage with the duration calculated using thermal time. The total length of GS3 for Souna is 600 ℃ d.

3.3.4 Impact of water and nutrient stress on development

The overall rate of development of some crops is slowed if the crop suffers water stress but millet development is only slowed by extreme water stress (Ritchie and Alagarswamy, 1989b). Mild water stress can actually increase the rate of development as a result of the plant temperature increasing.

In CROMSAS, water and nutrient stress are assumed to not affect the rate of development of the crop.

3.4 Plant growth

The growth of a plant refers to the actual growth rate of the organs, so the plant growth rate determines the final size of the plant. Plants grow by converting atmospheric CO_2 and minerals into carbohydrates in leaves, a photosynthetic reaction that is driven by the interception of solar radiation (Ong and Monteith, 1985). So for many plants, the growth rate is proportional to the amount of radiation that the plant is able to intercept.

Water is used to transport mineral nutrients around the plant, as both a solvent and a reactant in the photosynthesis reaction, and as a coolant for the plant as it evaporates through the leaf stomata in a process called transpiration (Ehlers and Goss, 2003). If insufficient water is available to the leaves then the photosynthesis reaction rate reduces and plant growth is impaired. Many nutrients are also required for plant growth and shortages of any will also cause plant growth to be impaired. The most important nutrients, in terms of the quantity required by plants, are nitrogen (N), phosphorus (P) and potassium (K). Plants develop root systems to extract water and nutrients from the soil.

Soil water originates as rainfall or through irrigation schemes. Nutrients are released by the decomposition of organic residue within the soil or are added through the application of mineral fertiliser or manure. The interactions between soil water and nutrients can be complicated. If there are insufficient quantities of either then growth will be impeded (Bacci *et al.*, 1999). A greenhouse study by Ashraf *et al.* (2001) recorded a further reduction in the millet yield when high doses of N were applied to plants suffering severe water stress. This phenomenon has been recorded in field studies where a crop with plentiful nutrients transpired more water than a crop in a more infertile field which caused severe water stress during grain filling, reducing the final yield (e.g. Affholder, 1995). The timing of any droughts strongly influences the final yield; in a study of 25 varieties of millet in India, grain yields were reduced by up to 33 % due to drought in GS2 but the impact of drought in GS3 was much greater with 50 %–75 % reductions in the yield (Bidinger *et al.*, 1982). The availability and uptake of N can be affected by the weather because poor rainfall restricts uptake and reduces the rate of N mineralisation, while too much rainfall removes N through leaching and denitrification (Sivakumar and Glinni, 2002).

Photosynthesis and plant growth are affected by other factors in addition to water and nutrient stress. The photosynthesis reaction rate of millet reduces substantially if the plant temperature is reduced below 24 ℃ (Pearson and Derrick, 1977). The reaction rate peaks at leaf temperatures of 30 ℃ to 35 ℃ (McPherson and Slatyer, 1973) but is balanced at high temperatures by losses through respiration which increase almost linearly with temperature. The net result of these two processes is a relatively constant plant growth rate between 22 ℃ and 36 ℃ (Maracchi *et al.*, 1993), with the growth rate reducing outside of this range.

This section explains how plant growth is simulated in CROMSAS.

3.4.1 Transpiration use efficiency (TUE)

GLAM calculates the daily crop growth as a function of the transpiration rate and the vapour pressure deficit (VPD), following the approach of Bierhuizen and Slatyer (1965) and Sinclair *et al.* (1984):

$$\frac{\partial W_{trans}}{\partial t} = T_{Tmax} \min\left(\frac{TE}{e_o^s - e_o}, TE_{max}\right) \tag{3.5}$$

T_{Tmax} is the maximum transpiration rate, TE is the transpiration efficiency (the biomass increase per unit of transpired water), and $e_o^s - e_o$ is the VPD. TE_{max} is a threshold which limits the transpiration rate on days when the VPD is very low. The growth rate is reduced in Equation 3.14 if the actual transpiration rate is lower that the potential transpiration rate.

3.4.2 Radiation use efficiency (RUE)

Monteith (1977) established, for temperate climates, that the daily crop growth is proportional to the interception of radiation. The conversion of radiation into dry matter was calculated by Monteith (1972) as the product of seven factors. Begue *et al.* (1991) simplified these to produce:

$$\frac{\partial W_{rad}}{\partial t} = \epsilon_c \epsilon_a \epsilon_s R_{dsw} \tag{3.6}$$

R_{dsw} is the incident downward shortwave radiation at the top of the canopy ($\mathrm{MW\,m^{-2}\,d^{-1}}$). ϵ_a is the fraction of the photosynthetically-active radiation (PAR, 400 nm–700 nm) that is absorbed by the crop. ϵ_s, the climatic efficiency, is the ratio of PAR to total radiation. ϵ_c, the conversion efficiency, is the ratio of crop growth to PAR ($\mathrm{g\,MJ^{-1}}$).

The climatic efficiency is relatively constant throughout the year; for example, in Niger during one rainy season it varied between 0.44 and 0.48 (Begue *et al.*, 1991). CROMSAS uses the mean experimental measurement from Begue *et al.* (1991) of $\epsilon_s = 0.466$.

In the absence of plant stress, the conversion efficiency is typically $1.5\,\mathrm{g\,MJ^{-1}}$ to $1.7\,\mathrm{g\,MJ^{-1}}$ for tropical C_3 plants (e.g. groundnut) and up to $2.5\,\mathrm{g\,MJ^{-1}}$ for C_4 plants (e.g. millet) (Black and Ong, 2000).

The growth rate is reduced in extreme temperatures. The average daytime temperature is estimated using the same method as CERES Ritchie and Alagarswamy (1989c):

$$T_{avday} = 0.25T_{min} + 0.75T_{max} \tag{3.7}$$

and the impact on growth is simulated using a user-supplied broken-linear function with growth reducing when T_{avday} is lower than 20 °C or higher than 35 °C.

3.4.3 Calculating the daily crop growth rate

Some studies have argued that plant growth is primarily limited by RUE (e.g. Arkebauer *et al.*, 1994; Azam-Ali *et al.*, 1989; Monteith, 1994) while others have argued that TUE is limiting (e.g. Azam-Ali *et al.*, 1984b; Demetriades-Shah *et al.*, 1992). Other studies have concluded that RUE is limiting for some crops and TUE for others (e.g. Cisse and Vachaud, 1988). The most appropriate approach is to simulate the daily crop growth as the minimum of the two methods:

$$\frac{\partial W_{pot}}{\partial t} = \min\left(\frac{\partial W_{trans}}{\partial t}, \frac{\partial W_{rad}}{\partial t}\right) \tag{3.8}$$

The PARCH (Stephens and Hess, 1999), CropSyst (Stöckle *et al.*, 2003) and APSIM (Keating *et al.*, 2003) models all use this approach. Section 2.1.1 explains why it is the most appropriate for models that are used to simulate the impacts of climate change.

3.4.4 Modelling rising carbon dioxide

Carbon fertilisation is expected to increase the yields and reduce the water use of some crops as the atmospheric CO_2 concentration increases. Field studies have identified the photosynthetic pathway, species, radiation intensity, growth stage and management regime (e.g. irrigation and nitrogen application) as factors which determine the magnitude of the fertilisation effect (Ainsworth and Long, 2005; Jablonski *et al.*, 2002; Kimball *et al.*, 2002; Norby *et al.*, 2003).

Early crop modelling studies simulated the impact of carbon fertilisation by applying coefficients to increase the daily crop biomass production and to decrease the transpiration rate (Ritchie and Alagarswamy, 2002). A similar approach is adopted in CROMSAS, except that the coefficients are instead applied to the RUE and TUE constants, ϵ_c in Equation 3.6 and TE in Equation 3.5), so that the impact of water and nitrogen stress can be properly assessed. The two coefficients are interpolated from broken-linear functions supplied by the user. The parameters for these coefficients are discussed in Section 7.2.1.

3.4.5 Canopy radiation interception by a single crop

Following the approach of Monteith (1972) and the experimental results of Squire *et al.* (1984), the radiation is assumed to decay exponentially through the canopy as a function of the leaf area index, L (the leaf area index (LAI) is the dimensionless ratio of the total upper leaf surface of the crop divided by the surface area of the field) and an extinction coefficient, k_c, which represents the efficiency of the leaves at absorbing radiation:

$$\epsilon_a = 1 - e^{-k_c L} \tag{3.9}$$

The efficiency of the leaves depends on many factors including the solar zenith angle, the fraction of diffuse radiation, the geometry and optical properties of the leaves, and the topography of the field (Begue *et al.*, 1991). Most of these factors vary as the plant develops so the extinction coefficient is unlikely to be constant throughout growth. For example, as leaves thicken over time they will intercept radiation more effectively, but this will be reversed when senescence commences and dying leaves intercept but do not absorb radiation.

Photosynthetically-active radiation (PAR) is more efficiently absorbed by leaves than the rest of the radiation spectrum. This phenomenon is particularly important for intercrops because the taller crop will absorb a greater fraction of the PAR than of the whole spectrum. Marshall and Willey (1983) describe the difference between the absorption of PAR and of total radiation in terms of a relationship between the extinction coefficients:

$$k_{c\_par} = 1.4k_c \tag{3.10}$$

They concluded that this relationship was independent of the canopy structure for millet. In CROMSAS, the PAR and radiation absorption calculations are performed separately for each crop. The PAR extinction coefficient is calculated using Equation 3.10.

3.4.6 Canopy radiation interception by multiple crops

Equation 3.9 is suitable for single crops but must be adapted for situations where more than one crop is growing in a field. Tsubo *et al.* (2005) have adapted this equation for two crops in the same field and a generalisation of their approach to simulate any number of crops was developed for CROMSAS.

The canopy is split into 1 cm thick layers. The radiation absorption in layer i (where $i = 1$ is adjacent to the ground), denoted ϵ_{ai}, is calculated using:

$$\epsilon_{ai} = \left(1 - \sum_{j=i+1}^{n} \epsilon_{aj}\right)\left(1 - e^{-\sum_{k=1}^{m} k_{ck} L_{ki}}\right) \tag{3.11}$$

where there are m crops in the field and L_{ki} is the leaf area of crop k in layer i. The first part of the equation calculates the fraction of the incident radiation at the top of the canopy which reaches the top of layer i. The second part is a generalisation of Equation 3.9 for several adjacent crops.

The total radiation absorption in the layer must then be split between each crop. For crop l in layer i, the total absorption is:

$$\epsilon_{ail} = \left(\frac{k_{cl} L_l}{\sum_{k=1}^{m} k_{ck} L_k}\right)\epsilon_{ai} \tag{3.12}$$

The total radiation absorption by each crop is then found by summing the absorption over all of the layers:

$$\epsilon_a = \sum_{j=1}^{n} \epsilon_{ajl} \tag{3.13}$$

This method is appropriate if the assumption that radiation decays exponentially through the canopy is reasonable and if the vertical leaf distribution of each crop is represented accurately. More complicated models have been proposed which calculate the radiation absorption from multiple crops as a function of the geometry of the plants and the field (e.g. Brisson *et al.*, 2004). There were neither field data to drive more complex approaches nor evidence from field studies that they would be more accurate in the Sahel, so it was concluded that a more complex approach would not improve the quality of the crop model simulations.

3.4.7 Water and nitrogen stress

The impact of water stress is simulated by reducing the daily crop growth:

$$\frac{\partial W}{\partial t} = \frac{T_T\left(t\right)}{T_{Tmax}\left(t\right)} \frac{\partial W_{pot}}{\partial t} \tag{3.14}$$

where T_T is the transpiration rate.

A similar approach is used by Gastal and Lemaire (2002) to simulate the impact of nitrogen stress on plant growth:

$$\frac{\partial W}{\partial t} = \frac{N_{cont}\left(t\right)}{N_{crit}\left(t\right)} \frac{\partial W_{pot}}{\partial t} \tag{3.15}$$

where N_{cont} is the nitrogen content of the crop and N_{crit} is the critical nitrogen content of the crop. The critical nitrogen content is defined as the nitrogen level required for the maximum growth rate (Greenwood *et al.*, 1990) and is a function of both the type of plant (C_3 or C_4) and the development stage of the crop. The ratio of the content to the critical content is sometimes called the nitrogen nutrition index (NNI). The NNI varies between zero and one.

It is assumed that the nitrogen stress always exceeds the stress caused by shortages of other nutrients, so no other nutrients are simulated in CROMSAS.

Shortages of micronutrients should not affect growth because sufficient quantities are thought to be supplied by the Harmatten winds in the Sahel (Harris, 1995). However, Payne *et al.* (1996) concluded that phosphorus is the most limiting nutrient in parts of Niger, so it would be incorrect to assume that high yields could be continuously achieved with the application of nitrogen alone.

One of the decisions that was encountered during model development was how to combine Equations 3.14 and 3.15 to calculate the cumulative impact of water and nitrogen stress on assimilate production. Two methods were considered. The water stress and NNI ratios are calculated independently in the literature so the first method used the smallest value of the two, assuming that the nitrogen uptake and transport are independent of the water uptake:

$$\frac{\partial W}{\partial t} = \min\left(\frac{T_T(t)}{T_{Tmax}(t)}, \frac{N_{cont}(t)}{N_{crit}(t)}\right)\frac{\partial W_{pot}}{\partial t} \tag{3.16}$$

In the second method, the impact of the ratios is cumulative:

$$\frac{\partial W}{\partial t} = \left(\frac{T_T(t)}{T_{Tmax}(t)} \times \frac{N_{cont}(t)}{N_{crit}(t)}\right)\frac{\partial W_{pot}}{\partial t} \tag{3.17}$$

Payne *et al.* (1995) examined the relationship between nitrogen uptake and transpiration for millet grown in pots in Texas. The nitrogen uptake was proportional to the transpiration rate but twice as much nitrogen was taken up when the plant was water-stressed. This experiment was probably not representative of Sahelian conditions because a relatively large amount of mineral fertiliser was used. Under field conditions, the authors stressed that nitrogen is not normally so well correlated with transpiration and the availability of nitrogen varies with many environmental factors. No similar field studies were found for the Sahel.

In view of the uncertainty, it was decided to follow the approach of the STICS and SARRA-millet model models and simulate the compound impact of water and nitrogen stresses (Equation 3.17).

A further change was made to Equation 3.17 to allow the sensitivity of the assimilate production to water and nitrogen stress to be increased or decreased:

$$\frac{\partial W}{\partial t} = \left(\frac{T_T(t)}{T_{Tmax}(t)}\right)^{C_{sens\_T1}}\left(\frac{N_{cont}(t)}{N_{crit}(t)}\right)^{C_{sens\_N1}}\frac{\partial W_{pot}}{\partial t} \tag{3.18}$$

In common with other models, the coefficients C_{sens_T1} and C_{sens_N1} were set to 1 in this equation. Similar coefficients were used in the calculation of root and leaf growth, where the impact of the stress is not always proportional to the level of the stress.

3.5 Soil water balance

The basic approach of GLAM to simulating the soil water balance was used in CROMSAS at first but the calibration of the model against field data from the village of Sob in Senegal (see Section 4.1.1) led to almost every parameterisation being changed. The water balance routines were also revised to simulate the uptake of multiple crops in the field.

CROMSAS splits the soil into many horizontal layers, each of depth 1 cm. Water arrives at the surface through rainfall (or irrigation). Following any runoff losses, the water percolates through the soil. If the soil water capacity in any layer is exceeded then water will drain to the next layer. Any water draining from the deepest layer is assumed lost to deep drainage. Plants extract water from the soil each day for transpiration. Water is also lost by direct soil evaporation. The water balance module simulates all of these processes and provides the crop transpiration rate for the photosynthesis calculation.

Lateral movement of water across soil layers is not represented in CROMSAS. While the model simulations should be acceptable for flat fields, the accuracy will reduce on sloping fields where lateral movement becomes important (Matthews, 2002).

3.5.1 Runoff

Runoff is potentially very high in the Sahel because the storms produce high rainfall rates and, particularly at the start of the rainy seabn, because the soil can form an impermeable crust after sustained drying which impedes drainage into the soil. Estimating runoff for individual fields is further complicated by the widely varying topography of the fields which is difficult to measure accurately and describe succinctly.

GLAM estimates runoff using the US Soil Conservation Service method (Choudhury *et al.*, 1987; USDA-SCS, 1964):

$$R = \frac{P^2}{P + k_{sat}} \tag{3.19}$$

where R is the runoff, P is the rainfall and k_{sat} is the saturated hydraulic conductivity of the soil. k_{sat} is estimated using:

$$k_{sat} = K_{ks} \left(\frac{\theta_{sat} - \theta_{dul}}{\theta_{dul}} \right)^2 \tag{3.20}$$

where θ_{sat} is the saturated water content of the soil, θ_{dul} is the soil water capacity (the maximum water content with no drainage) and K_{ks} is an empirical constant. Since CROMSAS, unlike GLAM, simulates different soil water capacities in each layer, k_{sat} was calculated for each layer and an average of the top 5 layers was used in Equation 3.19.

Runoff from this method was almost negligible and was felt to be underestimated for the Sob fields at the start of the rainy season. One alternative scheme, suggested by an agronomist with experience of Senegal, assumed that 40 % of all rainfall above a threshold of 20 mm would be runoff. While this scheme produces high runoff on days with heavy rainfall, it does not account for the early season underestimation at Sob. There is much uncertainty over the magnitude of the runoff from individual fields so the influence on simulation results should be assessed using a sensitivity study.

3.5.2 Drainage

GLAM simulates soil water drainage through the soil using the ‘tipping bucket’ scheme of Suleiman and Ritchie (2004):

$$\frac{\partial \theta}{\partial t} = -FD \left(\theta_{sat} - \theta_{dul} \right) \tag{3.21}$$

FD is the drainage rate; D is the basic rate, an empirical constant, and F takes account of any water draining from the layer above:

$$F = \frac{\ln \left(\theta_{in} + 1 \right)}{\ln \left(k_{sat} + 1 \right)} \tag{3.22}$$

θ_{in} is either the drainage from the layer above or, for the top layer, the rainfall (minus runoff).

Suleiman and Ritchie (2004) tested this scheme in the DSSAT model and recorded an improvement in the simulations. However, comparisons of CROMSAS with the soil water content measurements from Sob suggested that this scheme simulated water draining too slowly which occasionally led to large water reservoirs in some layers. In reality, fields in Sob tend to fully drain within a few hours of rainfall and the soil water content is never significantly higher than the field capacity in any layer (Dr F. Affholder, pers. comm.). The preferred approach was to change the saturated hydraulic conductivity of the soil but this had little effect on F. Two other schemes were tried in CROMSAS. The first simply increased the drainage rate D by 30 % to increase the flow of water through the soil. The second assumed that the soil would drain completely after rainfall so that the soil water content at the end of each day would not exceed the soil capacity in any layer. After testing with the three Sob fields, it was concluded that the first alternative scheme, with a faster drainage rate, gave the best agreement with measurements.

3.5.3 Evapotranspiration

Water loss from the soil by evaporation and transpiration is limited by the energy absorbed by the soil and the crop, respectively. The maximum energy-limited loss is called the maximum evapotranspiration rate (ET_m). Since the ET_m varies between crops, a reference evapotranspiration rate (ET_o) has been defined for a mature grass crop and is calculated purely from meteorological data (Allen *et al.*, 1998). The ET_m is calculated from the ET_o using:

$$ET_m = c_{crop} ET_o \tag{3.23}$$

where c_{crop} is a crop-specific empirical coefficient.

In GLAM, the ET_o is calculated from meteorological data and there is no crop coefficient (i.e. $c_{crop} = 1$). The GLAM parameterisation underestimated ET_m at Sob by around 50 % which led to poor simulations of water loss and crop yield.

Chapter 5 examines the most appropriate method to calculate ET_o in Senegal. CROMSAS can calculate ET_o using a meteorological data parameterisation or can use supplied data. For this calibration, following the approach of Affholder (1995), the ET_o was estimated from local evaporation pan measurements using the conversion coefficients derived by Dancette (1976). The crop coefficient was calculated as a linear function of the LAI up to a maximum of $c_{crop} = 1.53$, the value that was measured for Souna millet by Dancette (1983). This crop coefficient is very high compared with most crops (see Allen *et al.*, 1998) but is feasible for a tall aerodynamically-rough canopy. The crop coefficient represents an average over several days; since the measured evaporation is limited by the drying topsoil on days without rain, the peak crop coefficient is likely to be higher.

3.5.4 Evaporation and transpiration

The GLAM methodology for splitting the evapotranspiration into evaporation and transpiration is unusual. Most crop models split the energy for evapotranspiration between the crops and the soil according the solar radiation intercepted by the crop; this is not reduced in the absence of a crop because the evaporation from wet soil can exceed the reference evapotranspiration (Rosenberg *et al.*, 1983). In contrast, the energy fraction absorbed by the soil is artificially reduced by 40 % ($C_G = 0.4$) in GLAM:

$$E_{max} = (1 - C_G)\,(1 - \epsilon_a)\,ET_o \tag{3.24}$$

The calculation of the ground heat flux is also unusual in GLAM; several climatological and agronomic studies have found a ground heat flux close to zero with minor long-term trends (Dodds *et al.*, 2005), but the GLAM parameterisation produces relatively large positive values ($\approx 3\,\mathrm{MW\,m^{-1}\,d^{-1}}$) which reduce the reference evapotranspiration rate.

A more consistent approach with other crop models is used in CROMSAS. The net radiation is calculated as the sum of the shortwave and longwave radiation balances. The ground heat flux is set to zero, unless supplied by the user, and the maximum evaporation is calculated using Equation 3.24 but with $C_G = 0$.

The evaporation rate is also limited by the depth to which the absorbed energy can penetrate the soil; if the topsoil is dry then the soil temperature will rise and the heat will dissipate as sensible rather than latent heat. GLAM calculates the water-limited evaporation, E_{pot}, using the scheme of Cooper *et al.* (1983) for bare soil:

$$E_{pot} = \frac{E_{max}}{t_R} \tag{3.25}$$

The water loss is spread equally over the evaporation soil layers, which are specified using a parameter. While simple and elegant, this method led to poor simulations of the soil water content in the Sob fields. The soil was not bare for the majority of the rainy season and evaporation was observed to a depth of 50 cm rather than the 22 cm depth used by GLAM. An alternative empirical scheme was used in CROMSAS which was developed by Affholder (2001) for tropical soils:

$$\begin{aligned} E_{max}(z) &= \left(\frac{\gamma E_{max}}{1000}\right)^{\frac{z-1}{z_{max}-1}} \\ E_{pot}(z) &= E_{max}(z)\left(\frac{\theta(z)-\theta_{ll}(z)}{\theta_{dul}(z)-\theta_{ll}(z)}\right)^{\delta} \\ E_{pot} &= \min\left(\frac{E_{max}}{\sum_{z=1}^{z_{max}} E_{pot}(z)}, 1\right)\sum_{z=1}^{z_{max}} E_{pot}(z) \end{aligned} \tag{3.26}$$

where γ and δ are empirical constants. Affholder (2001) used $\gamma = 0.4$ and $\delta = 3.5$ and, after some experimentation, these values were used in CROMSAS as well. This scheme simulates soil evaporation reducing gradually from a peak at the surface to near zero at 40 cm.

The maximum transpiration is calculated in GLAM as a function of the absorbed radiation and the reference evapotranspiration:

$$T_{Tmax} = \epsilon_a ET_o \tag{3.27}$$

This approach was not used in CROMSAS because a crop coefficient is applied to represent the greater water use of some crops. Instead, the transpiration for crop i in a field with n crops is calculated as a function of the radiation that is not absorbed by the soil:

$$T_{Tmax} = (ET_m - E_{pot})\frac{\epsilon_{ai}}{\sum_{i=1}^{n}\epsilon_{ai}} \tag{3.28}$$

In effect, the crop is assumed to absorb the majority of the additional energy which is presumed to arrive through horizontal sensible heat advection. The crop evapotranspiration, ET_m, can vary for each crop. If there were large differences between crop coefficients for crops in the same field then a more thorough approach would calculate the total energy absorbed as a function of the canopy structure. This would greatly increase the complexity of the calculation and would probably lead to little improvement in the accuracy so was not attempted in CROMSAS.

3.5.5 Estimating the potential soil water uptake

The transpiration rate depends on the ability of the plant to extract water from the soil. The potential uptake (the soil water that is available to the plant for transpiration) is calculated in GLAM using a parameterisation based on the study of Passioura (1983). The uptake from each layer depends on the water content and the crop root density in the layer. Two issues were identified with this approach:

1. the Passioura approach does not have an upper root density threshold for maximum uptake so a mature crop with a well developed root structure is simulated having access to all of the soil water each day; however, field studies have concluded that such a threshold does exist which limits uptake (e.g. Dardanelli *et al.*, 2004); and,

2. the parameterisation of Passioura (1983) was found to have been inaccurately interpreted in GLAM (although the impact on the model results was probably minor).

Dardanelli *et al.* (2004) measured the plant soil water uptake in drying soils and found a close relationship with the soil water content:

$$\theta_{pe} = \sum_{z=1}^{z_{max}} k_{up} \left(\theta_z - \theta_{ll\_plant}\right) \tag{3.29}$$

θ_{pe} is the potential uptake, k_{up} is a constant, θ_z is the fractional water content of layer z (the water content, in units mm, divided by the depth of the layer) and θ_{ll_plant} is the wilting point of the soil for the plant (a lower 'wilting point', θ_{ll}, is used in CROMSAS to limit soil evaporation). The plant cannot extract water from a layer if the soil water content falls below the wilting point. Dardanelli *et al.* (2004) found $k_{up} = 0.096$ for several crops, including millet.

The extent to which water uptake is limited by the root density is not well understood. The uptake is likely to depend on the rooting pattern as well as the density. Passioura (1983) and Dardanelli *et al.* (2004) have both produced empirical parameterisations of water uptake; the former assumes that there is a strong relationship between uptake and root density while the latter assumes that there is no relationship. Where a relationship is assumed, the threshold for full growth is uncertain. For example, the STICS model estimates the water and nitrogen uptake as a function of the root density but only up to a threshold of $0.5\,\mathrm{cm\,cm^{-3}}$. While this threshold is higher than the millet root densities in most soil layers that have been observed by field studies, there is no conclusive proof that such a meaningful threshold exists. The STICS approach does not account for the important role of the deep central tap root which transports much of the water for transpiration. This root is larger and more effective than other roots but is counted as a single root in STICS, so it is possible that the model will underestimate the plant uptake at depth. In view of these concerns it was decided to not limit the uptake as a function of the root density in CROMSAS.

Affholder (1995) estimates the potential uptake using more complex empirical functions from Eagleman (1971). Both the Eagleman and Dardanelli *et al.* (2004) methods were tested in CROMSAS for the Sob fields. Both produced very similar estimates of potential uptake throughout growth but only when $k_{up} = 0.4$. When the lower Dardanelli constant was used, the simulated uptake was too low to explain either the crop yield or the measured soil water content in the Sob fields, so it was concluded that $k_{up} = 0.4$ was more appropriate for sandy soils in Senegal. Since the estimates of the Eagleman and Dardanelli approaches were so similar, the simpler Dardanelli approach was chosen for CROMSAS. The crop is effectively able to extract 40 % of the soil water above the wilting point each day rather than the 10 % derived by Dardanelli. It is likely that crops can more easily extract water from the sandy soils of Senegal than from the clay soils that were examined in the Dardanelli *et al.* (2004) study.

3.6 Soil nitrogen balance

The aim of the soil nitrogen balance module is to calculate the NNI, which affects assimilate production, leaf growth and the development of grain sinks. GLAM simulates nitrogen stress by applying a fixed coefficient to either the LAI or the final yield. CROMSAS has two methods to simulate nitrogen stress.

The first method is similar to the GLAM approach, with the NNI being a fixed, calibrated parameter. This approach acknowledges that many field studies have experienced difficulty linking fertiliser application to yield; for example, Kennedy *et al.* (2002) observed different pearl millet responses to fertiliser in each of five environments in the USA and concluded that each environment should be treated individually.

The second method was developed in response to two weaknesses with first method. The first weakness is the implicit assumption that the plant density and the NNI are independent. In reality, if the number of plants is increased then the soil nitrogen is exhausted more quickly and the final crop yield is not necessarily higher. By assuming a constant NNI, the model assumes that nitrogen availability increases with planting density so using this method always produces higher yields at higher plant densities. The second weakness is related to the objectives of this study. By calibrating the NNI, there is no direct quantification of the effect of applying a particular amount of fertiliser on the crop yield. Since the cost of applying fertiliser has been identified as a constraint to farm system intensification, it was desirable to be able to quantify the impact of particular nitrogen application strategies.

The second method simulates the soil nitrogen balance as shown in Figure 3.2a. The soil is assumed to have a pool of accessible nitrogen for the plant to tap each day. The contents of the pool are estimated from soil organic matter decay, manure decomposition and mineral fertiliser application. The pool is reduced by nitrogen uptake, volatilisation and leaching.

Many more complex models of soil nitrogen flows and nitrogen uptake have been developed (for example, several approaches are compared by Frissel and van Veen (1981)). Models of nitrogen flows typically simulate a number of interlinked pools containing residue and soil humus that are converted by soil microbes into plant-accessible NH_4 at varying rates (Ahuja and Ma, 2002). Required parameters include: *a*) the crop residue decomposition rate; *b*) residue and humus pool sizes; *c*) transformation rate constants for each conversion process and coefficients to simulate their strong dependence on soil temperature, moisture content, O_2 concentration, ion strength, pH, and microbial populations; *d*) interpool transfer coefficients; and, *e*) rate coefficients for nitrification and denitrification and their dependence on environmental factors. The conversion of mineral fertiliser into water-soluble NH_3 is normally simulated separately to the other pools. Such models require each parameter to be accurately calibrated for the environment being simulated and there was scanty information available in the literature for Senegal, so there was little potential benefit in developing a more complex model for this study.

3.6.1 Production of plant-accessible soil nitrogen

In the absence of fertilisation, the quantity of nitrogen in Sahelian sandy soils is generally low because the soil organic matter is particularly low. Bationo and Mokwunye (1991) measured soil organic carbon fractions of between 0.32 % and 0.72 % in sandy soils across the Sahel, with the total nitrogen content ranging between $103\,\mathrm{mg\,kg^{-1}}$ and $197\,\mathrm{mg\,kg^{-1}}$. A wider survey of 31 soil types in the same study found the total nitrogen content ranged from $31\,\mathrm{mg\,kg^{-1}}$ to $1800\,\mathrm{mg\,kg^{-1}}$, with a mean of $266\,\mathrm{mg\,kg^{-1}}$, so there is much natural variability. Much of the soil nitrogen is locked in a form that is inaccessible to plants. For example, Hafner *et al.* (1993) observed the soil nitrogen content reducing from $180\,\mathrm{mg\,kg^{-1}}$ to $110\,\mathrm{mg\,kg^{-1}}$ in a field which was cultivated without fertilisation for 6 continuous years; much of the remaining nitrogen was unavailable. The rate of mineralisation of soil organic matter depends on the structure of the organic matter; molecules decay at different rates and the mineralisation rate is very low after several seasons. The contribution of mineral nitrogen from the soil depends on the number of years of cultivation and the nitrogen application in those years.

The contribution to the nitrogen pool from soil organic matter decay, N_{som}, can be estimated using the equation:

$$N_{som} = c_{Ndecay} N_{tot} \tag{3.30}$$

where N_{tot} is the total nitrogen in the soil and c_{Ndecay} is the fraction that is converted to a plant-available form each year. For a predominantly sandy soil with a soil nitrogen content of approximately $150\,\mathrm{mg\,kg^{-1}}$, the total soil nitrogen is estimated to be $1400\,\mathrm{kg\,ha^{-1}}$. Assuming a conversion factor of $c_{Ndecay} = 3\,\%$, there would be $42\,\mathrm{kg\,ha^{-1}}$ nitrogen available to the crop from this source. 15 % of the available nitrogen is assumed to be released at the first rains (the nitrogen flush) and the remainder is released over the following 50 days in equal amounts each day. All of these parameters can be optimised to the field being simulated.

Manure has a higher nitrogen concentration and decays more quickly than other soil organic matter. For example, Affholder (1995) measured a mean concentration of 1.4 % nitrogen in manure sourced from 20 farms in Senegal. Harris (1995) assumes that manure decays over three years in the ratio 0.5:0.3:0.2. Affholder (1997) similarly assumes a decay ratio of 0.5:0.25:0.16 over 3 years, with 9 % presumably lost to volatilisation. The Affholder decay rate was adopted in this study.

Mineral fertiliser can be used to increase the soil fertility but only if there is sufficient soil organic matter (see Section 1.5.2). The effectiveness of mineral fertiliser is measured by the fraction of nitrogen that is recovered by the crop. Breman *et al.* (2001) state that 33 % is recovered while Fofana *et al.* (2008) conclude that 34 % is recovered from house fields and 20 % from bush fields. Bationo and Mokwunye (1991) conclude that the recovery rate depends on both the form of the fertiliser (they tested urea and the less volatile ammonium nitrate) and the method of incorporating it into the soil, with values ranging from 31 % to 82 % at Sadoré in Niger. They also concluded that mineral fertiliser would be relatively ineffective if it were not accompanied by the incorporation of crop residues or manure. So while mineral fertiliser is nominally in a plant-available form, there is clearly much uncertainty about the effectiveness of mineral fertilisation, with at least some of the variability depending on the soil management regime. In CROMSAS, mineral fertiliser is made available to the crop at the time of application but the total amount is reduced by a factor that accounts for the recovery fraction.

There is also a contribution to the nitrogen pool from nitrogen-fixing soil bacteria. The magnitude of this contribution is uncertain but Hafner *et al.* (1993)

conclude that it is likely to be relatively modest (perhaps 5 kg ha^{-1} per year).

3.6.2 Losses of plant-accessible soil nitrogen

Plant-accessible nitrogen can be lost from the soil through plant uptake, volatilisation, leaching and denitrification.

In an experiment in Niger, 36 % of mineral fertiliser was lost by volatilisation (Hafner *et al.*, 1993). The loss should be proportional to the amount of fertiliser that is applied, but depends on the management regime, so volatilisation is represented in CROMSAS as a reduction in the fertiliser recovery factor.

The loss of nitrogen by leaching depends primarily on the rainfall and the quantity of plant-accessible nitrogen of the soil. Only large rainfall events cause leaching but the impact is substantial, with Hafner *et al.* (1993) measuring an average loss of 30 kg ha^{-1} per year. The non-linear pattern of leaching is difficult to represent in models and some complex routines have been developed for this purpose (e.g. Brisson *et al.*, 1998). In CROMSAS, for simplification, the loss due to leaching is either constant throughout the season or is simulated by reducing the contribution from decaying soil organic matter. The frequency of large storms is unusually high in the Sahel so further work on a more sophisticated simulation of nitrogen leaching might improve this part of the model.

Since the sandy soils of the Sahel are very low in organic matter and nitrate, the potential for denitrification losses is small and assumed negligible.

3.6.3 Soil nitrogen supply

The total pool of accessible nitrogen, $N_{accessible}$, is calculated on the first day of significant rains as:

$$N_{access} = 0.15N_{som} + 0.5N_{man}(y) + 0.25N_{man}(y-1) + 0.16N_{man}(y-2) + c_{min}N_{min} \tag{3.31}$$

where N_{manure} and $N_{mineral}$ are the accessible nitrogen content of the manure and mineral fertiliser, y is the current year and c_{min} is the recovery fraction (which also accounts for losses due to volatilisation). The size of the pool is recalculated each day using:

$$\frac{\partial N_{access}}{\partial t} = \frac{\partial N_{som}}{\partial t} - \frac{\partial N_{uptake}}{\partial t} - \frac{\partial N_{leach}}{\partial t} \tag{3.32}$$

where N_{uptake} and N_{leach} are the plant uptake and the loss of nitrogen due to leaching, respectively. Any additional manure or mineral fertiliser can also be added if they are applied on a particular day.

The total supply of nitrogen to the plant on each day is calculated as a fraction (6 %) of the sum of the total plant-accessible nitrogen described above.

There was concern that the model would overestimate nitrogen uptake in the early stages because it was assumed that the whole soil was immediately available to the plant. In reality, the soil nearest the seed is tapped first and the spreading roots gradually extend the uptake radius over the following days. The model overestimation therefore increases at low planting densities. A simple spatial function was added to the model that restricts nitrogen as a function of the plant root length in the top 50 cm of soil, using data from Bruck *et al.* (2003a). This spatial approach assumes that the field nitrogen pool is initially homogeneous. If the farmer chooses to only fertilise soil in the immediate vicinity of plants then this spatial approach will be inaccurate and either the whole nitrogen pool should be made immediately available or the initial distribution of nitrogen in the field should be altered to reflect the management decisions.

3.6.4 Plant nitrogen demand

The nitrogen demand from the plant was calculated from the critical nitrogen content of the crop, N_{crit}. In a well fertilised field, millet plants will contain up to 3 % nitrogen in the stem and 4 %–5 % nitrogen in the leaves and grains (Maman *et al.*, 1999). Hafner *et al.* (1993) observed little variation in the nitrogen content of the organs of plants grown under a range of fertility conditions. Plants are able to recycle nitrogen from older leaves and the stem to young leaves and grains, so the critical nitrogen content tends to reduce over time. For this reason, Gastal and Lemaire (2002) model this threshold as an allotropic relationship with total plant biomass.

A different approach was adopted for CROMSAS because the Gastal and Lemaire (2002) method implicitly assumes that the total plant biomass is a good proxy for the plant development and this assumption is only valid for irrigated crops with plentiful nutrients. The critical nitrogen content of the whole plant was instead interpolated from an empirical function that was derived from Gastal and Lemaire (2002) and the millet field studies of Kennedy *et al.* (2002) and Maman *et al.* (1999). The critical nitrogen content steadily reduces as plant development progresses from 4.5 % nitrogen at emergence to 2.9 % nitrogen at harvest.

The plant demand is calculated to keep the plant nitrogen content at the critical level. If there has previously been a shortfall then the demand increases to a maximum of 5 % of the daily assimilate production.

As the atmospheric carbon dioxide concentration increases to 550 ppm due to climate change, the critical leaf nitrogen concentration is expected to reduce by approximately 5 % in C_3 species because the plants acclimate by producing the less of the enzyme Rubisco, so the nitrogen requirement of these crops reduces (Ainsworth and Long, 2005). It may be necessary to adjust the critical nitrogen curve as a function of the $[CO_2]$ if C_3 crops are modelled in the future. For C_4 plants, the demand for nitrogen does not change (Ghannoum *et al.*, 2007).

3.6.5 Calculation of the nitrogen uptake

A simple supply and demand model is used to calculate the nitrogen uptake. The total uptake is calculated as the minimum of the nitrogen supply and demand. The total nitrogen content of the plant is increased to reflect the nitrogen uptake and the NNI is then calculated.

Some studies have observed grain yield reductions at high fertility levels (e.g. Payne *et al.*, 1991; Powell and Williams, 1993). The cause of the reductions is not identified by these studies but could result from acidification of the soil. Conversely, the reduction could be caused by a shortage of soil water in the grain-filling stage if extra growth overly depletes the soil water in the earlier stages. CROMSAS does not simulate acidification or other chemical effects, but will simulate soil water shortages. Further research is required to identify the causes of these reductions.

The first soil nitrogen method assumes that the NNI is fixed throughout growth. The second method, with a full soil nitrogen balance, shows that the

NNI is only constant when unlimited nitrogen is available. At low fertility levels, the NNI often varies substantially throughout growth as the nitrogen demands of the crop fluctuat.

3.7 Assimilate partitioning and growth of plant organs

All of the crop models that are discussed in this chapter simulate both phenological development and assimilate production using the philosophy that the crop maximises use of the available light and water resources. In contrast, each model adopts a different approach to partitioning the assimilate to the plant organs. One of the difficulties is the diversity observed in nature; different species develop different organs at different times, while plants under stress respond in different ways. For example, leaf growth is often impaired in favour of root growth under nutrient stress (Squire, 1990, p160). Deciding how to partition the assimilate between plant organs and deciding how the plant organs grow is one of the most difficult tasks for a crop modeller. In the absence of an all-embracing theory of mass partitioning, each crop model chooses a different route.

Plant growth is inherently non-linear: growth is very slow at first but the crop mass and growth rate increase exponentially as the leaf area and root depth increase. A small perturbation in the early stages of growth can significantly affect the final yields. Similarly, small changes to model parameters that control early partitioning or organ growth can also affect the final yields. Some models (e.g. GLAM) avoid these issues by increasing the leaf area and root depth linearly and independently of plant growth. But in reality, organ growth depends on the rate of assimilate production and much understanding of the underlying physiological drivers of crop yields can be gained by examining partitioning and the development of organs throughout development.

This section examines the partitioning of assimilate to the plant organs and the subsequent growth of the organs. This part of the model received more attention than most of the others because of the range of possibilities and the relative dearth of field study data for Sahelian millet. The resilience of the model partitioning was tested during development under a wide range of conditions to identify problems at an early stage.

3.7.1 Partitioning to plant organs

GLAM has the simplest partitioning scheme of the models discussed here. Individual plants are not modelled. Grain partitioning is simulated as a function of the total crop dry matter using a linearly increasing harvest index (the ratio of grain to total dry matter) which is specified as an input parameter. In contrast, but in common with the approach of APSIM, CROMSAS simulates the growth of several plant organs for each plant: the roots, leaves, stems, reproductive organs and grains. Assimilate is also partitioned to tillers in the period following their formation.

Studies have shown that the partitioning fractions to each organ change throughout development but are relatively stable at any point in time (Squire, 1990). For example, root and leaf growth dominates in the early growth stages with the stem and the grains growing later. Variations occur as a response to environmental factors. If sunlight, water or nutrients are in short supply then the plant responds by allocating a greater fraction of the assimilate to the structure which obtains the limiting resource (Brouwer, 1983). For example, an irrigated experiment in India observed 10 % of the total biomass being partitioned to the roots (Gregory, 1982) but crops growing on stored water in Niger partitioned up to 34 % to the roots (Azam-Ali *et al.*, 1984a). 10 % to 20 % of the plant biomass is typically partitioned to the roots (Squire, 1990, p160).

In DSSAT, the demand from each organ continuously changes throughout development (Jones *et al.*, 2003, p33). APSIM takes a different approach, defining a large number of stages of development and then using fixed partitioning fractions in each stage. The partitioning in CROMSAS follows a number of rules. The partitioning to the vegetative and reproductive organs is set by the user for each development period and the value is then linearly-interpolated from this data according to the degree-days accumulated by the plant. This approach is consistent with the findings of Azam-Ali *et al.* (1984a) who observed that this partitioning fraction was not affected by planting density or drought. The only exception is if the plant has not achieved a minimum size required for reproduction, in which case the reproductive organs do not develop. This threshold mass is only 4 g for millet (Carberry *et al.*, 1985).

The roots and stems demand a fixed fraction of the daily assimilate while the leaf demand is calculated using the maximum growth rate of all of the leaves on that day. The most important difference between CROMSAS and the other models is the more flexible approach that was developed to satisfy plant assimilate demand. If sufficient assimilate is available to satisfy demand then any excess is partitioned to the stem and roots as directed by input parameters in each growth stage. More importantly, if there is insufficient assimilate to meet demand due to water or nutrient stress then the leaf demand is reduced and the roots receive a greater proportion of the assimilate. This approach is based on field observations from a number of field studies (Squire, 1990, p160). The fixed partitioning approach adopted by other models is less accurate for stressed plants.

These partitioning rules are based on both field studies and the partitioning parameters of other crop models. Unfortunately, few field studies have measured the mass partitioning throughout growth for a range of environmental conditions and none were available for Senegal. Only one prior study was available which observed stressed crops in Senegal and the only relevant measurements were of the leaf area at weekly intervals (Affholder, 1995). The more flexible approach that is used in CROMSAS therefore requires a number of parameters to guide the partitioning rules that have not been measured in field studies. The use of such parameters is contrary to the guidelines set out in Section 3.2 but is broadly consistent with observations that are available and is considered to be a model improvement. There is a need for a field study to examine assimilate partitioning to organs throughout plant development. In practice, the more flexible approach of CROMSAS is realised as small perturbations rather than large changes to the partitioning fractions, so it is unlikely that large errors have been introduced.

3.7.2 Root growth

The plant root depth is used to identify the soil layers from which water can be extracted. In GLAM, the root depth increases linearly with LAI. This approach was considered unsuitable for CROMSAS because a reduction in the plant density should not lead to a reduction in the root depth, so a thermal time approach was adopted instead:

$$z_{EF} = \left(\frac{t_{tt}}{tt_{root}}\right) z_{pot} \tag{3.33}$$

where z_{EF} is the vertical root velocity, tt_{root} is the anticipated root growth thermal time and z_{pot} is the potential root depth under ideal conditions. This approach led to unreasonable early root growth in dry conditions and hence to significantly overpredicted yields. Root growth was also quite different to the observations of Chopart (1980, referenced in Affholder, 1995), who recorded vertical root growth, in the absence of water stress, averaging $1.5\,\mathrm{cm\,d^{-1}}$ for the first 15 days, $3.5\,\mathrm{cm\,d^{-1}}$ for days 15 to 45 and $1\,\mathrm{cm\,d^{-1}}$ for days 45 to 60. Inspired by the DSSAT model (Ritchie and Godwin, 2000, Chap. 2), an alternative approach was devised for CROMSAS in which the growth rate varies under water-limited conditions. Equation 3.33 is modified by three factors: *a*) growth accelerates if the water content of the soil layers containing roots is low; *b*) growth slows if plant growth is being impeded through water stress (the roots are simulated as being less sensitive to water stress than the rest of the plant); and, *c*) growth is limited to a maximum speed of $0.5\,\mathrm{m\,g^{-1}}$ root mass assimilated each day, which slows growth in the early and late stages. The vertical root growth prior to emergence is fixed at $2\,\mathrm{cm\,d^{-1}}$. The resulting root growth is consistent with both the measurements of Chopart and the observations of millet roots in Niger by Gregory and Squire (1979) and Azam-Ali *et al.* (1984a). There was some concern that drought in the early growth stages could overly reduce root growth and prevent the plant from tapping deeper sources of water, leading to poor crop yield simulations. Further experimental work is required to guide model development.

In GLAM, the root length density (the length of root in each unit volume of soil, denoted RLD) is independent of the plant mass. The RLD is simulated empirically as a function of the root density at the top of the soil and the root depth. The RLD in CROMSAS is a function of the assimilate that is partitioned to the roots. The total root demand is highest at emergence and reduces gradually to zero as partitioning to the leaves increases. The actual growth in each layer is calculated each day according to the assimilate that is partitioned to the roots.

The root mass is converted to root length using a fixed specific root length (the root length per unit mass, denoted SRL) which is specified as an input parameter. The next step in CROMSAS is to model the root growth profile through the soil. CROMSAS assumes a similar initial shape to GLAM but uses this only to define the demand in each layer. The assimilate is shared according to the relative demands of all of the layers. In a well-watered soil, this leads to a similar pattern to those observed by Gregory and Reddy (1982) for millet and groundnut. If layers are dry then root growth is inhibited, as observed by Azam-Ali (1984). In common with DSSAT, the total root assimilate demand does not reduce until the water available to the plant falls below 25 % of the maximum transpiration rate.

Experimental measurements of the Souna millet SRL were not available. Two studies at Niamey, Niger, which used several varieties of millet, produced substantially different measurements. A value of 1.5 cm mg^{-1} was derived from the results of Azam-Ali *et al.* (1984a) after 31 days growth. The SRLs of four varieties from the study of Bruck *et al.* (2003a) were estimated to range between 10–30 m g^{-1} at flowering and 30–55 m g^{-1} at maturity. Since the SRL is only used for water partitioning between multiple crops in CROMSAS and little influences the predictions, it was acceptable to use a constant SRL which was set to 25 m g^{-1}.

Observations of root systems are rare because of the practical difficulties of such experiments. The root length density is highest at the soil surface and decreases rapidly with depth (Bruck *et al.*, 2003b; Gregory and Reddy, 1982). In an irrigated field study at high plant densities, on a field station in India, Gregory and Reddy (1982) measured maximum root length densities of 1.0 cm cm^{-3} for millet. In Niger, Azam-Ali *et al.* (1984a) measured maximum densities of up to 0.8 cm cm^{-3} for millet, while Bruck *et al.* (2003b) measured densities of up to 5.6 cm cm^{-3} in the top 10 cm of the soil. No target density is set in CROMSAS as the density is calculated from the root mass and the SRL, but the maximum root length density in all layers is set to 2.5 cm cm^{-3} as the literature suggests that this is unlikely to be exceeded in most layers.

3.7.3 Leaf growth and senescence

Vegetative primordia are initiated during GS1 which form leaves and tillers. Ong (1983a) observed leaves being initiated every 26 °C d in addition to the four leaves in the seed for the BK560 variety of millet. The first tiller was initiated 145 °C d after germination and subsequent tillers were initiated every 40 °C d. The final number of leaves and tillers depends on the length of GS1. The rate of expansion of leaves is also temperature-dependent; expansion slows if the leaf temperature exceeds an optimum (Ong, 1983c) but little is known about the impact of unusually high temperatures (Soussana *et al.*, 2010).

In Section 2.1.1, a number of drawbacks were identified with the simulation of leaf expansion in existing models. A new approach was developed in CROMSAS to avoid the discrepancies over the SLA in particular. Leaves are initiated in CROMSAS on both the main stem and the tillers during GS1. The leaf initiation rate is affected by water and nutrient stresses (Squire, 1990) so in CROMSAS, following the observations of Norman *et al.* (1995, p167), the thermal time between leaf initiations lies in the range 25 °C d with no stress to 35 °C d for highly stressed plants.

The appearance of each leaf is delayed by a fixed thermal time after the previous leaf, as observed in (Ong, 1983a). Once a leaf has appeared, it extends by up to 6 cm per day if there is sufficient assimilate. The rate of leaf extension peaks at 33 °C and is reduced at sub-optimal temperatures as observed in (Ong, 1983c). The rate of extension is not affected by the VPD in accordance with the observations of millet leaves (Ong, 1983c). The potential leaf extension is converted into leaf area and then leaf mass using empirical relationships derived by Payne *et al.* (1991):

$$L_{area} = 2.08 \ln (L_{length}) - 3.53 \tag{3.34}$$

$$SLA = c_l L_{mass}^{-0.216} \tag{3.35}$$

where the units of L_{area}, L_{length} , L_{mass} and SLA are cm^2, cm, g and $\mathrm{cm}^2\,\mathrm{g}^{-1}$, respectively and c_l is a variety-specific constant which is set to 300 for Souna. The maximum SLA is set to $850\,\mathrm{cm}^2\,\mathrm{g}^{-1}$. The total demand for assimilate is calculated by summing over all of the leaves on the plant. The growth of each leaf ceases when a maximum length of 1 m is reached, when the leaf reaches a certain age or if assimilate ceases being partitioned to the leaves. The maximum leaf size is a variety-specific parameter; millet leaves can grow to a length of 1.5 m (Andrews and Kumar, 2006)

The maximum LAI of the crop is limited by the number of plants, the number of leaves (which depends on the phenological development and the availability of nutrients) and the assimilate that is partitioned to the leaves. Leaf growth is simulated as being more susceptible to water stress than the other organs. A sensitivity coefficient for leaf demand, C_{sens2}, is used in a similar way to the coefficient for photosynthesis:

$$\frac{\partial W_{leaf\_demand}}{\partial t} = \left(\frac{T_T}{T_{Tmax}}\right)^{C_{sens2}} \frac{\partial W_{leaf\_demand\_max}}{\partial t} \tag{3.36}$$

To reflect the extra sensitivity of leaves to drought, $C_{sens2} = 1.5$ for millet.

During grain filling, millet leaves tend to senesce as nutrients are transferred from the leaves to the grains, causing the total *green* leaf area to reduce. If senescence is not simulated then the model will overestimate light interception and transpiration in the final growth stage. The rate of senescence tends to increase at higher temperatures, suggesting that the rate is linked to thermal time (Squire, 1990, p46). The rate of senescence is also usually proportional to the maximum LAI. Since the driver of LAI variability within a species is normally varying leaf sizes rather than a change in the number of leaves, the senescence parameterisation in CROMSAS treats each leaf individually, irrespective of the size of the leaf. The thermal time for the start of senescence and the number of leaves remaining on the plant at maturity are supplied as model parameters. The model then senesces fractions of leaves each day, starting from the leaves that developed first, so that the requested number of leaves is present at maturity. Leaf growth and senescence can take place concurrently in the model (although not for the same leaf).

3.7.4 Stem growth

CROMSAS calculates the stem demand using a simpler approach than for the roots and leaves. The stem is assumed to take a fixed fraction of the available assimilate each day. This fraction is supplied for each growth stage as an input variable and tends to vary between plant species. In the absence of field observations to support a relationship between the stem height and the stem mass, three methods for simulating the extension of the stem were included:

1. The stem height linearly increases with thermal time on days when assimilate is partitioned to the stem. This method assumes a weak relationship between stem mass and height, as might be encountered for a small spreading plant. The plant height is denoted h and c_{can} is a constant:
$$\frac{\partial h}{\partial t} = c_{cantt} t_{tt} \tag{3.37}$$
2. There is an allotropic relationship between stem mass and plant height. This is similar to the approach in the land surface scheme of the UKMO climate model (Osborne *et al.*, 2007), although the stem mass is used in CROMSAS rather than the LAI. The CROMSAS approach is consistent with ecological studies which have shown that allotropic relationships govern the size and mass of a wide range of species (Niklas and Enquist, 2001). It was necessary to derive a new power constant for CROMSAS because the stem mass rather than the total above-ground biomass was used in the relationship. In the following equation, a_{ch} is a constant and W_{stem} is the total plant stem mass:
$$h = (a_{ch} W_{stem})^{0.25} \tag{3.38}$$
3. The stem height linearly increases with stem mass using a specific stem height (the stem height per unit stem mass, denoted SSH). This method, which is also used by APSIM, assumes that the stem is vertical and of uniform thickness throughout growth. The SSH is denoted c_{canw} in the following equation:
$$\frac{\partial h}{\partial t} = c_{canw} \frac{\partial W_{stem}}{\partial t} \tag{3.39}$$

In the initial growth stages, millet leaves and roots receive almost all of the assimilate. Once a number of leaves have developed, stem elongation commences and the plant can grow to a height of 1 m to 4 m. In CROMSAS, stem demand is set to zero in the vegetative growth stage as elongation is assumed to occur primarily during the flowering stage, when at least 50 % of assimilate is partitioned to the stem, flowers and grains. The stem is also a sink, together with the roots, for excess assimilate at any time. The most appropriate option to model the stem height of millet is to use either an allotropic or linear relationship with stem mass (options 2 or 3).

3.7.5 Estimating the vertical leaf area distribution

In Section 3.4.6, the LAI in each canopy layer is used to calculate the radiation absorption in that layer. It is therefore necessary to split the leaf area of the individual leaves between layers. This is particularly complicated for millet because the leaf height changes with time as the stem elongates, and because the leaves change shape as the plant grows.

CROMSAS offers two methods to split the leaf area between layers: *a*) the total stem leaf area is smeared evenly between the top and bottom of the stem, assuming that the canopy is vertically homogeneous; and, *b*) the contribution of each leaf to each layer is calculated from the height of the leaf on the stem and the angle of the leaf.

If there are several crops in the same field then the taller crop tends to absorb the majority of the radiation. For example, since millet is a much taller plant than groundnut, most millet leaves are above the groundnut leaves and small errors in the height of either plant will have little impact on the crop model results. Conversely, if two crops of similar size are modelled, the height of the leaves of each crop will have to be simulated carefully so that the radiation interception of each crop is calculated accurately.

3.7.6 Flower and grain growth

Millet plants begin to produce reproductive primordia at panicle initiation in GS2. The reproductive spikelets flower at anthesis, are pollinated and develop grain sinks. The number of flowering spikelets depends on the growth rate of the crop during GS2: Ong and Squire (1984) found a close relationship between the number of grains and the thermal interception rate (defined as the intercepted radiation per degree day of development per plant) for temperatures in the range

22 °C to 31 °C, but at 19 °C the number of grains was substantially reduced. Other studies have concluded that low temperatures during GS2 (less than 20 °C) substantially reduce the number of surviving spikelets and can restrict the final yield (Fussell *et al.*, 1980; Ong, 1983b). Little is known about the impact of high temperatures on the number of grain sinks. In maize, the number of grain sinks reduces rapidly when the temperature exceeds 38 °C during flowering (Barnabás *et al.*, 2008), but similar studies have not been performed for millet.

In common with APSIM and DSSAT, CROMSAS simulates a discrete number of grain sinks. The number of sinks is simulated as being proportional to the biomass that is partitioned to the reproductive organs during GS2, which is proportional to the thermal interception rate unless reproductive partitioning is reduced as a result of the plants not reaching the minimum threshold biomass for reproduction. The main stem and all of the surviving tillers produce heads if biomass has been partitioned to their reproductive organs. The number of sinks on each head can be reduced if extreme temperatures affect the crop during GS2. This mechanism currently uses the average temperature but a future model development, which would have to be supported by experimental studies, could use the maximum and minimum temperatures and could make a more accurate estimation of the duration of extreme temperatures (e.g. Challinor *et al.*, 2005).

Flowering lasts for several days with new flowers appearing each day. The number of flowers can be reduced by drought, nutrient stress and excessively high or low temperatures. Based on the studies of Fussell *et al.* (1980) and Ong (1983b), the number of grain sinks was reduced if the average temperature moved outside of the range 25 °C to 35 °C; the impact of this mechanism on model simulations is examined in Section 4.2.4.2. The surviving flowers become grain sinks.

GS3 is dominated by grain filling and the grain yield of the plant depends on the duration of this period and the daily growth rate of the grains (Bieler *et al.*, 1993). The daily grain growth rate is approximately constant so plants grown at lower temperatures, which have longer grain-filling periods, produce larger grains (Fussell *et al.*, 1980). Measurements of the grain growth rate in the literature vary, with Fussell *et al.* (1980) reporting 0.21–0.34 $\mathrm{mg\,grain^{-1}\,d^{-1}}$ in a glasshouse study, van Oosterom *et al.* (2002) reporting 0.4–0.5 $\mathrm{mg\,grain^{-1}\,d^{-1}}$

in India and Bieler *et al.* (1993) reporting 0.25–0.58 mg grain^{-1} d^{-1}. After some experimentation, a value of 0.25 mg grain^{-1} d^{-1} was chosen for CROMSAS.

APSIM reduces the grain growth rate as a function of temperature using a broken-linear function with T_b = 3.7 °C, T_o = 30 °C and T_m = 56.3 °C. No justification for this approach could be identified, with both Fussell *et al.* (1980) and Ong (1983b) concluding that the growth rate is independent of temperature between 20 °C and 31 °C. Since it is very unlikely that grain filling will not be impaired at extreme temperatures, grain growth in CROMSAS is unaffected when average temperatures are in the range 20 °C–35 °C but is reduced outside of this range. More research is needed to examine the effects of high temperatures on grain filling in particular.

Bieler *et al.* (1993) recorded grain weights at harvest increasing from 3.4 mg to 10.9 mg as a result of the GS3 duration lengthening at lower temperatures. These weights are consistent with both measurements of the Souna variety from Dakar of 6.4 mg (Gueye and Delobel, 1999) and the findings of Haussmann *et al.* (2006) who recorded weights in the range 4 mg to 14 mg from 269 varieties across Africa. The maximum grain mass is set to 11 mg for Souna in CROMSAS.

Some cereals are able to move assimilate from the stem to the grains in a process called translocation. This means that the grains continue to develop during drought periods and that, under ideal conditions, the daily grain mass increase can even exceed the total biomass increase. An option is included in CROMSAS to translocate assimilate from the stem to the grains.

3.7.7 Tillers

A particular challenge for crop models is the representation of tillers. Tillers are semi-independent stems that are grown by some cereals in parallel to the main stem which can produce grain heads when assimilate is plentiful. Tillers represent an adaptation mechanism for the plant (and hence the farmer). High tillering species planted at low plant densities can produce several tillers when resources are plentiful, greatly increasing the yield, but will allow the tillers to wilt while producing at least a basic yield when faced with water stress (Azam-Ali *et al.*, 1984b). However, the highest grain yields are normally achieved by using low-tillering genotypes at high plant densities.

Souna millet is a low-tillering variety which rarely develops more than one productive tiller. For this reason, Affholder (1995) ignored tillering in the SARRA-millet model. Despite this, a tillering model was developed for CROMSAS to investigate the impact of tillers and to simulate high-tillering crops and varieties.

The tiller model uses a broadly similar approach to APSIM (van Oosterom *et al.*, 2001a). Tillers appear from leaf nodules and then grow as separate axes which grow their own leaves and sometimes grain heads. The maximum number of tillers is set as an input parameter. If the growing conditions deteriorate after a tiller has emerged then the tiller can senesce and die.

The radiation absorption of the leaves on each tiller is calculated separately as if the tillers were separate crops. Each tiller is therefore effectively treated as a separate crop for above-ground partitioning and organ growth. However, assimilate partitioning to the roots is taken from all of the stems. Model experimentation suggested that it is necessary for main stem assimilate to be transferred to the tillers for the first 100 ℃ d to properly simulate tiller growth. Only a small fraction of the total assimilate is transferred and this reduces from a maximum to zero over this period.

It was necessary to make several assumptions about the growth and death of tillers due to the lack of field observations. While the modelling of the tillers themselves should be acceptably accurate, it would be necessary to conduct field studies on high-tillering species to gain greater confidence that the modelling of the appearance and senescence of tillers is appropriate. Low-tillering species should be less affected by these assumptions.

There was a second concern with the tiller model regarding the distribution of tillers in a field. The number of tillers can vary widely between plants in the same field, particularly for high-tillering species (e.g. Azam-Ali *et al.*, 1984a). It is not clear that the CROMSAS approach of modelling a single representative plant is valid under these circumstances. In particular, the appearance or death of a single tiller in CROMSAS is assumed to affect every plant in the field and can significantly affect the final crop yield because only a small number of discrete tillers appear. A better probabilistic approach would simulate the crop several times with different numbers of tillers and then average the resulting yields.

3.8 Plant death

Plants which suffer sustained stress often die without producing any grain. The death of a young crop is a particular problem in the Sahel where early rains are often followed by several weeks of drought, leading to a late re-planting. Death tends to be a gradual process because some plants are stronger than others and because each plant in the field lives in a slightly different micro-environment. The number of fatalities depends on the degree of stress in the field (Squire, 1990).

Simulating plant death is challenging because it is difficult for field studies to attribute the death of plants to particular source(s) and it is even more difficult to link the magnitude of the stress with the fatality rate. Some varieties are hardier than others so field studies on one crop and variety will not generally translate to another variety (Matthews *et al.*, 1988, 1990). Hardier varieties are generally more responsive to stress and store higher water reserves than other varieties, but produce lower yields as a trade-off.

The version of GLAM that was used for this thesis did not model plant death (although a parameterisation has been added to a more recent version). APSIM sums the daily water stress factors and assumes plant death once a threshold total has been reached (van Oosterom, 2000). No account is taken of the length of any particular stress period in APSIM.

CROMSAS has an optional plant death parameterisation which adopts an alternative approach. Only periods of concurrent days with severe water stress ($< 5\,\%$ of the potential transpiration) can cause plant death. Plants do not die on the first few days as they are assumed to survive on water reserves. After this time, the death rate each day is calculated using an exponential function, so the death rate increases with time. The plant density of the crop is reduced as required. Plant death ceases when either the transpiration rate exceeds the $5\,\%$ threshold or if all of the plants are dead. Hardier crops can be modelled by increasing the time before plant death commences, by changing the water stress threshold and by dampening the exponential increase in deaths.

Testing CROMSAS with drought periods from Senegal in the period 1950–2008 suggested that the yield would be significantly reduced even in the absence of a plant death model. It is likely that simulating plant death would only make a significant difference in a small number of years which suffered sustained drought periods early in the growing season.

3.9 Summary

This chapter has described the CROMSAS crop model. Where possible, model development has followed the guidelines of Sinclair and Seligman (1996). CROMSAS has been designed with a similar structure to the existing crop models described in Section 2.1.1. In common with the RESCAP model (Monteith *et al.*, 1989), CROMSAS has been designed to conserve resource flows and to grow organs as a function of their mass so that the plant geometry is always realistic.

A number of original features have been introduced into the model:

- a new leaf expansion sub-model simulates the growth of the leaves and the interaction between the leaf mass and the leaf area in a more realistic way than has been achieved in any of the existing models;
- a fixed-length juvenile stage has been introduced that is more consistent with experimental findings than the thermal time relationship used in other models;
- a comprehensive simulation of tillers has been designed which is more elegant than the approaches used elsewhere;
- intercropping can be simulated between any number of crops and weeds;
- the soil evaporation, runoff and drainage have been redesigned; and,
- some of the potentially-important impacts of climate change (the impact of rising CO_2 on growth and the influence of temperature on leaf expansion and reproductive growth) are simulated.

CROMSAS was designed to examine the impact of changing the planting date, planting density and the nitrogen application. Together with the choice of crop variety, these are the most important crop management decisions for Sahelian smallholders. These management decisions also represent the best options for adapting to climate change in this region, meaning that CROMSAS can be used to examine the role of adaptation in reducing the negative impacts of climate change.

The calibration and evaluation of CROMSAS are presented in Chapter 4.

Chapter 4

Calibration and Evaluation of the CROMSAS Model

The CROMSAS crop model was described in Chapter 3. Before using the model to examine farming systems, it is necessary to examine the accuracy of the model for the purpose that it was built, which was to examine the impacts of crop management strategies and climate change. This chapter discusses the calibration and evaluation of the model.

4.1 Calibration of the CROMSAS model

Most crop models have empirical relationships which require calibrated parameters. Calibration is also required to adapt the model to the soil and climate of a particular region. This section describes how CROMSAS was calibrated for millet in Senegal. Field study measurements of three smallholder fields in the same village were chosen for the calibration. The first field was intensively farmed while the other two were more extensive, one with manure and one without. These fields are typical examples of smallholder fields in Senegal. The aim was to be able to accurately simulate all three fields with only the nitrogen application strategies differing between them in the model. The model design and calibration were iterated several times with feedback from the calibration being used to improve the model.

Models that are designed and calibrated for one environment often do not perform well in another environment. For example, the majority of crop research and modelling has focused on high-input intensive farming in temperate climates where solar radiation is the limiting factor to growth (Section 2.1.1). It is unlikely that such a model would accurately simulate a low-input extensive crop in a semi-arid climate, where radiation is not limiting, without modifications and re-calibration. The climate, soils and crops are very different in tropical regions.

A further need to calibrate models became apparent when meteorological data were being produced (Chapter 5). Several instantaneous temperature and humidity readings were available each day and several averaging methods were tested to estimate the daily averages (both daytime and 24-hour averages). While the methods showed similar trends, each produced daily averages with different magnitudes and these affected the growth rate in CROMSAS. It is necessary to calibrate the model parameters to account for any offset that has been introduced by the meteorological data averaging. Model parameters will vary from the literature where the studies use different techniques to average meteorological data. Since information about the dependence of the parameters to meteorological data is rarely available in the literature, it is inevitably necessary to calibrate the model to the local conditions.

4.1.1 Description of the field study

Comprehensive field studies of farmers' fields in the Sahel are rarely performed. Most agricultural studies take place on field stations under idealistic growing conditions that are often not representative of regional agricultural management practices. The only available large-scale study of farmers' fields in West Africa was from the ESPACE project (Affholder, 1992). There was insufficient information in the main database to properly calibrate the crop model because observations of the crop itself (biomass and grain yields) were only collected at harvest and there was no information about the path that the crop followed to produce those yields. It is necessary to examine the performance of the model throughout the season to properly assess the model skill. However, the ESPACE study included several small-scale field studies that collected additional information about the

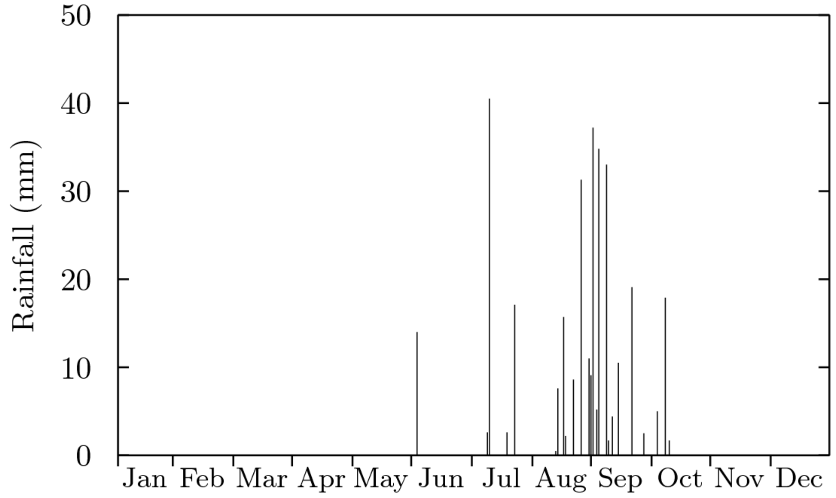

Figure 4.1: Daily rainfall measured in the Sob house field in 1991. Similar rainfall was recorded in the other two fields.

fields. The most suitable study for calibrating a millet model was performed on several fields in the village of Sob in 1991 and subsequently published by Affholder (1995). Additional observations of the rainfall in each field, the crop LAI and the soil water content were taken at regular intervals for each crop. Unfortunately, the only crop yield measurements were made at harvest.

Three fields were studied. The first was a house field which received manure during the study year and the two previous years. The second and third were bush fields, one which also received manure over three years and another which received none. Crops were planted in all three fields prior to the first rains in May. The first storm arrived on 3 June (Figure 4.1), which caused the crop to germinate, but the next rains did not arrive for another month and the first crop died. A second crop was planted in the intervening period which is the subject of this calibration. There was another mini-drought between mid-July and mid-August which affected the crops in all three fields. The village enjoyed regular rainfall between mid-August and mid-October and the crops did not suffer water stress during this time. The rainfall varied only slightly between the three fields; the distributions were almost identical and the total rainfall ranged from 336 mm to 343 mm.

4.1.2 Comparison of the three Sob fields

The original raw data of Affholder (1995) were obtained for this study. Table 4.1 summarises the three 1991 fields. The plant densities of the two manured fields were similar and substantially higher than the density of the unfertilised bush field; since both bush fields were owned by the same farmer, it is likely that he deliberately adapted to the lack of manure by reducing the stand density. The germination dates were the same for all three fields and followed a large rainfall event. The crops were harvested after 90 days.

All of the fields were fully weeded on two occasions but more attention was paid to the house field. Similarly, while caterpillars attacked crops in all three fields, the bush field crops suffered greater damage. The house field received more manure and was weeded more carefully, and this was reflected in the final yields, with both the grain and total biomasses being far higher than those of the bush fields. The yields were particularly low in the unfertilised bush field.

4.1.2.1 Soil water balance, radiation absorption and crop yield

The water loss varied between fields, with the high-yielding crop in the house field using far more water than the low-yielding crop in the unfertilised bush field (Table 4.1). The house field soil water content at harvest was almost unchanged while the water content of both bush fields increased substantially. It is interesting that the soil water content of the each field at harvest was quite different to the start of crop growth; stored water from the previous season was used in the house field and contributed to an increased yield. This ‘memory’ effect can presumably lead to increased crop yields in the years following poor growing seasons. Since the soil water changes occurred below a depth of 1 m, only mature crops, trees or other deep-rooted plants would have been able to access the stored water. The water content near the surface is always low as a result of evaporation and weeds.

It is interesting to examine the relationship between the crop yield and the water loss from the soil (due to evaporation, transpiration, drainage and runoff). Graph 4.2a shows that there is a linear relationship for the three fields, which suggests that the transpiration efficiency approach (Equation 3.5) would be valid if the offset was caused by evaporation, drainage and runoff. The higher density

	House field	**Bush fields**	
		Manured	**Unfertilised**
Soil type	Sand	Sand	Sand
Manure application	3 years	3 years	None
Stand density (stands ha^{-1})	15000	10800	9200
Plants per stand	4.1	5.6	4.8
Plant density (plants ha^{-1})	61666	60000	44000
Planting date	5 Jul	20 Jun	20 Jun
Germination date	10 Jul	10 Jul	10 Jul
Harvest date	3 Oct	3 Oct	3 Oct
Weeding visits	2	2	2
Weed prevalence (scale 1–5)	1	2	2
% crop affected by pests	10 %	30 %	30 %
Maximum LAI	3.2	1.7	1.1
Grain yield (kg/ha)	1654	800	269
Total biomass yield (kg/ha)	5743	3240*	1880
Harvest index	0.29	0.25	0.14
Rainfall (mm)	297	303	309
Soil water before planting	60.1	56.3	35.1
Soil water content at harvest	63.2	75.5	66.3
Change in soil water	3.1	19.2	31.1
Water loss (mm)	286	234	197

Table 4.1: Summary of data from the Sob 1991 field study which was used to calibrate CROMSAS for use in Senegal. The three fields are described in the main text. The weed prevalence is measured using a scale of 1–5 where 1 indicates no weeds and 5 means the plot is overrun. The pest damage was caused by caterpillars. The soil water content is measured in units mm water per m soil; the top 3.6 m was measured. *This yield was higher in the CIRAD ESPACE database (4187 kg ha^{-1}) than in Affholder (1995); the cause of the discrepancy is not known.

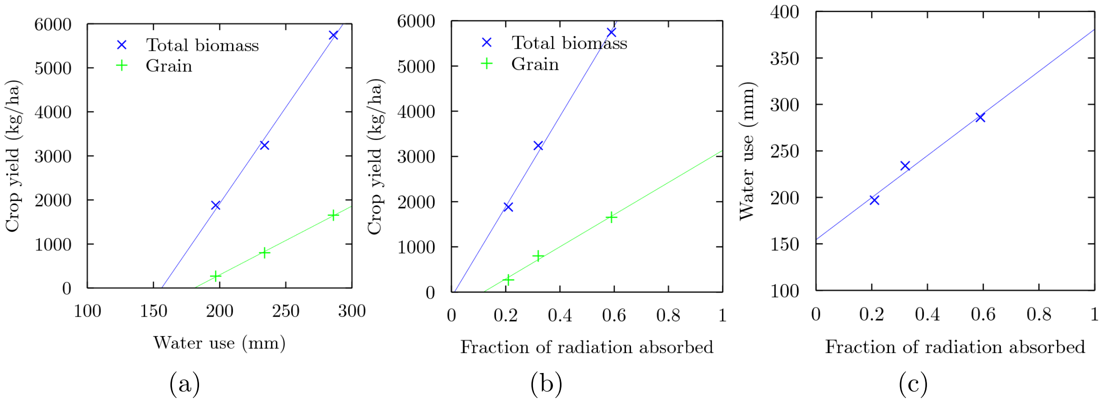

Figure 4.2: Relationships between water use, radiation absorption and crop yield for the three fields in the Affholder (1995) field study at the village of Sob in 1991.

crops in the more fertile fields used substantially more water. However, the water use efficiency of these crops was higher, presumably because the evaporation rate was similar for all three crops and the transpiration rate increased linearly with growth. The transpiration efficiency approach to calculating growth would therefore be valid for these fields (Equation 3.5).

The other approach to estimating growth in CROMSAS uses the radiation use efficiency concept. The radiation absorption of each crop was estimated from the measured LAI by assuming the light extinction coefficient $k_c = 0.55$ for each crop. This value is close to the values measured by Begue *et al.* (1991) of $k_c = 0.65$ during the growing phase and $k_c = 0.56$ during senescence; a wide range of values are used in different crop models (Section 3.2.1). Graph 4.2b shows that there is also a linear relationship for the three fields between yield and radiation absorption. So it is not clear from these graphs whether growth is radiation-limited or transpiration-limited.

4.1.3 Soil water content comparison

The most useful measurements at Sob were a series of soil water content observations in each field. The water content of each 10 cm layer in the top 360 cm of soil was measured weekly.

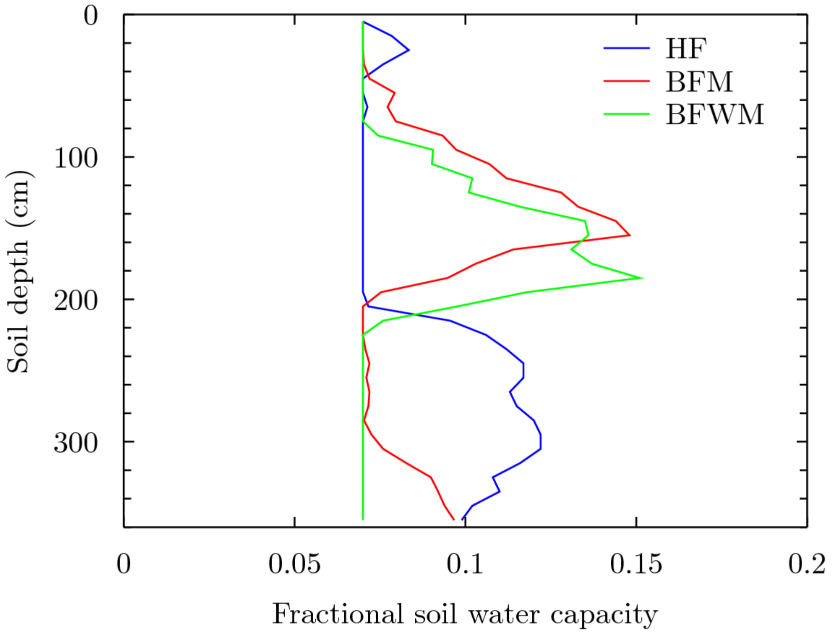

Figure 4.3: Soil water capacity in each Sob field in 1991. The water capacity in each layer is set to the maximum measured in that layer during the season, with a minimum of 7 %.

The soil water capacity of each layer, θ_{dul}, was estimated from the maximum observed water content in each layer (Figure 4.3). The lowest soil water capacity was set to 7 %, a typical value for a sandy soil (IRAT, 1983). The water content is probably underestimated in some layers which would cause the plant water uptake to be slightly underestimated. Following the measurements of IRAT (1983), and advice from an experienced agronomist, the wilting point in each layer, θ_{ll_plant}, was set to 2 % and the minimum soil water content, θ_{ll}, to 1 %. The first soil water measurements were performed two weeks prior to crop germination on 27 June 1991. The water content in each model layer was set to the measured value on this day so that a proper comparison could be performed.

Water was added to the soil from rainfall and lost from evapotranspiration and drainage below 3.6 m. It was assumed that no runoff occurred.

The measurements were generally performed a few days after rainfall. This allowed any rainfall to fully drain through the soil but prevented the soil drainage from being analysed directly. Figures 4.4a, 4.4b and 4.4c show histograms of water loss from the three fields. Negligible water was lost through deep drainage in any field in the model simulations.

Figures 4.5, 4.6 and 4.7 compare simulations of the water distribution through the soil against experimental measurements from the three field. In all three cases, the model simulates too much water in the soil at the start of the season, slightly too little in the middle and a reasonable amount at the end. Further field study observations would be required to identify the factors controlling these trends. Overall, the simulations produce good estimates throughout the season, despite the complexity of the plant—soil system.

4.1.3.1 Early growth stages

Water loss was underestimated by $1\,\mathrm{mm\,d^{-1}}$ in the first period of observations in all three fields. The discrepancy was probably caused by evaporation being underestimated or by runoff, which was not measured. Sahelian topsoils tend to form a hard impermeable crust while drying and it is likely that the crust impeded inflow during the single but large rainfall event ($\approx 40\,\mathrm{mm}$) that occurred in this period, causing substantial runoff. Crop transpiration was negligible at that growth stage and an investigation showed that transpiration from the initial millet crop (and weeds) which germinated a month earlier was also negligible. Interestingly, a validation of the CERES-Millet model for Niger also overestimated soil water in the early growth stages (Allison *et al.*, 1995).

After the 40 mm rainfall event, which caused crop germination, only 20 mm fell during the first month of growth. The soil dried and the crops were not able to tap deeper water so water loss reduced to almost zero. CROMSAS broadly simulates this mini-drought in all three fields but overestimates the transpiration rate. A number of sensitivity studies failed to find a flaw in the model which would explain this overestimation, but did show that both the water and nitrogen uptake were very sensitive to the vertical root growth in the early vegetative phase. Little information is available about the vertical growth of millet roots, either in stressed or unstressed conditions.

Rainfall arrived at regular intervals after the first month. The water loss increased to a high at 50 days after germination as the leaf area expanded rapidly.

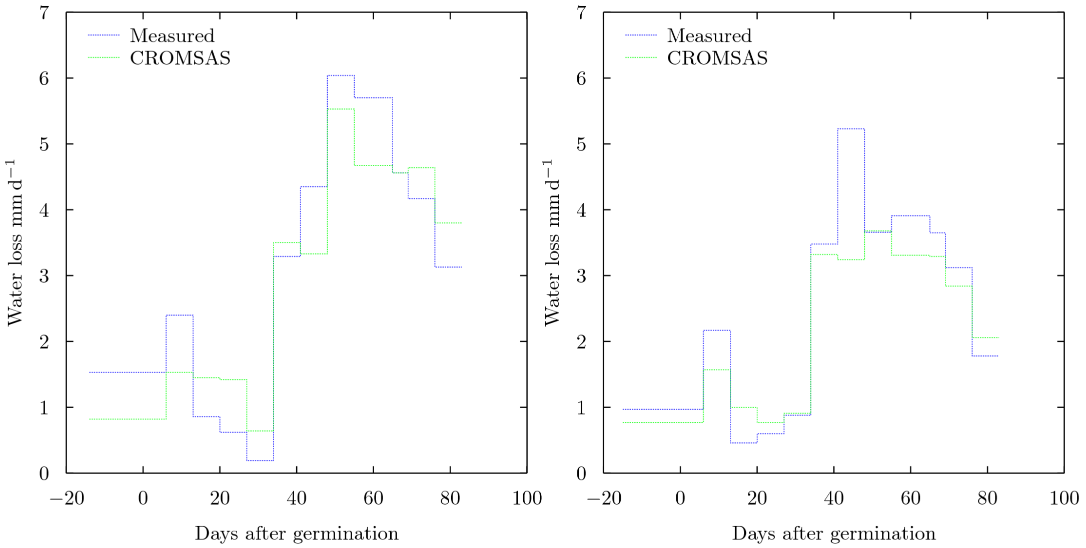

(a) House field (b) Bush field fertilised

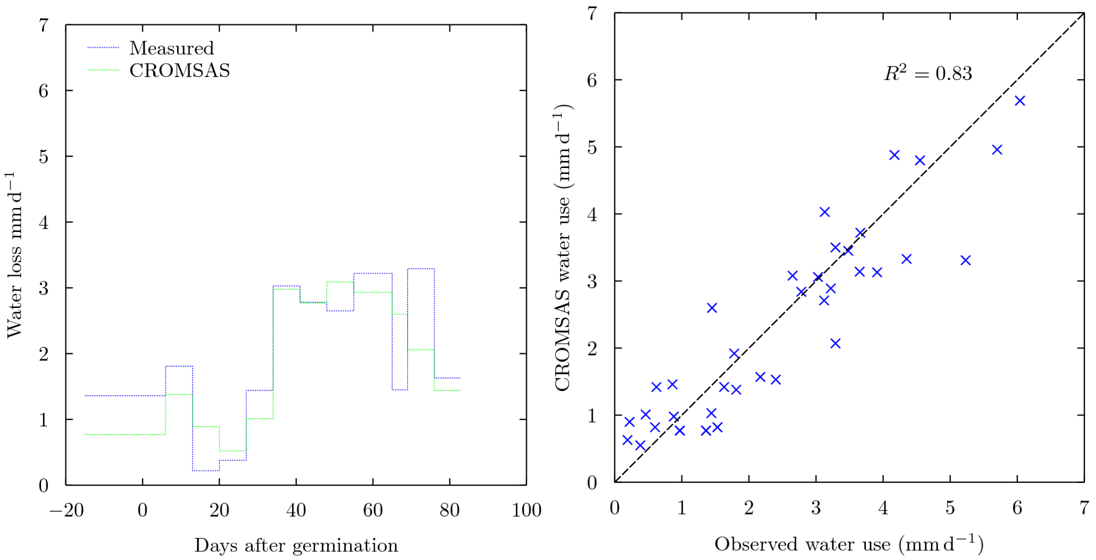

(c) Bush field unfertilised (d) Experiment–model comparison

Figure 4.4: Comparison of soil water balance measurements and CROMSAS simulations for the Sob calibration fields. The final graph includes comparisons from all three fields.

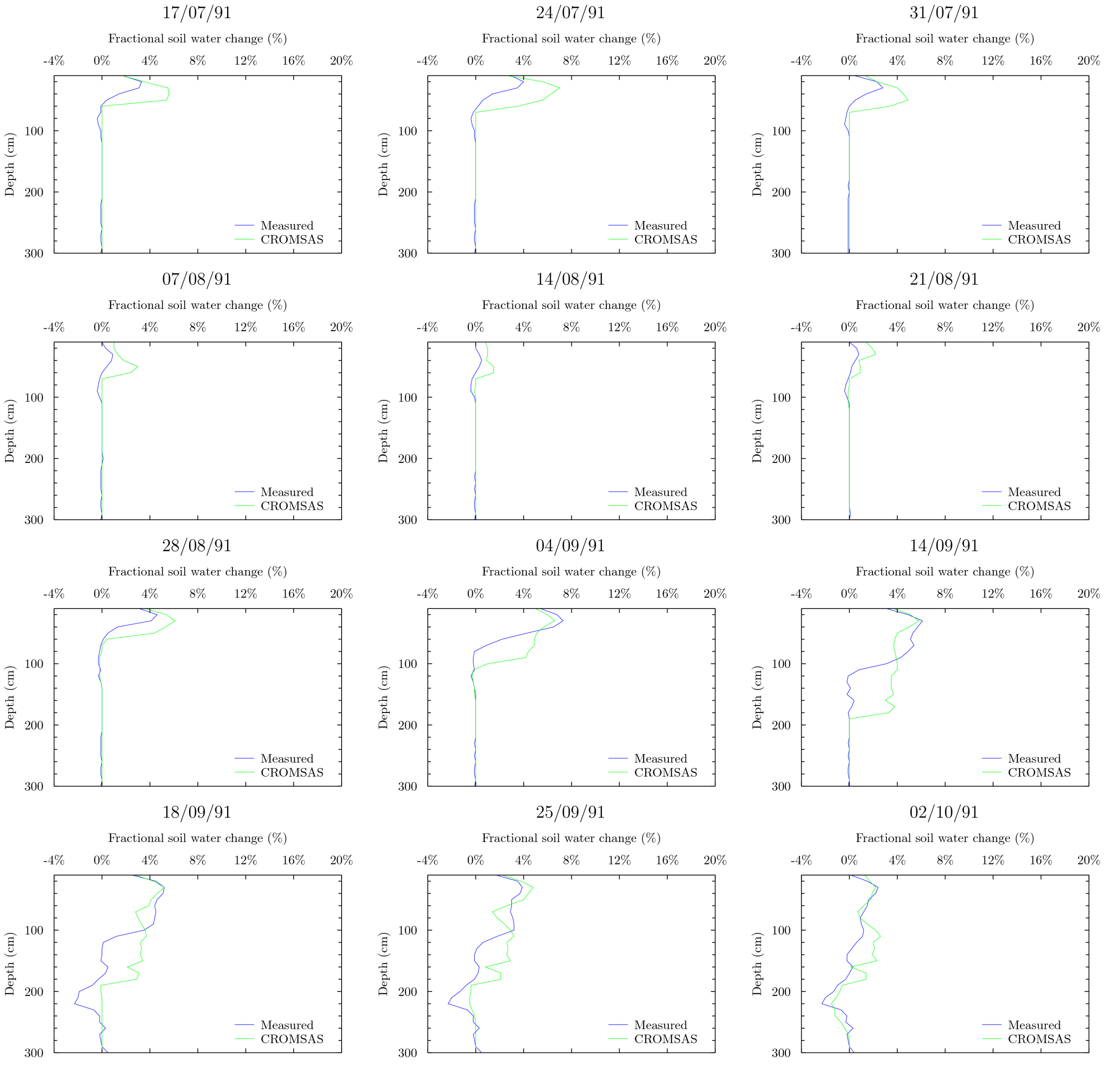

Figure 4.5: Comparison of the measured and simulated soil water content through the 1991 growing season in the Sob house field. These graphs show the absolute change from the first measurement of the season, which was performed two weeks prior to crop germination.

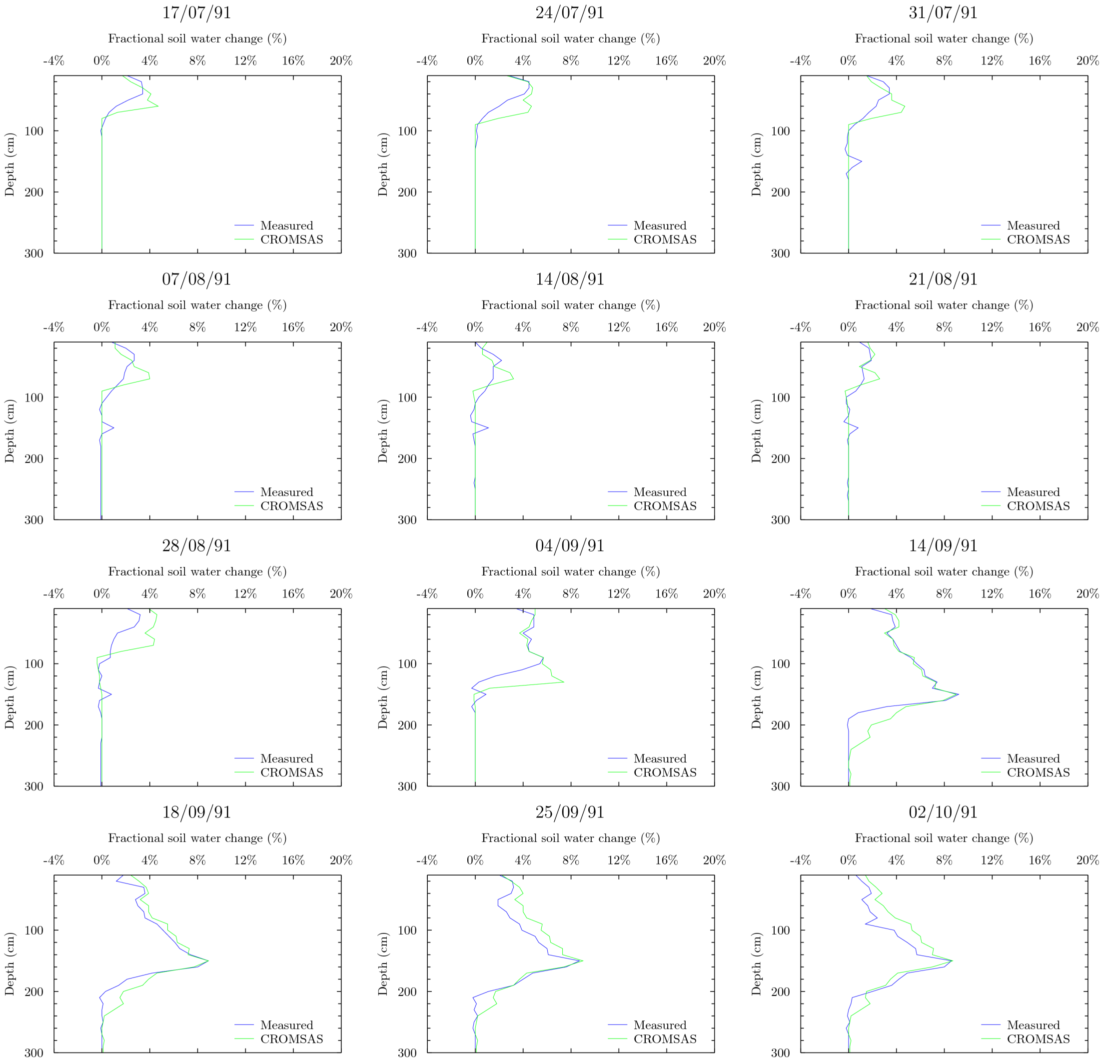

Figure 4.6: Comparison of the measured and simulated soil water content through the 1991 growing season in the manured bush field at Sob. These graphs show the absolute change from the first measurement of the season, which was performed two weeks prior to crop germination.

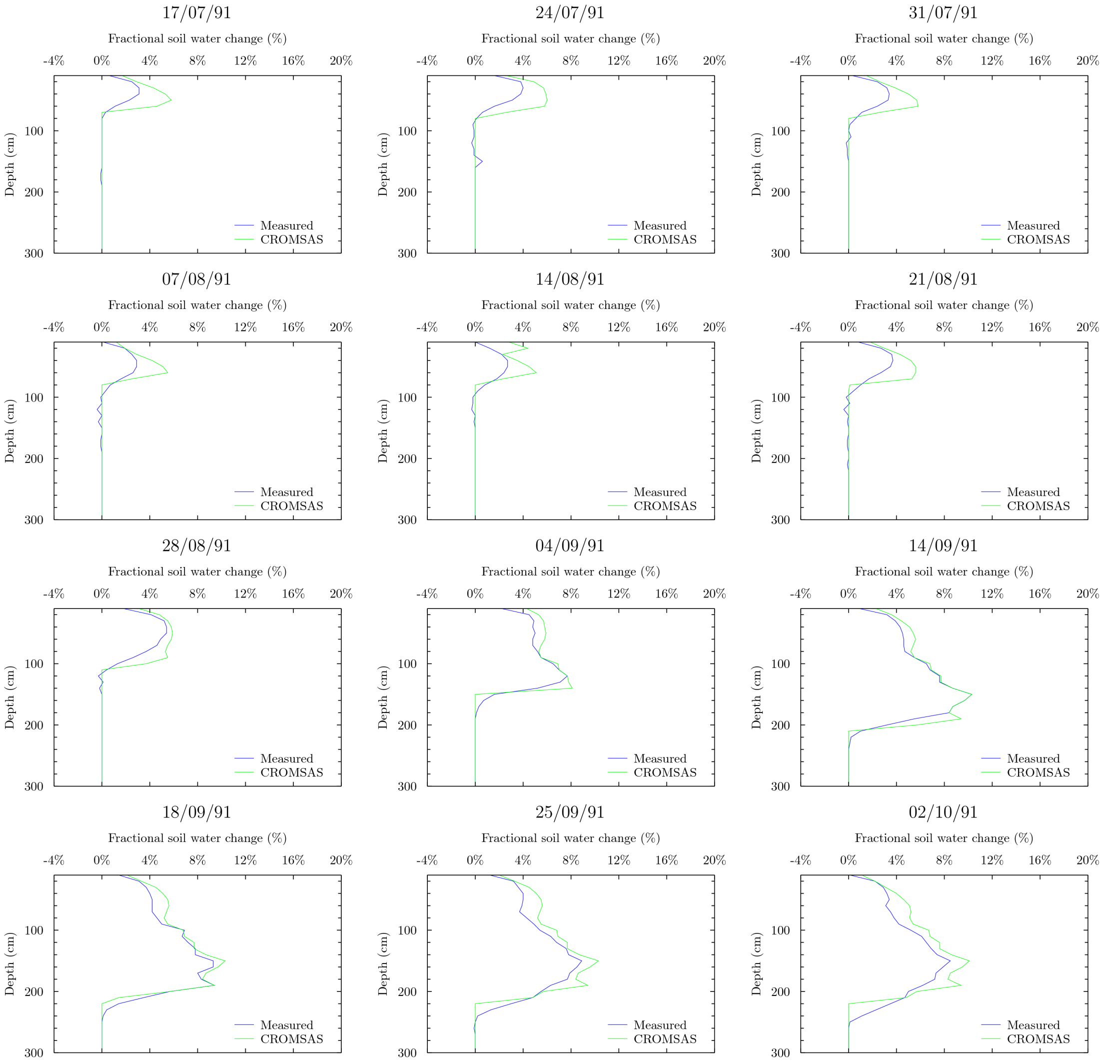

Figure 4.7: Comparison of the measured and simulated soil water content through the 1991 growing season in the unfertilised bush field at Sob. These graphs show the absolute change from the first measurement of the season, which was performed two weeks prior to crop germination.

The rate of water loss during this time in the two manured fields was higher than that calculated by the model, despite the model using a high crop coefficient of $c_{crop} = 1.53$ (Section 3.5.3). Run-off was considered as a possible explanation, but further investigations showed that the simulated crop growth was lower than measured as a result of the transpiration rate being too low. A possible explanation was that the energy absorbed by the crop for transpiration was higher than that calculated using Equation 3.27, either because the crop intercepted a much greater proportion of advected heat or because sensible heat on days with dry soil was intercepted by the crop. The latter phenomenon has been observed in a crop of bulrush millet (Begg *et al.*, 1964), so a mechanism was added to the millet model which allowed energy absorbed by the soil, which did not lead to evaporation, to be reflected back to the crop as sensible heat. The crop was assumed to absorb only a fraction of this sensible heat. This mechanism slightly increased the biomass and grain yields and improved the model simulations of the soil water content.

Water use was underestimated in the period between 55 and 70 days in all three fields. This period covers the end of flowering and the start of grain filling in the model. It is possible that the crops were still developing green structures (stems and leaves) during this time as a result of the earlier drought; while the model alters assimilate partitioning in response to drought, the phenological timing of the end of leaf emergence and the start of leaf senescence are fixed and are not influenced by water stress. Targeted field studies would be required to improve the simulation of the crop phenology.

4.1.3.2 Model performance in the towards crop maturity

During the final grain-filling stage, water loss was overestimated in the two bush fields. A comparison of the biomass:transpiration ratios showed that the model transpiration rate was too high in these two fields. Plant growth tends to slow in this stage as grains are relatively complex organs in comparison with the plant greenery and the plant needs to produce more complex molecules which require more energy per unit mass. Growth of the non-reproductive organs is impeded during this stage; in fact, assimilate is often transferred from the senescing leaves and the stem to the grains (in CROMSAS, the only plant demand in the final growth stage is from the stem and is limited to 10 % of the grain demand on that day). It was concluded that the millet crop was restricting the transpiration rate to that required for growth; as growth reduced towards harvest, transpiration also reduced. This conclusion is surprising because transpiration has often been viewed as a mechanism for limiting plant temperatures rather than a by-product of growth. By restricting transpiration, the plant conserves water for the future but at the cost of potential heat damage to itself.

Unfortunately, experiments that examine transpiration during grain-filling for high and low-yielding fields are rare; Azam-Ali *et al.* (1984b) examined three planting densities in Niger but the water loss for all three was very low in the final growth stage due to drought (less than 1 mm d^{-1}), so no conclusions could be drawn. Most field studies examine high-yielding crops at research stations where this phenomenon would not be observed and is generally not measured anyway.

A mechanism was added to the model to limit the transpiration rate as a function of the growth rate. If the assimilate production is limited by the transpiration rate then the water loss does not change, but if assimilate production is limited by radiation absorption or by a lack of demand for assimilate from the crop in the final growth stage then the transpiration rate is reduced appropriately. Unfortunately, this mechanism required several changes to CROMSAS. It was necessary to first calculate the assimilate demand, potential transpiration and potential growth. The actual growth rate was then calculated and finally the soil water balance and the plant growth were assessed. The mechanism had little effect on the house field but the water balance simulations in both bush fields improved. The water use was initially slightly low but this was rectified by introducing a lower transpiration efficiency parameter for the final growth stage to reflect the greater reduction in the photosynthetic efficiency when producing more complex molecules in the grains.

4.1.4 Balancing the model

A crop model has numerous interdependent parameters which drive many complex and variable processes. In general, field data are available for only a few of these parameters. The others are normally estimated and often calibrated so that the model simulations agree with field study observations. A concern for all modellers is the very real possibility that several parameters are inaccurately calibrated in a way that produces a good simulation for the test fields but is inaccurate elsewhere.

The calibration process for CROMSAS was designed to minimise such inaccuracies. Where available, parameters were taken from the literature or advice was sought from agronomists with experience in Senegal. Unfortunately, little information was available about the response of Souna millet to drought. For example, drought affects the partitioning fraction, which was simulated, and the phenological development rate, which was not. There was also little information about the growth of individual plant organs, although the outcomes could be inferred from observations of the roots, LAI and plant height. Fortunately, sensitivity studies showed that many parameters had little impact on the plant growth simulations and it was possible to identify a subset for calibration. Table 4.2 lists the most important parameters and the methods used to set each one.

The best strategy to avoid mis-calibration is to compare the model against studies of several fields with differing characteristics. The planting densities and the manure applications varied between fields at Sob which led to quite different growth characteristics (Table 4.1). With the exception of these crop management strategies, all of the parameters were the same for all three fields.

4.1.5 Results of the calibration exercise

The model simulations were compared with a range of field observations (the soil water content and LAI through the season, and the biomass and grain harvest yields). Many combinations of the parameters were tested to find the most appropriate calibration for all of these observations in all three fields, and to better understand the model sensitivity. Following calibration, the soil water loss was accurately simulated by the model in all three fields (see Section 4.1.3).

The observations and simulations of the LAI are shown in Figure 4.8. The LAI trend and magnitude are simulated reasonably well in all three fields. The

Parameter	Method to set the parameter
Light extinction coefficient, k_c	Estimated from the literature at 0.55 and verified by comparing the water use through the season and the biomass to transpiration ratio with observations
Radiation use efficiency, ϵ_c	Similar values as APSIM and RESCAP ($4\,\mathrm{g\,MJ^{-1}}$ PAR)
Transpiration use efficiency, TE	Estimated from the field study to balance the ratio of observed biomass to transpiration (see Section 4.2.5)
Water and nitrogen stress coeffs, $C_{sens_T}1$, $C_{sens_T}2$, $C_{sens_N}1$ and $C_{sens_N}2$	Both water and nitrogen stress constants are set to 1.0 for plant growth and 1.5 for leaf growth
Maximum evaporation depth	Set to 50 cm from sensitivity studies which compared the soil water content in the three fields in the early stages of plant growth
Root vertical growth rate	Calibrated in accordance with the deep soil water observations throughout growth
Leaf appearance rate	Taken from the literature (Ong, 1983a; van Oosterom *et al.*, 2001b) and photographs
Specific leaf area	Varies in the range 30–85 $\mathrm{m^2\,g^{-1}}$
Daily potential leaf extension	Relationship with temperature from Ong (1983c)
Maximum leaf size	Calibrated to 1 m from the field study LAI observations
Timing and rate of leaf senescence	Taken from the literature and calibrated for the field study LAI observations
Crop ET coefficient	Taken from Dancette (1983) for Souna millet
Coeffs for the number of grain sinks	Calibrated to simulate the final crop yield measurements

Table 4.2: Methods used to calibrate the most important parameters in the CROMSAS crop model. The importance of each parameter was assessed using sensitivity studies.

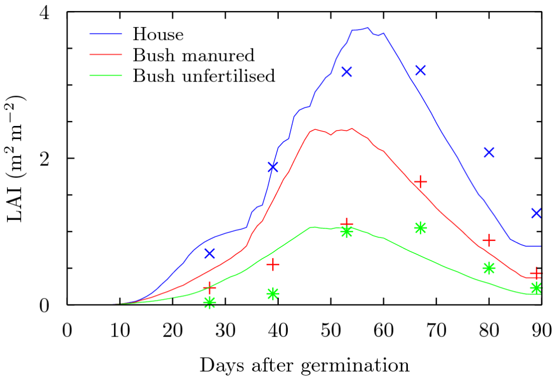

Figure 4.8: Observed and simulated LAI evolution in each Sob field in 1991. The points are the observations and the lines the CROMSAS simulations.

manured bush field LAI is overestimated in the early stages and the LAI peaks too early in both bush fields.

The measured and simulated grain and biomass yields are shown in Table 4.3. The biomass and grain yields are well simulated in all three fields. The simulated grain yield in the unfertilised bush field is overpredicted by the model, and the biomass underpredicted, although it should be noted that the harvest index of this crop (0.14) is substantially lower than that of the other crops. An examination of the ESPACE field database suggested that harvest indices were independent of the field type and fertilisation strategy so it is possible that this field is not representative of the larger region for reasons that could not be identified.

4.1.6 Discussion of the calibration findings

Three very different fields were used for the calibration. The model produced accurate estimates of the soil water content changes, the LAI evolution and the final biomass and grain yields. The simulation of the mini-drought in the first month was particularly pleasing as drought is difficult to simulate well because it requires all parts of the water balance and plant growth modules to be well balanced.

The GLAM water module was initially used but was did not simulate the water balance sufficiently accurately. Virtually all parts of the water module were redesigned during the calibration. Several new ideas were introduced:

	House field	**Bush fields**	
		Manured	**Unfertilised**
Measured grain yield	1654	800	269
CROMSAS grain yield	1694	745	345
Measured biomass	5743	3240*	1880
CROMSAS biomass	5990	3271	1438

Table 4.3: Comparison of the observed and modelled harvest yields for the three Sob fields in 1991. Simulated yields are presented for the full CROMSAS model and for the CROMSAS model with the GLAM water module. The house and manured bush fields were simulated receiving 127 kg ha^{-1} and 40 kg ha^{-1} manure, respectively, following the estimate of Affholder (1995). Measured yield data were also taken from this study. All of the yields have units kg ha^{-1}. *This yield was higher in the CIRAD ESPACE database (4187 kg ha^{-1}).

- the field capacity varies in each layer to allow heterogeneous soils to be simulated;
- plant growth can be affected by stored soil water from the previous year (the 'memory' effect, which is generally small but could be important under certain circumstances);
- drainage occurs faster than is possible under the scheme used in GLAM;
- soil evaporation reduces gradually from a maximum at the surface to zero at a depth of about 40 cm;
- the plant water uptake appears to be significantly higher than that found by Dardanelli *et al.* (2004);
- some of the energy that is intercepted by soil when it is dry appears to be convected to the crop as sensible heat;
- plant growth is often limited by the absorption of energy for transpiration, which includes advected heat from upwind regions, rather than the absorption of photosynthetic radiation; and,

- millet actively conserves water to the extent that it will close leaf stomata during grain-filling once the demand for assimilate has been met.

It was only possible to identify these phenomena because frequent high-quality measurements of soil water content were taken and because much information was recorded about each field. However, only three fields were tested and all had similar climatic conditions so these conclusions should ideally be tested in a larger, more extensive field experiment. This is particularly important for the parts of the model for which there was insufficient information to perform a proper calibration. The partitioning and organ growth need to be tested in a field experiment which considers a range of plant densities. In addition to the soil water content measurements, it would be very useful to record the total crop biomass and the biomass of each organ at frequent intervals throughout growth, and to observe the LAI and the extension of individual leaves more frequently. Reddy and Willey (1981) present a good experimental design for understanding the growth of a crop, although their study suffers from a lack of soil water content measurements.

One difficulty was the lack of information about rainfall runoff. In the early stages of growth in particular, the water loss could not be explained without assuming significant runoff (perhaps resulting from the soil being encrusted after a long hot dry season). In future field studies, additional measurements in the early stages of growth would be informative. For this study, since runoff can significantly impact the crop yield, it seems appropriate to perform one set of calculations with no runoff and another set with significant runoff, following the approach of Affholder (1997).

4.2 Evaluation of the CROMSAS model

It is difficult to comprehensively evaluate the skill of a crop model. The nature of the assessment depends on the purpose and required accuracy of the model (Monteith, 1996; Wallach, 2006b). For example, the evaluation of a model which is designed to accurately simulate the yield of a particular crop in an irrigated field, as a function of the fertiliser application, will be quite different to a research model that is used to estimate the yield of several crop varieties, in several regions, in variable rainfed fields. In the former case, the variability is limited but accurate simulations are expected. For the latter, which is closer to the purpose of CROMSAS, the required accuracy is lower but the climatic range is much broader and the fields are much more variable.

The term 'model validation' is often used in the literature as an assessment of whether the model is adequate for its intended purpose (Wallach, 2006b). The model is judged against its objective and it is either deemed suitable or unsuitable. CROMSAS has a wide-ranging objective: to simulate crop yields under a wide range of environmental and management conditions. There are insufficient field data to perform a thorough assessment in every possible environment under all conditions. A broader approach is adopted here which uses a diverse set of studies to consider whether the model simulations adequately represent crop responses to environmental conditions, so the term 'evaluation' is used in preference to 'validation'.

Plants are complex organisms and under identical environmental conditions, different varieties of the same species can react quite differently. Many different millet varieties are used across the Sahel; for example, in northern Nigeria the range of genotypes within a village is often greater than the range between villages (Mortimore and Adams, 1999). Souna is an improved cultivar but many farmers in Senegal still use traditional varieties. The differences between Souna and the traditional varieties were discussed in Section 3.1 and are further examined in Section 4.2.4.1.

In view of these difficulties, a thorough evaluation often involves several components. For example, Challinor *et al.* (2004) examine the consistency of the GLAM simulations against field observations from the literature and assess the skill of the model using statistical weather—yield correlations. The evaluation of CROMSAS also had several components. The principal component was a comparison of model simulations against measurements from Senegalese fields. Sensitivity studies were performed to characterise the model response to a range of meteorological data. The model skill to simulate the impact of crop management strategies (nitrogen application, planting date and planting density) was also considered. Finally, the consistency of the parameters with the literature was examined.

4.2.1 Evaluation against the SARRA-millet model fields

The millet fields identified by Affholder (1997) to evaluate the SARRA-millet crop model were extracted from the ESPACE database. The original study used 89 fields but these were found to consist of 80 unique fields and 9 duplicates with slightly different parameters. Other fields in the database were excluded because at least one of the following occurred: *a*) rainfall data were not available for the village; *b*) a substantial part of the field was replanted, so effectively two crops sown on different dates were present (only fields which were not replanted or were totally replanted were considered); *c*) the grain and ear yields were poorly correlated (normally the grain yield was approximately 60 % of the ear yield, and large deviations indicated errors in the measurements); and, *d*) the three harvest samples in each field differed substantially, indicating that the yield across the field was too heterogeneous. Affholder (1997) achieved a close correlation ($R^2 = 0.76$) between his model and the experimental grain yields, so this dataset presented a good opportunity to test the CROMSAS simulations.

The 9 duplicated fields were discarded. Each of the remaining fields was unique, with the rainfall, soil, topography, pests, disease, planting pattern, fertiliser application and weeding intensity all varying. The observed grain yield was invariably affected by several of these factors so each simulated field required an individually-calibrated plant-accessible nitrogen supply. Unfortunately, although the study recorded the type of fertilisation, the quantity of fertiliser that was applied to each field was not measured so it was difficult to relate the actual nitrogen application to the nitrogen content of the crop. One method would have been to calibrate the accessible nitrogen in each field to simulate the correct grain yield, but this would have rendered the evaluation pointless. Instead, for fields receiving manure or mineral fertiliser, it was assumed that similar quantities were used on all fields in each category (house, bush or distant). Fields that had been fallowed were assumed to be more fertile than those that had been cropped in the previous year. The total accessible nitrogen in each field was estimated from these assumptions and used by CROMSAS to simulate the crop yields.

4.2.1.1 Quantification of the model performance

The simulated yields are compared to experimental yields in Figure 4.9a. There was a close correlation between measurements and simulations of $R^2 = 0.71$, slightly lower than the correlation of $R^2 = 0.76$ achieved by the SARRA-millet model (Figure 4.9d) of Affholder (1997). The SARRA-millet model and the original data could not be traced but it was possible to retrieve some data of unknown provenance. The field fertility was calculated for SARRA-millet as a function of both the fertilisation strategy and the clay and silt content of the soil. Soil data were not available more widely so the field fertility in CROMSAS was calculated as a function of only the fertilisation strategy.

The CROMSAS grain yield root mean squared error (RMSE) was 292 $\mathrm{kg\,ha^{-1}}$ and the mean absolute error (MAE) was 234 $\mathrm{kg\,ha^{-1}}$. There was a small model bias with the simulated yields exceeding the measured yields by an average 45 $\mathrm{kg\,ha^{-1}}$. The maximum error, an underprediction of 637 $\mathrm{kg\,ha^{-1}}$, occurred in a field where the duration of crop development was underpredicted. The relative root mean squared error (RRMSE) can be used to compare the skill of the model against other models. The RRMSE for CROMSAS was 34 %, close to the 32 % achieved by the SARRA-millet model (Affholder, 1997).

The simulated biomass yields at harvest in Figure 4.9b were slightly lower than the measured yields with a bias of 228 $\mathrm{kg\,ha^{-1}}$ and with $R^2 = 0.57$. The biomass residues (the differences between measured and simulated yields) in Figure 4.10b show that the higher yields tend to be underpredicted while lower yields are overpredicted. One contribution to this trend might be errors in the estimation of the plant-available nitrogen for some fields, but the most likely cause is discrepancies between the actual and simulated duration of crop development. This issue is discussed in Section 4.2.4.1.

It is interesting to compare the CROMSAS predictions with the performance of the model prior to changing the soil water sub-model. Figure 4.9c shows that the correlation is poorer ($R^2 = 0.54$) with underpredictions for fields with

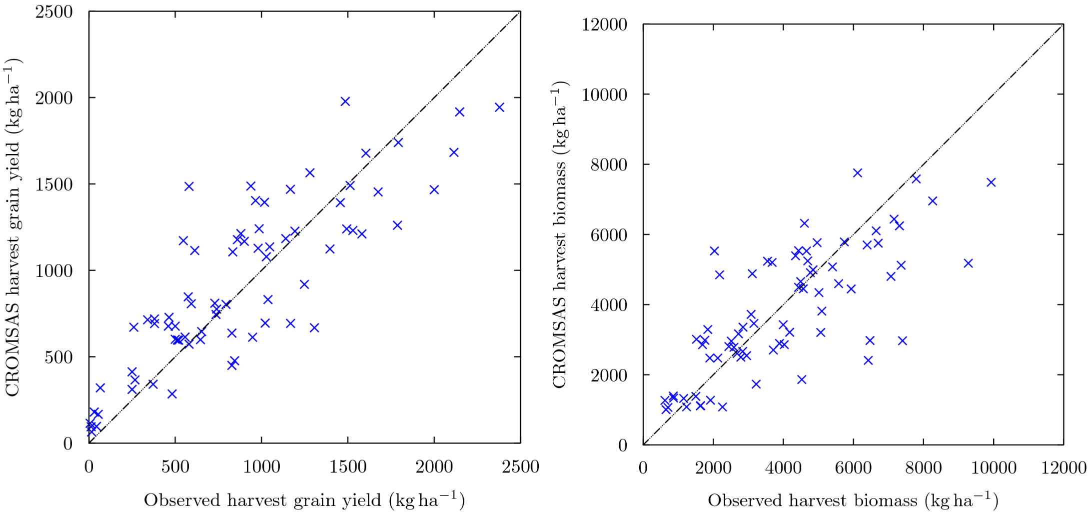

(a) CROMSAS grain yield (b) CROMSAS biomass

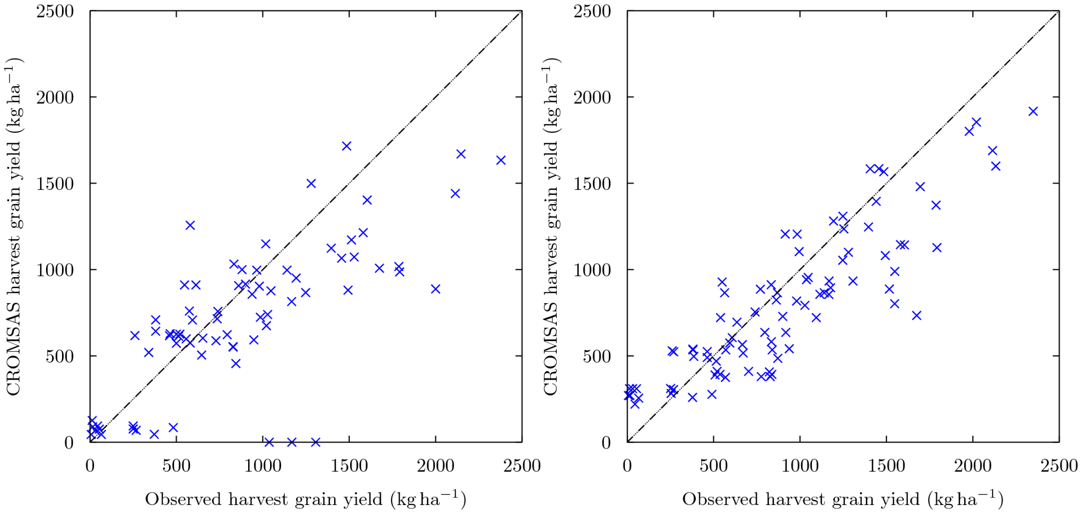

(c) CROMSAS original water sub-model (d) Affholder model grain yield

Figure 4.9: Evaluation of CROMSAS yield predictions for 80 smallholder fields in Senegal. The accessible nitrogen in each field was estimated because measurements of manure and mineral fertiliser application were not available. The soil water capacities were based on the measurements of IRAT (1983) and the soil was at wilting point at the start of the year. The original water sub-model was similar to the soil water method used by GLAM (Challinor *et al.*, 2004). The fields were chosen by Affholder (1997) and the results of his SARRA-millet model are shown for comparison.

higher yields and with several fields being simulated failing to produce grain. The simulated biomass yields (not shown) were also substantially poorer with a 1063 kg ha^{-1} bias and $R^2 = 0.29$.

The model grain yield residues are shown in Figure 4.10a. There is a similar but less pronounced trend to the biomass yields with higher yields being underpredicted and lower yields being overpredicted. The most likely causes are the discrepancies between the actual and simulated duration of crop development that were mentioned earlier and errors in the estimate of available nitrogen in each field.

It is useful to graph the residues against important model variables to identify any systematic errors in the model. Figure 4.10c shows the residues plotted against the plant density in each field. There is no trend that would indicate that any systematic error is affecting the simulation of the planting density. A similar graph of the residues plotted against the nitrogen application is shown in Figure 4.10d. Again, the lack of any bias suggests that the results are not skewed as a function of the nitrogen parameterisations, although the usefulness of this particular graph is limited because the field fertility is estimated rather than being measured so no authoritative conclusions can be reached without further field studies.

4.2.1.2 Evaluation against the ESPACE database fields

The performance of the ESPACE model was also compared with measurements of all of the fields in the ESPACE database for which there was sufficient information (408 fields in total). It became clear that the data quality of the larger dataset was insufficient to allow the fertilisation strategy to be estimated to an adequate accuracy. Instead, an alternative evaluation method was used which examined whether the model simulations, when operating under ideal conditions, produced yield forecasts which bounded the observed yields in each field. Sultan *et al.* (2005) also used this approach to evaluate the SARRA-H model. CROMSAS was run with daily rainfall data measured in each village and with the potential evapotranspiration calculated using the FAO56 method (see Section 5.2.3 for a description of evapotranspiration methodologies).

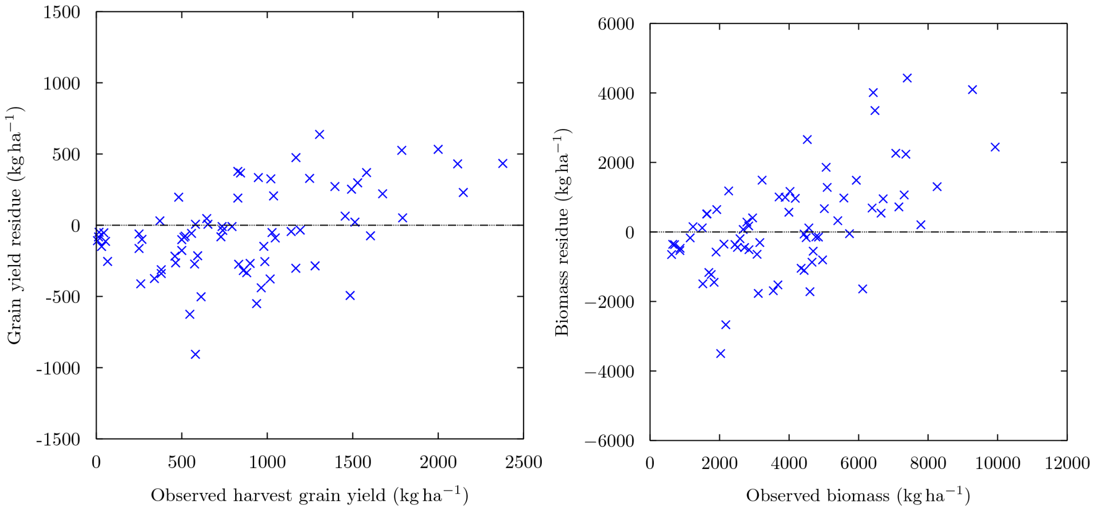

(a) Grain yield residues (b) Biomass residues

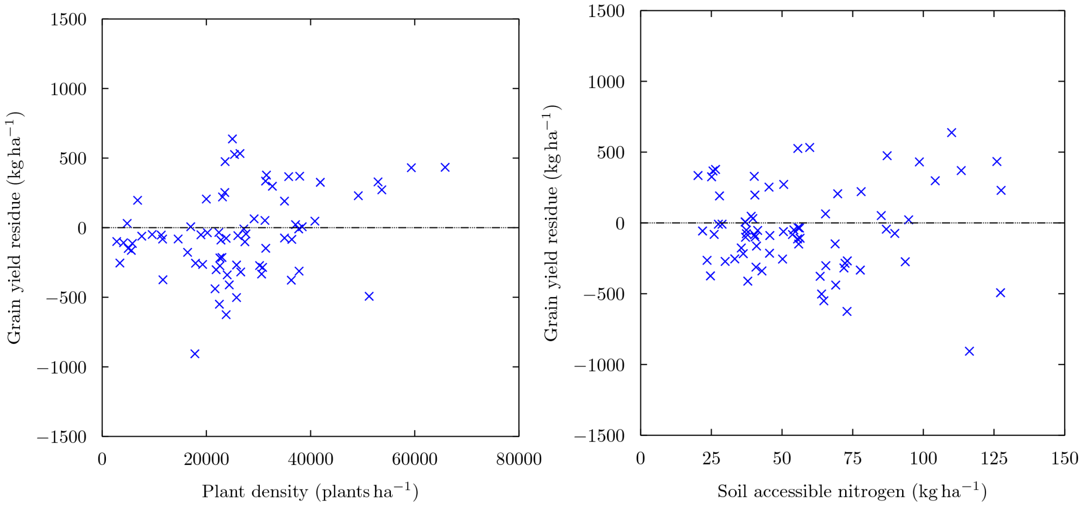

(c) Residues and plant density (d) Residues and soil fertility

Figure 4.10: Yield residues from the CROMSAS evaluation with smallholder fields. The residues are the difference between the measured yield and the model yield. The plant densities were measured at harvest. The accessible nitrogen in each field was estimated as measurements of manure and mineral fertiliser application were not available. The fields were chosen by Affholder (1997).

The observed and simulated biomass yields are shown in Figure 4.11b. All of the fields which lie to the top left of the line have observed yields that are lower that the simulated yield. A number of fields lie to the bottom right of the line; these had higher observed than simulated yields so these simulations were inconsistent with the field study. The majority of the fields with the poorest simulations were in the village of Keur Lamine (denoted with red crosses). This village is located further south than the others and smallholders appear to take advantage of the longer growing season by cultivating longer-duration varieties of millet. CROMSAS underestimated the duration of growth and hence underestimated the yield. A secondary reason for underpredicting some fields in Keur Lamine was the assumption that 'ideal conditions' was equivalent to an unlimited nitrogen supply. Using an unlimited nitrogen supply led to water stress during grain filling which reduced the harvest yields. Higher biomass and grain yields were simulated when the nitrogen supply was limited because the soil water was used less quickly. Affholder (1995) observed the same phenomenon in fields of the village of Sob in 1990.

The grain yield predictions were better than the biomass predictions, with only 3 % of the fields having grain yield discrepancies (Figure 4.11a). Longer-duration millets produce substantially more biomass than short-duration varieties but have lower harvest indices so the grain yield difference is much lower. The highest model yield was approximately 500 kg ha^{-1} higher than the highest observed yield, which raised concern that the model could be overestimating grain yields in good conditions. However, higher grain yields than those predicted by CROMSAS have been achieved under ideal conditions at research stations (Baron *et al.*, 2005) so this yield gap could simply reflect other on-farm difficulties (e.g. weeds, pest damage and soil deficiencies) that were not simulated by CROMSAS.

4.2.2 Sensitivity to environmental variations

The ESPACE field observations that were used to evaluate the performance of CROMSAS in the previous section were taken over only four years so do not fully represent the wide range of meteorological conditions that are found in Senegal over long time periods. A sensitivity study can be used to assess how the model

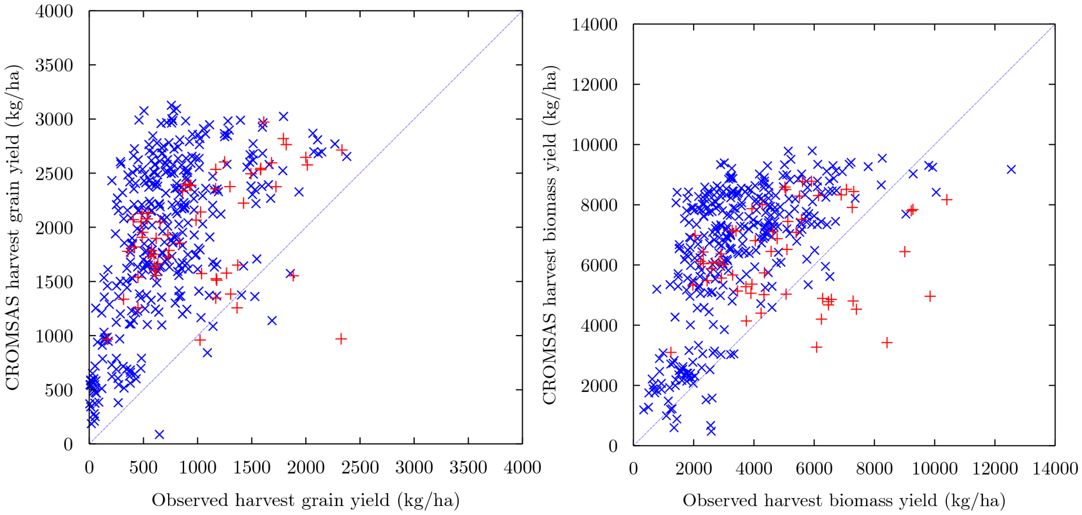

(a) Grain (b) Biomass

Figure 4.11: Comparison of observed and simulated maximum yields for smallholder fields in Senegal. The fields from the village of Keur Lamine are denoted with red crosses. The soil water capacities were based on the measurements of IRAT (1983) and the soil was at wilting point at the start of the year.

responds to a large range of environmental conditions, with the aim of identifying whether the model behaviour is consistent with expectations (Monod *et al.*, 2006). This section presents a number of sensitivity studies that examine the response of CROMSAS to changes in the rainfall, potential evapotranspiration, temperature and soil water-holding capacity. The impacts of varying the root growth rate and the LAI are also examined.

4.2.2.1 Sensitivity to idealistic climatic and soil variations

A particular difficulty with any sensitivity study that examines the impact of drought is that the impact of each parameter depends on the other parameters and the exogenous data; for example, the root growth rate will be very important in cases where deep soil water is required to support plant growth, but unimportant where the rainfall does not penetrate through the upper soil layers during a season. The impact of these difficulties can be reduced by using a probabilistic approach which includes many simulations that are created using either deterministic or stochastic (e.g. Monte Carlo) processes. A deterministic methodology was used here. A typical value was calculated for each variable by averaging meteorological data from the Bambey research station in Senegal. The variability in that value was assessed and used to define a range of either three or five alternative values for each variable. Simulations were performed for all possible combinations of the values and the grain yield and water stress were averaged for each range.

An idealistic weather dataset was created for the sensitivity studies. Rainfall was assumed to occur at regular intervals over four months between June and September. Table 4.4 shows the typical values and variations. The rainfall frequency refers to the period between each rainfall event; the total rainfall was conserved so there were longer gaps between larger events. Solar radiation, temperatures and the VPD were constant throughout the year. The crop was always planted after the first rainfall, on 9 June, at a planting density of 8 plants m^{-1}. The calculations were performed for all five soil categories in the ESPACE project. Variations in the potential evapotranspiration and rainfall (both magnitude and distribution) were tested.

The first sensitivity study used a fixed LAI shape throughout plant development which was independent of the crop growth rate. This removed the non-linear behaviour discussed earlier. The peak LAI was chosen for a well-fertilised crop with no nitrogen stress. Table 4.5 shows the impact of each factor on the grain yield, with each value representing the average of more than 1000 simulations. The means of each variable can be compared to identify how that variable affects the simulation. The coefficient of variation indicates the relative importance of the variable: smaller values indicate that the crop yields are particularly sensitive to the variable.

The soil type had little influence on the grain yield; the lowest yield was simulated for sand because these soils have lower water capacities so dry out more quickly (the impact of increased runoff in the other fields due to slower soil drainage was not simulated).

The influence of the LAI is more pronounced, particularly for the lowest peak value of 1.2, because the reduction in the absorption of solar radiation and advected energy leads to a reduction in the growth and transpiration rates.

	Typical Value	**Other values**			
		1	2	3	4
Maximum LAI	2.4		−50 %	+50 %	
Root growth rate	3 cm d^{-1}		−50 %	+50 %	
ETo	5.5 mm	−15 %	−7.5 %	+7.5 %	+15 %
Total rainfall	480 mm	−75 %	−37.5 %	+37.5 %	+75 %
Rainfall frequency	14 days	1	7	21	28
Solar radiation	24 MJ m^{-2} d^{-1}				
Maximum temperature	40 °C				
Minimum temperature	20 °C				
VPD	1.6 kPa				

Table 4.4: Plant growth and meteorological values for the idealistic sensitivity study. Up to four alternatives are used around the typical value. Percentages indicate the change from the typical value. Data are typical values and variances for the research station at Bambey.

The roots only reach a depth of around 90 cm in the slowest root growth simulations and the grain yields reduce substantially because much of the soil water is unavailable to the plant. Increasing the root growth rate beyond 2.4 m has only a minor effect on the biomass yield because the total rainfall is too low to penetrate to depths beyond 2 m.

The simulations of the potential evapotranspiration (ETo) are particularly interesting. Increasing the ETo causes the overall yield to increase at first because the transpiration rate (the main factor that is limiting growth) increases. The yield begins to fall at the highest ETo as a result of water stress.

The most important variable is the rainfall magnitude because the interannual range is so large. The grain yield increases rapidly as the rainfall magnitude is increased, as demonstrated by the low CV in comparison with the other variables. The rainfall frequency can also be important. When small quantities of rainfall occur daily, a greater proportion of soil water is lost to evaporation so growth is slower. Conversely, widely-spaced rainfall events provide a great deal of rainfall at once which percolates to the deeper soil layers, but the upper layers dry out

		Grain yield		
		Mean	Stdev	CV
Soil type	Sand	974	768	0.79
	Silt	1104	856	0.78
	Clay	1093	847	0.77
	Gravel	1060	818	0.77
	Sand/clay	1060	822	0.78
LAI factor	1.2	857	497	0.58
	2.4	1080	809	0.75
	3.6	1238	1031	0.83
Root growth factor (cm/d)	1.5	901	696	0.77
	3	1115	841	0.75
	4.5	1158	899	0.78
ETo magnitude (mm)	4.7	1029	722	0.70
	5.1	1053	779	0.74
	5.5	1067	831	0.78
	5.9	1074	873	0.81
	6.3	1068	902	0.84
Rainfall magnitude (mm)	120	47	32	0.68
	298	525	242	0.49
	480	1219	383	0.31
	662	1668	601	0.36
	840	1831	724	0.40
Rainfall frequency (days)	1	784	702	0.90
	7	1169	848	0.73
	14	1272	870	0.68
	21	1024	821	0.80
	28	1042	787	0.76

Table 4.5: Influence of the environment and plant development on the grain yield ($\mathrm{kg\,ha^{-1}}$). Each mean, standard deviation (Stdev) and coefficient of variation (CV) represents more than 1000 simulations. See the text for more details.

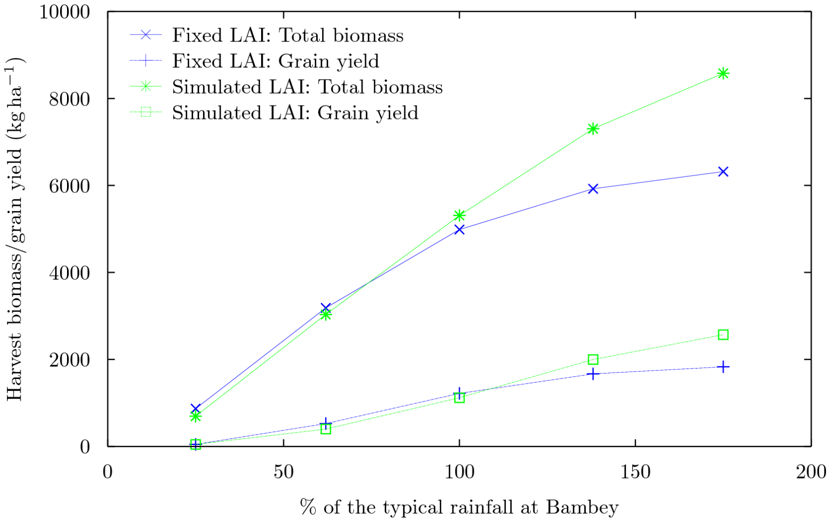

Figure 4.12: Sensitivity of the biomass and grain yield to rainfall. The first study uses a fixed LAI shape with a peak LAI of 2.4, while the second study dynamically simulates LAI. Each value is an average of approximately 1000 deterministic simulations.

between events and water stress occurs if the roots have not penetrated deeply enough.

The first sensitivity study used a fixed LAI to limit non-linear behaviour so that the impact of changing each parameter could be clearly observed. Since this is not representative of reality, a second study was performed with the LAI simulated by the model. Figure 4.12 shows that both the grain and biomass yields were larger in the dynamic-LAI simulations when rainfall was plentiful, as leaf growth responded to favourable conditions, but that there was little difference otherwise. The dynamic-LAI simulations produced similar trends to those described above for the fixed-LAI simulations.

4.2.2.2 Sensitivity to climatic and soil variations for a range of rainfall distributions

One weakness of the idealistic study was that the simulated rainfall distribution was very regular and not representative of the irregular distributions that are normally observed in the Sahel. To examine the simulations under a range of rainfall patterns, the sensitivity study was repeated for each annual rainfall pattern that was observed at Bambey in the years 1975 to 1991. The magnitude of each rainfall event was normalised so that the total rainfall each season equalled the totals in the idealistic study. The crops were planted after the first large rainfall event each year. The observed meteorological data from each year were used instead of idealised data so that the climate data would be internally consistent. This particular range of years was chosen because pan evaporation data were available and because the quality and availability of the meteorological data were particularly good.

Figure 4.13 shows histograms of the grain yields for the five rainfall magnitudes (vertically) and for three methods of calculating the reference evapotranspiration (ETo, horizontally). The rainfall in each year was normalised to the amount shown on the graph so only the rainfall distribution differed between years. The LAI was simulated by CROMSAS. In this figure, each of the 5625 simulations is an average of the 17 annual rainfall distributions from 1975–1991. Grain yields are all below 500 kg ha^{-1} at 120 mm rainfall. Yields increase with rainfall and the variability also increases, with a 1000 kg ha^{-1} range being simulated at 840 mm.

The FAO56 histograms are similar to the pan evaporation histograms at all rainfall magnitudes and, on this evidence, the FAO56 method is the most suitable for estimating the ETo. The FAO24 histograms are less similar but would still produce acceptable estimations.

The second series of graphs, in Figure 4.14 shows the interannual impact of the rainfall distribution. The rainfall in each year was normalised to 480 mm and the crops were planted following the first rainfall event. The rainfall distribution clearly has a strong influence on crop yield. In some years (e.g. 1975) the range of yields is very wide, while in others (e.g. 1984) there is little variation between runs. Rainfall distribution has a non-linear influence on grain yields. In countries like Senegal, where the influence is strong, statistical models of crop yields will produce poor results and it is necessary to use a crop model to produce reasonable yield projections.

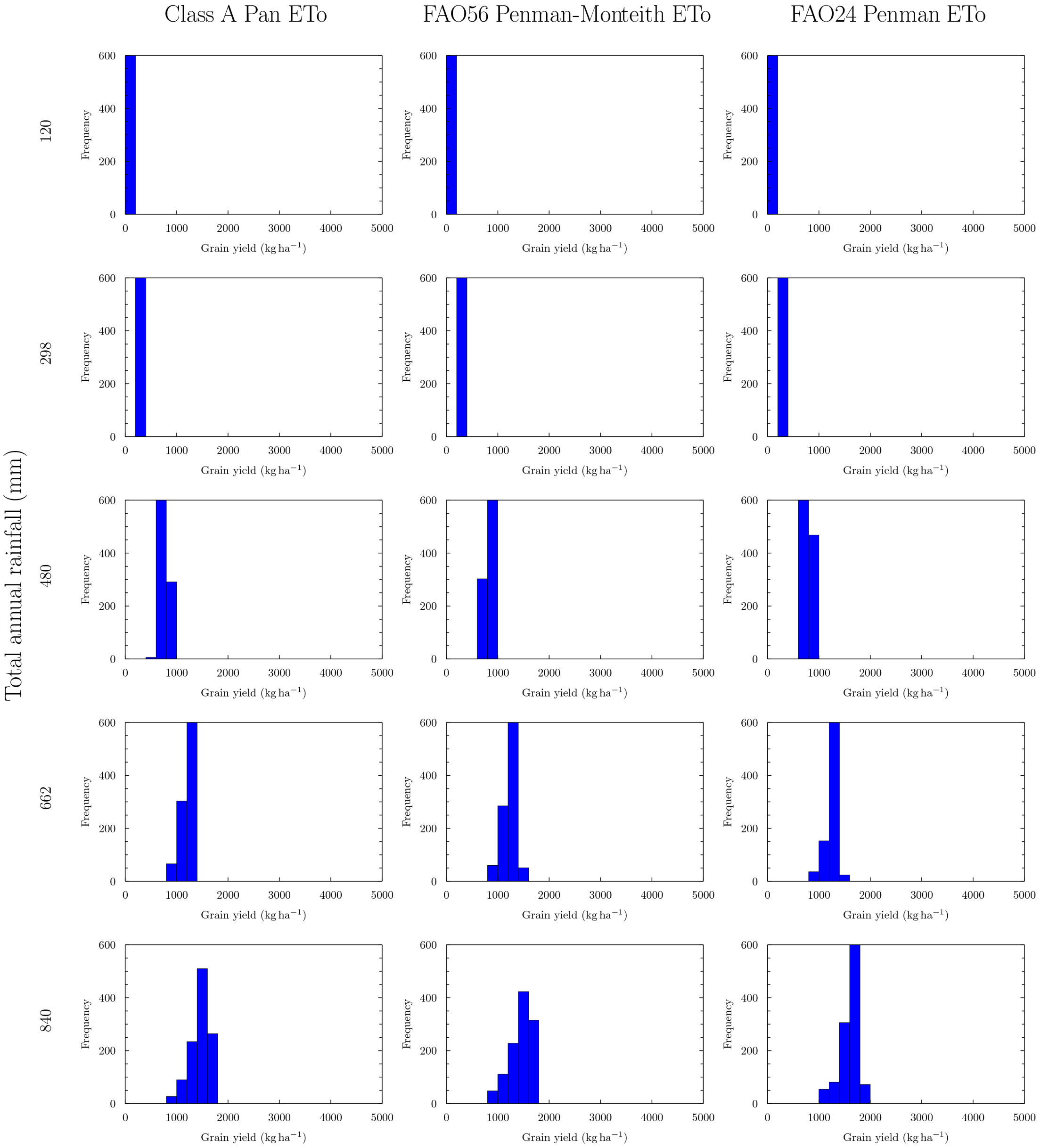

Figure 4.13: Histograms of the grain yields for the five rainfall magnitudes and for the three ETo methods (Pan, FAO24 and FAO56). Each histogram shows 1125 simulations, with each simulation being an average of the grain yield for 17 different rainfall distributions, which were taken from Bambey for the years 1975–1991. The total rainfall is normalised to the value shown to the left of the graphs. The LAI was simulated by the model in all of the runs.

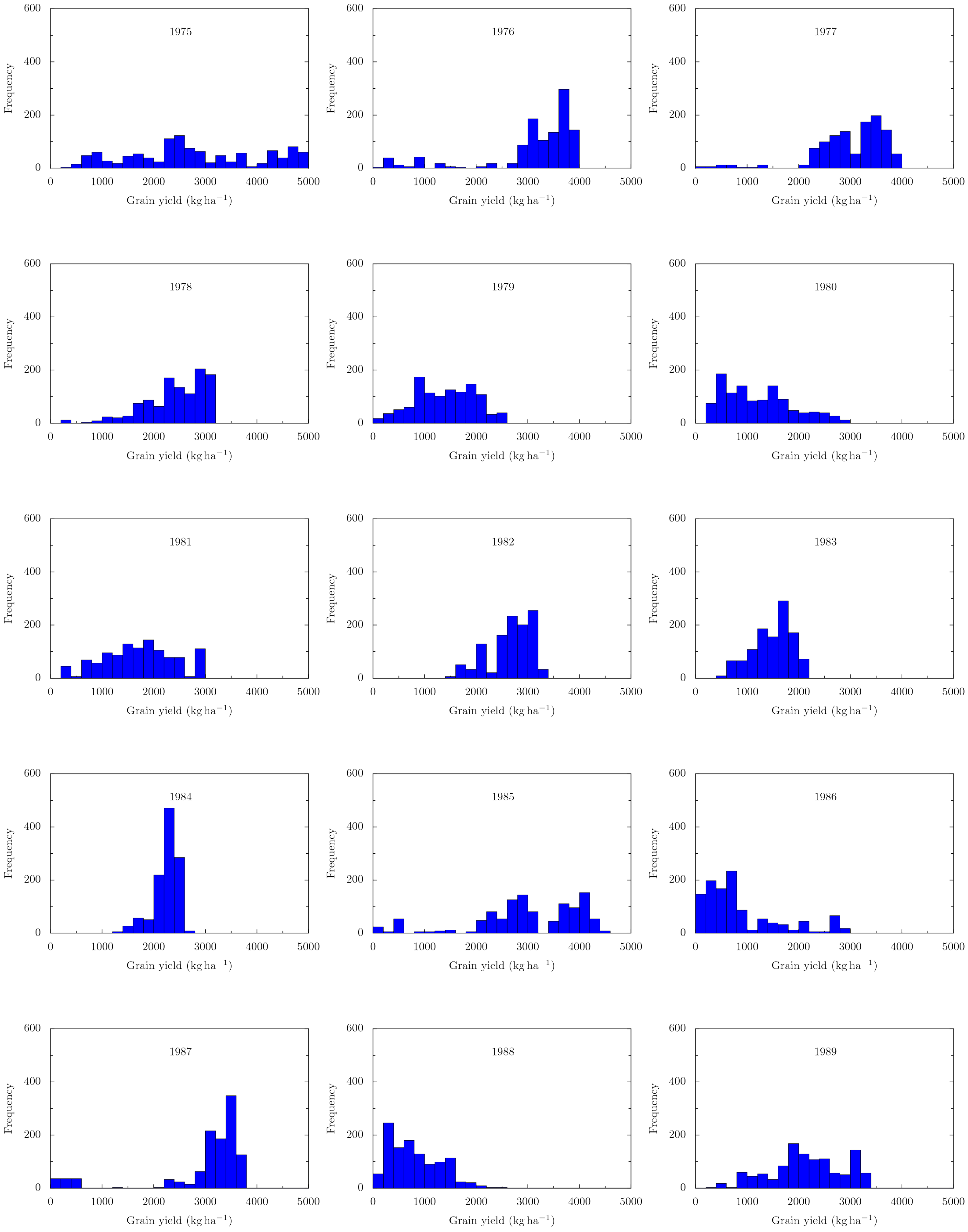

Figure 4.14: Impact of the rainfall distribution at Bambey in the period 1977–1990 on grain yields. The total rainfall each year is normalised to 480 mm.

4.2.3 Sensitivity to temperature

CROMSAS is designed to simulate the impact of climate change on crop yields so it is important that the model responds accurately to temperature variations. This sensitivity study examined the model response to a range of average temperatures from 0 ℃ to 50 ℃. The diurnal range was assumed to be 10 ℃ in each case so, for example, an average temperature of 35 ℃ was simulated as $T_{min} = 30$ ℃ and $T_{min} = 40$ ℃. The study used the sensitivity model described above with a fixed VPD at all temperatures.

There was a complex interaction between temperature and rainfall for both the grain and biomass yields, as shown in Figures 4.15a and 4.15b. The highest yields were simulated at around 20 ℃ for 840 mm rainfall and at 25 ℃ for lower rainfall. The crop development duration is substantially longer at 20 ℃ than 25 ℃ and this increases crop growth if there is sufficient water. For this reason, biomass production peaks at an even lower temperature, even though no grain sinks are formed because the temperature is too low. Millet is cultivated as a forage crop as far north as Denmark because of the high biomass yields that can be produced at low temperatures. Grain yields reduce to a minimum at 33 ℃ because the crop duration is a minimum at this temperature. Yields increase again beyond 33 ℃ until high temperature damage reduces the number of grain sinks.

The number of grain sinks is not reduced by temperature damage in the range 25 ℃–35 ℃ so peaks at 25 ℃ due to the longer crop duration (Figure 4.15c). Grains are simulated growing by the same amount each day so the individual grain mass peaks at 20 ℃ because of the long duration of grain-filling. These simulations are consistent with the experimental studies of Fussell *et al.* (1980) and Ong and Squire (1984).

Some sensitivity studies are shown in Figure 4.15d. A fixed VPD is an unrealistic assumption when the temperature is changing so the calculations were repeated with the VPD being estimated from the temperature. As expected, low VPDs at lower temperatures led to higher yields while high VPDs depressed yields at high temperatures. Another study was performed to examine how temperature influences the number of grain sinks in the simulations. Removing temperature

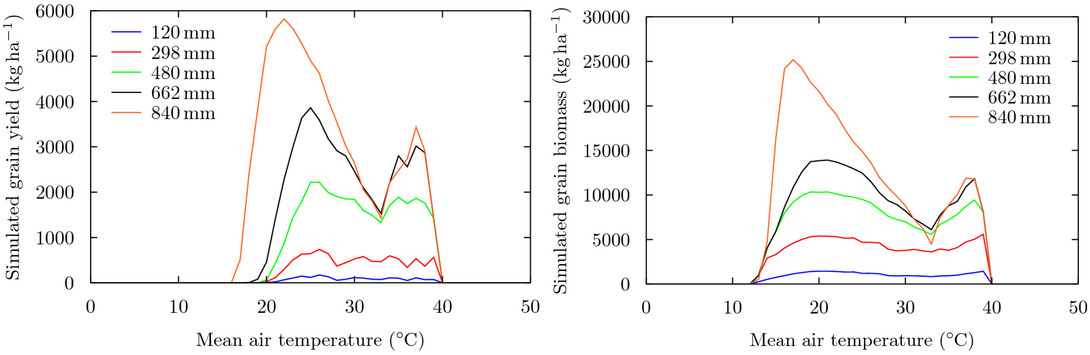

(a) Yield (b) Biomass

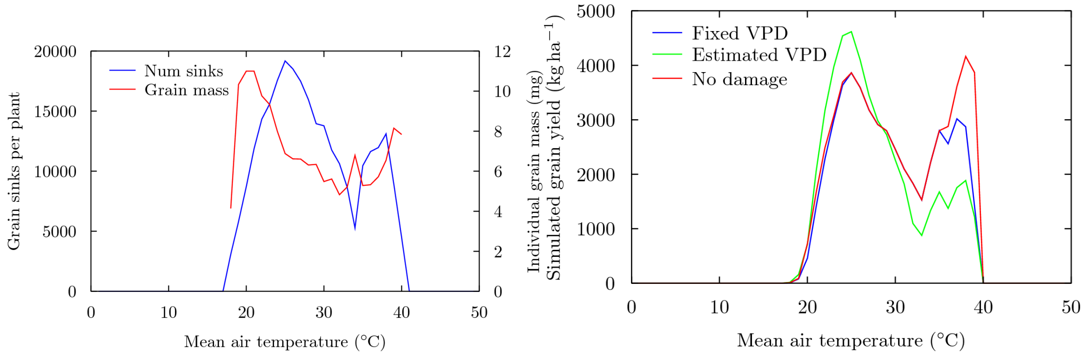

(c) Grain statistics (d) Yield variations

Figure 4.15: Sensitivity of CROMSAS to temperature variations. All of the other variables were held constant except for the VPD in the yield variations graph. The grain size and number of grain sinks were simulated for 840 mm rainfall.

damage caused little change at low temperatures but very high yields at high temperatures with the peak yield at 38 °C. This behaviour seems unrealistic and is contrary to the experimental study of Ashraf and Hafeez (2004), who observed reduced yields at high temperature.

4.2.4 Simulating crop management strategies

CROMSAS simulations of varying planting dates, planting densities and nitrogen management strategies were evaluated to confirm that the model could be used for crop management strategy simulations.

4.2.4.1 Planting date evaluation

The influence of the planting date on crop growth was examined in Section 2.2.2, with the review concluding that it is necessary for crop models to simulate the rate of crop development and the impact of extreme temperatures and water stress on the crop. The Sahel has a short monsoonal rainy season so there is limited flexibility to change the planting date; crops must be planted after the first rains and must complete grain-filling before the soil moisture is depleted if high yields are to be achieved. Previous studies have examined whether planting should be delayed beyond the start of the first rains; for example, Sivakumar (1988) identified a relationship between the date of onset of rains and the length of the rainy season across Niger and Sultan *et al.* (2005) examined the best long-term planting date using a model for one of those locations. Bacci *et al.* (1999) examined two planting dates in a field experiment in Mali, with the first planting at the beginning of the rainy season and the second delayed by 20 days, but found no statistical differences in yields. Experimental planting date studies are expensive and time-consuming to perform (Soler *et al.*, 2008) and are likely to have little practical impact compared to, for example, nitrogen application experiments, and no comprehensive, systematic field studies of the impact of changing the planting date in the Sahel have been published.

The influence of temperature and rainfall on the CROMSAS predictions are discussed in Section 4.2.2.1. The ESPACE database contained the most comprehensive survey of planting patterns so was used to examine the impact of the planting date on the duration of crop growth; since harvest dates were only collected in a minority of the villages, the whole millet database was used. Based on the GS1 duration measurements that were discussed in Section 3.3.1, it was expected that the choice of planting date would have little influence on the crop duration because the temperature is reasonably constant throughout the growing season, but Figure 4.16a shows that the discrepancy in the simulated duration of growth ranged from an underestimation of 60 days to an overestimation of 25 days. Figure 4.16b suggests that the mean harvest date is weakly dependent on the planting date, either as a result of longer-duration millets being selected for earlier planting dates or because the varieties used were strongly photoperiodic.

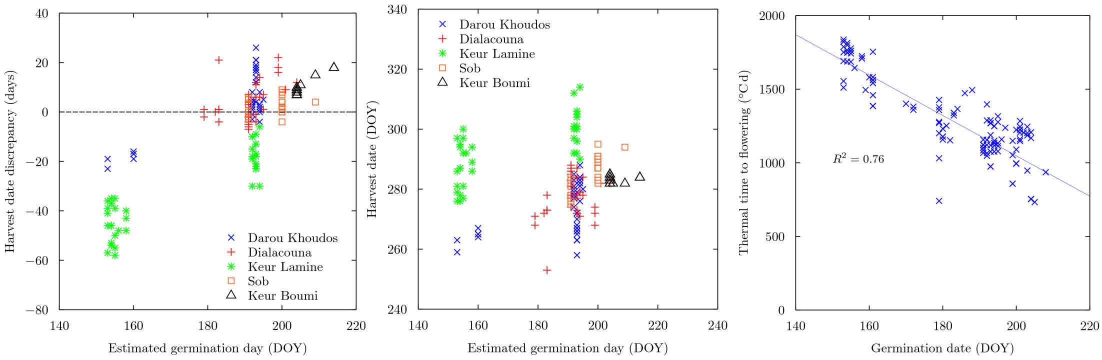

(a) Harvest date discrepancies (b) Observed duration dates (c) Photoperiodicity of millet

Figure 4.16: Harvest date simulation discrepancies and photoperiodicity of millet in Senegal. The harvest date discrepancy is the difference between the experimental day of the year (DOY) and the CROMSAS DOY. The thermal time values in the photoperiodicity graph were calculated using Equation 3.1. The field data were extracted from the ESPACE database Affholder (1992).

The photoperiodicity is examined in Figure 4.16c, which shows a close relationship between the germination date and the thermal time to flowering and suggests that some of the varieties are strongly photoperiodic (note that there were difficulties identifying the correct flowering date in some cases as there were different observers in each village and the definition of the flowering date was interpreted differently by each observer; dates from the time of panicle initiation to the end of flowering were recorded). While thermal time is plotted in this graph, there is no evidence from these results that the time to panicle initiation is sensitive to temperature because the temperatures were reasonably constant throughout growth in all villages.

The Souna variety and the Serere 10 B variety that was examined in Section 3.3.1 are improved varieties of millet. In contrast, most of the varieties in the ESPACE database, including all of those that are planted early in the season, are recorded as local varieties. One of the major goals of plant breeding in the past has been to remove photoperiodic behaviour, but late flowering has the advantage of avoiding yield losses that result from heavy rain during grain-filling, and the additional biomass provides extra feed for livestock (Niangado, 2001).

The varieties in the ESPACE database must be strongly photoperiodic since the longest day in Senegal has only 13 hours of sunlight.

The most evident differences between varieties are the rate of development and the photoperiodic sensitivity (Carberry and Campbell, 1985; Craufurd and Bidinger, 1988b). CROMSAS should accurately simulate the impact of changing the planting date of Souna millet as the impacts of drought are simulated (Sections 4.2.1 and 4.2.2) but the model will not accurately simulate the duration of local strongly-photoperiodic varieties without appropriate re-calibration of the crop phenological development.

Figures 4.16a and 4.16b show that the duration varies substantially between varieties in different villages. However, there is also great variety within villages with some crops maturing 30 days earlier than other crops. A series of millet varieties could be defined from these data, with perhaps 1–2 varieties per village, which differ only in the development time and sensitivity to photoperiod. The benefits of a crop management strategy which uses alternative varieties could then be assessed. Changing crop varieties could be a particularly important strategy to reduce the impacts of climate change. Such an investigation is not included in this thesis but is a potential future investigation (Section 8.2).

A sensitivity study was performed to examine the long-term impact of changing the planting date by examining the relationship between the planting date and the grain yield throughout each year at Bambey in the period 1977–1991. Figure 4.17 shows that there are substantial variations in the yields each year. The crops did not suffer nitrogen stress and temperatures varied little through the season, so the differences were caused by the rainfall pattern. The first possible planting date each year varied between mid-May and the start of July. In contrast, the end of the season was more stable and crops not planted by the end of August produced poor yields. In some years, planting early produced high yields, while it was better to delay planting in other years. Crop management simulations are used to identify the optimum planting dates in Senegal in Chapter 6.

4.2.4.2 Planting density evaluation

An experiment was performed at Niger to examine the growth of millet at three planting densities (2.9, 5.8 and 11.5 $\text{plants}\,\text{m}^{-2}$, denoted wide, medium and nar-

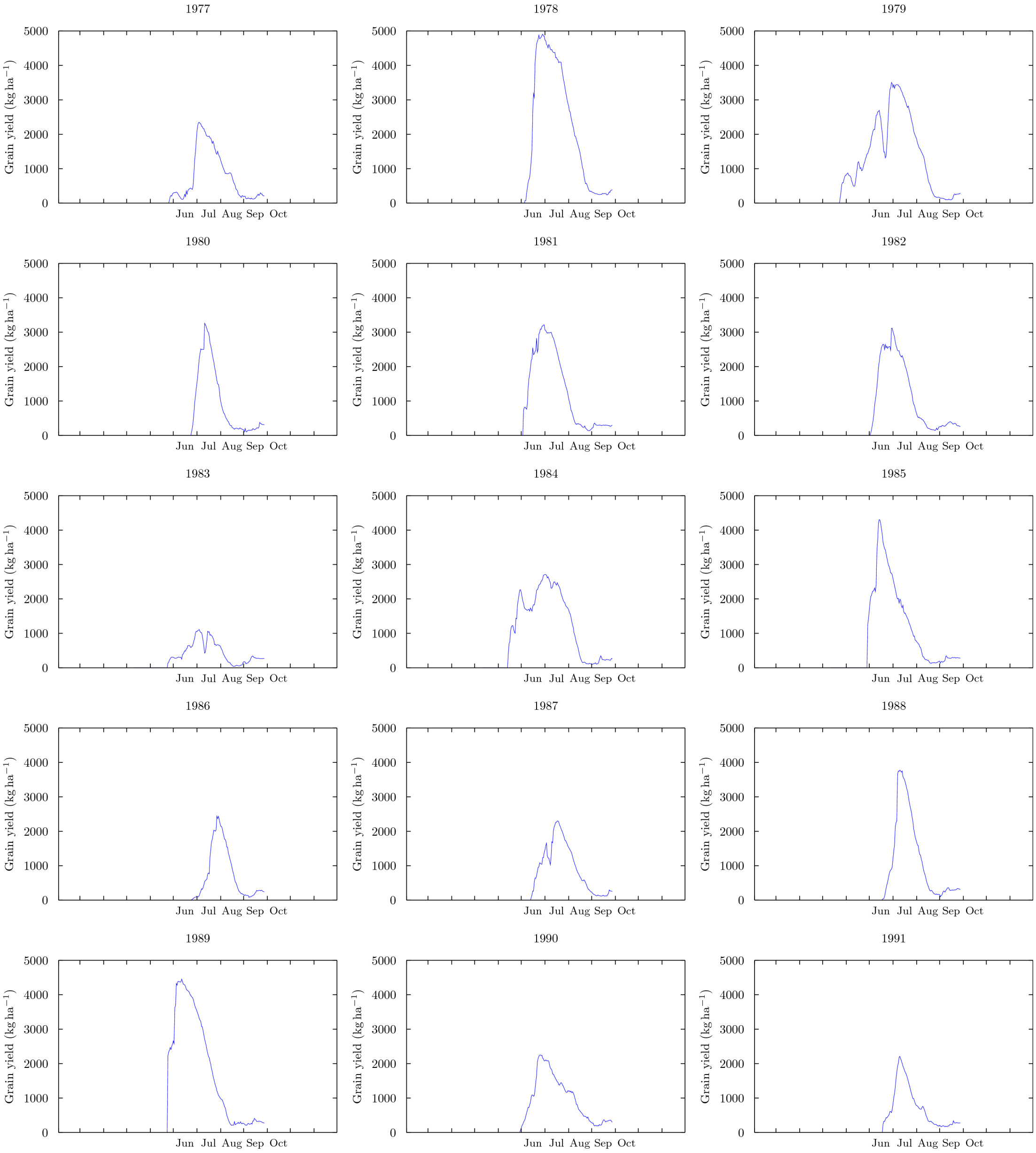

Figure 4.17: Impact of changing the planting date on the grain yield at Bambey in the period 1977–1991. Each point shows the final yield if the crop is planted on that day.

row spaced, respectively) (Azam-Ali, 1984; Azam-Ali *et al.*, 1984a). All three crops were irrigated for the first 20 days then grown on stored water. The experiment was simulated in CROMSAS to evaluate the model skill at a range of planting densities. The experiment used the Indian BK560 variety of millet and it was necessary to create a new variety in CROMSAS with different phenological development times and a different leaf growth rate using experimental data from Ong (1983a) and Ong (1983b).

The total biomass of the wide-spaced crop was well simulated but that the narrow-spaced crop biomass was overestimated and the medium-spaced crop underestimated (Figure 4.18). The simulations are more accurate in the early stages, suggesting that the most likely reason for the discrepancies is the modelling of the water available to the plant in the drying soil; a sensitivity study showed that these discrepancies could be caused by the root depths being underestimated and overestimated, respectively. The individual plant masses are well simulated for all three crops (Figure 4.19), despite the large differences between the crops, which suggests that the approach of CROMSAS to simulating individual plants is appropriate. Figure 4.20 shows that the wide-spaced crop has the best LAI simulation. The medium-spaced LAI is simulated peaking too late, while the narrow-spaced LAI is too high, presumably because the magnitude of the water stress is too low despite the first day of water stress being predicted accurately. Overall, this comparison shows that CROMSAS simulates crops planted at a range of densities with reasonable accuracy.

A sensitivity study was performed to examine the CROMSAS predictions for a range of planting densities. The sensitivity model described in Section 4.2.2.1 and Table 4.4 was used with only the planting density varying between runs. Both grain and biomass yields increase substantially as the total rainfall is increased (Figure 4.21). Initially, grain and biomass yields increase proportionally with the planting density to a plateau. At this point, growth is restricted by the light resources being fully utilised and increasing the density leads to smaller plants. Barrenness (van Oosterom *et al.*, 2001a) causes grain yields to reduce to zero at high planting densities because the plants fail to reach the minimum mass required for reproduction (set to 4 g in CROMSAS). The optimum planting density is lower for crops with lower rainfall. The biomass yields have similar trends to the

Figure 4.18: Crop growth evaluation for crops grown at three planting densities. The experiment was performed in Niger for three crops that were irrigated for the first 20 days then grown on stored water (Azam-Ali, 1984; Azam-Ali *et al.*, 1984a)

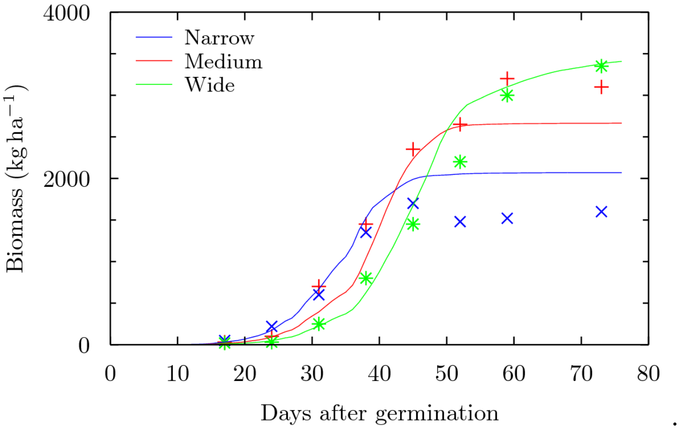

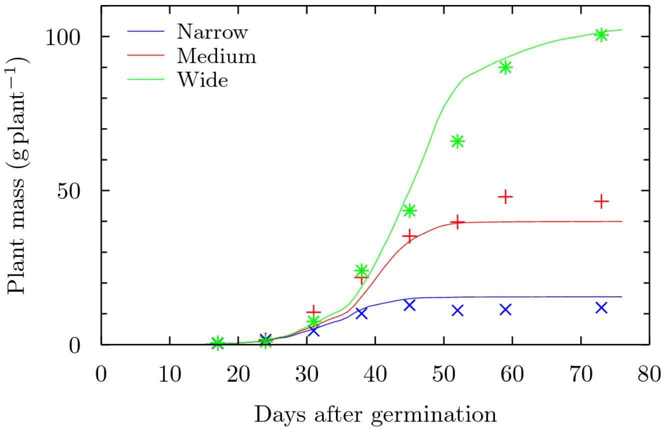

Figure 4.19: Plant mass evaluation for the same experiment.

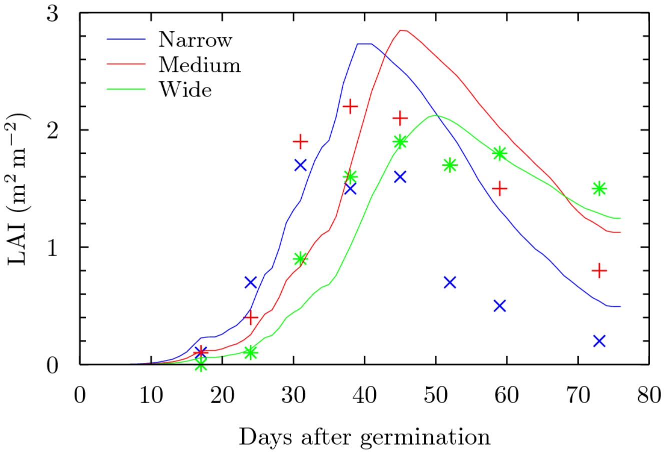

Figure 4.20: LAI evaluation for the same experiment.

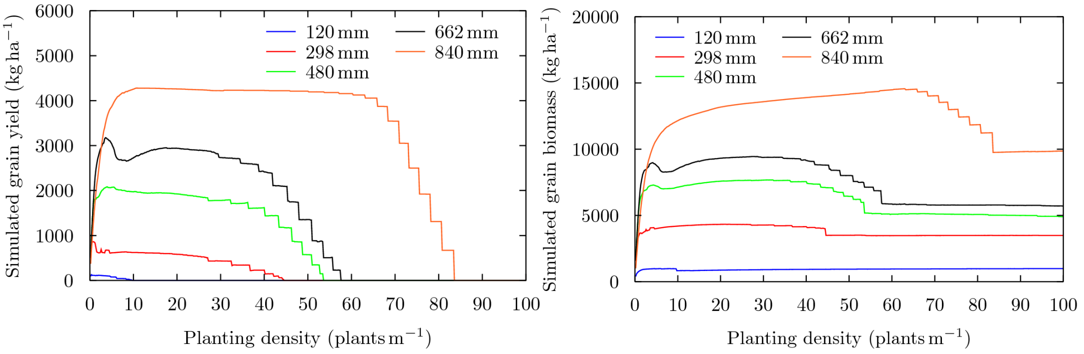

(a) Grain

(b) Biomass

Figure 4.21: Planting density sensitivity study.

grain yields except that a minimum biomass is produced at all planting densities because plant death due to poor growth is not simulated in CROMSAS. The trends presented here are broadly consistent with field experiments of many crops (Azam-Ali and Squire, 2001).

4.2.4.3 Nitrogen management evaluation

An experiment was performed at Nioro-du-rip in Senegal to examine the impact of applying manure and mineral fertiliser on the growth of millet (van Duivenbooden and Cissé, 1993). The experiment was simulated in CROMSAS to evaluate the model skill at different levels of nitrogen application. Souna was planted in the experiment so no changes to the CROMSAS parameters were necessary.

The crop yields were high on the plot with no applied fertiliser or manure so the intrinsic soil fertility at the research station must have been very high. The field fertility in CROMSAS was increased accordingly. CROMSAS accurately predicted the change in the biomass yields in the cases with applied fertiliser but was inaccurate in the manure-only case (Table 4.6), where an unexpected biomass reduction was experienced in the experiment that was not simulated in CROMSAS. The simulations of the change in the grain yields were slightly worse due to an underprediction of the grain yield in the control field. The RRMSE for the grain and biomass yields were low, at 3 % and 9 % respectively, showing that the model can accurately simulate the impact of nitrogen application on

	Biomass		Grain	
	Experiment	Model	Experiment	Model
None	7897	7817	2397	2019
Fertiliser	8924	9054	2448	2513
Manure	7354	8811	2029	2409
Fertiliser & Manure	9789	9480	2717	2780

Table 4.6: Nitrogen application evaluation of CROMSAS for a field experiment performed by van Duivenbooden and Cissé (1993) at Nioro-du-rip in Senegal using Souna millet.

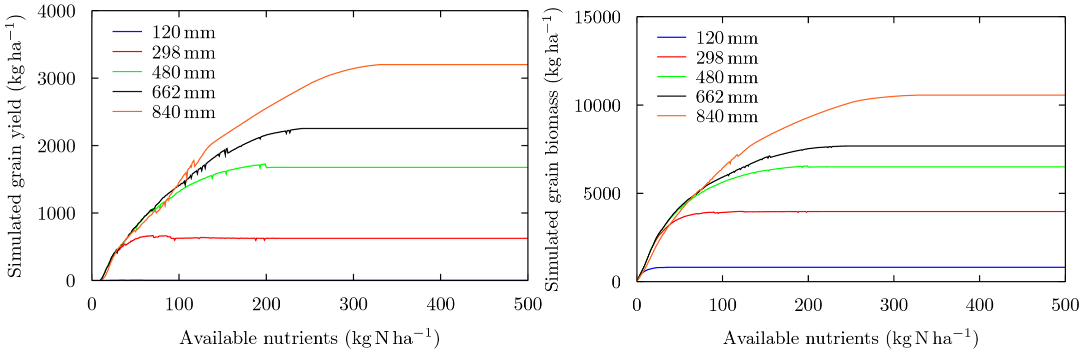

(a) Grain (b) Biomass

Figure 4.22: Nitrogen application sensitivity study.

fertile fields. The evaluation of CROMSAS against the SARRA-millet model fields (Section 4.2.1) has already indicated that the model accurately simulates the effects of nitrogen application on smallholder fields.

A sensitivity study was performed using the sensitivity model in Section 4.2.2.1 and Table 4.4 to examine the response of CROMSAS to nitrogen application. A constant planting density of 8 plants m^{-1} was used throughout. Figure 4.22 shows that the crop responds to steadily increasing nitrogen with increased grain and biomass yields. The nitrogen requirement for the maximum yield is substantially lower in fields receiving less rainfall. There is no grain yield in the 120 mm rainfall simulation because the planting density is too high and the plants are too small for reproduction to occur.

4.2.5 Consistency of the model parameters with the literature

There was concern that the calibrated TUE constant, *TE*, was lower than values found in previous studies. Ehlers and Goss (2003) present transpiration use efficiencies from Tanner and Sinclair (1983) for several C_3 crops (in the range 3.1 Pa–6.2 Pa) and C_4 crops (7.4 Pa–13.8 Pa). These experiments did not include millet, but since millet is a C_4 species, one would expect it to lie in the latter range. In fact, the maximum calibrated CROMSAS value for millet is lower, at 6 Pa, which is within the C_3 crops range. This discrepancy was particularly surprising because the observed ratio of transpiration to biomass for Sob ($333\,\mathrm{l\,kg^{-1}}$) is similar to millet measurements in the USA ($296\,\mathrm{l\,kg^{-1}}$) where the transpiration use efficiency studies were performed. Squire (1990) presents transpiration use efficiencies for millet in India (9.5 Pa–10.6 Pa) and in Niger (8.4 Pa). These are all higher that the calibrated value in CROMSAS. However, close inspection of the Squire values revealed that *TE* was calculated using the maximum daily VPD rather than the daylight average that is used in CROMSAS. For comparison, if the maximum VPD were used in CROMSAS then $TE = 9.0\,\mathrm{Pa}$ which is close to the observed value from Niger. It appears that millet has a lower *TE* than most C_4 crops, suggesting that there are opportunities for improved varieties (Sinclair *et al.* (1984) present some suggestions). Another possible reason for the discrepancy is that the leaf temperature of the African crops is higher than that of similar crops elsewhere as a result of higher incident radiation, and that this leads to a higher localised VPD across the leaf than elsewhere.

The location of the VPD measurements might also have affected the comparison; in this study the VPD data were taken from the closest synoptic weather station which might not be representative of the Sob micro-climate. This example shows why a crop model needs to be calibrated for a particular climatic dataset, but also highlights that a calibration is unlikely to be valid if the source or processing of the meteorological data are changed. Careful steps were taken to produce a self-consistent meteorological dataset (Section 5.1).

4.2.6 Discussion of the evaluation

Crop models are simple simulations of a complex reality and there is a danger that the calibration process camouflages some model inadequacies which then leads to inaccurate simulations under other conditions; for example, Monteith (1996) believes that "model development often runs ahead of the measurements needed for rigorous calibration and validation". The evaluation of CROMSAS examined model performance using a range of techniques to ensure that such inadequacies are not present and to identify the limits of the model.

The ESPACE database contained observations from 7 villages, taken over 4 years, giving 13 village × year combinations in total. While much information was collected, a crucial missing component was the amount of manure and fertiliser that was applied to each field, which meant that the fertility of each field was not known. Fortunately, a subset of 80 fields with higher-quality data were available and it was possible to estimate the fertility of each field and evaluate the model against a range of rainfall patterns and crop management schemes across the range of environments found in the groundnut basin. The correlation between the model predictions and the measurements ($R^2 = 0.71$) was slightly lower than that achieved by Affholder (1997) with the SARRA-Millet model. The RMSE error in the CROMSAS simulations was $292\,\mathrm{kg\,ha^{-1}}$, or $34\,\%$ of the average grain yield. The sensitivity study simulations (e.g. Figure 4.22a) showed that grain yields an order of magnitude higher than this RMSE could be achieved with optimal crop management strategies (i.e. high nitrogen input and high planting density). Any model error would be lower than changes in the yield caused by altering crop management strategies so it was concluded that the model accuracy met the requirements of the study. The lack of a trend in the plots of the yield residue against the planting density and nitrogen application show that the model does not contain biases which would skew the results of crop management strategy simulations involving these variables.

There was a relationship between the biomass error and the total biomass that was caused primarily by poor simulation of the crop duration. This issue was investigated as part of the of the evaluation of CROMSAS for simulating varying planting dates and it was concluded that the improved variety that was used to calibrate the crop development in CROMSAS was weakly photoperiodic but that some of the local varieties in the ESPACE study were strongly photoperiodic. It is also likely that there were several varieties in each village, with a range of development durations, so it is not surprising that modelling only a single variety led to discrepancies. The ESPACE observations could be used to define a number of varieties for use in crop management simulations in the future. It was concluded that the model should simulate the consequences of varying the planting date if the crop duration discrepancy is small and if the temperature dependence and water uptake can be simulated accurately. The model should accurately simulate the development of improved varieties but will not accurately simulate the duration of local varieties unless the development time and photoperiod sensitivity are recalibrated. Even if the duration is poorly simulated, the evaluation against the ESPACE fields shows that the magnitude of any errors in the grain yield are likely to be small because the duration primarily affects vegetative growth.

The influence of temperature and rainfall were examined using a series of sensitivity studies. The model responded to drought and other stimuli as expected from the model design. The rainfall magnitude was identified as the most important factor affecting crop growth in Senegal. Crop growth was sensitive to mean daily temperatures outside of the range 20 °C–30 °C. This upper threshold will be exceeded regularly in the twenty-first century (Chapter 7) so it is important to characterise how the model responds, particularly because very few experiments have examined the growth of millet at high temperatures. A sensitivity study was used to examine the simulation of grain yield reduction at high temperatures in CROMSAS and it was concluded that the model simulations were consistent with the experimental findings of Ashraf and Hafeez (2004).

There was concern that the irregular rainfall distributions of the Sahel were not tested in the sensitivity studies. A second study was performed using rainfall distributions from 17 consecutive seasons at Bambey to investigate this concern. The rainfall distribution influenced the grain yield, as surmised elsewhere (Baron *et al.*, 2005), although the total annual rainfall was more important in most years. This study also showed that both the FAO24 and the FAO56 methods would adequately estimate the ETo for the crop model.

An experiment in Niger which examined the growth of millet at three planting densities (Azam-Ali *et al.*, 1984a) was simulated using CROMSAS. The growth of all three crops, and the size of the individual plants, were reasonably well predicted. A planting density sensitivity study showed that model simulations were broadly consistent with the findings of field experiments of many crops.

Another series of CROMSAS simulations evaluated the impact of nitrogen application. The experiment examined the impact of applying fertiliser and manure on the yields of Souna millet in Senegal (van Duivenbooden and Cissé, 1993). CROMSAS accurately simulated the influence of nitrogen application that was observed in the experiment with the exception of a manured field, where a yield reduction was observed but an increase was simulated. It was unfortunate that the base fertility of the fields was much higher than that of farmers fields in the region, presumably because of heavy fertiliser application in previous years.

4.3 Summary

The calibration study was performed using three fields with different nitrogen application strategies. A number of issues were identified which led to the entire water module being redesigned for use with millet in Senegal (Section 3.5). Following the redesign, the model was able to reproduce the field study observations throughout growth with reasonable accuracy. This outcome vindicated the decision to develop a new model instead of using an existing model where the model structures could not have been changed.

The evaluation showed that the model simulates the growth of Souna millet, under the range of environmental conditions found in Senegal, to an acceptable accuracy for this study. The model simulated both the onset and impact of water stress for a range of conditions.

The model has been calibrated for Souna millet with the meteorological data that has been produced from observations by this study. Different millet varieties could be simulated by changing the crop parameters. If a different crop were to be modelled which responded differently to environmental stress (e.g. maize), more fundamental changes to the model might be required. The performance of the model for any new variety would need to be evaluated prior to use.

Chapter 5

Meteorological Data

This chapter explains how the meteorological datasets were produced and the data quality checked. It is split into two parts. Section 5.1 describes the production of complete meteorological datasets with daily data for the period 1950–2009 at each synoptic station in Senegal. Section 5.2 assesses the most suitable method for estimating the reference evapotranspiration in Senegal.

5.1 Dataset production and quality assurance

The sensitivity studies in Chapter 4 showed that the crop yield is very sensitive to the availability of soil water. In most areas of Senegal, rainfall is the only water source for agriculture and there are large spatial variations across the country (Figure 1.7). It was necessary to obtain high-quality daily rainfall data to drive the crop model.

Other meteorological data are required by the model. Air temperature data are used as a proxy for the plant temperature to simulate the phenological development of the plant. Solar radiation and humidity data are used by the radiation and transpiration assimilate production methods, respectively. Wind data are required for some evapotranspiration calculations. The quality of crop yield simulations is limited by the quality of the data that are used to drive the model so it was necessary to produce an internally consistent meteorological dataset with no temporal biases.

Meteorological data were obtained from four sources: *a*) AGRHYMET (Centre Regional de Formation et d'Application en Agrométéorologie et Hydrologie Opérationnelle, in Niger); *b*) CIRAD (Centre de coopération Internationale en Recherche Agronomique pour le Développement, a French research organisation); *c*) UK Met Office; and, *d*) NCAR (National Center for Atmospheric Research, in the United States). This section describes each source then explains how these data were combined to produce a full record. Where necessary, values were estimated to fill gaps. Extensive quality checks were performed and these are also described.

5.1.1 AGRHYMET and CIRAD meteorological data

In the late 1980s, a research project was undertaken by the AGRHYMET organisation in Niger to characterise the climate across the Sahel region. The region was split into 0.25° squares and the daily measurements from synoptic and rainfall weather stations were used to estimate a value in each box. The project concluded with the publication of an 11-volume agro-climatic atlas (Morel, 1992). Another output was a complete dataset for each synoptic station for the years 1950–1980 with values estimated to fill all of the gaps. Meteorological data were obtained for the 11 synoptic stations in Senegal from this dataset.

The ESPACE project was being undertaken by CIRAD at the same time as the AGRHYMET project was operational. One of the outputs of the ESPACE project was a complete rainfall record, with gaps filled where necessary, for all 11 synoptic stations and 13 other rainfall stations in Senegal. This data were obtained and covered the years 1950–1991.

Morel (1992) identified many errors in the observations. There were confusions between the universal time and the local time when recording measurements. Some errors resulted from mistakes (from poor memory recollection, different operators, transmission errors or even dyslexia). Some readings were repeated. Since the timescale was so long, relocated weather stations and particularly pluviometers were also an issue. Both the AGRHYMET and CIRAD datasets underwent careful consistency checks to identify and remove errors and biases.

5.1.1.1 Daily average temperature

The maximum and minimum daily temperatures were supplied for each station on each day. The average temperature each day was estimated by averaging the maximum and minimum, in common with many other studies (e.g. Doorenbos and Pruitt, 1977):

$$T_{av} = \frac{T_{max} + T_{min}}{2} \tag{5.1}$$

5.1.1.2 Daily average humidity

The average relative humidity (RH) was supplied for each day. The actual vapour pressure of the air, e_a, was calculated using the equation of Bolton (1980):

$$e_a = c_{ea} \times \frac{RH}{100} \times 0.6108 \exp\left(\frac{17.27T_{av}}{T_{av} + 237.3}\right) \tag{5.2}$$

The method that was used by Morel (1992) to calculate RH was not known. The factor c_{ea} was included in this equation to correct any bias from calculating e_a using only T_{av} (the most accurate method would be to average the observations of e_a through the day but this data were not available in the AGRHYMET dataset). The UK Met Office MIDAS data (Section 5.1.2.2) were used to estimate the bias factor. The MIDAS RH was calculated for the 06:00 and 18:00 observations and averaged to estimate the daily RH. This was then substituted into Equation 5.2 to calculate the 'AGRHYMET-equivalent' MIDAS vapour pressure. By comparing this vapour pressure with the actual MIDAS average vapour pressure (calculated by averaging at least four daily measurements, where possible), it was possible to derive a value for the coefficent $c_{ea} = 0.91$ as an average over all of the synoptic stations. However, using this factor in Equation 5.2 led to the average AGRHYMET humidity being 10 % lower than average MIDAS humidity. A long-term rising minimum temperature trend was considered as an explanation because the air would be able to hold more moisture throughout the night and condensation would be reduced. A more likely explanation was that Morel had calculated RH using Equation 5.2 in reverse rather than by averaging observations at 06:00 and 18:00. This hypothesis was supported by the NCEP/NCAR reanalysis model time series, which simulates a flat trend (Figure 5.1). It was

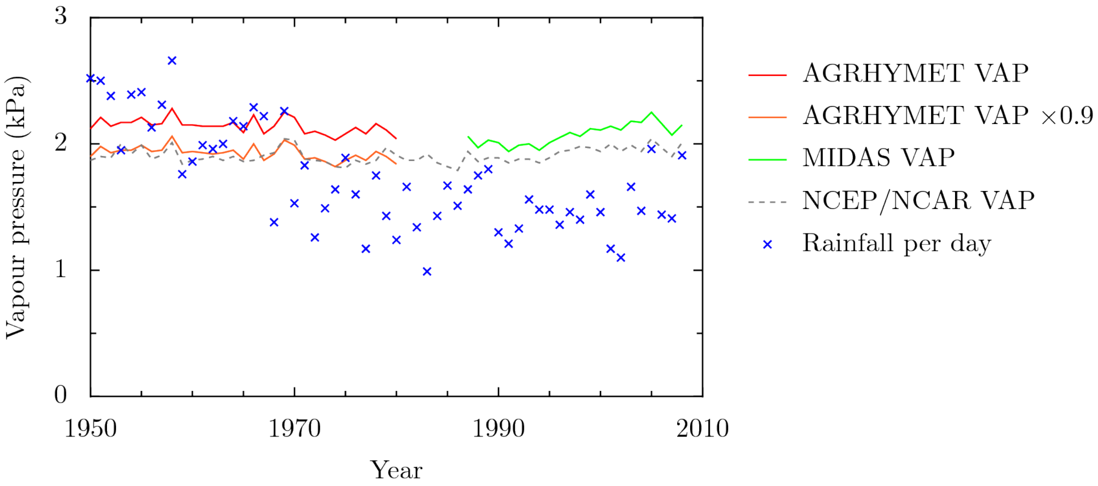

Figure 5.1: Humidity time series for the AGRHYMET, MIDAS and NCEP/NCAR reanalysis datasets. Each value is an annual average of all 11 synoptic weather stations in Senegal. Two AGRHYMET datasets are presented; the second is multiplied by a factor $c_{ea} = 0.9$ as described in the text.

concluded that using a factor $c_{ea} = 0.91$ would underestimate the humidity, and it was decided to set $c_{ea} = 1$.

Over large areas, humidity is correlated to the rainfall (Le Houérou, 2009, p62). Averaging over all of the stations, there was a positive correlation between humidity and rainfall in Senegal with $R^2 = 0.35$. The rainfall in 1950–1970 was higher than in later years (Figure 5.1) so the humidity should be higher in the AGRHYMET dataset, supporting the rejection of the 0.91 factor.

The saturated vapour pressure (SVP) is the quantity of water vapour required to saturate the air at a particular temperature. Denoted e_a^s, it can be calculated using Equation 5.2 by setting $c_{ea} = 1$ and $RH = 100$. The equation is non-linear so tends to underestimate the SVP if the average daily temperature is used. Instead, following the advice of Allen *et al.* (1998), the SVP was calculated as the mean of Equation 5.2 using the maximum and minimum temperatures:

$$e_a^s = c_{ea} \frac{0.6108 \exp\left(\frac{17.27 T_{max}}{T_{max}+237.3}\right) + 0.6108 \exp\left(\frac{17.27 T_{min}}{T_{min}+237.3}\right)}{2} \tag{5.3}$$

Since the SVP depends only on the temperature, there is a strong diurnal variation. A comparison with the instantaneous SVP values calculated from the

MIDAS database showed that Equation 5.3 underestimated the average daytime SVP (defined as 07:30 to 19:30) but overestimated the 24-hour SVP. The factors in each case varied somewhat by station but appropriate averages were $c_{ea} = 1.06$ for the daytime SVP and $c_{ea} = 0.92$ for the 24-hour SVP.

The vapour pressure deficit (VPD) is used to calculate the transpiration-limited growth rate and is also used by some equations to calculate the reference evapotranspiration. It is calculated as the difference between the SVP and the actual vapour pressure of the air:

$$\mathrm{VPD} = e_a^s - e_a \tag{5.4}$$

5.1.2 UK Met Office meteorological data

The World Meterological Organisation (WMO) World Weather Watch stations provide an almost continuous record of weather data across the globe. The African network is considered to be the poorest in the world because the distribution of stations across Africa is very uneven, the density of stations is much lower than the WMO minimum recommended level and because Africa has the lowest reporting rate of any region (Washington *et al.*, 2004). Fortunately, the relatively stable political environment in Senegal has led to an almost continuous record from all 11 Senegalese stations. The synoptic data for each station were obtained from the UK Met Office MIDAS database (UK Met Office, 2009) for the period 1985 to 2009.

Each station was able to submit up to eight records each day, at three-hourly intervals from midnight, but for most days there were readings at 06:00, 18:00 and perhaps at a couple of other times. The instantaneous air temperature, dew point temperature and wind speed were recorded in each record, and some records also contained the minimum or maximum temperature for the day and the rainfall over a stated period prior to the reading. There were numerous short gaps in the datasets. All of the parameters contained some inconsistent and unrealistic data, no doubt caused by the same factors that were identified in Section 5.1.1. It was necessary to identify and remove the poor quality data and to fill gaps with appropriate data.

Parameter	Maximum	Minimum	Unit
Maximum temperature (T_{max})	50	10	°C
Minimum temperature (T_{min})	40	0	°C
Observed temperature (T_{obs})	50	0	°C
Dew point temperature (T_{dew})	30	−10	°C
Wind speed	10	0	$\mathrm{m\,s^{-1}}$
Rainfall	250	0	$\mathrm{mm\,d^{-1}}$
Cloud cover	8	0	oktas
Sunshine duration	0	15	hours

Table 5.1: Acceptable range of values for meteorological parameters in the MIDAS database.

The dataset was far too large to be checked by hand so automated algorithms were developed to identify and remove data that were likely to be erroneous. The most basic test checked that each value lay within an acceptable range (Table 5.1). The ranges were found by plotting annual time series in several climatic zones. They represent a compromise between being overly tight, which causes unusual but valid observations to be removed and reduces the variability of the dataset, and being overly lax, which leads to more erroneous observations being included. The list of removed data values was checked to ensure that the range was not overly tight. Where possible, each parameter was also checked for consistency with other parameters. For example, the maximum temperature was required to be higher than the minimum temperature. Further checks were made on the rainfall data and these are described in Section 5.1.2.4. In total, discrepancies were identified in 4.6 % of observations across the 11 weather stations (88 000 discrepancies out of 1.9 million observations).

5.1.2.1 Daily average temperature

The instantaneous air temperature was measured and recorded as part of each observation. Gaps in the time series were filled using two methods. The first method used estimates from other observations on the same day, using the assumption that the temperatures follow a predictable diurnal cycle. Each observed temperature was compared with the temperatures at other times on the same day and the highest correlations between times were identified. Coefficients were then derived to link the observations. The second method examined the correlations between the observation in question and observations at the same time on the surrounding days (averaging 1, 2 or 3 days each side).

The product of the analyses was a list of the relationships between temperature observations at each of the eight measurement times on the same day and at the same time on surrounding days. Each month was split into three periods (days 1–10, 11–20 and 21–end). The best correlations were identified in each 10-day period and used to fill gaps in the dataset. The highest correlations exceeded 0.9.

Unfortunately, it was difficult to estimate the daily average temperature because observations were only regularly made at 06:00 and 18:00 each day. It was not possible to accurately estimate the temperature at other times of the day because the analysis was generally skewed by the small number of unrepresentative observations that were available. In the absence of a full temperature record, the average temperature could not be accurately estimated because of the magnitude of the diurnal cycle in the Sahel. In view of these difficulties, the daily average temperature was instead calculated from the daily maximum and minimum temperatures, which were recorded in addition to the instantaneous temperatures, using Equation 5.1. The correlations between these temperatures and the eight instantaneously measured temperatures were assessed over all of the years for each 10-day period and the strongest relationships used to estimate the maximum or minimum temperature where data were not available.

Both the evapotranspiration rate and the rate of phenological development depend on the temperature. Producing an appropriately-averaged temperature for both processes is difficult because phenological development occurs both day and night, while evapotranspiration is broadly a daytime phenomenon. The difference between the daytime and 24-hour average temperatures is related to the magnitude of the diurnal cycle, with the daytime average temperatures being around 3 °C higher in the south and 6 °C higher in the more arid north.

The most common approach of calculating the daily average temperature in other models, for both evapotranspiration and phenological development, is to use the maximum and minimum temperatures in Equation 5.1 (e.g. Challinor *et al.*, 2004; Doorenbos and Pruitt, 1977). The bias that is introduced into the evapotranspiration calculation is removed through calibration. Using this approach for the MIDAS data also ensured consistency with the AGRHYMET data. Comparisons with the instantaneously measured temperatures showed that this equation tended to overestimate the 24-hour average temperature while being lower than the average daytime temperature. The error was judged small enough to be ignored.

5.1.2.2 Daily average humidity

The specific humidity of the air was recorded in the MIDAS database using instantaneous observations of the dew-point temperature. These temperatures were analysed and gaps were filled using the same methods as those described in Section 5.1.2.1.

The actual vapour pressure of the air, e_a, was calculated from each observed dew point temperature, T_{dew}, using the relationship derived by Bolton (1980):

$$e_a = 0.6108 \exp\left(\frac{17.27T_{dew}}{T_{dew} + 237.3}\right) \tag{5.5}$$

The lack of observations at certain times of the day also affected the humidity daily averaging. In this case, however, the actual humidity had only a small diurnal variation at the synoptic stations and it was acceptable to estimate the daily average using the average of the observations at 06:00 and 18:00, which were available for most stations.

In contrast to the actual vapour pressure, the saturated vapour pressure is closely related to the diurnal cycle so there are large variations throughout the day. The most accurate method to calculate a daily average would be to average the SVP at each observational time, but there were insufficient observations on most days to allow a simple average to be representative so this method was judged too inaccurate. Instead, the SVP was calculated from the maximum and minimum temperatures using the same method as for the AGRHYMET dataset

(Equation 5.3). The two methods were compared where possible for the MIDAS data. As explained in Section 5.1.1.2, two factors were derived to estimate the 24-hour and the daytime SVPs. These factors were also applied to the MIDAS data.

The vapour pressure deficit was calculated using the same method as for the AGRHYMET dataset (Equation 5.4).

5.1.2.3 Daily average wind speed

The wind speed is only used in the evapotranspiration calculations and these require measurements at a height of 2 m. Since the synoptic stations record the wind speed at a height of 10 m, it was necessary to convert the observations using the relationship from Allen *et al.* (1998):

$$u_2 = u_z \frac{4.87}{\ln\left(67.8z - 5.42\right)} \tag{5.6}$$

24-hour wind run data were not available so it was necessary to estimate the wind speed from instantaneous observations. Surprisingly, the wind speed was found to be only very weakly related to the time of day, so the daytime average wind was calculated as the average of the observations at 06:00, midday and 18:00. On a few days, the averaged wind speed exceeded $10\,\mathrm{m\,s^{-1}}$ which was considered an unrealistic representation of the 24-hour wind run; it is likely that the instantaneous observations on these days were affected by storms or that mistakes had been made. Also, for well developed crop canopies, the wind speed within the canopy is limited by the roughness of the canopy. These observations were removed and alternative values estimated.

In view of the difficulties estimating the average wind speed, the MIDAS measurements for 1985 to 2008 were compared with the values of Morel (1992) for 1950 to 1980. The wind speeds were consistent for the more northerly stations but the MIDAS values were significantly higher in the south-east (Figure 5.2). It is not known whether the discrepancy results from methodological issues or is due to climatic variations between the two periods. As a further check, the MIDAS observations were also compared against and found to be broadly consistent with the wind climatologies of Hayward and Oguntoyinbo (1987, p51).

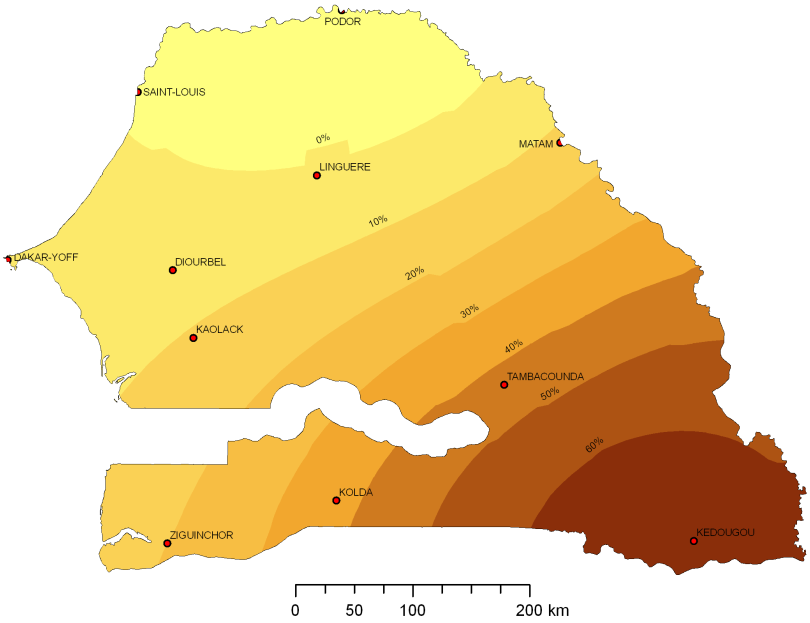

Figure 5.2: Map of the wind speed discrepancy between the CIRAD and MIDAS databases. The CIRAD measurements (Morel, 1992) are averages for the period 1950–1980 while the MIDAS measurements (UK Met Office, 2009) cover the period 1985–2008.

Allen *et al.* (1998) recommend that the minimum wind speed be set to $0.5\,\mathrm{m\,s^{-1}}$ to account for boundary layer instability and the buoyancy of air in promoting the exchange of vapour at the surface when the air is calm. This was applied within CROMSAS rather than in the meteorological datasets.

5.1.2.4 Daily rainfall

Only some records in the MIDAS database contained rainfall data. Each of these records contained the total rainfall to that point over a number of specified hours; if either the rainfall or the number of hours was missing then the record was ignored (500 cases). Each day was split into eight 3-hour periods in line with the MIDAS database records. For some periods, there were no rainfall data, while for others, there were multiple records. In view of the importance of obtaining accurate rainfall data, the records were processed carefully.

The first step was to examine each period containing more than one record to see if any of the records were unreasonable. The criteria for unreasonable records were: *a*) the number of hours of rainfall was not a multiple of 3 (so the period covered by the record was inconsistent with the 3-hourly reporting convention); *b*) the record covered a period that was longer than 24 hours; *c*) there was high rainfall (>30 mm) outside of the rainy season (between November and May); and, *d*) at least 50 % of the periods that were covered by a particular record were also covered by another record. The record was removed if three of these criteria were satisfied; 16 records were removed in total.

The next step was to delete superfluous entries, which occurred where rainfall records for short periods were completely covered by subsequent records with longer periods. The short period records were deleted. In 380 of these cases, the short period rainfall was higher than and therefore inconsistent with the long period rainfall. Even after these steps were performed, there were still almost 2000 periods which were covered by two records (although in most cases, both records contained zero rainfall).

Long-term daily rainfall records, for the years 1950–1991, were available for all eleven synoptic weather stations from CIRAD. The two datasets overlapped between 1985 and 1991. Analysing the discrepancies between the two datasets, by eye, showed that the MIDAS database contained many consecutive entries with identical rainfall totals in places where the CIRAD database only contained one reading, suggesting that a single reading was counted twice when the data were being processed; this problem was also regularly encountered by Morel (1992). Since it was very unlikely that two consecutive rainfall events would have had the same rainfall to within 0.1 mm, the repeated record was set to zero rainfall in each case. More than 900 records were affected. Most duplications occurred during the years 1985–1989, suggesting that the errors were made when older records were being prepared for submission to the WMO.

After data processing, there were 4500 days between May and November (the nominal monsoon season) with no rainfall records, which is on average about 19 per year at each weather station. Zero rainfall was assumed on each of these days. There were 53 periods of particular concern when no rainfall records were available for five or more consecutive days.

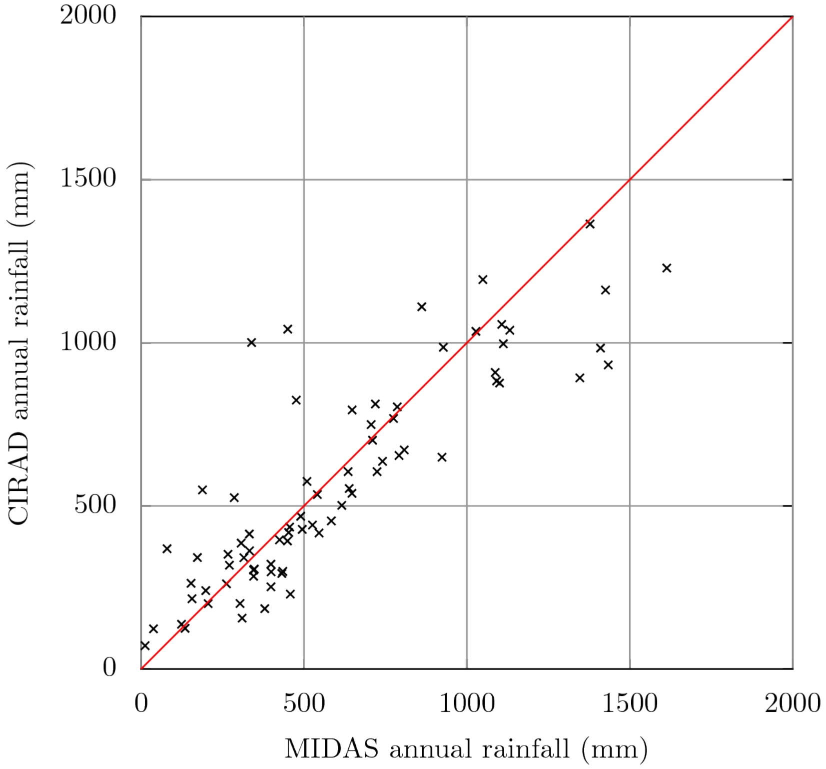

Figure 5.3: Comparison of the total annual rainfall recorded in the CIRAD and MIDAS databases for 11 weather stations in the years 1985–1991. The linear regression line has the equation $y = 0.73x + 135$ with $R^2 = 0.74$ (P < 0.0001).

Although day-to-day rainfall patterns could be identified in the CIRAD and MIDAS records, in some cases there were substantial differences between the annual rainfall totals of the two datasets (Figure 5.3). Despite the removal of significant numbers of records from the MIDAS database, and despite many days having no records, the CIRAD annual totals still tended to have only 90 % of the rainfall of MIDAS totals in the same year. A systematic discrepancy of this scale has the potential to introduce errors into crop simulations. So despite a correlation between the two datasets of $R^2 = 0.74$, these discrepancies were a cause for concern.

An investigation was performed to examine whether the two datasets were well matched in terms of the distribution and magnitude of rainfall events, which meant examining individual days rather than the annual totals. For each year between 1986 and 1991, the rainfall pattern at each weather station from the MIDAS database was compared against all of the annual CIRAD records (all weather stations and all years) and given a daily score that depended on the proximity of the daily rainfall values, with zero awarded where only one of the datasets recorded rainfall. The highest score was identified for each weather station in each year. In 62 out of 65 combinations, the closest time series for each weather station in the MIDAS dataset was the equivalent record in the CIRAD dataset. In the remaining three cases, a nearby weather station in the same year was closest. The scores ranged from 10 % to 63 % (where 100 % represents a perfect match). While the high number of correctly matched records demonstrated a relationship between the two datasets, some of the scores were surprisingly low. It is possible, but unlikely, that the rainfall measurements were taken from different gauges in the same area. It is also very difficult to avoid making mistakes when processing rainfall data and inconsistencies have been found in both datasets; the particularly large number that were found in the MIDAS dataset suggests that the quality of the MIDAS records is poorer.

The rainfall analysis raised concerns about the accuracy of the MIDAS dataset. The CIRAD dataset appears to have far fewer errors; a test for consecutive identical rainfall totals found only five instances and the only large event was also repeated in the MIDAS dataset so was most likely correct. The same test over the same period found 900 consecutive identical records in the MIDAS dataset. It was concluded that the CIRAD dataset was the most suitable for crop simulations. The MIDAS data were judged adequate for post-1991 studies in cases where there were few days with no data; it is comforting that the majority of the identical rainfall cases occurred before 1991, which suggests that quality control procedures might have been improved in later years.

5.1.2.5 Daily average cloud cover and the sunshine duration

The cloud cover and the sunshine duration can be used to estimate the daily incident solar radiation (Section 5.1.3).

Sunshine duration data were available for the period 1950–1980 in the AGRHYMET data. It was also available in the MIDAS database from around 1998. In the MIDAS dataset, the sunshine duration was generally recorded at 06:00 and showed

Cloud	0	1	2	3	4	5	6	7	8
n/N	0.95	0.85	0.70	0.65	0.55	0.45	0.30	0.15	0.05

Table 5.2: Empirical relationship between the cloud cover and the fractional sunshine duration from (Doorenbos and Pruitt, 1977). The cloud cover is estimated in oktas by a human observer. n is the number of hours of sunshine and N is the number of hours of daylight.

the sunshine recorded on the previous day, using the same data format as the rainfall. A methodology was developed to identify the correct day and basic consistency checks were performed.

No sunshine duration data were available in the years 1981–1997. In these years, where possible, the sunshine duration was estimated from the cloud cover. The cloud cover was estimated by eye and was recorded using the okta scale with 0 representing no cloud and 8 representing a completely overcast sky. The quality of each observation would have depended upon the skill of the observer. The daily average cloud cover was estimated by averaging the individual readings each day, weighted by the hours of daylight that they represented.

Two methods were considered to estimate the sunshine duration from the cloud cover. The FAO method uses a look-up table (Table 5.2) to convert from the cloud cover to fractional sunshine duration (Doorenbos and Pruitt, 1977). An investigation using the post-1998 data showed that this method tended to underestimate the sunshine duration in Senegal. An alternative method was suggested by Morel (1992), who calculated the fractional sunshine duration using an empirical equation:

$$I = 93.38 - 0.040456cld - 0.0087653cld^2 - 0.18518cld^3 \tag{5.7}$$

where *cld* is the cloud cover in oktas. This method was derived for the Sahel region, had a close correlation ($R^2 = 0.97$) and produced a better estimation of the sunshine duration than the FAO method, so was used in this study.

5.1.3 Estimating the downward solar radiation from the sunshine duration

The incident solar radiation at the top of the atmosphere, known as the *extraterrestrial radiation* and denoted R_a, can be calculated as a function of the latitude and altitude of the location and the day of the year. This study used the method recommended by Allen *et al.* (1998, p45) to estimate the solar radiation.

Even in the absence of clouds, only a fraction of the incident solar radiation reaches the ground; this is called the *clear sky radiation* (R_{so}) and can be estimated using:

$$R_{so} = (a_s + b_s)\, R_a \tag{5.8}$$

where a_s and b_s are constants.

On most days, the downward solar radiation is further reduced by the presence of clouds and other atmospheric aerosols. Equation 5.8 can be altered to estimate the incident downward solar radiation reaching the field, R_{dsw}, as a function of the number of hours of sunshine (Allen *et al.*, 1998):

$$R_{dsw} = \left(a_s + b_s \frac{n}{N}\right) R_a \tag{5.9}$$

where n is the number of hours of sunshine and N is the number of hours of daylight.

Values for the constants a_s and b_s have been derived by a number of studies (Table 5.3). Unfortunately, solar radiation measurements are not performed by synoptic weather stations so it was not possible to derive appropriate values for the constants across the country. However, some solar radiation and sunshine duration measurements were made available by CIRAD from the Bambey research station for the period 2004–2008. Equation 5.9 was rearranged and R_{dsw}/R_a was plotted against n/N for 1100 days. Regression analysis was used to derive values for the two constants of $a_s = 0.31$ and $b_s = 0.38$ ($R^2 = 0.61$). The maximum value of $a_s + b_s$ for any day was 0.75. The Morel constants for the Northern Sahel were clearly the most suitable of those listed in the table and were adopted for all of the stations.

Study	Region	a_s	b_s	$a_s + b_s$
Page (1961)	Dakar	0.10	0.70	0.80
Page (1961)	Tropics	0.23	0.52	0.75
Davies (1965)	West Africa	0.19	0.60	0.79
Morel (1992)	Northern Sahel	0.29	0.42	0.71
Morel (1992)	Southern Sahel	0.25	0.45	0.71
This study	Bambey	0.31	0.38	0.69

Table 5.3: Empirical constants for calculating the incident solar radiation (R_{dsw}) from the extraterrestrial radiation (R_a). The constants derived by Page (1961) and Davies (1965) were taken from the literature review of Linacre (1967). See the text for an explanation of the constants.

In the absence of cloud cover or sunshine hour observations, Allen *et al.* (1998) suggests using Hargreaves' radiation formula to estimate R_{dsw}:

$$R_{dsw} = k_{R_{dsw}} \sqrt{T_{max} - T_{min}} R_a \tag{5.10}$$

where $k_{R_{dsw}}$ is an adjustment coefficient ($0.16 < k_{R_{dsw}} < 0.19$).

Table 5.4 compares the measurements of the solar radiation with estimates from the sunshine duration method, Hargreaves' equation and the NCEP/NCAR reanalysis model for Bambey in 2004–2008 (see the following section for details of the NCEP/NCAR reanalysis model). The sunshine duration method is the best in terms of both magnitude and correlation. The correlations for the other two methods are lower and the NCEP/NCAR model in particular tends to overestimate the solar radiation; in a crop model, this would lead to an overestimate of the reference evapotranspiration and to an overly high growth rate if the radiation use efficiency method was being used (and was not recalibrated).

5.1.4 NCEP/NCAR reanalysis model data

The use of weather models for hindcasting was discussed in Section 2.5. The NCEP/NCAR reanalysis model has been used to perform daily calculations of the global weather system for the period from 1948 to the present time on a

Method	Mean	Standard Deviation	R^2
Measured solar radiation	20.6	3.6	
Sunshine duration estimate	20.1	3.6	0.71
Hargreaves' formula	21.3	3.5	0.36
NCEP/NCAR reanalysis model	25.0	3.5	0.30

Table 5.4: Comparison of measured and estimated downward solar radiation at Bambey in 2004–2008. The correlations are between the estimates and the measurements. All figures have units $\mathrm{MJ\,m^{-2}\,day^{-1}}$.

spatial scale of 1.88° × 1.88° (Kalnay *et al.*, 1996). A small number of points cover the whole of West Africa; for example, since the latitudinal rainfall gradient is approximately $2\,\mathrm{mm\,km^{-1}}$ in Senegal, then between two grid points there is a annual rainfall change of approximately 400 mm. Figure 5.4 shows that the Senegal is entirely covered by just 12 grid boxes. The spatial scale limits the resolution of the data to large-scale trends but the model is still useful as a source of simulated meteorological data for times when observed data are not available. The solar radiation, temperature and humidity tend to have low spatial variability near sea level so the errors caused by using low-resolution data are likely to be less important than errors caused by inadequate modelling of atmospheric processes. The next section compares the long-term model simulations with observed data to remove any bias from model data.

The NCEP/NCAR data were retrieved from the NOAA website (Kalnay *et al.*, 1996). For each weather station, the data from the four surrounding model grid points were linearly interpolated to the weather station coordinates. The model projections are compared with observations in Sections 5.1.5.1 to 5.1.5.5.

5.1.5 Producing a complete dataset for 1950–2009

The datasets discussed above were combined to produce a complete dataset for each synoptic station which covered the years 1950–2009. Different approaches were used for the non-rainfall and rainfall data.

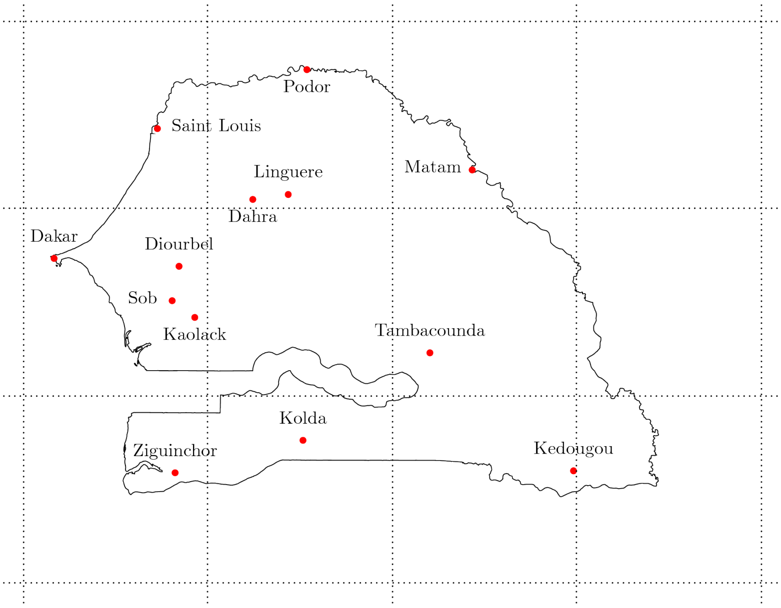

Figure 5.4: Map of the Senegalese synoptic weather stations in the MIDAS database. The overlying grid shows the NCEP/NCAR reanalysis grid boxes. The grid points lie in the centre of the boxes. The village of Sob, which was used to calibrate CROMSAS, and Dahra, the location of the radiation measurements, are also shown. The map data were obtained from `http://www.maproom.psu.edu/dcw/`.

For the non-rainfall data, the AGRHYMET data contained an almost complete record for 1950–1980 (the gaps having been filled by that project). The MIDAS dataset contained a less complete record from around 1985–2009. Hence there were no records available for 1981–1984. The NCEP/NCAR model was used to generate data for these years and to fill gaps in other years. The gaps were filled using two methods. The first method compared the combined Morel/MIDAS observations with the NCEP/NCAR simulations for each day and derived coefficients to link the two datasets. The second method compared each observed value with the average of the surrounding days (1, 2 or 3 days on each side). Correlations and offset factors were calculated for both methods in each 10-day period throughout the year (i.e. 3 periods per month). For each 10-day period, the highest correlation of either method was identified and the offset factors were used to fill all of the gaps in the dataset.

For the rainfall, the CIRAD data were used for 1950–1991 and then the MIDAS data for 1992–2009. The NCEP/NCAR model was judged to be too inaccurate to be used to fill rainfall gaps (Section 5.1.5.5) so zero rainfall was assumed on days where data were not available.

The following sections examine the data from each of the datasets.

5.1.5.1 Temperature

The reanalysis model produced a reasonable estimate of the minimum temperature trends at most of the synoptic stations (Figure 5.5). Despite there being a strong north—south rainfall gradient across the country, the minimum temperature trends are more affected by the proximity to the coastline with an east—west pattern being observed at all stations. At Saint Louis, a northerly coastal station, the model simulation was flatter than the observed trend. The simulation here is particularly good when one considers the strong influence from two oceanic grid cells (Figure 5.4). Similar temperature trends were observed for the other five western and central synoptic stations, with the model tending to overestimate in some cases and underestimate in others. The peak minimum temperature observed in late-May at the two easterly stations was not observed at the other stations. In each case, the model underestimated the minimum temperature throughout the year.

The NCEP/NCAR simulations of the maximum temperature were poorer than the simulations of the minimum temperature (Figure 5.6). The dry northern stations of Podor and Linguere were simulated most accurately. The temperatures at Dakar and Kaolack were consistently underestimated by up to 10 °C. An east—west pattern was also noticeable for the maximum temperature with the both the high and low peaks being overestimated at the easterly stations (Tambacounda, Kolda and Kedougou). With the exception of St Louis, all of the stations had peak temperatures in May and a second smaller peak at the end of the rainy season in November. This trend was consistently underestimated for the western stations and overestimated for the eastern stations.

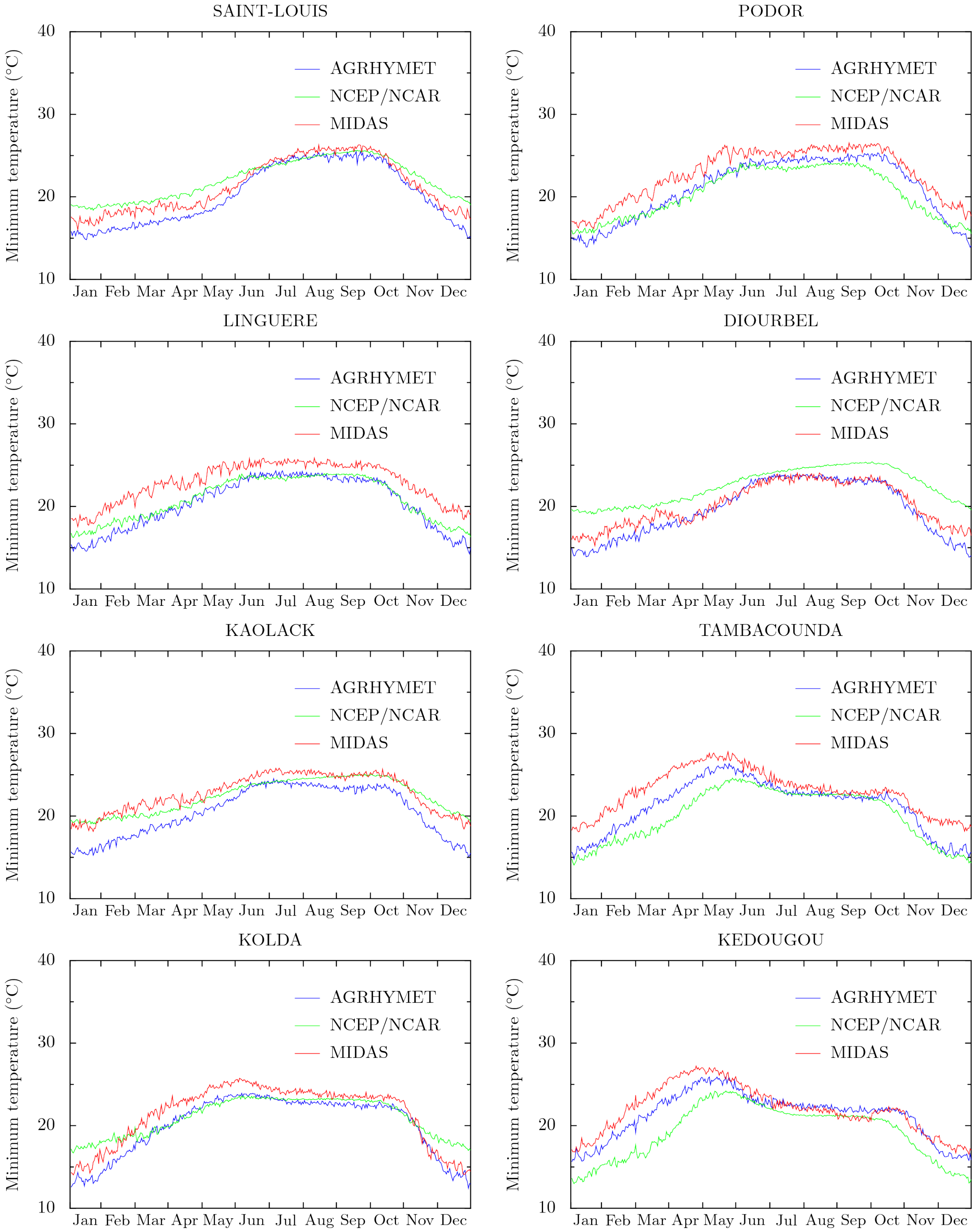

Figure 5.5: Observed and simulated minimum temperatures at eight synoptic stations in Senegal. Each day represents the mean of the period 1950–2008. The observations were extracted from the AGRHYMET dataset (Morel, 1992) and the MIDAS database (UK Met Office, 2009), and the simulations were performed by the NCEP/NCAR reanalysis model (Kalnay *et al.*, 1996).

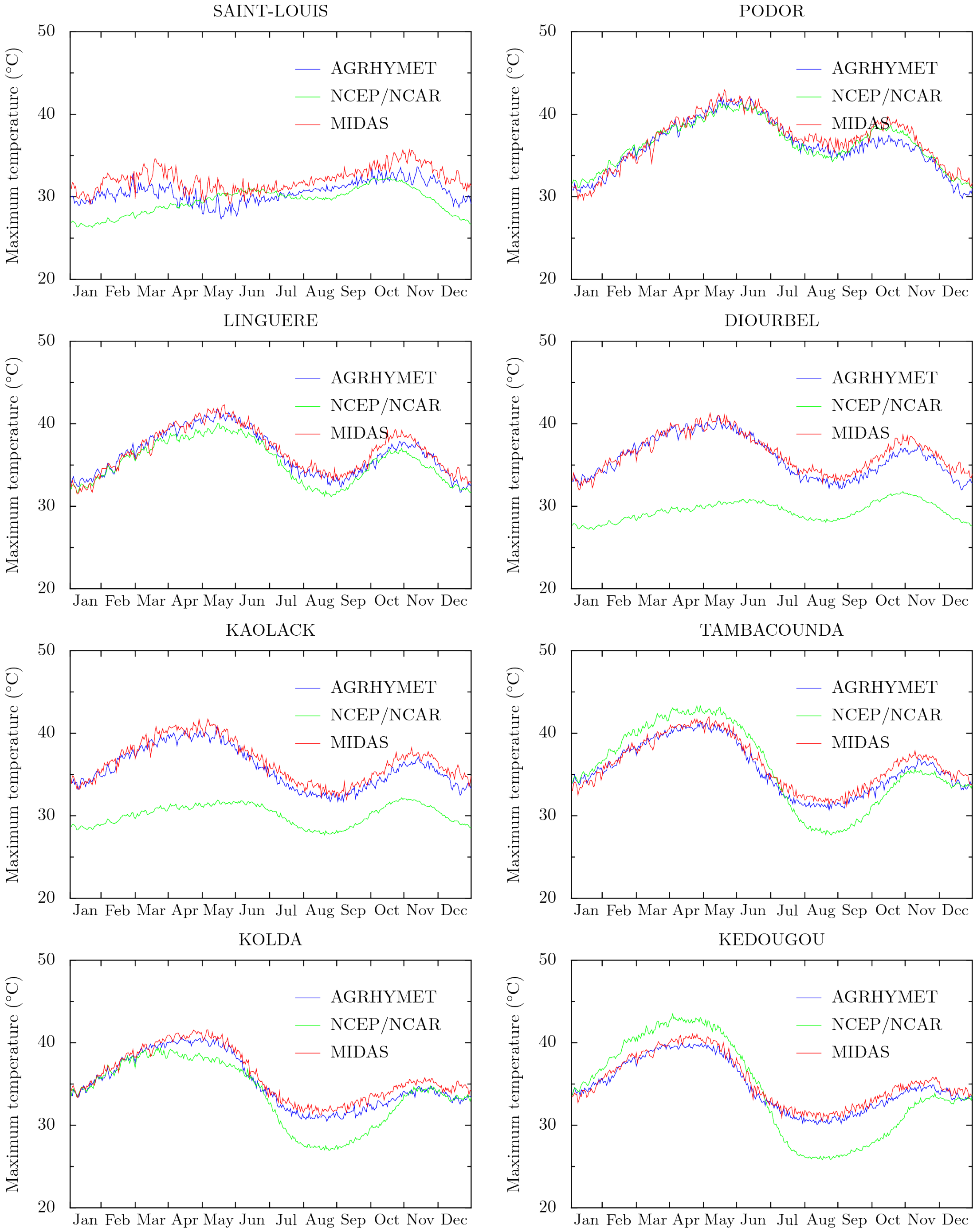

Figure 5.6: Observed and simulated maximum temperatures at eight synoptic stations in Senegal. Each day represents the mean of the period 1950–2008. The observations were extracted from the AGRHYMET dataset (Morel, 1992) and the MIDAS database (UK Met Office, 2009), and the simulations were performed by the NCEP/NCAR reanalysis model (Kalnay *et al.*, 1996).

Parameter	Correlations (R^2)	
	Annual	Rainy season
Minimum temperature (°C)	0.61	0.03
Maximum temperature (°C)	0.54	0.18
Mean temperature (°C)	0.59	0.14
Actual vapour pressure (kPa)	0.86	0.22
24-hour SVP (kPa)	0.57	0.28
Wind speed ($\mathrm{m\,s^{-1}}$)	0.20	0.18

Table 5.5: Statistical correlations for observed and modelled temperature, humidity and wind speed at 11 weather stations in Senegal, for the years 1950–2008. The model simulations were performed by the NCEP/NCAR reanalysis model. The daily values at each station were compared to produce a correlation for each year at each site. The means of these correlations from all of the stations are presented here. All days were included in the annual correlation, while the rainy season correlation considered only the period July–September of each year.

The model simulation of the annual temperature trend at each station is reasonable with an average annual correlation $R^2 = 0.61$ for the minimum temperature and $R^2 = 0.54$ for the maximum temperature (Table 5.5). The correlations within the rainy season (defined here as July–September) are much poorer.

A common characteristic of tropical climates is that the diurnal temperature range is larger than the annual temperature variation. In order to accurately forecast the diurnal temperature range, a model needs to accurately simulate the incoming solar radiation (in fact, the diurnal temperature range is used by Hargreaves' formula, Equation 5.10, to estimate the solar radiation). In contrast with the maximum and minimum temperature trends, the simulations of the diurnal range produced a noticeable north—south pattern of discrepancies (Figure 5.7). Skilful simulations were produced for the northern stations (Podor and Linguere) but the magnitude of the diurnal cycle was too low during the rainy season further south. At Diourbel and Kaolack, in the groundnut basin, the strength of the diurnal cycle was underestimated by up to 10 °C throughout the year.

The mean temperature is used to calculate both the evapotranspiration rate

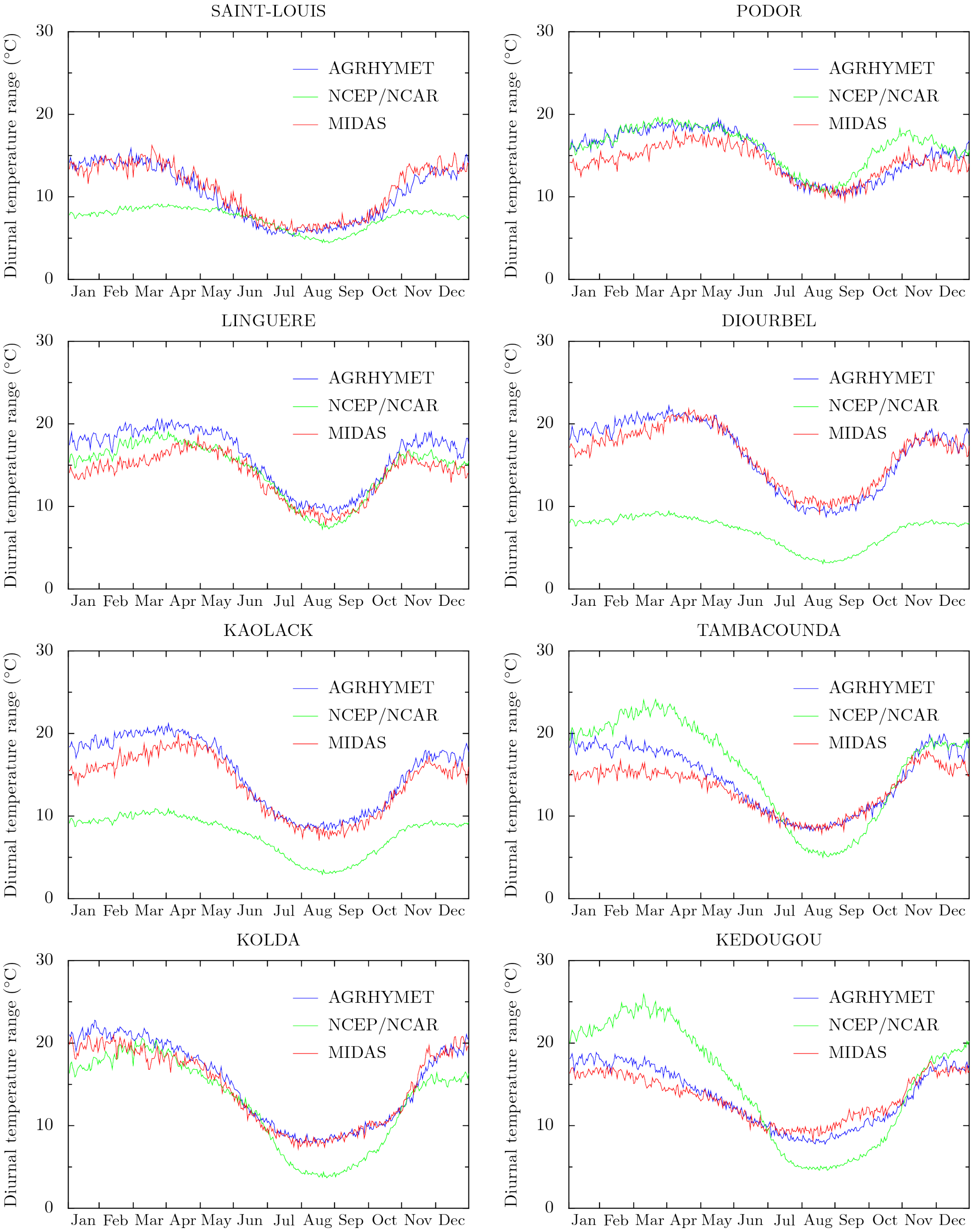

Figure 5.7: Observed and simulated diurnal temperature range at eight synoptic stations in Senegal. Each day represents the mean of the period 1950–2008. The observations were extracted from the AGRHYMET dataset (Morel, 1992) and the MIDAS database (UK Met Office, 2009), and the simulations were performed by the NCEP/NCAR reanalysis model (Kalnay *et al.*, 1996).

and the plant phenological development. While the observed trend was broadly reproduced by the model at all of the sites, it tended in particular to underestimate the mean temperature during the rainy season at the more southerly stations (Figure 5.8).

While the model tended to reproduce the overall temperature trends, the discrepancy tended to increase towards the west and the south, perhaps as a result of the clouds being poorly simulated in the wetter regions. The discrepancy in the rainy season was generally different to that of the dry season (which is why the relationships between the model and the observations were assessed for 10-day periods rather than for the whole year).

5.1.5.2 Humidity

As one would expect from Equation 5.3, the saturated vapour pressure (SVP) trends were very similar to the mean temperature trends, with the model underestimating the rainy season SVP at Diourbel and Kaolack but producing good simulations elsewhere (Figure 5.9). The annual SVP correlation between the model and the observations was similar to the temperature correlations (Table 5.5).

The model underestimated the actual vapour pressure at some of the stations, particularly during the dry season (Figure 5.10). The rainy season simulations were generally good, as reflected by the close annual correlation between the model and the observations (Table 5.5).

The 24-hour SVP increased by 0.37 kPa and the daytime SVP increased by 0.43 kPa between 1950 and 2008. Since the vapour pressure was relatively unchanged (Figure 5.1), the annual average vapour pressure deficit has increased over time. The VPD has increased during the rainy season (July–September), which will have increased the demand for water from crops and could have led to droughts having greater impacts.

5.1.5.3 Wind

A reduction in the wind speed was observed at all of the stations during the rainy season (Figure 5.11). The model reproduced these trends but there was a

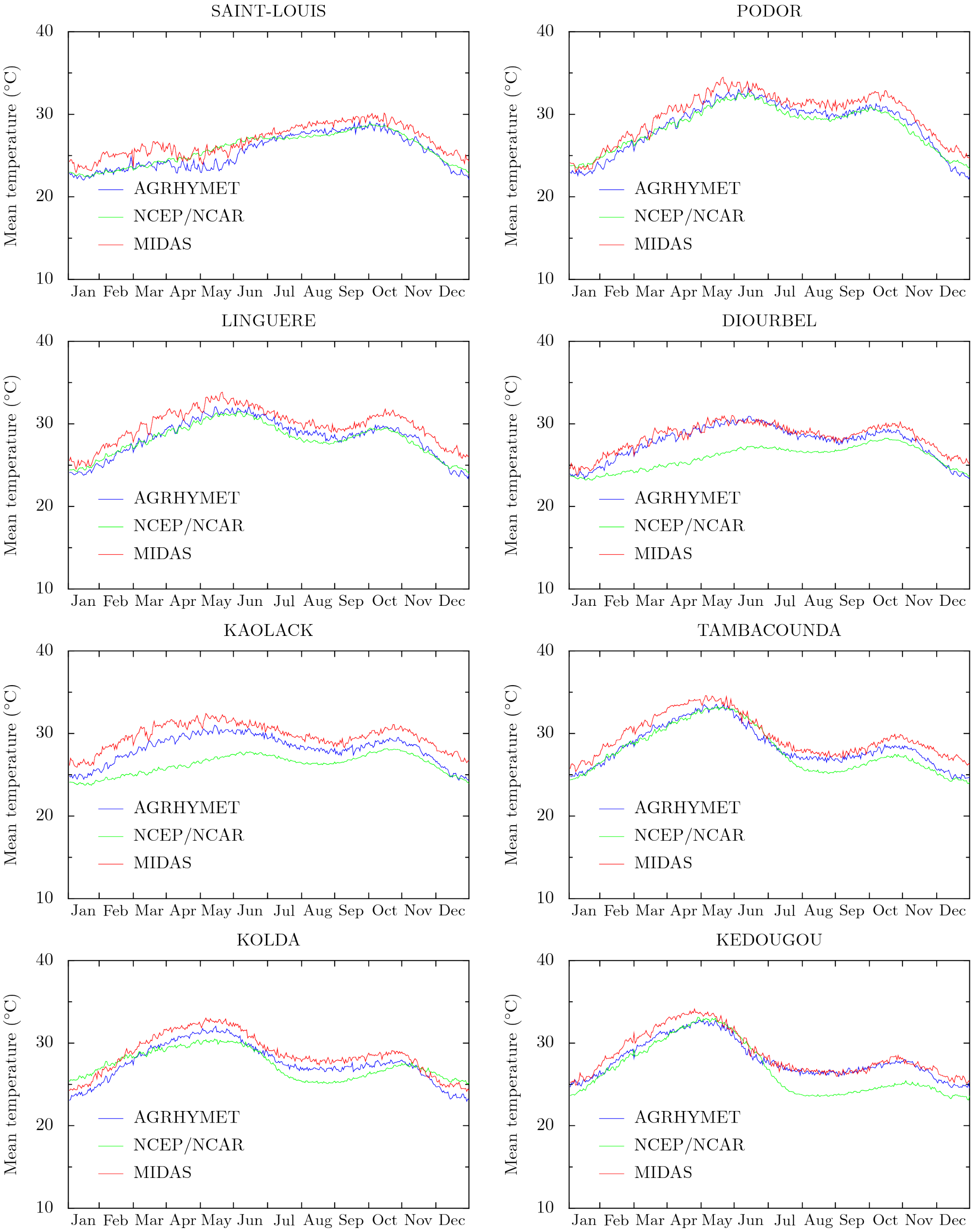

Figure 5.8: Observed and simulated mean temperatures at eight synoptic stations in Senegal. Each day represents the mean of the period 1950–2008. The observations were extracted from the AGRHYMET dataset (Morel, 1992) and the MIDAS database (UK Met Office, 2009), and the simulations were performed by the NCEP/NCAR reanalysis model (Kalnay *et al.*, 1996).

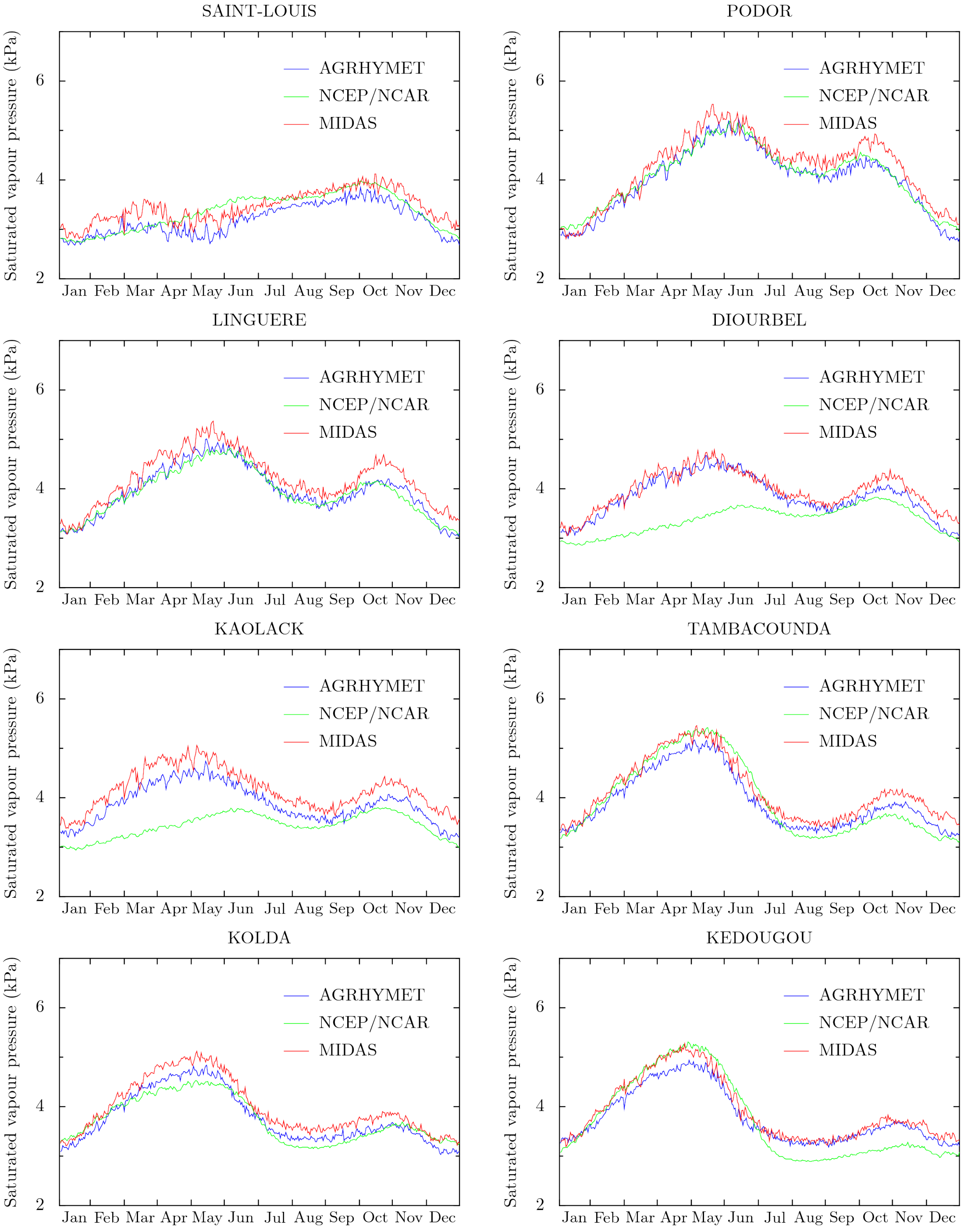

Figure 5.9: Observed and simulated saturated vapour pressure at eight synoptic stations in Senegal. Each day represents the mean of the period 1950–2008. The observations were extracted from the AGRHYMET dataset (Morel, 1992) and the MIDAS database (UK Met Office, 2009), and the simulations were performed by the NCEP/NCAR reanalysis model (Kalnay *et al.*, 1996).

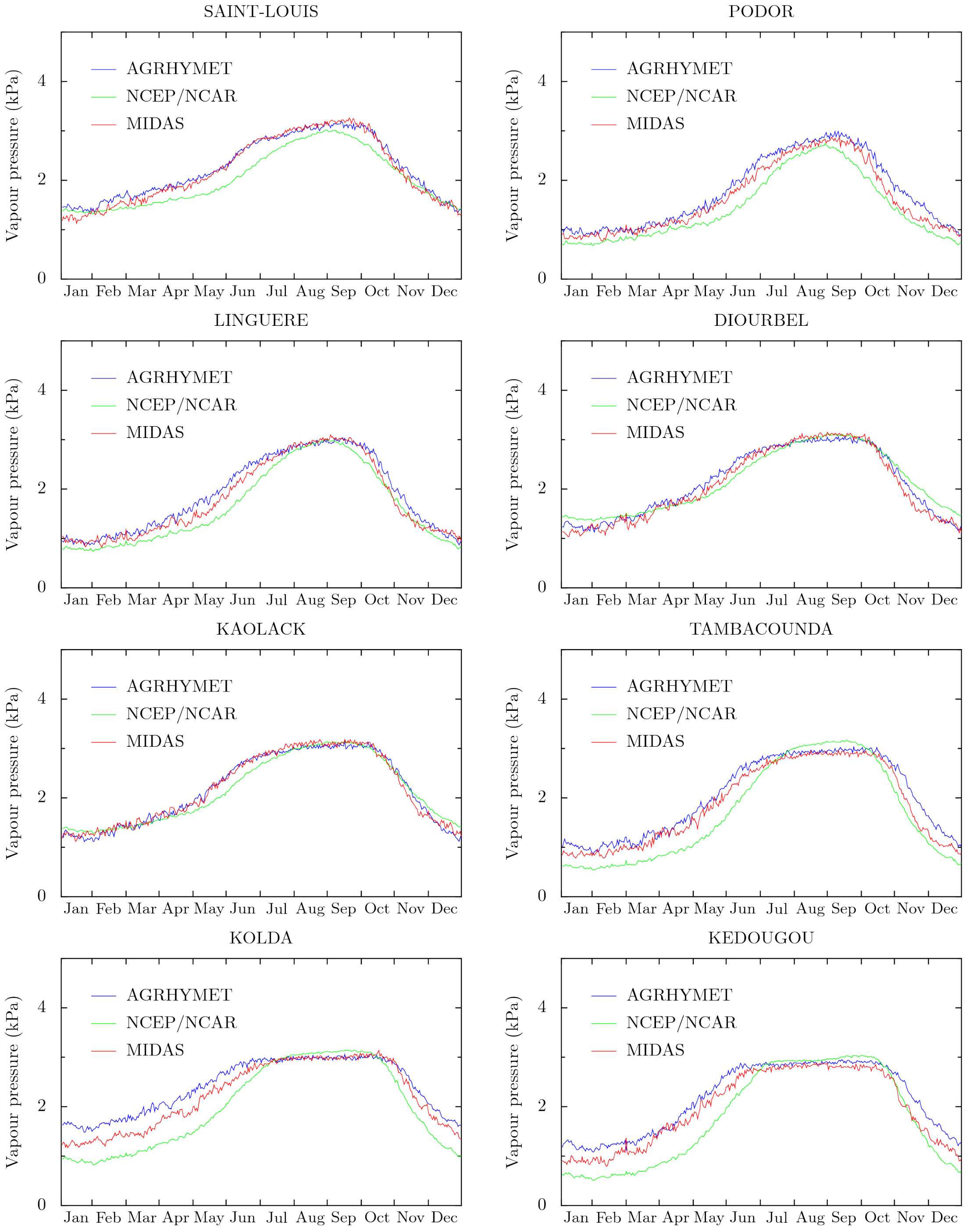

Figure 5.10: Observed and simulated vapour pressure at eight synoptic stations in Senegal. Each day represents the mean of the period 1950–2008. The observations were extracted from the AGRHYMET dataset (Morel, 1992) and the MIDAS database (UK Met Office, 2009), and the simulations were performed by the NCEP/NCAR reanalysis model (Kalnay *et al.*, 1996).

mix of over and underestimation at different stations. Wind speed is particularly difficult to simulate because the precise location of the anemometer can have a significant effect on the measurements, particularly if any orographic features are present in the area. The model simulation of the wind speed trend was much poorer than the simulations of temperature and humidity, with an overall annual correlation of $R^2 = 0.20$ (Table 5.5).

The average wind speed increased by 9 % in the period 1950–2008, although this was driven primarily by the increases observed at the south-easterly stations that were discussed in Section 5.1.2.3. The cause of this phenomenon is not clear (deforestation was considered as a possibility but the model of Sankhayan and Hofstad (2001) suggests that the rate of deforestation should be too slow to have such a profound effect on the climate).

5.1.5.4 Downward solar radiation

There was little variation in the solar radiation across Senegal (Figure 5.12). The NCEP/NCAR model overestimated the solar radiation at all of the stations during the dry season, which perhaps resulted from the impact of atmospheric aerosols in the dusty harmatten wind being under-represented. The simulations were better during the rainy season but the model still overestimated the solar radiation at most stations. The two measurement datasets were generally consistent although the AGRHYMET estimates were slightly higher during the rainy season at Kolda and Kedougou.

The average solar radiation reduced by 5.3 % across Senegal between 1950 and 2008, a phenomenon driven by a 10.3 % reduction in the sunshine duration (a reduction of 55 minutes per day on average). The reduction appeared to occur in the period 1981–1997 when directly-measured sunshine duration data were not available (Figure 5.13). It is not known whether the reduction was real or whether it was caused by the cloud—sunshine relationship being unrepresentative. The reduction is more pronounced at Kedougou than elsewhere. The decrease is small enough to have only a minor effect on the operation of the crop model.

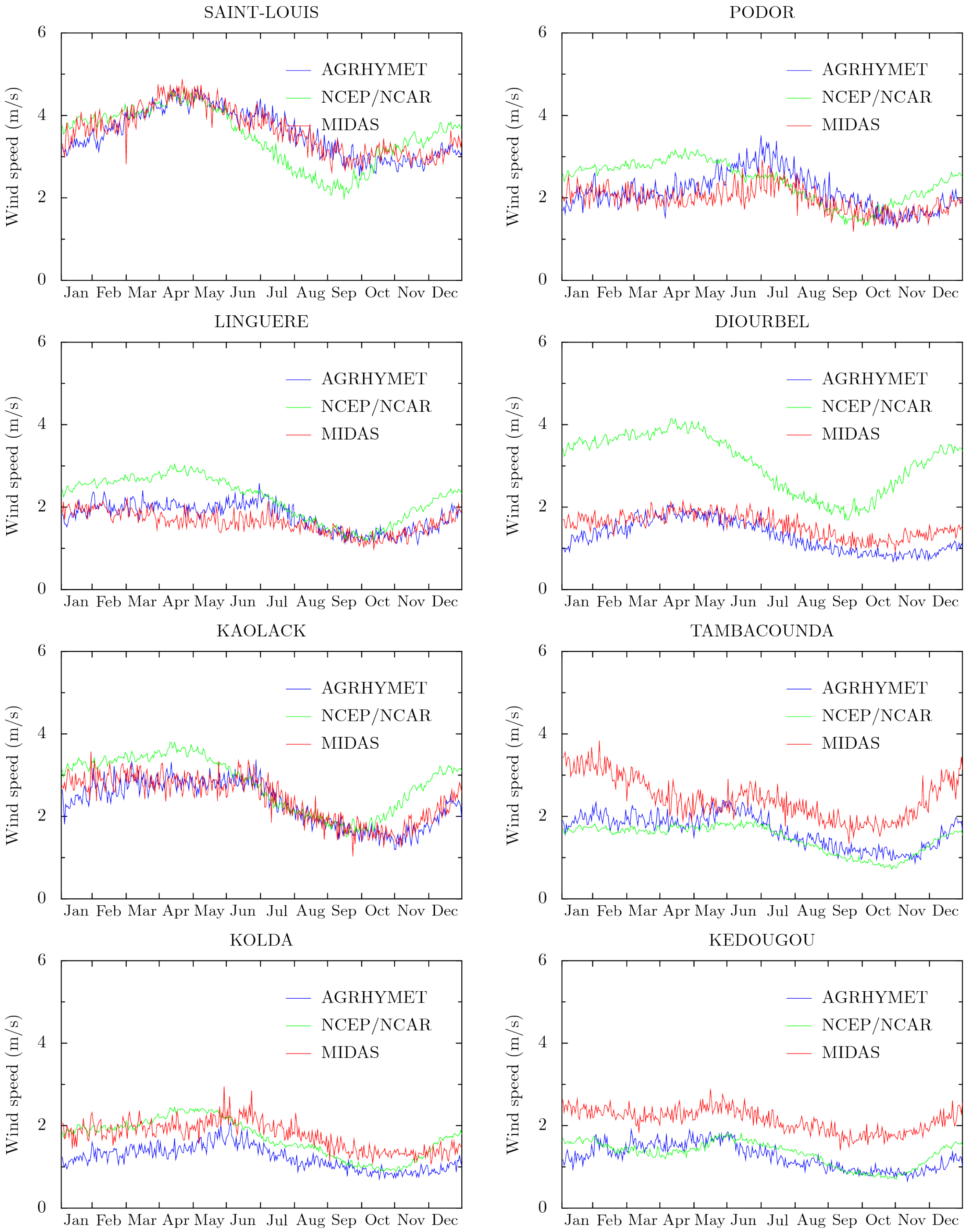

Figure 5.11: Observed and simulated wind speed at eight synoptic stations in Senegal. Each day represents the mean of the period 1950–2008. The observations were extracted from the AGRHYMET dataset (Morel, 1992) and the MIDAS database (UK Met Office, 2009), and the simulations were performed by the NCEP/NCAR reanalysis model (Kalnay *et al.*, 1996).

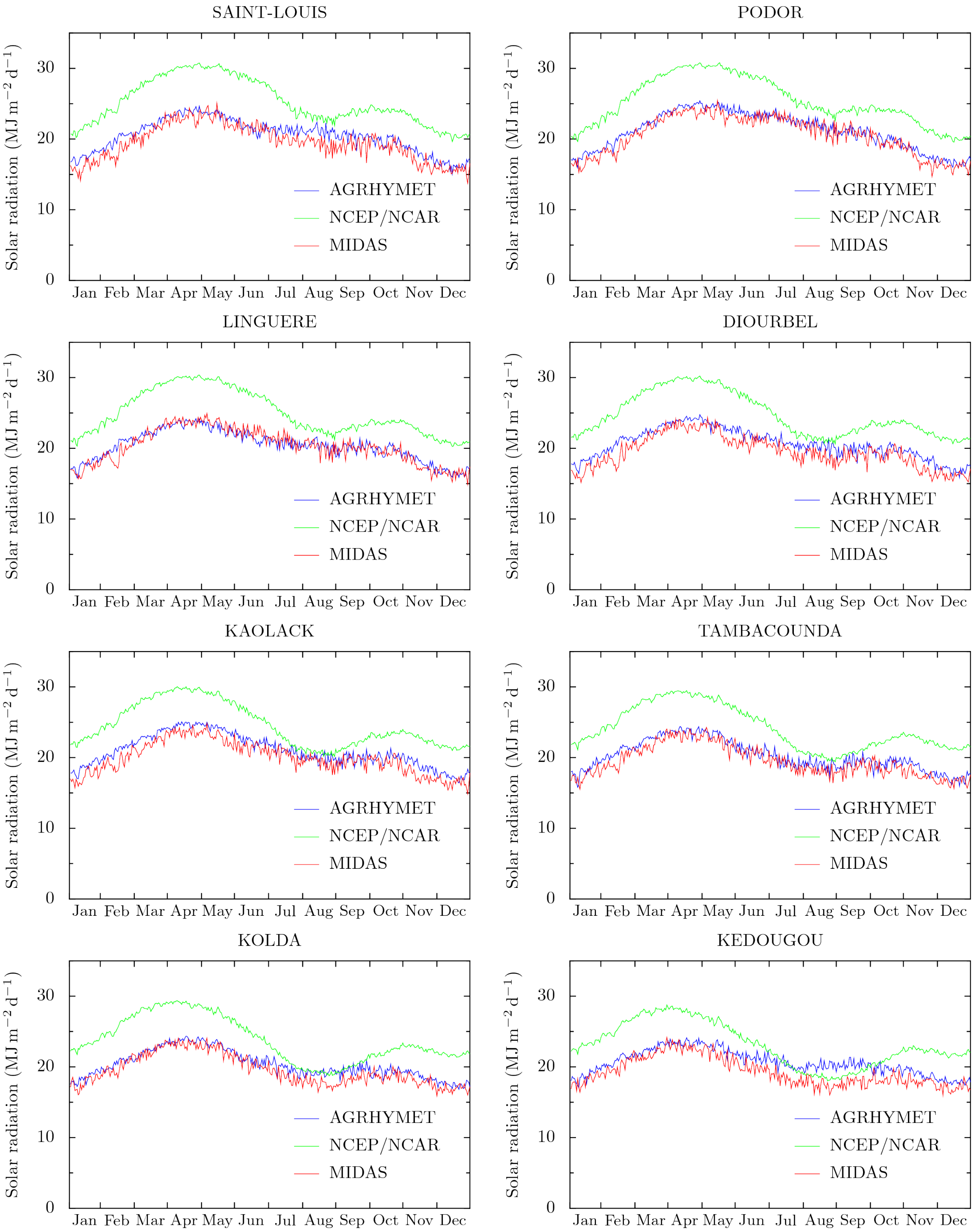

Figure 5.12: Observed and simulated downward solar radiation at eight synoptic stations in Senegal. Each day represents the mean of the period 1950–2008. The observations were extracted from the AGRHYMET dataset (Morel, 1992) and the MIDAS database (UK Met Office, 2009), and the simulations were performed by the NCEP/NCAR reanalysis model (Kalnay *et al.*, 1996).

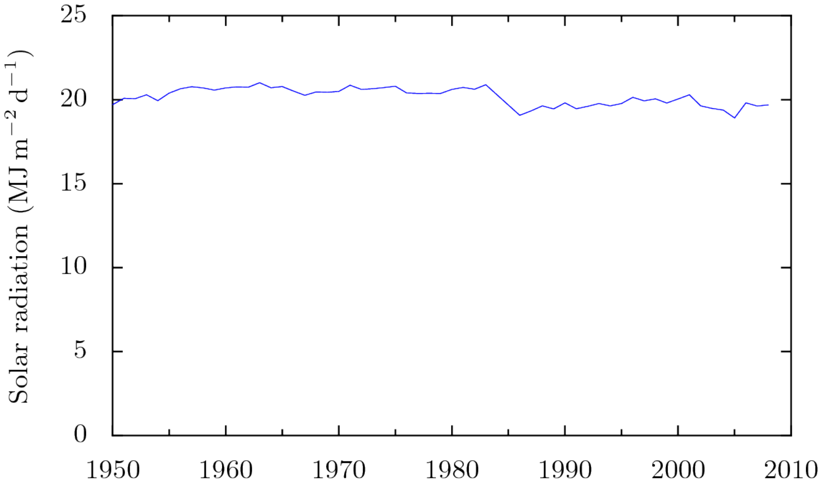

Figure 5.13: Time series of the observed downward solar radiation across Senegal between 1950 and 2008. The average represents the arithmetic mean of 11 synoptic stations across the country. The solar radiation values were calculated from sunshine duration data that were extracted from the AGRHYMET dataset (Morel, 1992) and the MIDAS database (UK Met Office, 2009), using the method described in the text.

5.1.5.5 Rainfall

Rainfall in Senegal is highly variable both spatially and temporally. Most rainfall events occur on smaller spatial scales than those used by the NCEP/NCAR reanalysis model and simulations of the number, size and intensity of events were poor. With the exception of the two most northerly stations, the model substantially overestimated the number of rainfall events; over all of the stations in the period 1950–2008, an average of 40 events per year were observed while the model simulated an average of 67 events per year. This was counterbalanced by an even larger discrepancy in the average magnitude of each event, with the model estimating 5.5 mm per event compared with the observed 15 mm per event.

The model simulated an overly late onset of the rainy season at all of the stations (Figure 5.14). In reality, the rains tend to commence earlier and with smaller, more irregular events than those simulated. The model simulation of the rainfall magnitude at the peak of the rainy season was too low at the drier northern stations and too high in the more humid south. The end of the rainy season was simulated reasonably well.

A time series of the averaged precipitation for the 11 synoptic stations is shown in Figure 5.15. With the exception of the first few years of the twenty-first century, the model consistently underestimates the annual rainfall.

In view of all of these findings, it was concluded that the NCEP/NCAR rainfall simulations were of insufficient quality to be used in the crop model.

5.1.6 Discussion

Producing a long, continuous and accurate meteorological data record is not an easy task. There are numerous discrepancies which must be identified and numerous gaps that must be filled. The dataset is derived from millions of observations so it is impractical to do this by hand. To further compound the difficulties, the original records were not available so it was necessary to use secondary data. Since only rainfall records were available for the years 1981–1984, other meteorological data for this period were derived from the NCEP/NCAR reanalysis model.

The AGRHYMET dataset was complete because the data had been checked and the gaps had already been filled using spatial and temporal extrapolations. It was necessary to develop techniques to fill the gaps in the MIDAS database. A combination of temporal factors and reanalysis model simulations were used to estimate values for erroneous and missing data. A more accurate approach would have been to also use spatial data from other synoptic stations, interpolated using an appropriate kriging technique, but it was concluded that the increase in the accuracy would have been insufficient to justify the additional effort. If the analysis were to be extended in the future from the synoptic stations to all areas of the country then appropriate kriging techniques would have to be developed and it would be reasonable at that point to use spatial techniques.

The rainfall data presented particular methodological difficulties because the required data quality is higher than that of other meteorological data and because the reanalysis model simulations were found to be of insufficient quality. Fortunately, the ESPACE project produced continuous, quality-checked rainfall

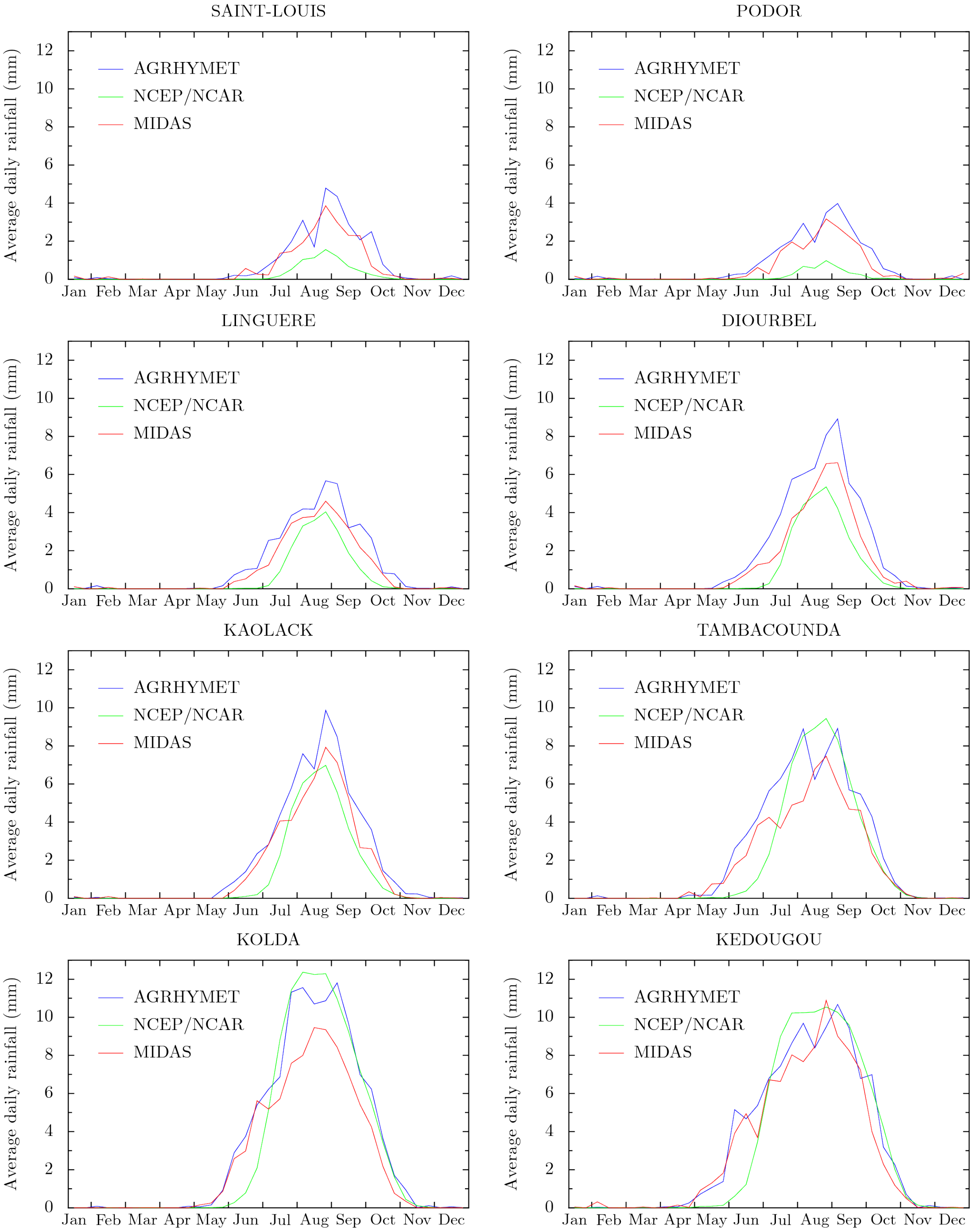

Figure 5.14: Observed and simulated daily average rainfall at eight synoptic stations in Senegal. Each month is split into three 10-day periods and the average daily rainfall for the years 1950–2008 is plotted for each period. The observations were extracted from the AGRHYMET dataset (Morel, 1992) and the MIDAS database (UK Met Office, 2009), and the simulations were performed by the NCEP/NCAR reanalysis model (Kalnay *et al.*, 1996).

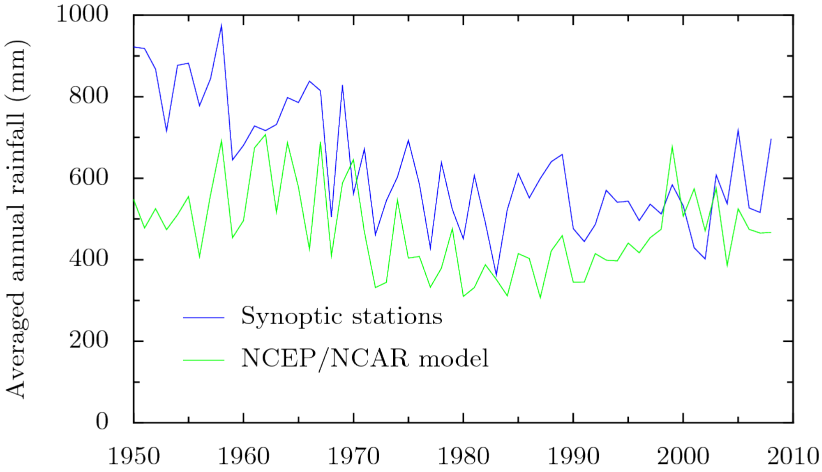

Figure 5.15: Time series of the observed annual rainfall across Senegal between 1950 and 2008. The average represents the arithmetic mean of 11 synoptic stations across the country. The observations were extracted from the AGRHYMET dataset (Morel, 1992) and the MIDAS database (UK Met Office, 2009), and the simulations were performed by the NCEP/NCAR reanalysis model (Kalnay *et al.*, 1996).

records for the synoptic stations in Senegal for the period 1950–1991 and the MIDAS database contained records for 1992–2009. There were some issues with gaps and inaccuracies in the MIDAS database that were difficult to resolve and these could merit renewed attention in the future.

It is possible that other sources of data will become available in the future. Satellite measurements could potentially offer more accurate estimates of the downward shortwave radiation (Stisen *et al.*, 2008) and could also be used to accurately estimate the rainfall across the country (Teo and Grimes, 2007).

Despite these difficulties, a continuous, self-consistent meteorological data record was produced for each synoptic station in Senegal for the period 1950–2009. This dataset provides all of the meteorological data that are required by the crop model.

5.2 Reference evapotranspiration

The loss of water from the soil is simulated in CROMSAS using the reference evapotranspiration (Equation 3.23). Since routine evapotranspiration measurements were not available from the synoptic weather stations, it was necessary to estimate the daily evapotranspiration from meteorological data. Several methods have been developed, the majority of which are derived from the surface energy balance. This section assesses the performance of each method against evapotranspiration measurements to identify the most suitable method for use in the crop model.

5.2.1 Estimating the net radiation

The downward solar radiation is only one component of the surface energy balance. Most methods of estimating the reference evapotranspiration require the net radiation at the surface rather than the downward solar radiation. This section identifies appropriate methods to calculate the net radiation from the downward solar radiation.

The net radiation can be calculated as the sum of the solar (shortwave, denoted sw) and longwave (infrared, denoted lw) radiation fluxes:

$$R_n = R_{nsw} - R_{nlw} = (R_{dsw} - R_{usw}) + (R_{dlw} - R_{ulw}) \tag{5.11}$$

where d and u refer to the downward and upward fluxes, respectively.

The net shortwave radiation, R_{nsw}, is normally calculated using the albedo, α:

$$R_{nsw} = (1 - \alpha)\, R_{dsw} \tag{5.12}$$

The net longwave radiation, R_{nlw}, can be calculated using (Allen *et al.*, 1998):

$$R_{nl} = \sigma \left(\frac{T_{max}^4 - T_{min}^4}{2} \right) (0.34 - 0.14\sqrt{e_a}) \left(a_{lw} \frac{R_s}{R_{so}} - b_{lw} \right) \tag{5.13}$$

where σ is the Stefan-Boltzmann constant ($4.903 \times 10^9\,\mathrm{MJ\,K^{-4}\,m^{-2}\,day^{-1}}$), e_a is the actual vapour pressure, a_{lw} and b_{lw} are constants and the temperatures have units Kelvin. Allen *et al.* (1998) recommend using $a_{lw} = 1.35$ and $b_{lw} = -0.35$, but Meyer (1999) derived alternative values for a hot dryland area of Australia with $a_{lw} = 0.92$ and $b_{lw} = 0.08$. The sum of the constants should always equal unity.

Solar radiation data were available from direct measurements, from indirect observations of the sunshine duration, from NCEP/NCAR reanalysis model simulations and from Hargreaves' formula (Equation 5.10). The data from each of these sources were used to estimate the net radiation at two locations in the Sahel.

5.2.1.1 Radiation measurements at Dahra, Senegal

Specialist equipment is required to perform direct radiation measurements and they are not routinely performed in Senegal. The only comprehensive data that were available within Senegal were recorded in a campaign at Dahra (15°55′N 15°31′W, see Figure 5.4), near Linguere, in 2006 (Stisen *et al.*, 2008). Three components of the surface energy balance were recorded at 15-minute intervals: *a*) downward shortwave radiation; *b*) upward shortwave radiation; and, *c*) net radiation.

Agricultural land in the tropics tends to have an albedo which varies from 0.15 for thick green vegetation to 0.4 for bare soil; for comparison, the reference grass crop for evapotranspiration calculations in Allen *et al.* (1998) has an albedo of 0.23. The evolution of the albedo through the 2006 rainy season is shown in Figure 5.16. Dahra has a short rainy season and the albedo was close to 0.38 until August. The three large peaks occurred on days of unusually low downward solar radiation (i.e. on particularly cloudy days). The first of these days brought heavy rainfall and the albedo reduced to around 0.25 as vegetation developed. Following a gradual increase to 0.35 in September, the albedo reduced again following further large rainfall events and settled at around 0.28.

There was an 8-day break in measurements at the end of September. Afterwards, the net radiation measurements steadily reduced to around $2\,\mathrm{MJ\,m^{-2}\,d^{-1}}$ by mid-December (Figure 5.17). While a reduction is expected towards the end of the year as the solar minimum approaches (see the NCEP/NCAR model simulation on the same graph), this decrease was considered to be too steep and

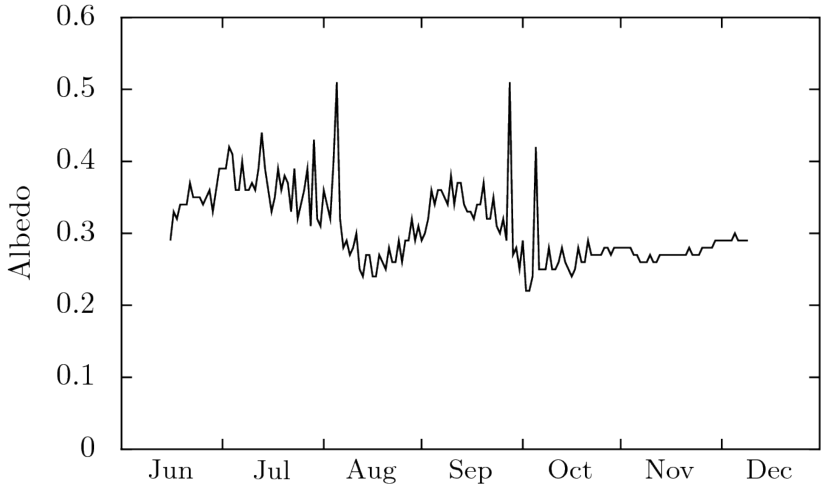

Figure 5.16: Evolution of the albedo at Dahra, Senegal in 2006. The peaks occurred on days of particularly low downward solar radiation.

more likely to result from a problem with the instrument. The net radiation measurements from October were not used in the analysis.

The net longwave radiation on each day was calculated from the shortwave balance and the net radiation by rearranging Equation 5.11. This was then compared with the estimates from Equation 5.13 and with the NCEP/NCAR model simulation.

A regression model was used to calculate new constants for Equation 5.13. At first, the fit was poor with $a_{lw} + b_{lw} = 1.1$ rather than unity and with an unexpectedly weak relationship between solar radiation and longwave radiation (low a_{lw}), which was caused by longwave radiation being underestimated. A possible cause of the underestimation was the assumption in Equation 5.13 that the surface temperature was equal to the air temperature. Since only sparse vegetation grows at such northerly climates, and since the solar radiation is so intense, it is likely that the surface temperature was higher than the air temperature during daylight hours. An investigation showed that using a surface temperature that was on average 10 °C higher than the air temperature produced a better fit, with $a_{lw} = 0.85$ and $b_{lw} = 0.15$. These values are close to those derived by (Meyer, 1999) for a dryland area of Australia.

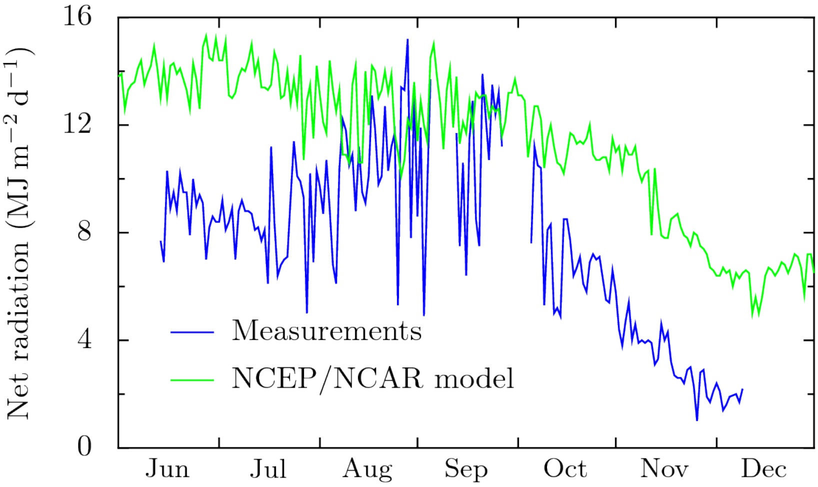

Figure 5.17: Net radiation measurements at Dahra, Senegal in 2006 (Stisen *et al.*, 2008), together with estimates from the NCEP/NCAR reanalysis model (Kalnay *et al.*, 1996). Gaps in the measurements indicate periods when the equipment was not operational.

The net longwave radiation estimates from Equation 5.13 were more closely correlated to the measurements than the NCEP/NCAR model estimates (Table 5.6). Although the correlations were poor, Equation 5.13 produced a similar mean and the variability was low. The NCEP/NCAR model estimates were too high as a result of the solar radiation being overestimated.

A comparison of the net radiation measurements with several estimates is shown in Table 5.7. The most closely correlated estimate came from a combination of the measured solar radiation with the net longwave radiation from the calibrated version of Equation 5.13. The average of this method was similar to the measured value. In contrast, the NCEP/NCAR model overestimated the net radiation and the correlation between the model and the measurements was very poor.

5.2.1.2 Net radiation measurements in the HAPEX-Sahel project

There was concern that the Dahra measurements might not be representative for Senegal because they were taken at a single site during only one rainy sea-

Method	Mean (MJ m^{-2} day^{-1})	R^2
Measured net lw radiation	4.5	
Estimated lw from measured R_s	4.6	0.36
Estimated lw from Hargreaves' R_s	4.1	0.28
NCEP/NCAR reanalysis model lw	5.1	0.17

Table 5.6: Estimates of the average net longwave (lw) radiation at Dahra, Senegal in June–September 2006. The measured figure was inferred from measurements of the shortwave radiation balance and the net radiation. The estimated lw figures were calculated using Equation 5.13, with only the solar radiation varying between the two rows. A 10 ℃ temperature correction was applied to the equation and calibrated coefficients were used (see the text for more details).

Method	Mean (MJ m^{-2} day^{-1})	R^2
Measured RN	9.6	
Estimated RN from measured R_s	9.4	0.66
Estimated RN from Hargreaves' R_s	8.9	0.19
NCEP/NCAR reanalysis model RN	13.1	0.02

Table 5.7: Estimates of the net radiation (RN) at Dahra, Senegal in June–September 2006. The estimated RN figures were calculated using Equation 5.13, with only the solar radiation varying between the two rows. A 10 ℃ temperature correction was applied to the equation and calibrated coefficients were used (see the text for more details). The Hargreaves' calculation assumed a constant albedo of 0.28 throughout the season.

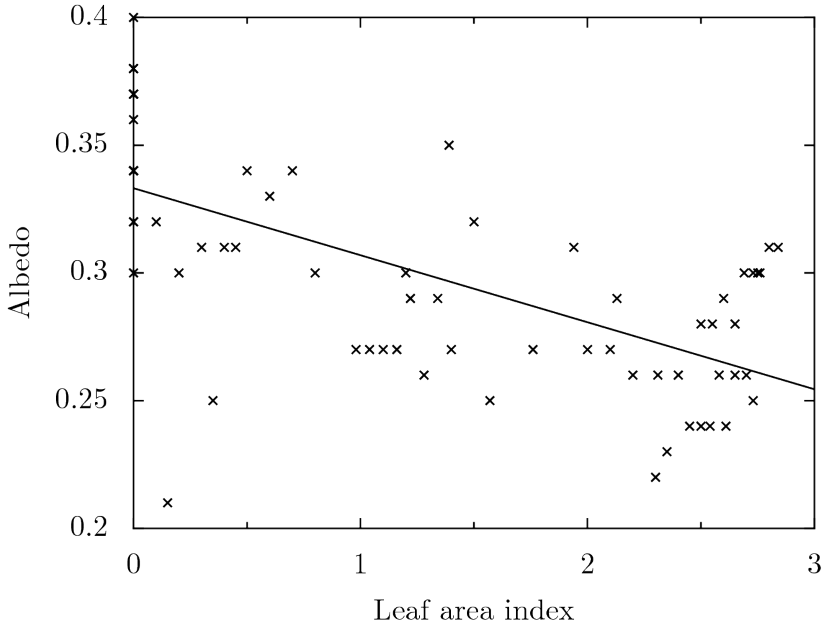

Figure 5.18: Relationship between the albedo and the leaf area index in a millet field, from the HAPEX-Sahel experiment in 1992. The albedo continued to decrease during leaf senescence after the LAI peaked at 2.8 and did not increase again until the crop was harvested.

son. Since alternative measurements of the net radiation were not available for Senegal, data from the HAPEX-Sahel project (H-S) in Niger were examined instead. Measurements were downloaded from `http://www.ird.fr/hapex` for the East-Central Supersite (13°40′N 2°32′E) in 1992. This site lies 2° south of Dahra. NCEP/NCAR reanalysis data were retrieved for the same location.

The clear sky radiation, R_{so}, was found from the maximum value of the ratio of the measured radiation to the extraterrestrial radiation (R_s/R_{et}). For Niger, in Equation 5.8, $a_s + b_s = 0.73$, which was similar to the Dahra and Bambey maximums of 0.75.

The H-S measurements were performed in a millet field so the relationship between the albedo and the leaf area index (LAI) of the crop could be examined. Figure 5.18 shows, as expected, that the albedo tended to decrease as the LAI increased, from around 0.34 to 0.26 ($R^2 = 0.41$).

Similar difficulties were encountered when estimating the net longwave radiation in the H-S experiment as were found in the Dahra experiment. A 20 °C temperature difference between the surface and air temperatures was required to produce a good fit to the measurements. The constants, again derived using regression analysis, were different to those at Dahra with $a_{lw} = 0.71$ and $b_{lw} = 0.29$. The estimated values were more closely correlated to the measured values in the H-S experiment than at Dahra (Table 5.8). While the NCEP/NCAR mean was similar at both sites, the measured mean was $1\,\mathrm{MJ\,m^{-2}\,d^{-1}}$ greater in the H-S experiment. The reason for this is not known; it could be a climatic phenomenon, but Lloyd *et al.* (1997) notes that there can be a 20 % discrepancy between two such instruments in the same place so the discrepancy is within the tolerance of the instruments.

A comparison of the net radiation measurements with the estimates is shown in Table 5.9. The trends are similar to those at Dahra, with Equation 5.13 producing the most skilful estimate. The NCEP/NCAR model overestimated the net radiation and there was no correlation with the measurements.

5.2.1.3 Discussion

Field campaigns in Senegal and Niger were used to assess the methods of estimating the net radiation. The albedo reduced as the leaf area increased.

Few studies have examined longwave radiation trends in the tropics. The derived constants indicate that the longwave radiation in the Sahel is less sensitive to the solar radiation than assumed in the approach of Allen *et al.* (1998). It was necessary to assume an offset between the surface and air temperatures for both field campaigns to derive reasonable estimates of the longwave radiation from Equation 5.13. In the calculations of reference evapotranspiration, which assume the presence of a well-watered crop, this temperature offset should not be applied because the surface and air temperatures should be similar.

The net radiation in both campaigns was skilfully predicted by this approach, demonstrating that it is suitable for reference evapotranspiration calculations. In contrast, the NCEP/NCAR model tended to overestimate the net radiation and the correlations with the measurements were poor.

Method	Mean ($\mathrm{MJ\,m^{-2}\,day^{-1}}$)	R^2
Measured R_{nl}	5.4	
Estimated R_{nl} from measured R_s	5.4	0.74
Estimated R_{nl} from Hargreaves' R_s	4.7	0.53
NCEP/NCAR reanalysis model R_{nl}	4.9	0.26

Table 5.8: Estimates of the average net longwave (R_{nl}) radiation during the HAPEX-Sahel experiment in July–October 1992. The measured figure was inferred from measurements of the shortwave radiation balance and the net radiation. The estimated lw figures were calculated using Equation 5.13, with only the solar radiation varying between the two rows. A 20 °C temperature correction was applied to the equation and calibrated coefficients were used (see the text for more details).

Method	Mean ($\mathrm{MJ\,m^{-2}\,day^{-1}}$)	R^2
Measured R_n	10.3	
Estimated R_n from measured R_s	10.3	0.90
Estimated R_n from Hargreaves' R_s	8.4	0.49
NCEP/NCAR reanalysis model R_n	11.8	0.00

Table 5.9: Estimates of the net radiation (R_n) during the HAPEX-Sahel experiment in July–October 1992. The estimated RN figures are calculated using Equation 5.13, with only the solar radiation varying between the two rows. A 20 °C temperature correction was applied to the equation and calibrated coefficients were used (see the text for more details). The Hargreaves' calculation assumed a constant albedo of 0.28 throughout the season.

5.2.2 Estimating the ground heat flux

The ground heat flux is the heat that is gained or lost when the ground heats or cools. The flux magnitude is related to the mineral composition and water content of the soil. It is normally much smaller than the net radiation flux and is often neglected or assumed to be zero.

Several methods have been proposed to estimate the ground heat flux. Based on the idea that the soil temperature lags the air temperature, several authors have calculated the ground heat flux as a function of the change in the air temperature over several days (Allen *et al.*, 1998; Jensen *et al.*, 1971; Meyer, 1988):

$$G = c_s \frac{T_{av\_i} - T_{av\_i-1}}{\delta t} \delta z \tag{5.14}$$

where c_s is the soil heat capacity, T_{av_i} and T_{av_i-1} are the air temperatures at times i and $i-1$ respectively, δt is the time interval and δz is the effective soil depth. The effective soil depth can range from 0.1 m for a couple of days to more than 2 m for monthly periods.

Alternatively, Challinor *et al.* (2004) estimates the ground heat flux as a function of the net radiation flux:

$$G = 0.4 R_n \mathrm{e}^{-kL} \tag{5.15}$$

where k is the light extinction coefficient and L is the LAI.

Both of these equations were compared against measurements of the ground heat flux from the HAPEX-Sahel campaign at the East-Central Supersite in 1992. For Equation 5.14, the best correlation was found against the average temperature 4 days previously (with $\delta t = 4\,\mathrm{day}$, $\delta z = 0.1\,\mathrm{m}$ and $c_s = 15\,\mathrm{MJ\,m^{-3}\,°C^{-1}}$). Equation 5.15 was tested for bare soil and for a fully developed millet crop canopy ($L = 3$).

Table 5.10 shows that the net radiation method was most closely correlated to the measurements but tended to overestimate the ground heat flux. This method has a significant disadvantage that negative values do not occur because the net radiation flux is always positive over 24 hours. The temperature lag method correlation was lower but the mean estimate was close to the measured mean. The NCEP/NCAR reanalysis model had a similarly close mean but was negatively

Method	Mean ($\mathrm{MJ\,m^{-2}\,day^{-1}}$)	R^2
Measured ground heat flux	0.3	
Temperature lag estimation	0.1	0.31
Net radiation estimation, $L = 0$	4.2	0.39
Net radiation estimation, $L = 3$	0.9	0.39
NCEP/NCAR reanalysis model	0.1	0.07

Table 5.10: Comparison of measured and estimated ground heat flux during the HAPEX-Sahel experiment.

correlated with measurements. It was concluded that the temperature lag method was the most appropriate of these methods to estimate the daily ground heat flux because the mean was close to the measured mean and a positive correlation was observed.

On most days during the growing season, the magnitude of the ground heat flux was less than 10 % of the magnitude of the net radiation flux at the HAPEX-Sahel site, so any errors were likely to have little impact on the surface energy balance. It was therefore acceptable to set the ground heat flux to zero to reduce the possibility of any large daily errors being introduced.

5.2.3 Reference evapotranspiration methodologies

Numerous methods have been developed to estimate the water loss from plants, soil and water bodies. The principal approach has been to identify a standard rate of evapotranspiration under particular conditions and then to calculate the actual evapotranspiration by applying coefficients that depend on the crop type, the growth stage and the soil water availability (e.g. Equation 3.23). At first, the standard rate was termed the *potential evapotranspiration* because it was considered to be the maximum possible rate of water loss (Penman, 1948). While this is reasonable in the relatively cool and humid climate of the UK, it is less accurate in hot dry climates where crop evapotranspiration can exceed the free water evaporation. The potential evapotranspiration was replaced by a *reference evapotranspiration* which represents the water loss from a "well-watered hypothetical grass crop with an assumed height of 0.12 m, with a surface resistance of $70\,\mathrm{s\,m^{-1}}$ and an albedo of 0.23" (Allen *et al.*, 1998). This section identifies the most appropriate method to estimate the reference evapotranspiration in Senegal.

5.2.3.1 Evapotranspiration formulae

The surface energy balance of a field can be written as:

$$R_n - G = \lambda E + H \tag{5.16}$$

where R_n is the net radiation at the surface, G is the ground heat flux, λE is the latent heat flux (the evaporation) and H is the sensible heat flux. Most evapotranspiration equations are derived from Equation 5.16 with the aim of estimating the latent heat flux term using available meteorological data.

Penman (1948) derived what is now known as the Penman equation by combining the surface energy balance with the Dalton equation. He assumed that the surface temperature was close to the air temperature, which was certainly true for the cool, humid English climate where he performed his work but is less certain in hot, dry climates (Dodds *et al.*, 2005). The first methodology that was recommended by the FAO for calculating reference evapotranspiration, denoted FAO24 in this study, was a variant of the Penman equation (Doorenbos and Pruitt, 1977):

$$\lambda E = \frac{\Delta\left(R_n - G\right) + \gamma\left(0.27 + 0.23u_2\right)\left(e_a^s - e_a\right)}{\Delta + \gamma} \tag{5.17}$$

where Δ is the gradient of the saturation vapour pressure curve (calculated at T_{av}), γ is the psychrometric constant, $e_a^s - e_a$ is the vapour pressure deficit and u is the wind speed (in units $\mathrm{m\,s^{-1}}$).

A subsequent report, denoted FAO56, recommended an alternative approach which was based on an equation derived from similar principles called the Penman-Monteith equation (Allen *et al.*, 1998):

$$\lambda E = \frac{\Delta\left(R_n - G\right) + \gamma\frac{900\lambda}{T+273}u_2\left(e_a^s - e_a\right)}{\Delta + \gamma\left(1 + 0.34u_2\right)} \tag{5.18}$$

Priestley and Taylor (1972) used a simplified version of the Penman equation to calculate the ETo over large areas (denoted P-T):

$$\lambda E = \alpha \frac{\Delta \left(R_n - G\right)}{\Delta + \gamma} \tag{5.19}$$

where α is a coefficient which is set to 1.26 by both Priestley and Taylor (1972) and Baron *et al.* (1996).

Challinor *et al.* (2004) uses an alternative form of the P-T equation with the coefficient altered to account for high vapour pressure deficits (denoted GLAM):

$$\alpha = 1 + \left(\alpha_0 - 1\right) \frac{\left(e_a^s - e_a\right)}{V_{ref}} \tag{5.20}$$

where $\alpha_0 = 1.26$ and V_{ref} is a reference value of the vapour pressure deficit which was set to 1 kPa in the GLAM model.

The final equation of interest here is Hargreaves' formula. In contrast to the equations described above, it is designed for locations where adequate net radiation data are not available (Allen *et al.*, 1998):

$$E = 0.0023 \left(T_{av} + 17.8\right) \left(T_{max} - T_{min}\right)^{0.5} R_a \tag{5.21}$$

where R_a is the extraterrestrial radiation flux.

All of these equations estimate ETo using only meteorological data. The choice of equation depends upon both the availability of data and the accuracy of the equation in a particular climatic zone. Where possible, the quality of the ETo estimates should be evaluated against experimental measurements.

5.2.3.2 Methods for measuring evapotranspiration

The reference evapotranspiration (ETo) is difficult to measure directly. The most common and oldest method is the evaporation pan, where a pan of standard size (generally a "Class A" pan) is filled to the same level each morning; the quantity of water required can then be used to calculate the evaporation from the previous 24 hours. The evaporation rate depends on many factors including the type of pan, the environment of the area in which the pan lies (cropped or bare soil), the exchange of heat between the pan and the ground and the weather (Jones, 1992). There are two major drawbacks with evaporation pans (Dodds *et al.*, 2005): *a*) pan evaporation, which is effectively free water evaporation, is different to evapotranspiration where the behaviour of the crop affects the water loss; and, *b*) the pan measurements depend on the placement of the pan, the surrounding environment and the skill of the operator, so some of the variation between sites is not related to the local atmospheric evaporative demand.

A better method to measure the evaporation uses an instrument called a weighing lysimeter. This is a set of scales which is buried underground in a cropped field with a slab of soil (perhaps 1 m deep) on top. Changes in the weight of the soil slab are principally caused by the addition or removal of water. The field is irrigated to capacity every day and the loss of water due to evapotranspiration is recorded. Placing the scales in a large homogeneous field reduces the influence of the local environment on the results. Unfortunately, lysimeter experiments are very expensive and time-consuming to perform and few have taken place in Africa.

Another method uses eddy correlation instruments to measure the relative magnitudes of the latent and sensible heat fluxes, called the Bowen ratio (Bowen, 1926). Although this method requires specialist equipment, the measurements are taken automatically. Eddy correlation was used to measure the Bowen ratio in the HAPEX-Sahel experiment. However, the instruments tend to measure a large upwind evapotranspiration footprint of unknown area so it is difficult to assess the effects of heat advection on the local evapotranspiration rate (Lloyd *et al.*, 1997). Additionally, the area around the instruments is often not irrigated so the only useful measurements for reference evapotranspiration are those on days immediately following rainfall.

5.2.3.3 Evapotranspiration measurements in Senegal

Time series of evaporation pan measurements were obtained from CIRAD for the Bambey agricultural research station for the years 1972–1991 and 2004–2007. The quality of the data was verified by plotting a time series of the total annual evaporation (Figure 5.19). The measurements in the period 1967–1971 were lower

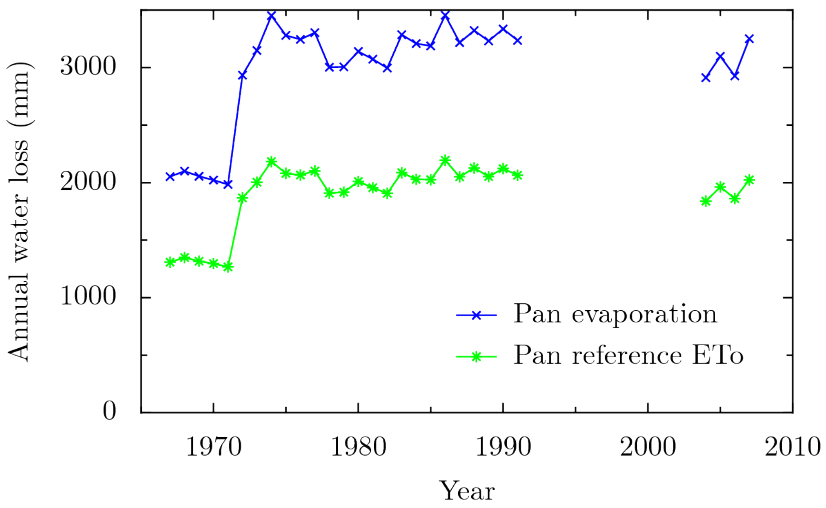

Figure 5.19: Time series of the annual measured pan evaporation at Bambey, Senegal between 1967 and 2007. The reference evapotranspiration (ETo) was calculated from the pan evaporation using the coefficients derived by Dancette (1976) for Bambey. The pan evaporation data were supplied by CIRAD.

than in the later years and were excluded. Otherwise, the two sets of measurements were consistent and it was therefore likely that the pan was operated under consistent conditions in the period 1972–2007.

The next step was to convert the pan evaporation to reference ETo. Dancette (1976) measured the reference ETo using a grass crop at Bambey in 1969–1970 and compared it with pan evaporation during the same period. Monthly coefficients were produced to translate pan evaporation measurements to reference ETo. These were used to estimate the reference ETo for Bambey for the period 1972–2007 as shown in Figure 5.19. The reference ETo is substantially lower than the pan evaporation. The average annual reference ETo measured by Dancette (1976) was 2011 mm, which was very close to the estimated average from the pan evaporation of 2018 mm and provided further evidence that the two sets of measurements were recorded using similar evaporation pans operated under consistent environmental conditions.

Meteorological observations from Bambey were available for the period 1975–2007. The reference ETo was estimated using the five equations in Section 5.2.3.2 and compared to the pan ETo. Table 5.11 summarises the annual averages for each method over the whole period. The Penman equations were best-correlated with the measured pan ETo. The annual mean of the FAO56 equation was close to the pan mean but the rainy season mean was slightly overestimated. In contrast, the FAO24 mean was significantly higher than the pan mean. A similar conclusion was also reached by Steiner *et al.* (1991), who found that the FAO24 equation overestimated the ETo by 30 % in a similar hot, dry climate in the USA when compared with measurements from weighing lysimeters. The scatter of the FAO56 estimates, measured using the standard deviation, was noticeably lower than that of the pan measurements. The accuracy of the other equations was significantly poorer, probably resulting from the horizontal advection of heat being more poorly represented.

The FAO56 Penman-Monteith equation is the most suitable for estimating the reference ETo if the required meteorological data are available. Figure 5.20 examines the variation of the methods through the year using data averaged over the period 1975–2007. The FAO56 estimate is close to the pan ETo throughout the year, although the April peak is underestimated and the September rainy-season trough is overestimated. The performance in the last four months of the year is poorer than that of the first eight months. The FAO24 trend is similar to the FAO56 trend throughout the year but the FAO24 ETo is consistently too high.

The only other daily evaporation pan data that were available for Senegal were for Nioro-du-Rip in the south of the country, for the period 1989–1990. Unfortunately, on-site meteorological data were not available so it was necessary to use data from the synoptic weather station at Kaolack, which lies 41 km to the north. The correlations between the equations and the pan ETo were poorer at Nioro and all of the equations overestimated the ETo during the growing season (not shown). This probably resulted from using meteorological data from a more northerly location, where the heat advection is greater and the evaporative demand higher, rather than being caused by the equations being inaccurate. The Nioro-du-Rip results were broadly consistent with the findings from Bambey but no further conclusions could be reached.

	Mean	St dev	Correl (R^2)
Annual			
Measured pan ETo	5.5	1.8	
FAO24 Penman	6.8	1.6	0.60
FAO56 Penman-Monteith	5.4	1.3	0.56
Priestley-Taylor	4.3	1.2	0.05
GLAM	6.1	1.9	0.19
Hargreaves	5.7	1.1	0.42
July–September			
Measured pan ETo	4.5	1.3	
FAO24 Penman	5.9	1.2	0.42
FAO56 Penman-Monteith	4.8	0.9	0.39
Priestley-Taylor	5.0	0.9	0.19
GLAM	6.2	1.4	0.24
Hargreaves	5.1	0.6	0.24

Table 5.11: Comparison of measured and estimated ETo at Bambey, Senegal. Each value is an average of the annual figures for the periods 1972–1991 and 2004-2007. The pan ETo is estimated from the pan evaporation using the coefficients derived by Dancette (1976). All values (except for the correlation) have units mm day^{-1}. “St dev” is the averaged standard deviation for the whole year. “Correl” is the correlation between the model estimate and the measured pan ETo.

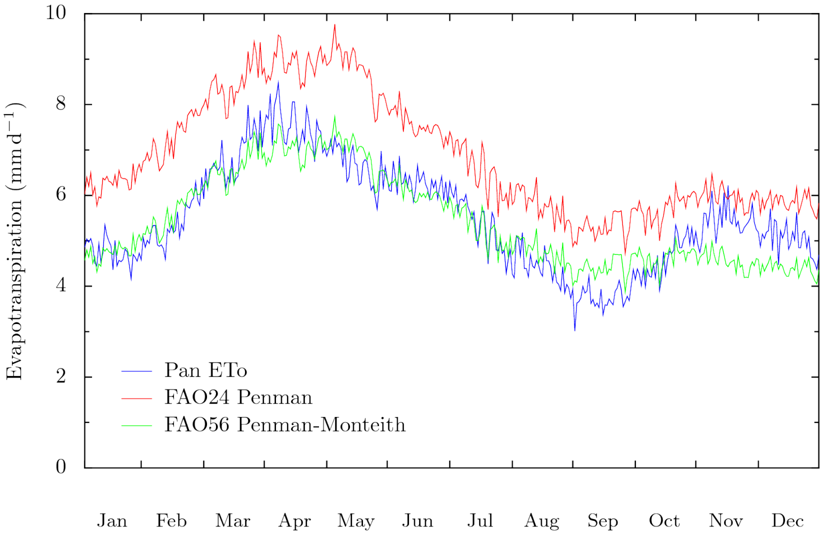

Figure 5.20: Observed and estimated reference evapotranspiration climatology for Bambey, Senegal. Each day represents the mean of the period 1975–2007 (excluding days where data were not available for one or more methods). The observations were derived from pan evaporation data supplied by CIRAD.

5.2.3.4 Evapotranspiration measurements from the HAPEX-Sahel experiment

The HAPEX-Sahel project used eddy correlation instruments to measure the Bowen ratio. At first, it was hoped that the measurements could be combined with local meteorological observations to examine the performance of the equations in another part of the Sahel. Unfortunately, the latent heat flux was assessed by measuring the net radiation and dividing this into latent and sensible heat fluxes, with the assumption that the advected heat flux would be negligible over large areas (Monteny *et al.*, 1997). The Priestley-Taylor equation, which takes no account of advected heat, was unsurprisingly the most accurate for these measurements.

This assumption is clearly not valid at the field-scale, in Niger or Senegal, and it was concluded that these measurements could not be used to assess the performance of the ETo equations. Other studies using eddy correlation instruments are likely to present similar difficulties.

5.2.3.5 Evapotranspiration methodology in this study

The FAO have recommended the FAO56 Penman-Monteith equation as the most suitable for calculating the reference ETo (Allen *et al.*, 1998). Previous studies (e.g. Baron *et al.*, 1996; Stisen *et al.*, 2008) adopted this approach for Senegal but did not present evidence of the suitability of the approach. This section used measurements to identify the most suitable approach for Senegal.

Few measurements of evapotranspiration were available in Senegal. Daily pan evaporation measurements were only available at two sites, and meteorological observations were only available at one of these. The conclusion of the analysis of a long time series for Bambey was that the FAO56 Penman-Monteith equation was indeed the most suitable method and should give adequate estimates of the evapotranspiration when combined with the meteorological dataset produced by this study and the crop coefficients of Dancette (1983). The suitability of the FAO56 equation would need to be evaluated again if the meteorological data were produced using a different approach to that outlined in this chapter.

5.3 Conclusion

The sensitivity studies in Chapter 4 showed that it was necessary to use accurate rainfall data and self-consistent meteorological data to produce accurate crop yield forecasts. This chapter has described the production of a dataset for the years 1950–2009 for use in CROMSAS. The quality of the dataset has been verified and all of the gaps have been filled.

An appraisal of several methods for estimating evapotranspiration concluded that the FAO56 Penman-Monteith equation was the most suitable for estimating the reference evapotranspiration in Senegal. Using this equation in conjunction with the meteorological dataset and the coefficients of Dancette (1983) should produce accurate estimates of the water requirements of a range of crops in Senegal.

Chapter 6

Influence of rainfall and crop management practices on millet yields

This chapter examines how rainfall and crop management practices affect smallholders in Senegal over the long term. First, a yield gap analysis is used to identify the causes of poor yields in the ESPACE villages (Section 6.1). Since this analysis represents only a few years, a more comprehensive long-term study is performed using CROMSAS with the meteorological data from Chapter 5 to examine how rainfall variations affected crops at several locations, representing all of the Sahelian rainfall regimes, in the period 1950–2009 (Sections 6.2 and 6.3). Optimal management strategies are assessed (Section 6.4).

The literature review identified the economics of intensification, and in particular the balance between the cost of fertilisation and the income from selling grain, as an important consideration for farmers (Section 2.2.4), so a simple analysis of the economics of intensification is presented in Section 6.5.

Smallholders have the option of adapting their management decisions each year. This chapter concludes by examining how smallholders might improve both crop yields and the financial returns from their farms by adapting their crop management practices in response to growing conditions in previous years (Section 6.6).

Cause	Yield reduction
Nitrogen stress	36 %
Planting too early	16 %
Nitrogen stress and planting too early	45 %
Nitrogen stress, planting too early and sub-optimal planting density	49 %

Table 6.1: Yield reductions caused by sub-optimal crop management in the ESPACE fields from Section 4.2.1.

6.1 Yield gap analysis

Climate variability and soil fertility were identified in Chapter 1 as key large-scale constraints on smallholders in Senegal. On a smaller scale, the ESPACE study observed great variability in the grain yields from smallholder farms within villages (Section 1.4.4), which suggests that the climate is not the principle factor in many fields.

A yield gap analysis was performed for the ESPACE fields that were used in the evaluation of CROMSAS (Section 4.2.1). Six fields with observed yields lower than 100 kg ha^{-1} were excluded as they had a disproportionate influence on the yield gap. Across 74 fields, achieved yields were estimated to be 51 % of the potential yields (Table 6.1). Sub-optimal nitrogen application had the greatest impact on yields. Planting too early also reduced yields while using sub-optimal planting densities had a reasonably small impact (it is likely that the planting densities chosen by smallholders were optimised for the lower nutrient application that was used in reality so this part of the yield gap is illusory).

This yield gap is typical of rainfed farming systems: worldwide crop yields are estimated to be 50 % of potential yields due to biota and crop management deficiencies (Lobell *et al.*, 2009) (irrigated yields are nearer 80 % of potential yields). CROMSAS does not simulate the impact of pests and disease on crops but a substantial fraction of smallholder farms are affected by these (Section 1.5.4). Since the bias between measurements and simulations was so small in Section 4.2.1, it is likely that the average field fertility was underestimated in the CROMSAS simulations and this cancelled out the yield losses due to biota. This means that the yield reduction due to sub-optimal nitrogen application was probably lower than 39 % and biota were responsible for the remainder.

6.2 Methodology

The ESPACE study, in common with other field studies, was necessarily short-term and spatially-restricted, covering only a few years and a few villages. If the four years of the study were not representative of the long-term climate then the yield gaps derived above would not be representative of the region because smallholder crop management practices are probably adapted to much longer timescales. A long-term study is required to understand the influence of climate on crop production in Senegal.

CROMSAS (Chapter 3) was used to simulate crop yields over 60 years to consider how climate variability has affected yields in the region (Section 6.3), using the meteorological dataset from Chapter 5.

Simulations were performed for each region using a range of planting densities, planting dates and fertility levels, which were chosen from the literature, the ESPACE study (Affholder, 1992) and the sensitivity studies in Chapter 4 to represent current and possible future farming practices in the Sahel.

The soil water capacity was chosen from IRAT (1983) for Sahelian sand (6 %). Additional sensitivity studies were performed for a very low soil water capacity (2.5 %) that was representative of a village that was analysed by Affholder (1997) (see Section 4.2.1), and for a higher soil capacity (9 %) that represented a local clay soil (again from IRAT, 1983). Similarly, while zero runoff was assumed for most cases, a sensitivity study was performed for high runoff with 40 % of the rainfall after the first 20 mm in any event assumed to be lost. The alternative values for the soil capacity and runoff are examined in a sensitivity study in Section 6.3.1.

The planting densities, which were based on the ESPACE study (see Table 1.3), varied in the range 1–12 plants m^{-2}. This range of densities is typical in both Senegal and the wider Sahel; for example, the lowest stem density simulated here is typical of the millet stand densities of 0.5 stands ha^{-1} found in Niger (Payne, 1997).

Smallholders generally plant crops during the dry season or immediately after the first rains (Section 1.5.3). In addition to this strategy, three equally-spaced planting dates were simulated each month during May, June, July and August. Planting earlier or later than these dates would lead to crop death from water stress. In all cases, it was assumed that the germination did not occur sufficient water was present in the topsoil.

The ESPACE study shows that the soil fertility tends to be higher in fields that are closer to the household compound because less labour is required to transport manure to the fields. Table 1.2 shows that there is much variability in the fertilisation strategies between fields so it is difficult to identify a typical fertility level. In one village, Affholder (1995) found that manure with approximately 130 kg N ha^{-1} was applied to house fields and 40 kg N ha^{-1} to bush fields by smallholders (in years when fields received manure). In these simulations, soil nitrogen applications varied in the range 0–400 kg N ha^{-1}. These figures are the quantity of plant-accessible nitrogen in the field from manure and/or mineral fertiliser application, after losses due to volatilisation, leaching or other phenomena. In each case, an additional 15 kg N ha^{-1} was assumed available from organic matter decay; 5 % of this was made available at the first rains, representing the 'nitrogen flush', and the remainder appeared over the following 50 days. 400 kg N ha^{-1} accessible soil fertility was unreasonably high but was included to ensure that the analysis was bounding.

A simple financial analysis was performed to assess the economic benefits of fertilisation. Another analysis examined the potential benefits of adapting crop management practices according to the conditions in previous years.

6.2.1 Study locations

Six regions of Senegal with synoptic weather stations were chosen to represent the range of annual rainfall totals across the country so that the importance of rainfall could be comprehensively analysed. Where possible, the chosen regions cultivated millet as the principal subsistence grain crop. Figure 6.1 highlights the

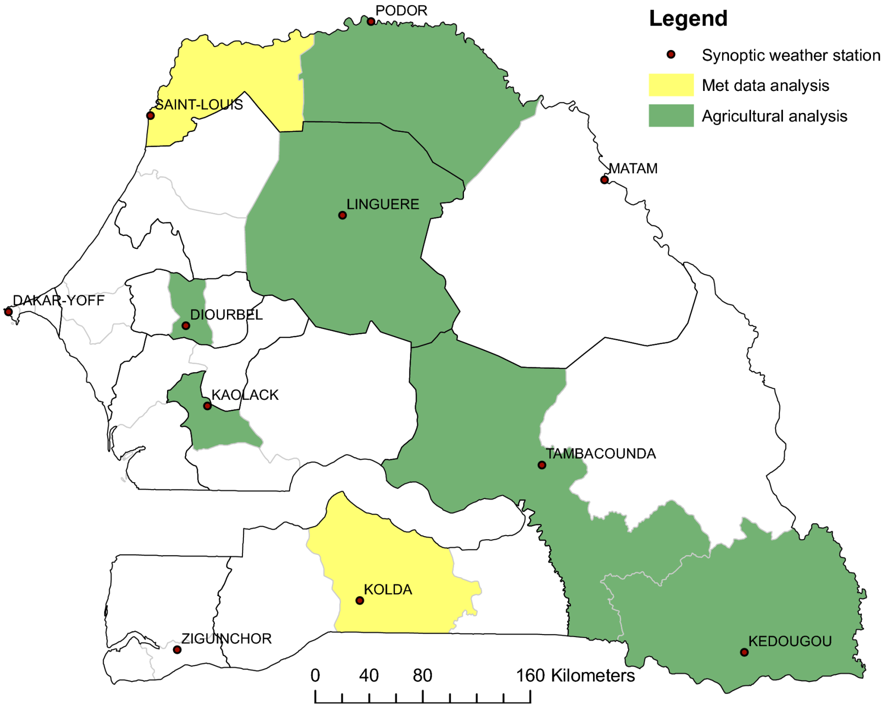

Figure 6.1: Regions selected for analysis by this study. Regions selected for full analysis are shaded green. Regions selected only for climatic analysis are shaded yellow. The locations of the eleven synoptic weather stations in Senegal are indicated.

six chosen *departements* in green. Diourbel, Kaolack and Tambacounda represent the range of rainfall rates in the groundnut basin. Linguere and Podor are typical low-rainfall areas, while Kedougou represents a climate with ample water.

Dakar, St Louis and Ziguinchor were not chosen because their coastal climates are not typical of the Sahel. The Matam climate was too similar to Linguere to justify separate analyses.

It was assumed that the observations from the synoptic weather stations in each region were representative of the climate in the region. Table 6.2 shows the rainfall statistics for each weather station for the period 1950–2008. The mean rainfall ranged from 239 mm to 1129 mm. There was high rainfall variability at the first five stations with the standard deviation being 28 %–46 % of the mean rainfall. Only Kedougou had no years of poor rainfall. These trends are visualised in Figure 6.2, which characterises the long-term probability of exceeding rainfall

Location	Mean	Minimum	Maximum	St dev
Podor	239	62	720	110
Linguere	396	135	679	122
Diourbel	538	248	1110	183
Kaolack	619	256	1118	201
Tambacounda	733	281	1235	203
Kedougou	1129	705	2075	234

Table 6.2: Rainfall statistics for the six chosen regions of Senegal. The statistics were averaged over the period 1950–2008. Data extraction is discussed in Chapter 5. All figures have units mm.

levels at each station.

6.3 Impact of water stress on grain yields

Simulations were performed to estimate the maximum achievable long-term grain yields at each location and to examine how yields are affected by rainfall. Figure 6.3 shows the distribution of simulated optimum yields (in the absence of nutrient stress) for the six locations. Cumulative distribution functions improve our understanding of the long-term risks of farming by highlighting the influence and frequency of particularly good and bad years. The simulations were performed for all of the planting dates and planting densities each year and the highest grain yields were plotted.

Two types of irrigation were simulated. The first, drip irrigation, assumed that no water was lost through evaporation (in effect, there was an impermeable mulch on the field). The second, flood irrigation, assumed that the soil was filled to capacity each day. The former case produced higher yields because water was not lost through evaporation so the transpiration rate, and hence the growth rate, increased. In fact, the rainfed yields were occasionally higher than the yields simulated using flood irrigation.

The irrigated yields varied substantially between locations, partly because slightly higher temperatures reduced the crop duration at the drier locations

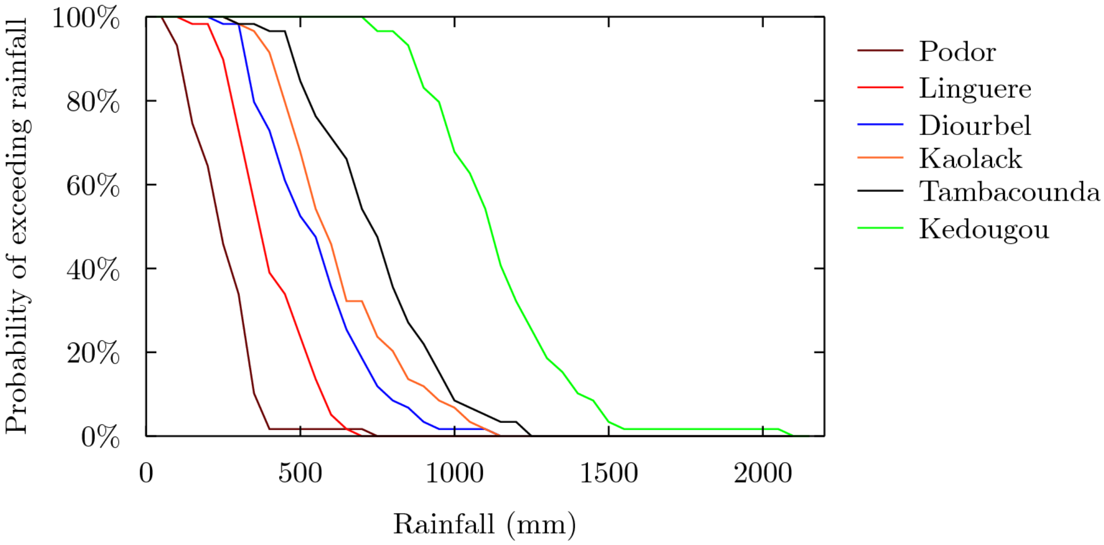

Figure 6.2: Rainfall cumulative distribution function at the six study locations for the 60-year period 1950–2009. Data extraction is discussed in Chapter 5.

but primarily because the growth was reduced in drier areas by higher vapour pressure deficits (VPDs). At Podor and Linguere, the locations with highest VPDs, the maximum yields ranged between 2–5 t ha^{-1}. The difference between the two irrigation methods was most apparent at these locations because the transpiration efficiency tended to limit photosynthesis. In more humid locations, where the radiation efficiency was more likely to be limiting, yields of almost 8 t ha^{-1} were simulated in some years.

The maximum yields from CROMSAS were similar to the highest observed yields of millet. The record yield for millet is 6 t ha^{-1} in the USA and India, but only 3.5 t ha^{-1} has been reported in Mali (Clerget and Traore, 2009). In the absence of irrigation, these authors estimate a maximum grain yield of 4 t ha^{-1} based on a 100 mm soil water reserve at the end of the rainy season. With irrigation, the theoretical yield rises to at least 7 t ha^{-1}. Potential yields in Senegal can exceed 4 t ha^{-1} under optimal resources (Baron *et al.*, 2005). The highest simulated yields in the groundnut basin (Diourbel) were around 5 t ha^{-1}, which is broadly consistent with these studies. Up to 7.5 t ha^{-1} were simulated for Kedougou but it is likely that plant physiological limits would prevent such a yield being realised. Sorghum and maize, which can achieve yields of this magnitude,

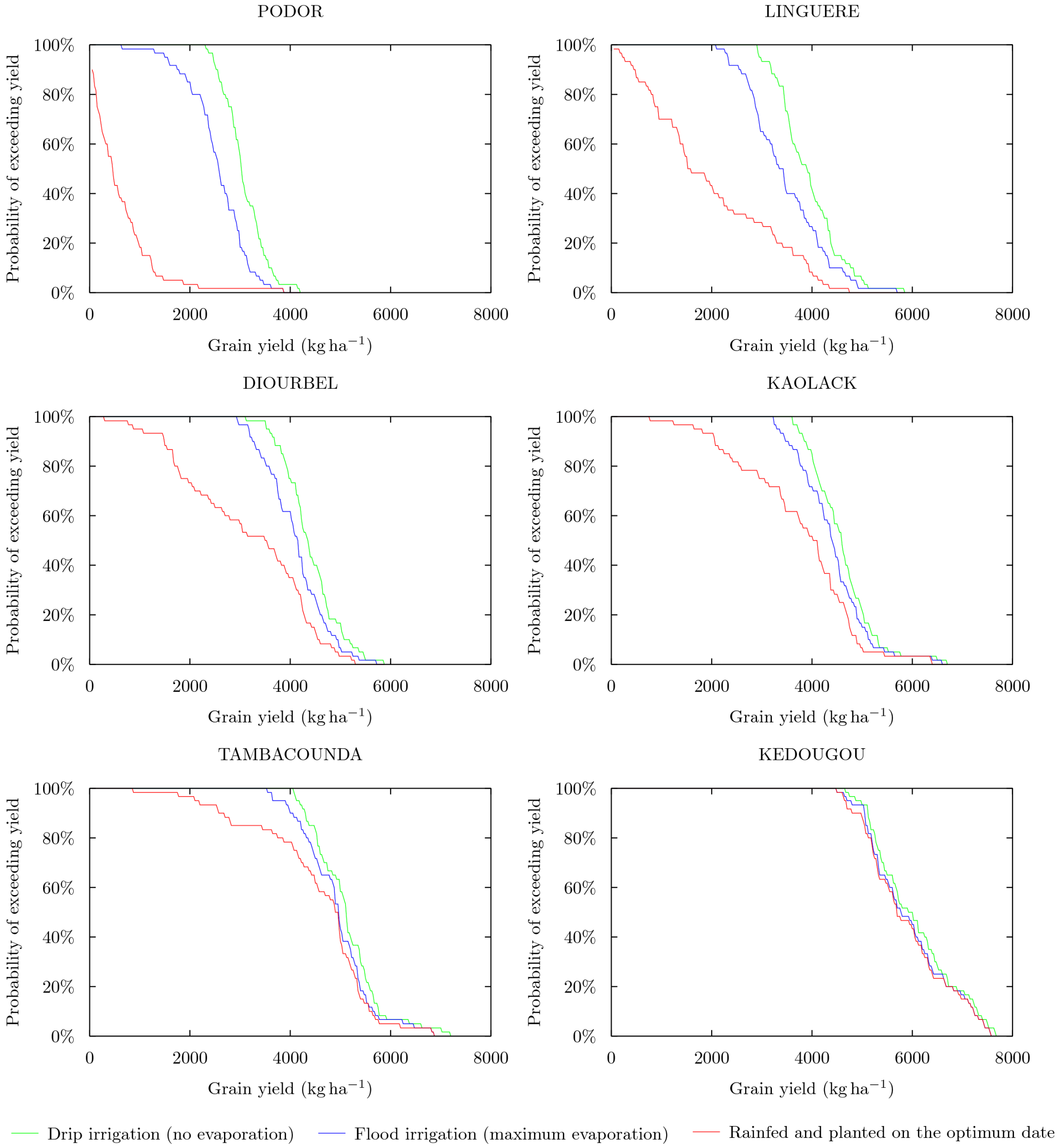

Figure 6.3: Long-term impact of water stress on grain yields at the six locations. Crop growth was simulated with no nitrogen stress. Each yield was chosen for the optimum planting date and planting density in that year.

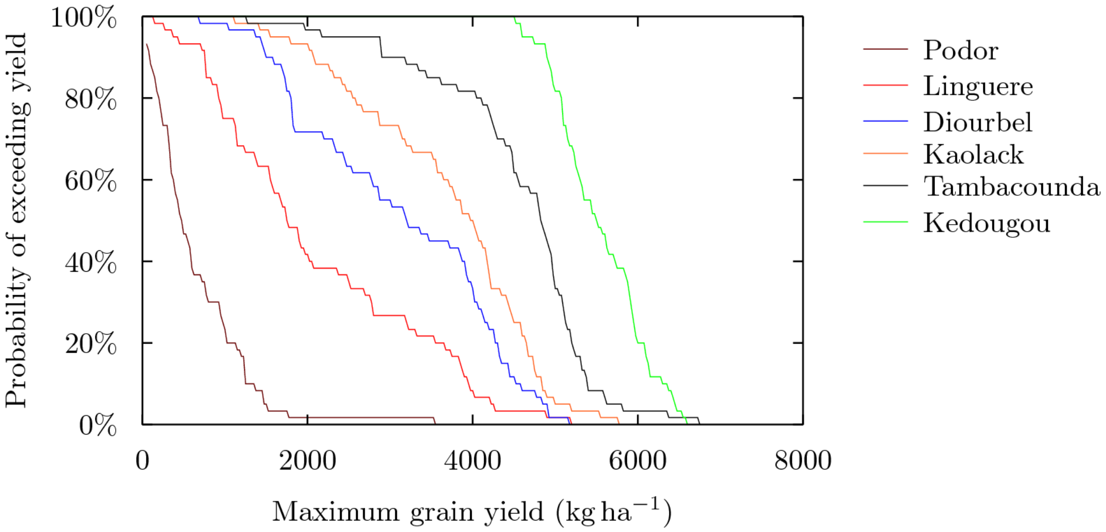

Figure 6.4: Comparison of rainfed crop yields at the six locations. Each yield was chosen for the optimum combination of crop management decisions in that year.

are more suited to the more humid climate at Kedougou and it is unlikely that millet would be cultivated there.

The differences between irrigated and rainfed yields are most pronounced at the drier locations. At most locations, there were few differences between rainfed and flood irrigation yields in the more productive years. However, there were substantial differences in the least productive years.

The rainfed yield distributions of each location are compared in Figure 6.4. Yields are broadly higher in locations with higher rainfall, but the different shapes of the curves show that the influence of rainfall is not consistent across the locations. Low-rainfall locations have a small number of good years while high-rainfall locations have a small number of bad years; for example, the trend at Linguere is close to the inverse of the trend at Tambacounda. The variability in these trends demonstrates why field experiments that are performed over a short period can produce misleading conclusions about the potential for crop cultivation in a region. Nevertheless, the maximum rainfed yields at most locations, in most years, are substantially higher than the yields currently achieved across Senegal (Section 1.4) so factors other than rainfall must have an important influence.

6.3.1 Soil and runoff sensitivity study

In the simulations presented above, it was assumed that the soils were predominantly sandy and that no rainfall was lost as runoff. In view of the concerns that were raised in the calibration and evaluation of CROMSAS about high runoff and low soil water capacities in some fields (Sections 4.1.3.1 and 4.2.1, respectively), a sensitivity study was performed to test these assumptions. Figure 6.5 shows the grain yields for each combination of soil and runoff at each location. There is little impact at Podor because the rainfall is so low and also little impact at Kedougou where water stress only substantially affects crops in 20 % of the years. The soil capacity is the most important factor at the other locations with grain yield reductions of up to 1.5 t ha^{-1} being simulated at Kaolack. High runoff reduces yields in soils with high water content but has negligible impact at low water content. These simulations suggest that low soil water content in particular should be considered as a potential constraint that reduces the effectiveness of agricultural intensification.

6.4 Impact of crop management decisions on grain yields

Three of the important decisions for smallholders are identified in Section 1.5 as the nitrogen application, planting date and planting density. This section examines each of these in turn, but first considers how the timing of crop management decisions affects yields.

6.4.1 Timing of crop management decisions

The simulations that have been presented so far have identified the optimum planting date and planting density in each year. Sahelian smallholders do not possess such perfect foresight and must choose their planting density, planting date and fertilisation strategies at the start of the rainy season with no knowledge of the magnitude of the coming rainfall.

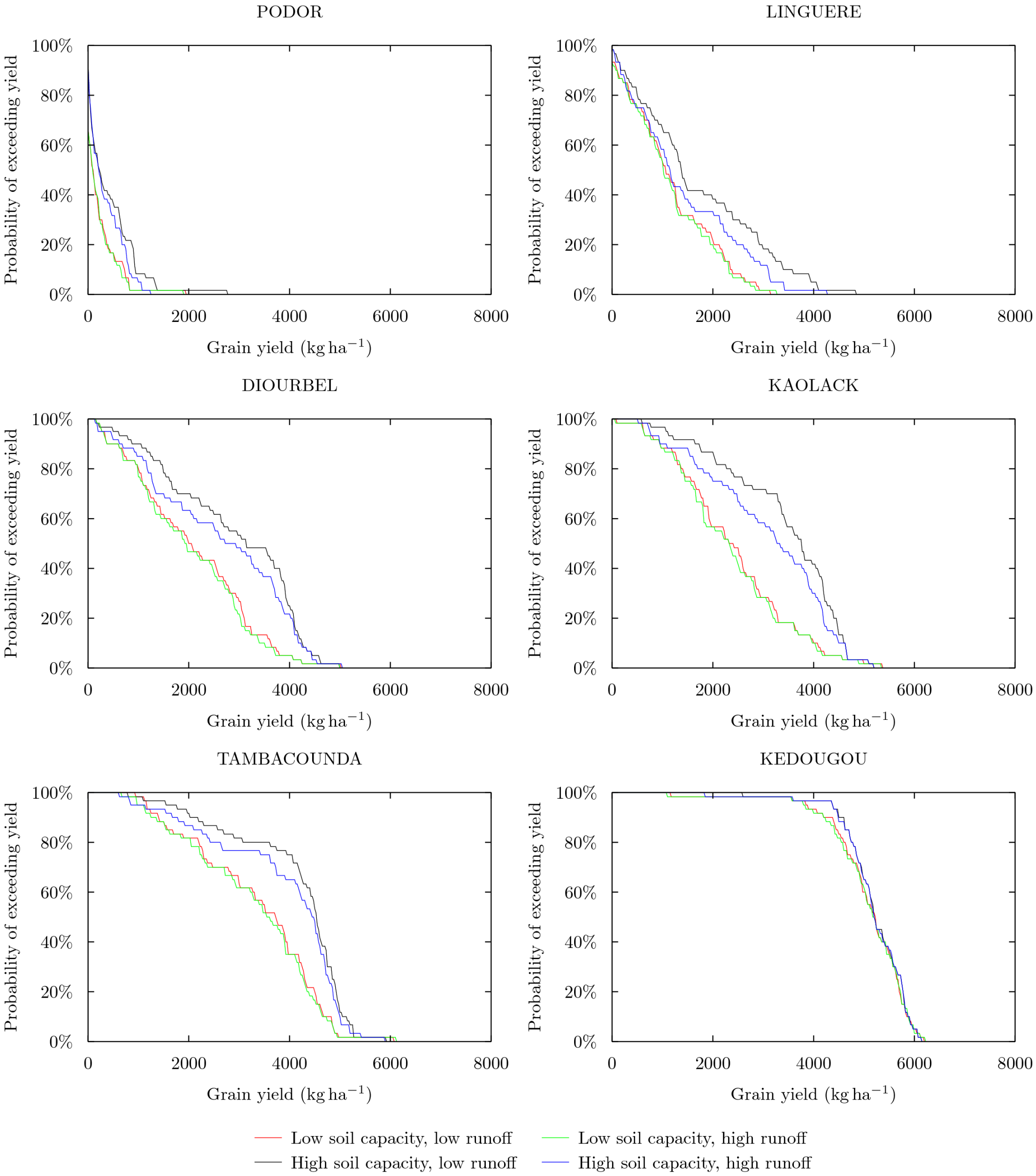

Figure 6.5: Influence of the soil water capacity and the runoff rate on grain yields at the six locations. Crop growth was simulated with no nitrogen stress. Each yield was chosen for the optimum planting date and planting density in that year.

A simulation was performed to determine the yield reduction due to this lack of perfect foresight. Figure 6.6 presents three situations. The first, perfect foresight, assumed that the optimal planting date and planting density were used each year. For the second, the optimal planting date and planting density for the period 1950–2009 were identified and used in all of the years. The third shows the grain yield for dry planting (planting prior to the start of the rainy season, and replanting if the first crop fails) with the optimal long-term planting density.

The achievable grain yields are lower in the absence of perfect foresight. At Podor, the optimal fixed planting date was prior to the start of the rainy season. For Linguere, Diourbel and Kaolack, dry planting slightly improved yields in the best 20 % of years but reduced yields in other years. Planting later in the season tended to produce higher yields at the high-rainfall locations. As the next section will show, fixing the planting date and planting density seems to have a relatively small impact on the yield compared to changing the level of nitrogen application.

6.4.2 Nitrogen management

Soil fertilisation strategies vary widely within Senegal (Section 1.5.2). Figure 6.7 shows a time series of the grain yield at five levels of nitrogen application. The simulated yields at Podor were very low for all nitrogen applications due to water stress. Elsewhere, yields greatly increased as the nitrogen application was increased. However, the interannual variability also increased substantially as the yield increased and was particularly high at the highest nitrogen level. At Podor and Linguere, virtually no grain yield was simulated in some years, even at the highest nitrogen level. At Diourbel and Kaolack, high nitrogen application had little impact on yields in some years. Yields at several locations reduce in the years from 1980, primarily as a result of drought but also because of increases in the temperature and the VPD.

The yield reductions due to drought in Figure 6.7 are particularly high for the highest nitrogen application. Table 6.3 shows the simulated average reduction in the grain yield over the period 1950–2009 at the six locations. Losses were higher at locations with lower rainfall. But increasing the nitrogen application beyond 100 kg N ha^{-1} also increased the losses (although the average yield was

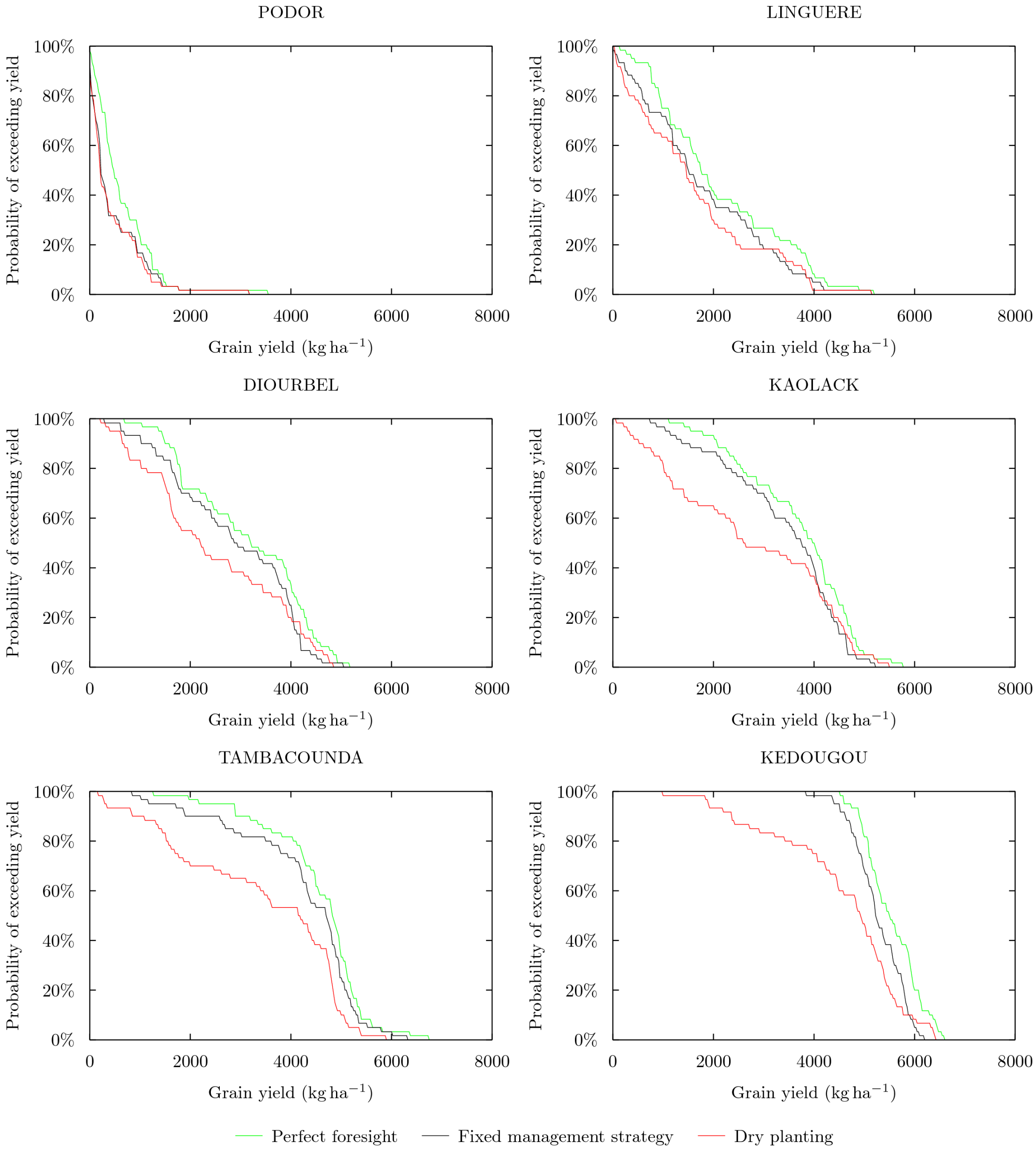

Figure 6.6: Graphs of the distribution of grain yields achieved under different assumptions about the knowledge of the farmers. Crop growth was simulated with no nitrogen stress. See the text for a description of each state of knowledge.

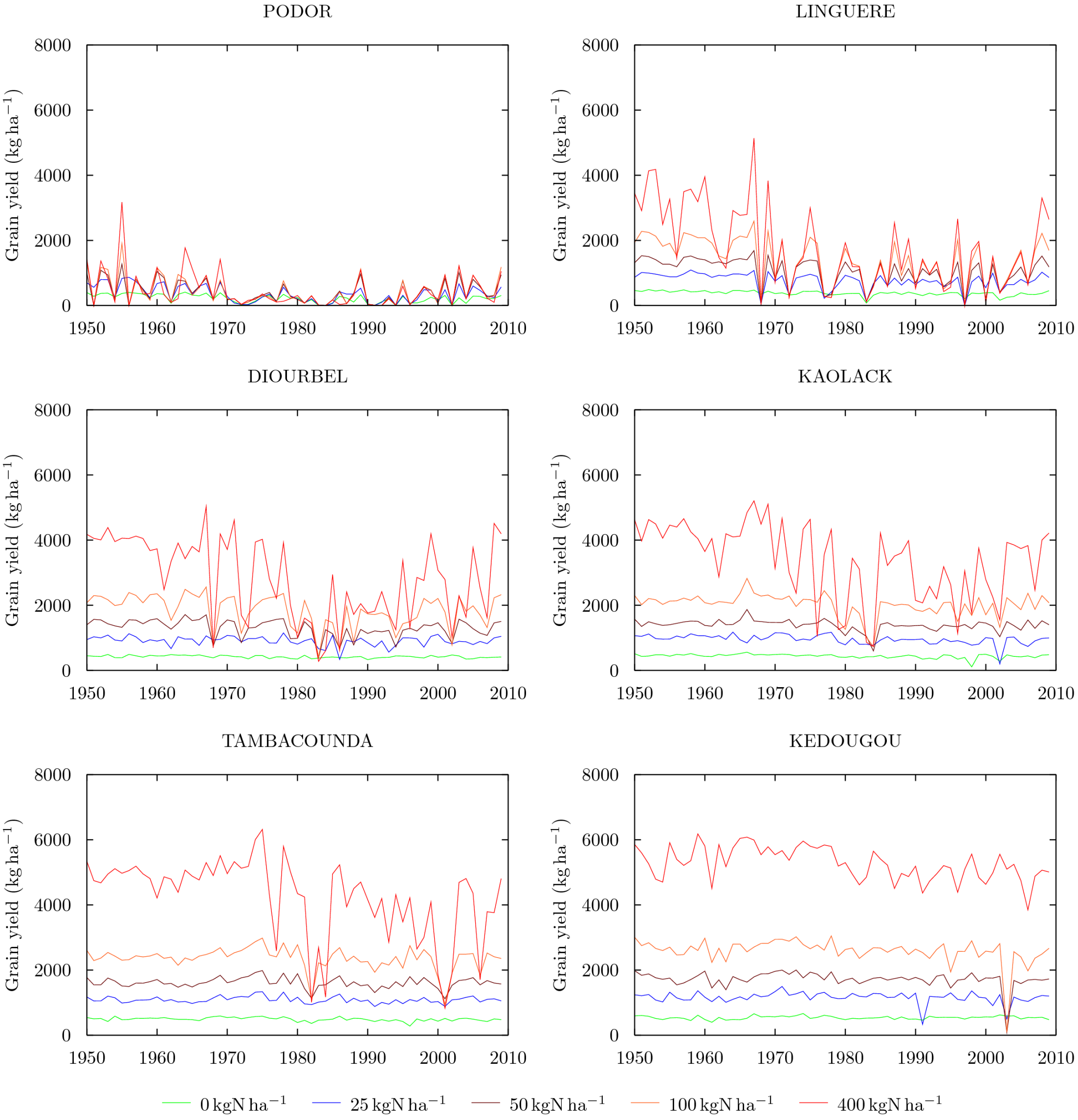

Figure 6.7: Time series of grain yield variations for a range of nitrogen applications at six locations in Senegal. The planting date and planting density were the long-term optimum for each nitrogen level.

Nitrogen (kg N ha^{-1})	25	50	100	200	400
Podor	−52%	−65%	−74%	−81%	−82%
Linguere	−18%	−24%	−33%	−45%	−50%
Diourbel	−10%	−13%	−17%	−28%	−33%
Kaolack	−8%	−9%	−11%	−19%	−23%
Tambacounda	−4%	−2%	−4%	−9%	−12%
Kedougou	−5%	−3%	−2%	−5%	−5%

Table 6.3: Average loss of grain due to drought for a range of nitrogen applications, at six locations in Senegal. The figures show the difference between the irrigated yield and the rainfed yield averaged over the period 1950–2009. Optimal long-term planting dates and planting densities were used for each year.

still substantially higher at higher nitrogen levels). The additional losses were principally caused by water stress during grain filling in some years, when the soil water was depleted more quickly than at lower soil fertility levels due to increased transpiration earlier in the season by the larger crop.

In some cases, increasing the soil fertilisation appeared to reduce the grain yield. Affholder (1995) has reported this phenomenon but other authors have concluded that increasing the soil fertility will not cause diminished yields (e.g. Payne, 1997). Table 6.4 shows that this phenomenon is simulated by CROMSAS but primarily at the two locations with the lowest rainfall. At the other locations, which have similar rainfall to the agricultural research stations in West Africa, the simulations suggest that yields would only rarely be reduced by increasing the soil fertility. The low frequency of this phenomenon means that it would be difficult to observe even in an agronomic study which was designed to search for it, so perhaps the contention in the literature is caused by the existence of only a small number of agricultural field studies from the region that have included measurements that could have identified this phenomenon. This issue illustrates an instance where a crop model can usefully guide field experiments and can examine issues for which the field studies have limited spatial or temporal coverage.

	Best planting date	Dry planting
Podor	29%	31%
Linguere	17%	17%
Diourbel	8%	8%
Kaolack	4%	9%
Tambacounda	4%	6%
Kedougou	1%	3%

Table 6.4: Simulated frequency of grain yield reductions caused by increasing the soil fertility at six locations in Senegal. The planting date and planting density were the long-term optimum at each fertility level.

6.4.3 Planting date

Dry planting is widely practised in the Sahel but there is evidence in the literature (e.g. Sultan *et al.*, 2005) that a later planting date would produce higher yields. Figure 6.6 shows that dry planting only produces higher yields in the best 20 %–40 % of years at the lower-rainfall locations. The optimum planting date was averaged over all of the years for each planting density × fertility combination. At low nitrogen levels, the optimum planting date was relatively late, between 30 June and 10 July, because organic matter decomposition was well advanced by then and the crops were able to survive on stored soil water. This date was very dependent on the magnitude of the initial nitrogen flush, which is not well understood. The optimum planting date moved forward at all locations for high plant densities because soil water became limiting. The optimum planting date for high nitrogen applications was between 23 May and 14 June as soil water availability was the most important factor. The best planting date depended on the latitude because more southerly locations have earlier starts to the rainy season.

There was an assumption in these simulations that the plant-accessible nutrient pool would be fully available to the crop for all planting dates. In reality, numerous weeds germinate at the first rains which irreversibly use available nutrients if they are not controlled, so the optimum planting date will be earlier than that identified above. For smallholders, the increase in the grain yield resulting from a planting delay is offset by the additional labour requirement for clearing the field prior to planting and, for those using photoperiod-sensitive crops, by a potential loss of animal feed from the extra biomass that would have been produced. It is therefore possible that dry planting was the best strategy for smallholder livelihoods at most of the locations. Appropriate livelihood surveys could help explain why dry planting continues to be the favoured option in many parts of the country.

It might be possible for smallholders to alter their nitrogen application strategies according to the timing of the rainy season. Figure 6.8 shows the most effective nitrogen application at each location as a function of the planting date. Since the optimal application is almost always the highest application, despite much of the nitrogen being wasted in some years, the most effective nitrogen application is defined here as the lowest application that produces 90 % of the maximum yield at that planting date. At all of the locations except Podor, the most effective nitrogen application reached a maximum late in the season. Crops planted earlier or later suffered water stress. Rainfall had a strong influence with the most effective application ranging from 25 kg N $\mathrm{ha^{-1}}$ at Podor to almost 400 kg N $\mathrm{ha^{-1}}$ at Kedougou.

6.4.4 Planting density

The planting density is varied by farmers to manage water stress and cope with nutrient deficiencies (Mortimore and Adams, 1999). One cause of low grain yields in the Sahel has been identified as the use of unnecessarily low planting densities by smallholders (Payne, 1997, 2000; Shapiro and Sanders, 1998). Simulations were analysed to identify the optimum long-term planting density strategy. The CROMSAS sensitivity study in Section 4.2.4.2 showed that the optimal planting density increased with rainfall. Figure 6.9 shows that the optimal density also broadly increases with the nitrogen level, although there is a reasonably large range of values at each level and yields vary little within each range. Even at the highest nutrient application, optimum planting densities were as low as 7 plants $\mathrm{m^{-2}}$. These simulations suggest that the smallholder planting densities

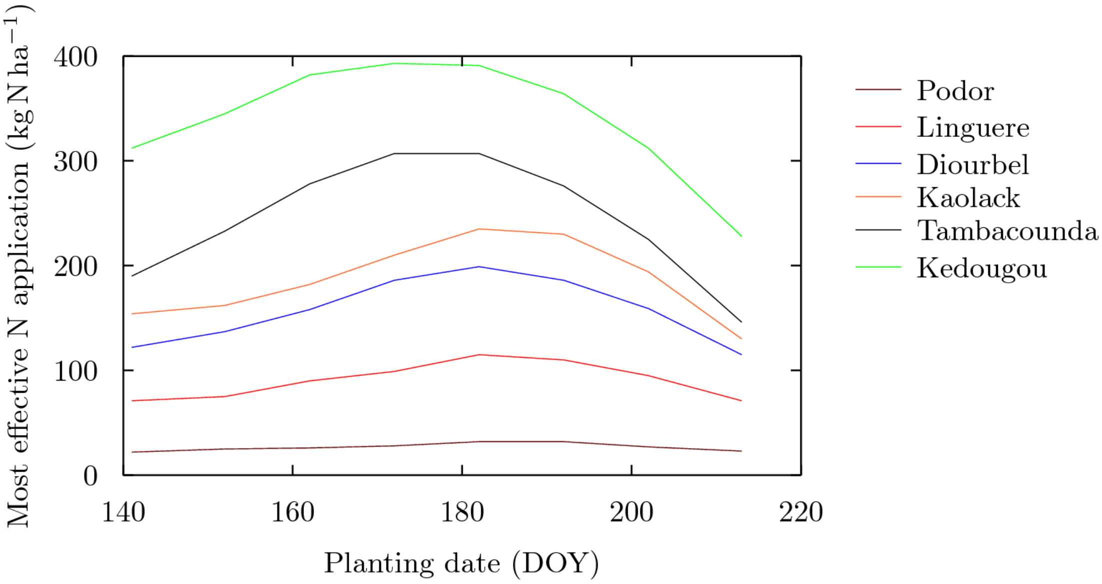

Figure 6.8: Optimal nitrogen application as a function of the planting date at the six locations. The optimal nitrogen is averaged over the period 1950–2009 for each planting date. In each year, the optimal nitrogen was the amount required to achieve 90 % of the maximum yield of that year.

measured by the ESPACE study were well-adapted to the climatic conditions and the fertility management of smallholders in Senegal. The large variations observed by that study reflect the broad range of optimum densities that are shown in Figure 6.9.

Payne (1997) recommended that planting densities in Niger should be doubled or quadrupled from 0.5 stands m^{-2}. This translates to a target planting density in this study of 2 to 4 plants m^{-2} (assuming that there are 2 plants (or stems) per stand). At Podor, the optimal density was not sensitive to the nitrogen application. At the other locations, the optimal density was approximately 3 plants m^{-2} at low nitrogen levels, which is within the range suggested by Payne (1997). Considering that Payne (1997) did not apply fertiliser to his lowest fertility plots, the grain yields were still surprisingly high in some years ($\approx$ 1350 kg ha^{-1}) which suggests that the intrinsic soil fertility at the research station was higher than found in most smallholder fields, perhaps as a result of latent fertilisation from experiments performed in previous years. Under these circumstances, the assumption

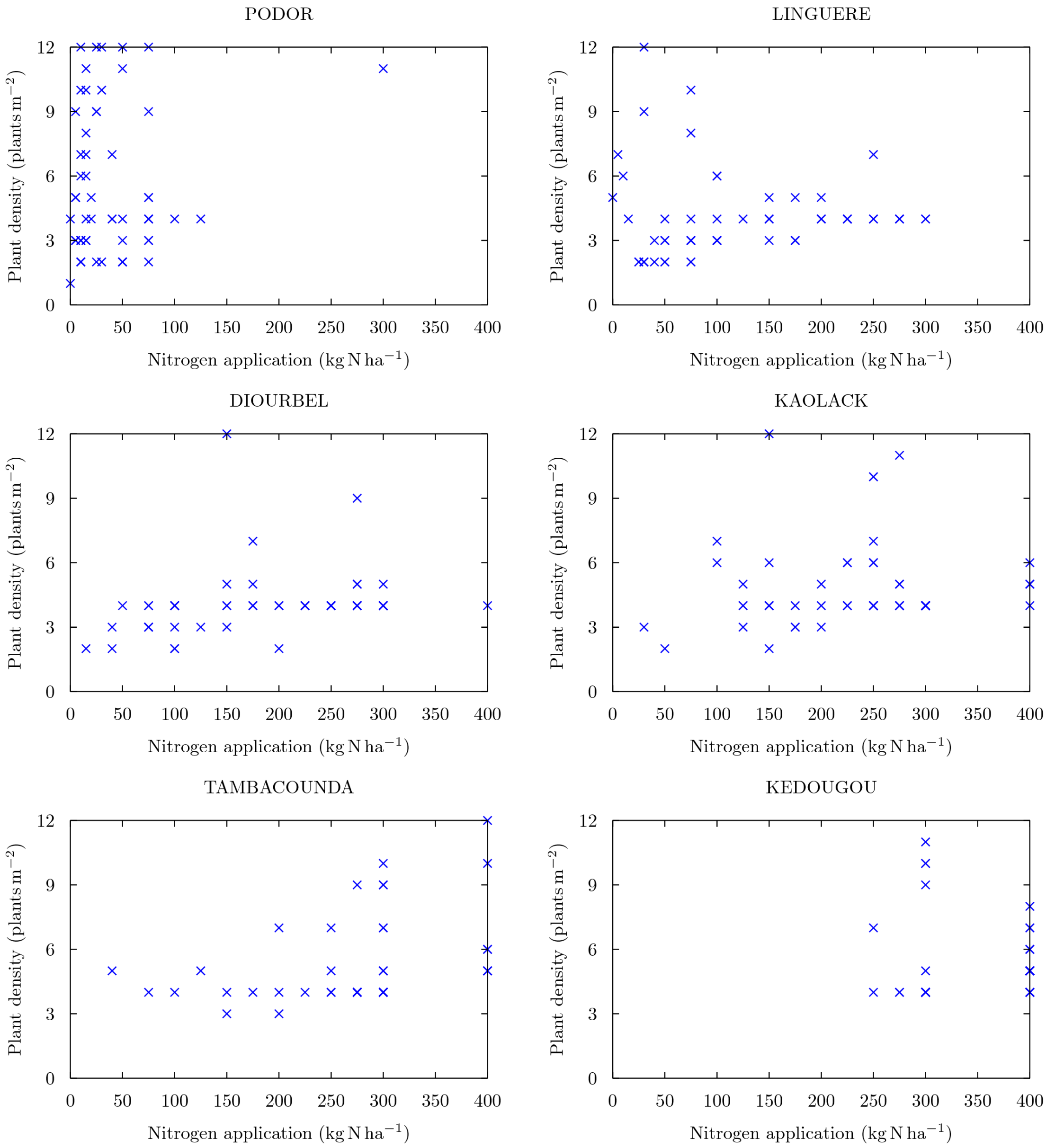

Figure 6.9: Optimum planting densities for a range of nitrogen applications. Each cross represents the planting density—nitrogen combination for one year. The lowest nitrogen application that produces 90 % of the maximum yield in that year is plotted as this is assumed to be the most effective nitrogen application in that year.

that the research station fields were representative of local smallholder fields was not valid and increasing the planting density would have increased yields on the research station but not necessarily elsewhere.

6.5 Economic considerations of nitrogen application

Varying the planting date or the planting density comes at a financial cost of extra labour and seed. These decisions are not greatly constrained by environmental or socio-economic factors so, as shown in the previous sections, the typical planting dates and planting densities are close to the optimum in each location. In contrast, the costs of increasing the soil fertility are much greater. If manure is being used then livestock must be bought and corralled in the family compound. Feed and water must be supplied each day. Manure must be collected, stored, transported then applied to the fields. The main difficulty is the sheer quantity of manure that is required; for example, to increase the nitrogen content of the field by $100\,\mathrm{kg\,N\,ha^{-1}}$, it is necessary to produce and apply around $7000\,\mathrm{kg\,ha^{-1}}$ manure (Affholder, 1995), which is very time-consuming when it is being transported by cart or by hand. Only half of this will decay into a plant-accessible form in the first year. If mineral fertiliser is being used then the fertiliser must be bought at great cost at the start of the season from a market, transported to the household then applied to the field (much lower quantities are involved so the transport costs are lower). Moreover, the effectiveness of mineral fertiliser depends on many factors and the recovery rate is often very low (Bationo and Mokwunye, 1991).

Although farmers can increase crop yields by raising the soil fertility in their fields through the application of fertiliser, it does not necessarily make economic sense to do so. Smallholders aim to grow economically-viable crops as one strand of their household activities, not subsistence crops at any cost for survival (Mortimore and Adams, 1999). Fields are abandoned if they become unprofitable.

A simple economic analysis was used to examine the long-term change of household income caused by increasing the soil fertility. The accuracy of economic analyses is often restricted by a lack of good-quality financial data. For example, producing and applying manure is a labour-intensive activity so the marginal cost of household labour dominates, but there are also costs to purchase the animals, build corrals, produce feed and purchase veterinary services, and these costs will vary between households. Although manuring is the main strategy for fertilising fields in Senegal (Section 1.5.2), in view of the complexity of pricing manure it was decided to concentrate on the economics of mineral fertiliser use. The analysis compared the income from selling the grain at market with the cost of buying fertiliser to increase the soil fertility. It was assumed that 14–7–7 NPK fertiliser was used since this was the most common mineral fertiliser recorded by the ESPACE study (Affholder, 1992). The costs of preparing the fields, planting the crop, weeding, transporting the fertiliser and incorporating it into the field, and harvesting, storing and selling grain were not included, so the analysis would have overestimated the net income. However, the change in the net income due to fertilisation was the important quantity and this should have been more accurately estimated because using mineral fertiliser should not substantially change the household labour costs.

Four principal factors were identified that affect the profitability of intensification:

1. the climate of the region, with higher and more regular rainfall increasing the profitability;
2. the recovery rate of mineral fertiliser by the crop, with higher rates being more profitable;
3. the market price of mineral fertiliser, with lower prices being more profitable; and,
4. the market price of grain, with higher prices being more profitable.

The effectiveness of mineral fertiliser can be measured as the fraction of applied nitrogen that is recovered by the crop. Field studies have variously reported recovery rates of 33 % in all fields (Breman *et al.*, 2001) and 34 % and 20 % in house and bush fields, respectively (Fofana *et al.*, 2008). Bationo and Mokwunye (1991) conclude that the recovery rate depends on both the form of the fertiliser (they tested urea and the less volatile ammonium nitrate) and the method of incorporating it into the soil, with recovery rates ranging from 31 % to 82 %. There is clearly much variability that is related to the soil condition and the fertilisation strategy. For this reason, a range of recovery rates was tested from 25 % to 100 %.

Historically, millet prices in Senegal have been volatile in comparison to groundnut prices (Kelly *et al.*, 1996). Figure 6.10a shows the millet price at Kaolack market for the period 2005–2010 (earlier data were not available). The price tends to peak just before harvest commences. A price of 175 CFA was chosen for the economic analysis. A similar time series of fertiliser prices was not available for Senegal, so the variability of the price of fertiliser was gauged instead by examining the long-term trends in the prices of the commodities that are used to make NPK fertilisers. Figure 6.10b shows that the prices were reasonably stable over 50 years until 2008. However, the price of fertiliser is also affected by the availability of government subsidies (Shapiro and Sanders, 1998), which were largely withdrawn in Senegal under structural adjustment programmes, and by currency devaluations which cause a step increase in the price. The Senegalese price is therefore likely to have been more variable than the world price of fertiliser. Gray (2002) records fertiliser prices in Senegal of 138–151 CFA, and, in the absence of better information, a price of 150 CFA was used in this study. The lack of information about long-term price trends means that this model is of limited use to understand the trends over several decades, but is useful for considering recent years and future possibilities.

6.5.1 Fertiliser use return on investment

The financial return on investment (ROI) is the ratio of money that is gained or lost on an investment relative to the amount of money invested. It can be used to examine the opportunities for smallholders to improve the profits from their farms by applying mineral fertiliser. Figure 6.11 shows the ROIs for each location for several nitrogen applications, assuming a recovery rate of 33 % (consistent with the observed rates of Breman *et al.* (2001) and Fofana *et al.* (2008) for smallholder fields). Nitrogen application led to large losses at Podor. The frequency of years

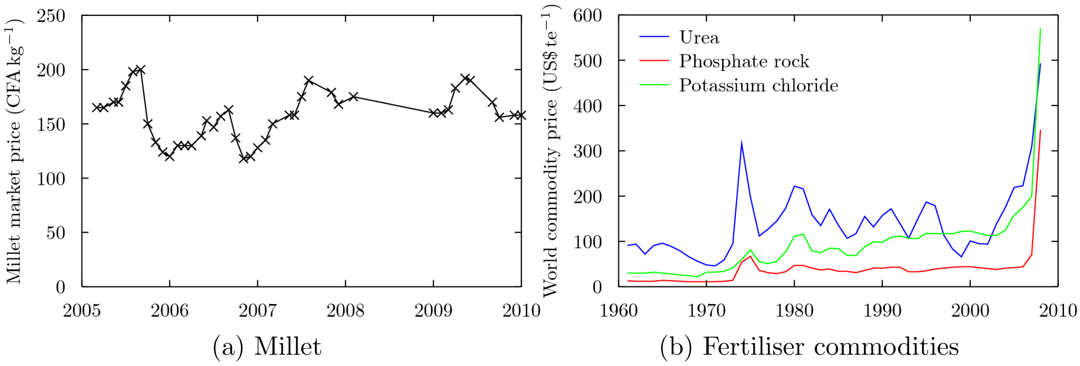

(a) Millet

(b) Fertiliser commodities

Figure 6.10: Time series of millet market prices and world fertiliser commodity prices. The millet prices are for Souna millet at Kaolack market in Senegal and were sourced from West-African Market Information Network (2010). The fertiliser commodity prices were taken from World Bank publications and compiled by International Rice Research Institute (2010).

with losses depended on the rainfall at the other locations. Using large amounts of fertiliser caused large losses at all locations, but applying microdoses produced a positive return at the four locations with the highest rainfall in more than 60 % of years. This conclusion is consistent with the findings of a maize study described in Cooper *et al.* (2008), which also found the economic returns from microdoses of fertiliser would be higher than the return from larger doses (the ROIs in that study had a much larger range from -8 to 5 CFA CFA^{-1}, which is particularly surprising at the lower end because it is not clear how the losses could be almost an order of magnitude higher than the cost of the fertiliser).

The influence of the recovery rate is shown in Figure 6.12 for an N application of 50 kg N ha^{-1}. With high recovery rates, large returns are possible in most years at all locations except Podor. Improving the nitrogen recovery rate to 50 % would lead to losses in only 20 % of years at the four locations with the highest rainfall.

6.5.2 Market price volatility

In view of the uncertainty in the price of millet and mineral fertiliser, a sensitivity study was performed to quantify the impact of price variations on the profit margins. Table 6.5 shows the results for Kaolack with 33 % and 75 % recovery

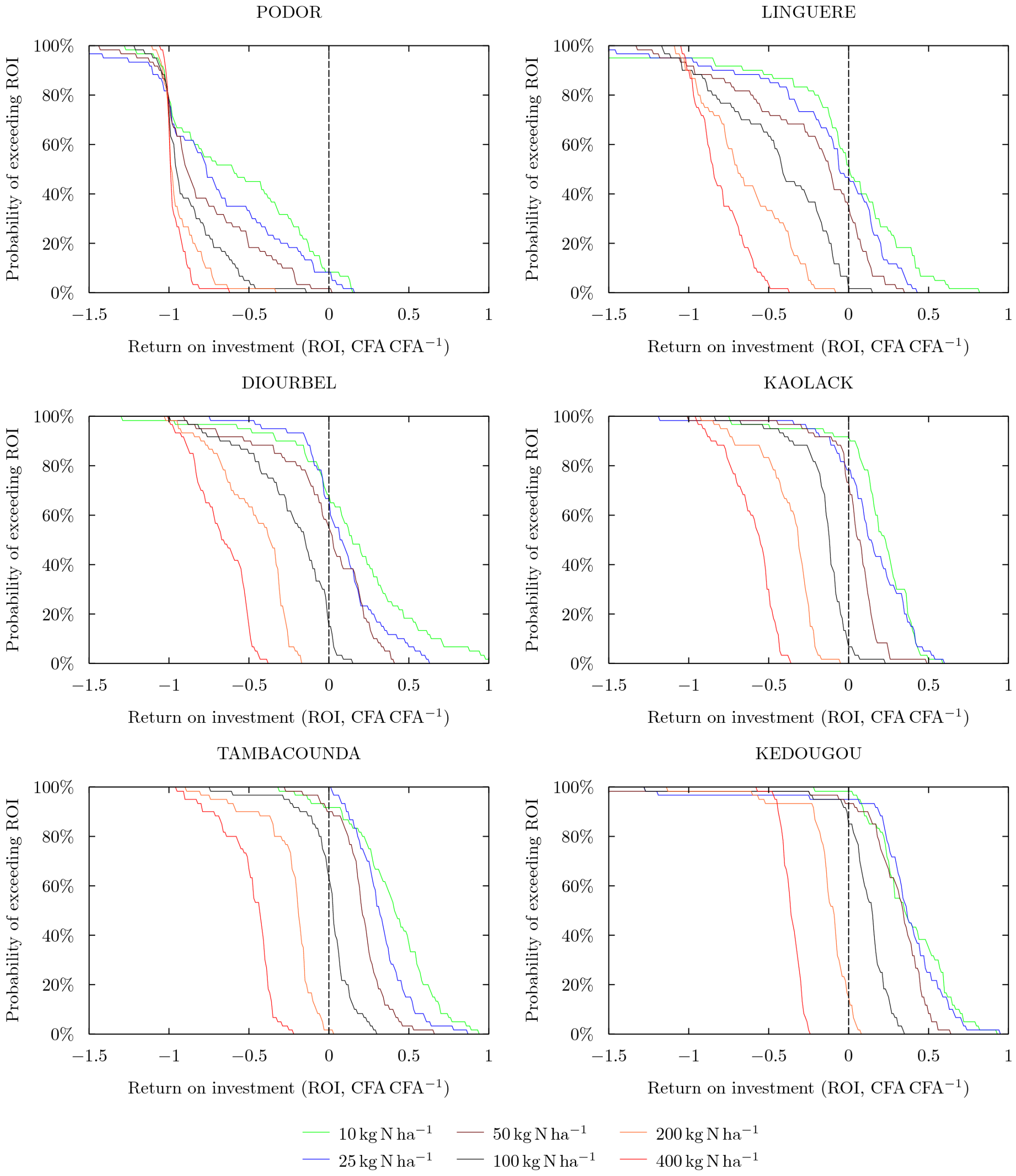

Figure 6.11: Return on investment for several levels of nitrogen application at the six locations. A nitrogen recovery rate of 33 % was assumed. The profit was calculated as the difference between the market price of fertiliser (150 CFA kg^{-1}) and the market price of millet (175 CFA). The costs of buying, transporting and applying fertiliser, and the additional costs of transporting millet to market, were not included in the calculation. Simulations were performed for the period 1950–2009 and the optimal long-term planting dates and planting densities were used each year.

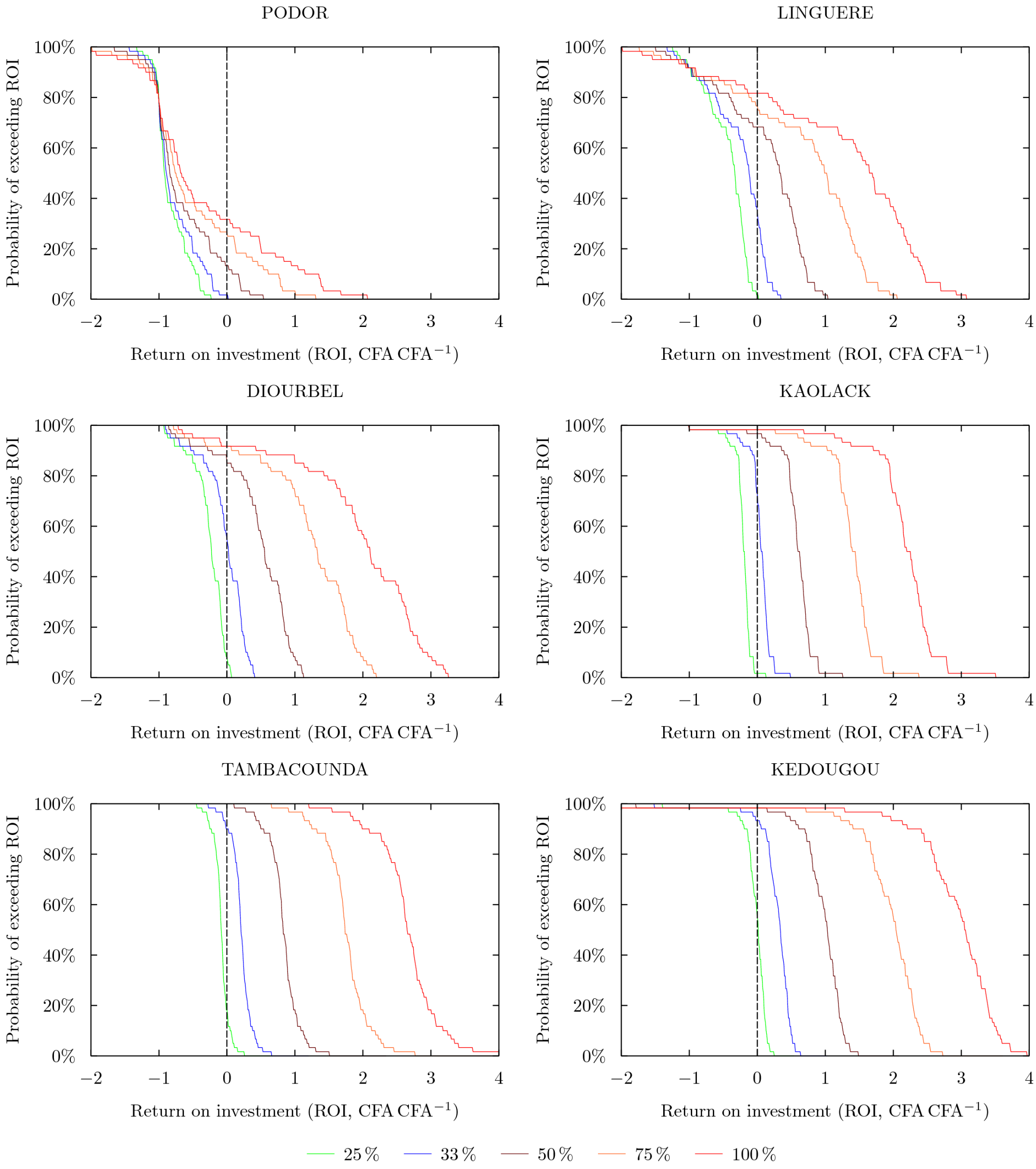

Figure 6.12: Influence of the nitrogen recovery rate on the return on investment at the six locations. 50 kg N ha^{-1} plant-available nitrogen was available in each case. The profit was calculated as the difference between the market price of fertiliser (150 CFA kg^{-1}) and the market price of millet (175 CFA). The costs of buying, transporting and applying fertiliser, and the additional costs of transporting millet to market, were not included in the calculation. Simulations were performed for the period 1950–2009 and the optimal long-term planting dates and planting densities were used each year.

Grain price ($\mathrm{CFA\,kg^{-1}}$)	Mineral fertiliser price ($\mathrm{CFA\,kg^{-1}}$) 100	150	200	250	300
33 % recovery rate					
100	−4	−50	−104	−157	−208
150	60	6	−48	−102	−156
200	116	62	8	−46	−100
250	172	118	64	10	−44
300	229	174	120	66	12
75 % recovery rate					
100	65	41	17	−7	−31
150	121	97	73	49	26
200	177	153	129	105	82
250	233	209	185	162	138
300	289	265	242	218	194

Table 6.5: Sensitivity study of the impact of grain and fertiliser price variations on profit margins. The profits are calculated as the difference between no fertiliser and $50\,\mathrm{kg\,N\,ha^{-1}}$ fertiliser being applied. All profits have units $1000\,\mathrm{CFA\,ha^{-1}}$.

rates. For a 33 % recovery rate, profit margins are finely balanced, with an increase in the fertiliser price or a reduction in the grain price leading to losses. Conversely, an increase in the grain price would make intensification economically very attractive to farmers. At a 75 % recovery rate, intensification is always profitable in the long-term unless fertiliser prices are very high and grain prices are very low.

This analysis ignores short-term price volatility caused by rainfall variations. In years of poor rainfall, total grain production will reduce and grain prices will rise. Farmers that produce excess grain will enjoy large profits. In years of good rainfall, with high yields, prices will drop and fertiliser use will be less profitable than shown here.

6.5.3 Managing the risk of income variability

Smallholders do not base their investment decisions solely on the long-term return from agricultural intensification (Mortimore and Adams, 1999). The variability of the return is also important because the risks to the household are reduced when the variability is reduced. Smallholders must invest in soil fertilisation before the start of the rainy season when there is much uncertainty about the final yield, so they need to be confident that the investment will not threaten their livelihoods in the short term. Figures 6.11 and 6.12 show substantial losses in some years, particularly when the recovery factor is low. In the past, fertiliser was subsidised by the Senegalese government so the financial damage to smallholders was lower. The analysis presented here could be extended to inform insurance schemes that would enable smallholders to manage the risk of agricultural intensification to their livelihoods. Another method of reducing the financial risk is to use manure instead of mineral fertiliser. Manure has the advantage of decaying over several years, so a single poor rainy season will not lead to the investments in the soil nutrients being completely lost. Manure also contains much organic matter which bolsters the low natural concentrations that are found in the sandy soils of Senegal.

6.6 Adaptation by smallholders

The simulations in this chapter have been underpinned by one of two assumptions. In each case, the farmer has been assumed to have had either perfect foresight of the optimum growing conditions or to have repeatedly used a fixed farming strategy over the whole period of analysis (1950–2009). The former is clearly impossible while the latter views the farmer as a robot that repeats the same pattern every year with no regard to changes in the environmental conditions. CROMSAS was designed to examine the potential for farmers to adapt their agricultural systems to changing environmental or climatic conditions. This section examines the impact of changing the soil fertility, planting date and planting density in response to the growing conditions in the previous years.

6.6.1 Adaptation to conditions in prior years

It was assumed in this analysis that farmers would choose the optimum soil fertility, planting date and planting density based on the optimum growing conditions in previous years. In reality, farmers are not able to observe the conditions each year and estimate how their crops could have grown with different management decisions as accurately as assumed in the model, but this approach permits a conservative appraisal of the benefits of adaptation.

Four adaptation periods are presented here: one, three, five and ten years. In each case, the optimum agricultural strategy is identified for the adaptation period prior to the current year and then used in the current year. Table 6.6 shows the average grain yield for each adaptation option for the period 1960–2009 (the period 1950–1959 is not included because there are insufficient preceding years for the ten-year adaptation calculation). The average yields with perfect foresight and with no adaptation are also shown for comparison. As expected, the perfect foresight method is the optimum at all locations. The no adaptation method is generally the next best option. Adaptation to the conditions in previous years leads to lower yields, with the shortfall increasing as the adaptation period is shortened. The explanation for this behaviour lies in the choice of a target of yield maximisation. The best long-term method to maximise the yield at each location is to always apply the most fertiliser possible because yields will be greatly increased in some years while losses due to over-fertilisation are minimal (other crops, for example maize, are more susceptible to drought damage than millet and would have higher losses due to high fertilisation in drought years). Choosing management decisions according to the optimal conditions in previous years leads to reduced yields in years with high rainfall when insufficient fertiliser is applied following a poor year.

In practice, farming is an economic activity and nitrogen application is limited by the cost of the fertiliser, so it is necessary to measure the success of adaptation strategies against the profit that they bring. Figure 6.13 shows the range of profits that could be made by following each adaptation option with the aim of maximising profits rather than the crop yield, for a 50 % recovery rate. The profits are calculated relative to a base case of dry planting at the lowest planting density

	Perfect foresight	No adaptation	Adaptation based on previous years			
			1	3	5	10
Podor	551	396	254	306	333	329
Linguere	1862	1524	1135	1307	1325	1514
Diourbel	2958	2601	2148	2367	2425	2540
Kaolack	3542	3202	2553	3086	3100	3099
Tambacounda	4447	4103	3685	3812	4082	4098
Kedougou	5500	5240	4763	5116	5135	5185

Table 6.6: Simulated yields for a range of agricultural adaptation options. The yields were calculated with the fertility level, planting date and planting density chosen according to the adaptation option. All yields have units $\mathrm{kg\,ha^{-1}}$.

with no application of nitrogen. The results have a broadly similar pattern to the crop yield results in Table 6.6. The profits from all strategies are similar in the best 80 % of years but there are substantial variations in the worst 20 % of years when large losses are experienced at all locations if crop management is are based on the most successful strategies of previous years. At several stations, adapting to previous years produces slightly higher yields than not adapting in the 10 % best years. However, the no adaptation strategy produces higher yields and smaller losses in poorer years and a slightly greater overall profit.

Similar results were found for recovery rates of 33 % and 75 % (not shown). The optimal level of nitrogen application for the no adaptation strategy depended on the recovery rate; for example, at Diourbel, the optimal applications were 0, 50 and 100 $\mathrm{kg\,N\,ha^{-1}}$ for recovery factors of 33 %, 50 % and 75 % respectively with crops in each case planted on 21 June at planting densities of 2–4 $\mathrm{plants\,m^{-1}}$.

The reason why adaptation to previous years is less unsuccessful than the no adaptation strategy is the absence of systematic trends in the interannual profitability of farming. This is demonstrated by Figure 6.14, which shows a Fast Fourier Transform of the interannual profits for a nitrogen application of 50 $\mathrm{kg\,N\,ha^{-1}}$ and a recovery rate of 50 % at Diourbel. There is little temporal coherence and there are no dominant frequencies, suggesting an absence of underlying cyclical behaviour. Basing adaptation on the profits of previous years is only

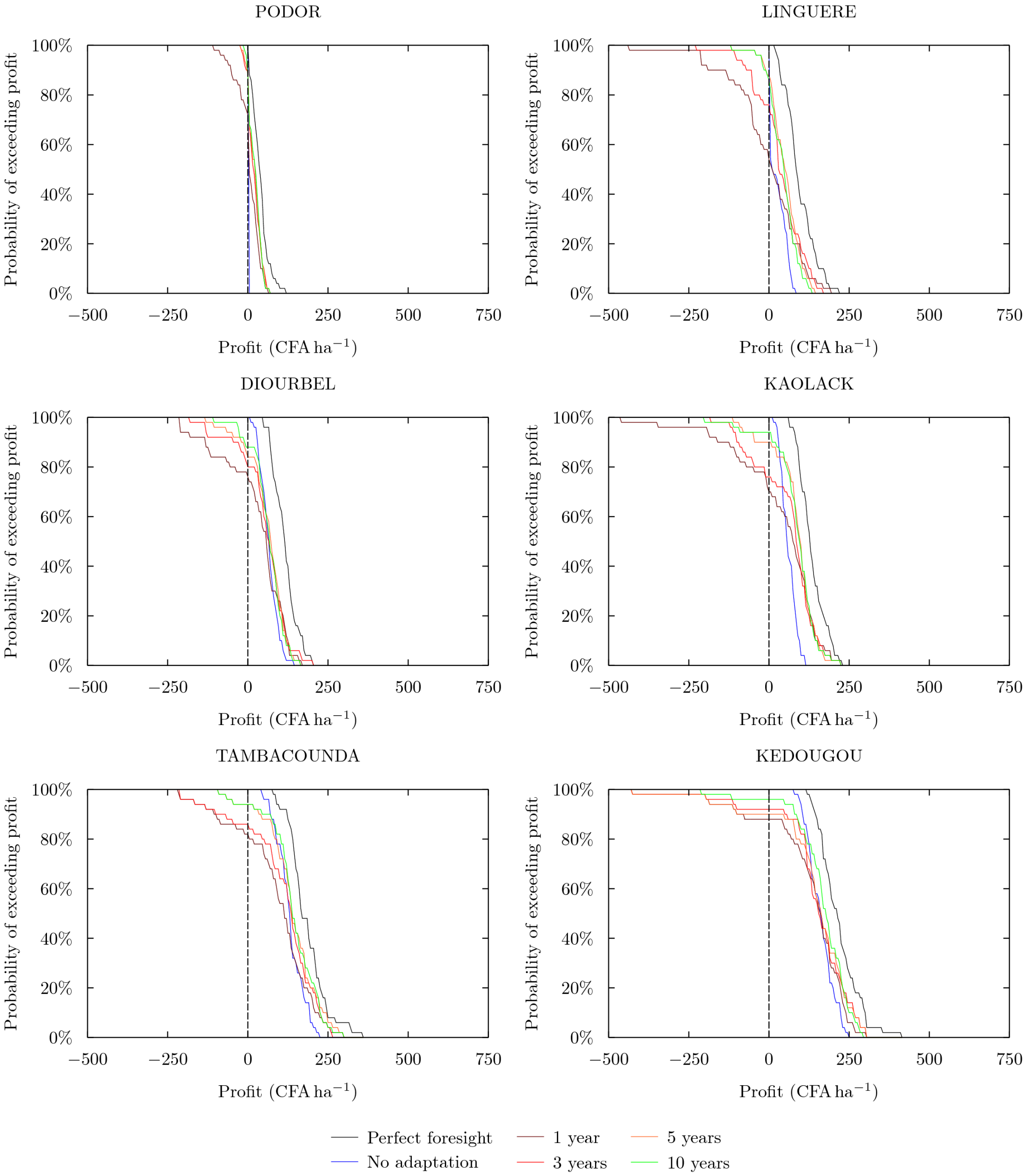

Figure 6.13: Long-term profits for a range of crop management adaptation options at the six locations. An nitrogen recovery rate of 50 % was assumed. The profit was calculated as the difference between the market price of fertiliser (150 CFA kg^{-1}) and the market price of millet (175 CFA). The costs of buying, transporting and applying fertiliser, and the additional costs of transporting millet to market, were not included in the calculation. Simulations were performed for the period 1950–2009.

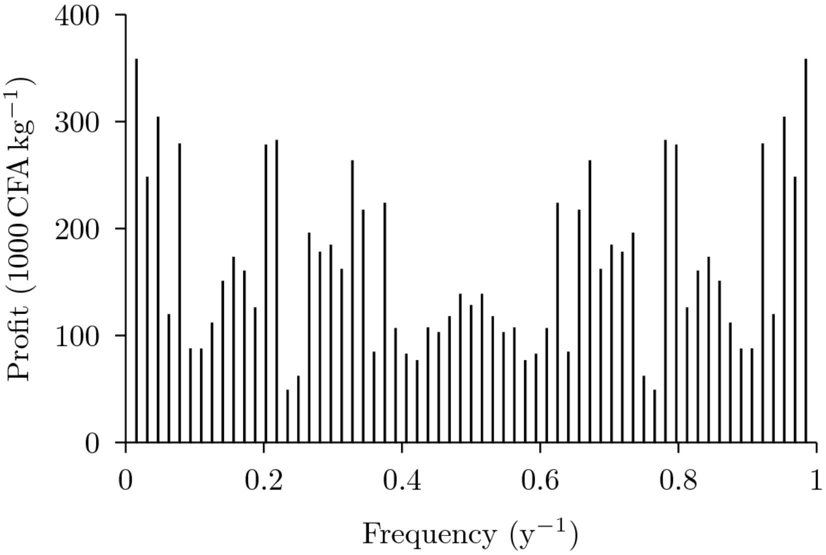

Figure 6.14: Frequency analysis of the interannual profits at Diourbel for a nitrogen application of 50 kg N ha^{-1} and a recovery rate of 50 %. A Fast Fourier Transform was used to identify the dominant interannual frequencies in the period 1950–2009.

likely to be successful if there are long-term trends that are poorly-represented by a simple average across all of the years, but the Sahel was dominated by a long drought during 1960–2009. Climate change could create such long-term trends in the future. Figure 6.14 shows that any alternative adaptation options that were based on cyclical rainfall patterns would also perform poorly.

6.6.2 Adaptation sensitivity study 1: environmental influences

A sensitivity study was performed to investigate how profits would be affected by variations in the temperature and rainfall patterns. Five new sets of meteorological data were created which had:

1. 50 % fewer rainfall events each year but with the total rainfall unchanged (the rainfall events were removed randomly);
2. decreased interannual rainfall variability, with the rainfall each year being

50 % closer to the long-term average for the location;

3. increased interannual rainfall variability, with the rainfall each year being 50 % further away from the long-term average for the location;
4. decreased temperature variability, with the diurnal temperature range being decreased by 50 % each day; and,
5. increased temperature variability, with the diurnal temperature range being increased by 50 % each day.

The adaptation studies were performed for each dataset.

The impact of the rainfall and temperature variations are shown in Figure 6.15 for the no adaptation strategy and Figure 6.16 for the adaptation strategy based on the previous year. While the variations between locations, which depend on the average rainfall, remain, variations in the rainfall distribution at each location generally have little impact on profits. Over the long-term, the mean rainfall is a more important determinant of profitability than either the intraseasonal or interannual rainfall variability. Temperature variations have a greater influence than rainfall, with higher diurnal variability reducing yield through a reduction in the crop growth rate (Equations 3.6 and 3.7), but the impact is still small compared to the differences between locations. Rainfall and temperature variations have a greater influence on the previous-year adaptation strategy than the no adaptation strategy but do not alter the overall trends between strategies that were identified in Figure 6.13.

6.6.3 Adaptation sensitivity study 2: risk-averse behaviour

Another sensitivity study was performed to investigate if yields and profits would be reduced if the smallholder were risk-averse. It was assumed that the principal aim of the smallholder was to minimise any losses from the farm, with profit maximisation being only a secondary aim.

With no adaptation, the most appropriate long-term strategy to meet these aims was to invest only a small amount in the soil fertility. For example, at Kaolack with a 33 % recovery rate, this strategy achieved lower average yields of

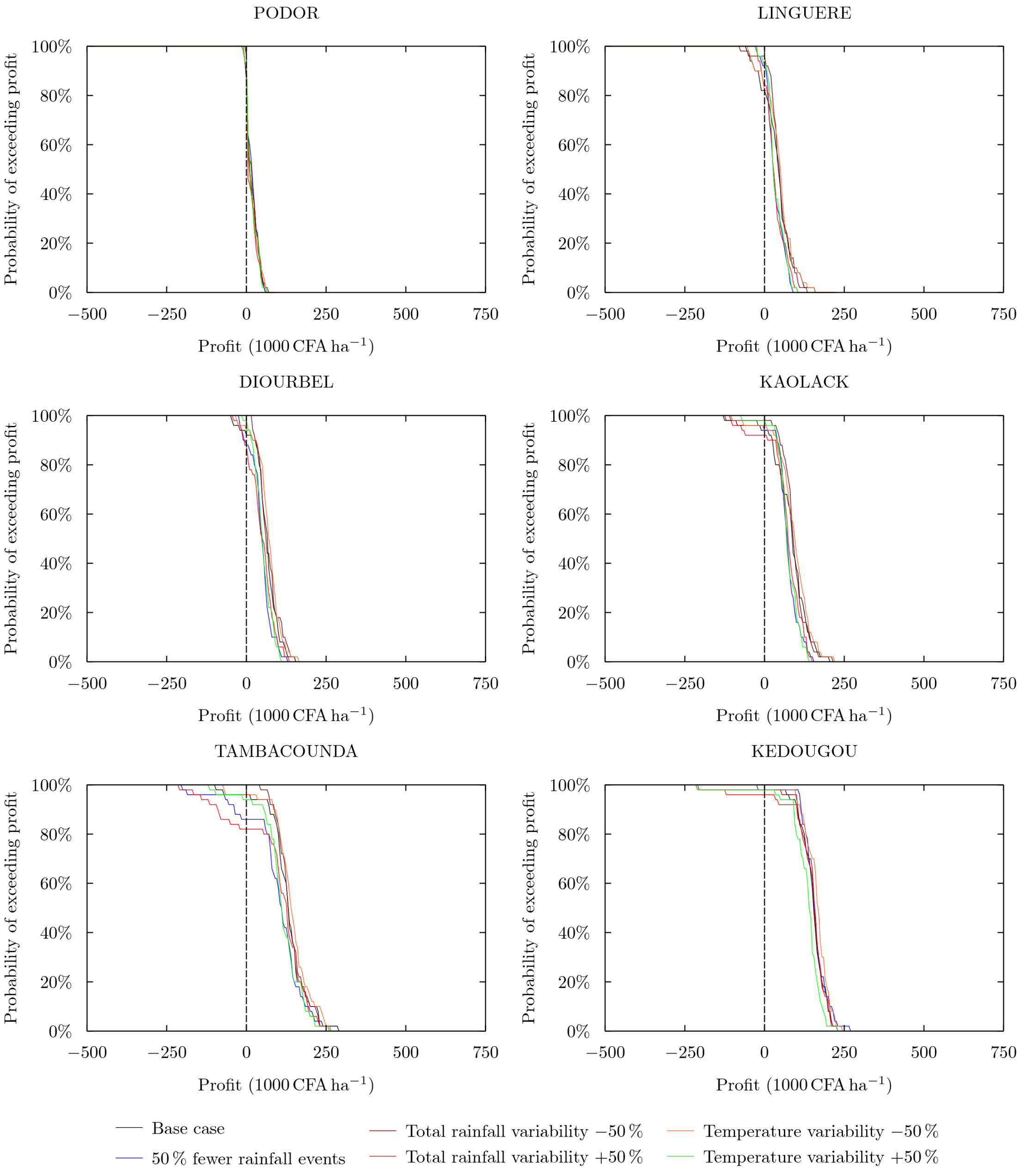

Figure 6.15: Influence of temperature and rainfall on long-term profits from a no adaptation strategy. Profits were calculated for a nitrogen recovery rate of 50 % over the period 1950–2009.

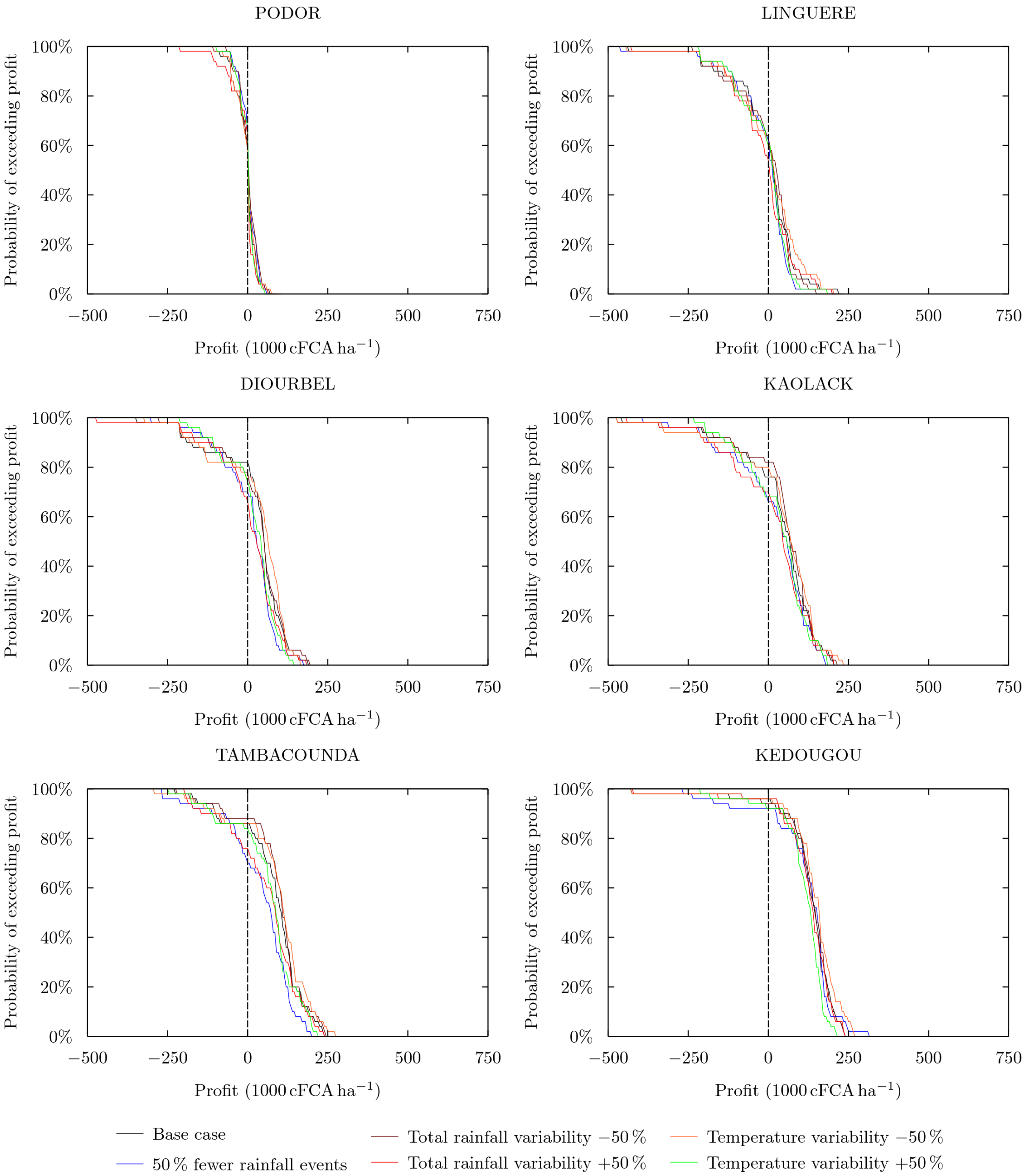

Figure 6.16: Influence of temperature and rainfall on long-term profits from a strategy based on the optimum conditions in the previous year. Profits were calculated for a nitrogen recovery rate of 50 % over the period 1950–2009.

only 394 kg ha^{-1} and profits were reduced on average by 16 000 CFA ha^{-1}, but the household did not suffer any losses. It was more profitable to adapt to conditions in previous years under these circumstances but this strategy led to occasional losses in some years because the risk of losses was underestimated following several profitable years.

Smallholders in Senegal normally farm several dispersed fields. An investigation was performed to see if the losses could be minimised while producing a higher grain yield by operating two different management regimes on two fields (for example, one could be intensively managed, to provide large profits, while the other could provide small but dependable grain yields in all years). Each field was assumed to be the same size (0.5 ha) with identical soils and rainfall, and all possible combinations of planting date, density and nitrogen application were tested for each field. While the optimal nitrogen application was generally the same in both fields, it was possible to increase the overall yields and avoid losses by planting crops in the two fields at different times. In several years, profits from one field covered losses from another. At Kaolack, with a 33 % recovery rate, using alternate strategies in two fields increased the grain yield by 63 % and the mean annual profit by 45 %.

6.7 Discussion

Rainfall has a strong influence on smallholder agricultural systems in Senegal. The low average rainfall at Podor prevents crop growth in many years, explaining why the region is predominantly pastoral outside of the Senegal river valley. Agriculture becomes feasible as the annual rainfall increases, for example at Diourbel and Kaolack in the groundnut basin, but the interannual grain yield variability is very high (Figure 6.7) as a result of rainfall fluctuations. In southerly high-rainfall locations, yields are higher and yield fluctuations are smaller.

Rainfall is not the only important climatic variable. The grain yield at the most humid location in unstressed growing conditions was twice the unstressed yield at the driest location, as a result of the VPD being much lower in humid conditions. There were also variations in the irrigated yields between sites caused by temperature and VPD variations (Figure 6.3). It is possible that the unstressed yield gap between humid and dry locations will widen in the future if the VPD increases due to climate change.

Farmers in Niger have been criticised in the literature for utilising planting densities that are lower than the optimum (e.g. Payne, 1997, 2000; Shapiro and Sanders, 1998). The planting densities of Senegalese smallholders that were reported in the ESPACE study (Section 1.5.3) were predominantly within the optimum range found here. It was concluded here that planting densities should be higher where rainfall and nitrogen are plentiful but that a broad range of planting densities would produce similar yields at particular rainfall and nitrogen levels. These conclusions are consistent with the studies of Keating *et al.* (1988) and Singh *et al.* (1993) (Section 2.2.3) except that the range of optimum densities is broader for millet than for maize because millet is a hardier crop which produces productive tillers in favourable conditions.

Dry planting is widely practised in Senegal but a modelling study for Niger by Sultan *et al.* (2005) concluded that delaying planting until the monsoon onset would be more appropriate. The results of this study show that higher grain yields would have been achieved if the planting date had been delayed by around two weeks after the dry planting germination date. Delaying planting reduces the impact of early-season droughts. As explained in Section 2.2.2, other studies have identified late planting as a risk reduction strategy that reduces the impact of bad years at the cost of reduced overall yields (Singels, 1992; Williams *et al.*, 1999). In Senegal, delaying planting reduces the impact of bad years and increases the overall yield. However, this investigation did not take account of either the loss of soil nutrients to weeds, the additional labour that is required to clear the weeds from the field prior to planting or whether delaying planting increased the susceptibility of the crop to pests or disease. Surveys of smallholders are required to identify the underlying reasons behind the dry planting strategy.

While the planting density and the planting date can be varied quite easily, it is much more difficult for smallholders to increase the fertility of their fields. Yet the soil fertility was found to be the main yield-determining factor when there was sufficient rainfall, with very low yields being simulated in unfertilised fields. Importantly, the fractional losses and the yield variability increased substantially as the soil fertility was increased, which reduced the effectiveness of fertilising the fields (the ratio of the grain yield to the applied nitrogen was reduced). Occasionally, in drier years, increasing the soil fertility even caused the grain yield to reduce as the limited pool of soil water was used up too rapidly. The existence of this phenomenon has been debated in the literature (e.g. Affholder, 1995; Payne, 1997); the analysis here suggests that the most likely reason for the discord is that the few field studies that have been performed in the Sahel have had little opportunity to measure these relatively infrequent events.

The increasingly inefficient use of fertiliser at high soil fertility levels, caused by increased fractional yield losses and increased variability, are important because nitrogen application is difficult and expensive. Generating tonnes of manure and applying it to fields is a time-consuming process. In some parts of Senegal, it is possible to buy manure from livestock herders or to make arrangements for herds to graze on the fields in the dry season. Otherwise, manure must be produced by the household: the animals must be purchased, corralled and fed, and the manure must be collected and transported to the fields, with the amount of manure that can be applied depending on the availability of household labour and the availability of feed. If mineral fertiliser is used then it must be bought at a market, transported and applied to the fields. There is a risk to the household that the labour and savings that are invested in the field fertility will not be recompensed if the rainfall is poor. A simple economic analysis identified the rainfall, the nitrogen recovery rate and the grain and fertiliser market prices as the four principal factors that determine the profitability of soil fertilisation. In Senegal, the rainfall variability is very high, the recovery rate is often very low (Breman *et al.*, 2001; Fofana *et al.*, 2008), grain prices are depressed by the availability of imported rice and fertiliser is expensive in comparison with other continents (Gray, 2002). For low recovery rates, the most profitable strategy is to apply microdoses of fertiliser at high-rainfall locations, a strategy also identified by Cooper *et al.* (2008) for Zimbabwe. Intensification becomes financially viable at higher recovery rates or if the cost of fertiliser is reduced.

Most of the simulations in this chapter assumed that the crop management decisions were either optimised each year (perfect foresight) or fixed for the whole period (no adaptation). An investigation was performed to examine the opportunities for smallholders to improve grain yields by adapting their crop management decisions in light of the growth conditions in previous years. Adaptation has been identified as a key strategy to mitigate the impact of climate change in the future (Easterling *et al.*, 2007). It was concluded that the best strategy to maximise both grain yields and profits was in fact to use a fixed strategy for the whole period and to not adapt to the conditions in recent years. The optimum nitrogen application depended on the recovery rate. An investigation was performed to examine whether adaptation would be beneficial if the rainfall or temperature distributions were different. The no adaptation strategy produced higher yields and profits with lower risk despite large changes in the distributions being simulated. It was concluded that the profitability of nitrogen application in Senegal is determined primarily by the mean rainfall rather than by the rainfall or temperature distributions. A second investigation examined how risk-averse behaviour (defined as avoiding financial losses) would affect yields. Yields and mean annual profits were substantially reduced at low recovery rates because the only acceptable strategy was to dry-plant with little nitrogen application. One method to produce higher yields and profits while still avoiding losses was to cultivate two fields with different crop management strategies. Using different planting dates and, occasionally, different nitrogen applications led to substantial long-term increases in the yields and profits while still avoiding losses.

These simulations took no account of damage caused by pests and disease, which were observed in many fields by the ESPACE project (Section 1.5.4). Over-fertilisation and flooding were also ignored in the simulations. All of these factors could have reduced the grain yields.

By characterising the long-term impacts of rainfall and nitrogen application, studies like this one can be used to inform insurance schemes that enable smallholders to manage the risk of agricultural intensification to their livelihoods and reduce the impact of large losses in the years with poor growing conditions.

Another method for smallholders to reduce their financial risk is to use manure instead of mineral fertiliser. Manure has the advantage of decaying over several years, so a poor rainy season will not lead to the investments in the soil nutrients being completely lost. Manure also contains much organic matter which bolsters the low natural concentrations that are found in the sandy soils of Senegal. It would be interesting to compare the relative long-term merits of manure and fertiliser use in a systematic modelling study across the country using a broad farm system model (Section 2.4).

6.8 Summary

This chapter has shown that a substantial yield gap exists in smallholder fields in Senegal. Interannual rainfall variability is the principle cause in low-rainfall regions, causing lower and more variable crop yields. Water stress has a greater impact on crop yields at higher levels of soil fertility, so the profitability of farming reduces with agricultural intensification unless fertiliser can be applied cheaply. The poor return on investment from nitrogen application is the principle barrier to intensification at locations with sufficient rainfall. This is affected by the prices of fertiliser and grain, and the nitrogen recovery rate. The optimum strategy to maximise profits while minimising the risk is to use little fertiliser and accept low yields, unless the price of fertiliser is very low or the recovery rate is very high.

Several crop management decisions were examined and there was little evidence to suggest that the smallholder farming systems in Senegal are not optimised for the Sahelian environment. The benefits of adapting crop management according to the growth conditions in previous years were assessed but the optimum strategy was to use fixed planting dates and planting densities each year.

Although adapting crop management decisions was not the optimum strategy in the past, it might become necessary in the future as a result of climate change. The impact of climate change on smallholder agricultural systems in the future is examined in Chapter 7.

Chapter 7

Climate change and smallholder farms

Having examined Sahelian smallholder farming over the last 60 years in Chapter 6, this chapter looks forward to assess how climate change could affect smallholder agriculture in the twenty-first century and to gauge the benefits of adapting crop management strategies. Rural smallholders have been identified as being particularly vulnerable to climate change and in danger of having to abandon rainfed farming altogether (Cline, 2007). Section 7.1 describes how the climate data from three climate models were processed for use in the crop model. The simulation of climate change in CROMSAS is discussed in Section 7.2. The impacts of climate change in Senegal are assessed in Section 7.3 and the potential for adapting crop management strategies to reduce these impacts is examined in Section 7.4. The chapter concludes with a sensitivity study that examines uncertainties in the literature regarding the effect of increased CO_2 on crop growth, in Section 7.5.

7.1 Climate projections for Senegal

From an ensemble of 18 GCMs, Cook and Vizy (2006) identified only four with moderately realistic rainfall variations in the Sahel region (Section 2.5.2). Three of these were chosen to produce climate change projections for this study (Table 7.1), from the centres of the Geophysical Fluid Dynamics Laboratory (GFDL),

IPCC GCM version	Short name	Grid spacing
GFDL-CM2.0	GFDL	2.0° lat × 2.5° lon
MIROC3.2(medres)	MIROC	∼2.8° lat—lon
MRI-CGCM2.3.2	MRI	∼2.8° lat—lon

Table 7.1: IPCC GCMs used by this study for climate change projections. The grid spacings were taken from Cook and Vizy (2006).

USA, the Centre for Climate System Research ('Model for Interdisciplinary Research on Climate', or MIROC), Japan, and the Meteorological Research Institute (MRI), Japan. These three were also chosen by Huntingford *et al.* (2005) for an agro-climatological analysis of the Sahel region.

It was necessary to process the GCM data to produce good-quality climate projections. GCM data can be used directly if the simulations are accurate. Figure 7.1 compares the daily temperature and precipitation projections of the three GCMs with observed data from Chapter 5. In each case, the data are a climatological average of the period from 1961 to 2000 and are averaged across the 11 synoptic weather stations in Senegal. The difference in the maximum temperature between models is up to 7 °C during the growing season. The minimum temperature simulations are more accurate with little variation during the growing season. The rainfall predictions are very variable with the peak annual average rainfall ranging from 3.5 mm in the MRI GCM to 10.4 mm in the GFDL GCM. Discrepancies of this magnitude would have a pronounced impact on crop model simulations.

Huntingford *et al.* (2005) avoid this problem by 'nudging' each daily value: the mean value calculated by the GCM for the period is subtracted and the observed mean is added instead. This approach assumes that each GCM underestimates or overestimates the actual value by the same fixed quantity at all times. Although easy to implement, there are several philosophical and practical issues with this approach. While GCMs have skilfully simulated temperature trends in the past (Hansen *et al.*, 2006; Randall *et al.*, 2007), Figure 7.1 shows that each GCM simulates different temperature and precipitation patterns for the twentieth century. Even the projections of the NCEP/NCAR reanalysis model, which

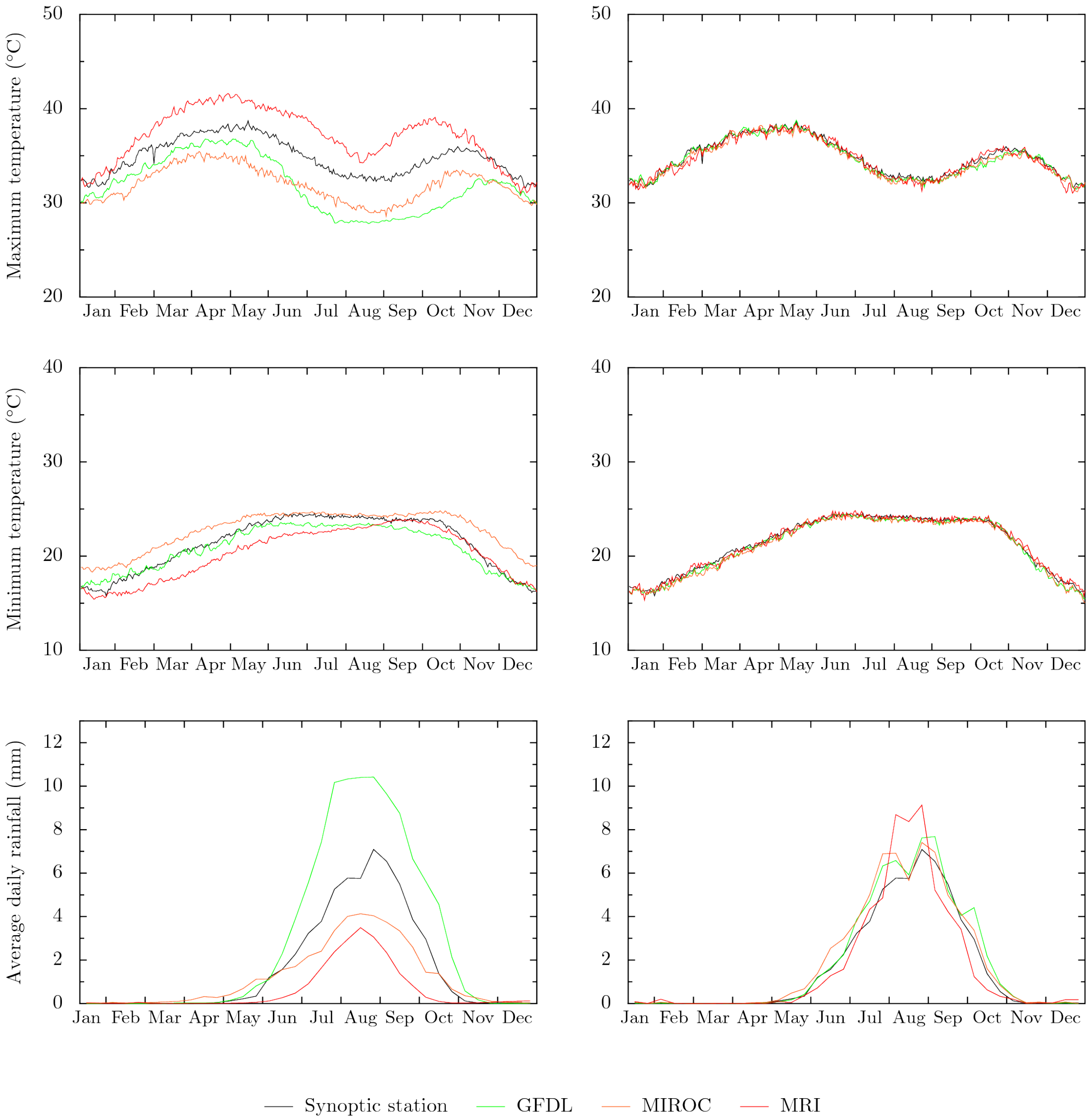

Figure 7.1: Comparison of observed and simulated temperatures (daily maximum and minimum) and rainfall across Senegal for the years 1961–2000. Climatologies for three IPCC GCMs are presented. The graphs on the left show the raw GCM daily averages (or 10-day averages in the case of rainfall). The graphs on the right show the daily averages of the climate change datasets created from the GCM projections by this study, using the method described in the main text.

should be more accurate than the IPCC GCMs, are systematically different to observations (Section 5.1.5). It is therefore preferable to apply GCM trends to observed data rather than relying on the GCM projections with an offset. Using offsets can also introduce inaccuracies to the GCM projections. If the offset is an annual mean then the GCM projections will become skewed if the rate of change is not constant throughout the year. This loss of accuracy can be avoided by calculating offsets for shorter periods, for example monthly, but the problem then arises of discontinuities being introduced between months if the rate of change is not constant throughout the year. These problems were encountered for the GCM data towards the end of the twenty-first century.

A different methodology was adopted in this study. The aim was to produce datasets with realistic daily meteorological data but which represented longer-term climatic trends. Several methods were tested to extract the long-term climate model trends. Linear regression analysis did not represent short-term variations and tended to underestimate the accelerated warming in some scenarios toward the end of the twenty-first century. Moving averages were found to be better; 11, 15 and 31-year averages were tried and the 15-year period was identified as the best for balancing shorter-term and longer-term variations. At the start and the end of each climate model dataset, where a full 15-year moving average could not be calculated because of insufficient data, it was necessary to extend the long-term trend to the edge of the dataset using regression analysis.

Rainfall was the most difficult to simulate realistically because of the relatively high variability and particularly poor GCM simulations compared to other meteorological data. The seasonal distribution of rainfall can be as important as the total magnitude (Section 4.2.2.2) so a methodology was developed which reproduced typical seasonal rainfall distributions. The GCM rainfall projections were judged to be too inaccurate to be used directly so observed rainfall data were used instead. The datasets were produced using a series of operations:

1. The total monthly rainfall was calculated for each year of the observed data and normalised to produce a series of monthly rainfall distributions.

2. Similarly, the total monthly rainfall was calculated for each year of the GCM data and normalised to produce a series of GCM monthly rainfall

distributions.

3. The closest observed year rainfall distribution was identified for each GCM rainfall distribution using least squares analysis.
4. The long-term annual rainfall trend between the observed and GCM years was calculated using a 15-year moving average.
5. The rainfall in each GCM year was calculated as the rainfall from the matched observed year perturbated by the long-term rainfall factor.
6. Trends in the other meteorological data were also calculated using a 15-year average. Data from the same observed year as for the rainfall were used to keep all of the meteorological data internally consistent. For each meteorological parameter, the long-term trend between the observed year and the GCM year was calculated using a 15-year moving average. Trends were separately calculated for each month and the distribution was then smoothed to avoid discontinuities at the end of months towards the end of the twenty-first century.
7. The non-rainfall meteorological data were calculated for each GCM year using the equivalent data from the observed year perturbated by the smoothed long-term trend function.

The resulting datasets had different short-term data to the GCM projections, but the long-term trends from the GCMs were represented. The datasets were internally consistent and properly represented the variability of the Sahelian climate.

Specific humidity data at the surface were only available for the MRI model. Since the humidity variations are relatively small, with a gradual rise being forecast in the twenty-first century, it was concluded that any errors resulting from the use of MRI trends in all three models would be negligible. The monthly trends of the maximum and minimum temperatures were only available for the MIROC model, with only the mean surface temperature being provided for the other two models. Since daily maximum and minimum temperatures were available for the periods 1961–2000, 2046–2065 and 2081–2100, these were used to establish relationships between the maximum, minimum and mean temperatures in the GFDL and MRI models. These relationships were interpolated to years where daily data were not available and used to estimate the maximum and minimum temperature trends for the whole period of analysis.

7.1.1 Comparison of observed and simulated climate data

The temperature and rainfall projections from the approach developed by this study are compared to observations and to the daily GCM projections of each model in Figure 7.1, for the period 1961–2000. The observed temperature climatology was skilfully reproduced with the projections being virtually indistinguishable from the observed pattern, a significant (albeit expected) improvement on the raw GCM projections. The observed rainfall climatology was simulated less skilfully but was greatly improved in comparison with the raw climate model data. The main discrepancy was the overly high MRI maximum, which resulted from the raw MRI projections being particularly low and the simulated rainy season being shorter than elsewhere. An unrepresentative number of observed years with short, intense rainy seasons were selected to represent the MRI model, and this led to a higher rainy season peak when the rainfall was approximately normalised to the observed total.

Figure 7.2 compares the observed and GCM rainfall variabilities for the period 1950–2000. The long-term Sahelian drought in the period 1970–2000 is clearly visible in the observed time series but only the MRI model simulates a long period of drought at the same time. The drought periods that are simulated by the MIROC and GFDL models rarely exceed 5 years in length. In view of the differences between the observations and the models, the conclusions reached in Chapter 6 are reassessed using the projections from the three GCMs in Section 7.2.2.

There is concern that climate change will increase the number of extreme weather events (Easterling *et al.*, 2007). For agriculture, it has been postulated that the frequency and intensity of droughts could increase if rainfall is brought by fewer but larger storms (Cubasch *et al.*, 2001; Hulme *et al.*, 2001). In this situation, the number of rainfall events would decrease even if the total rainfall

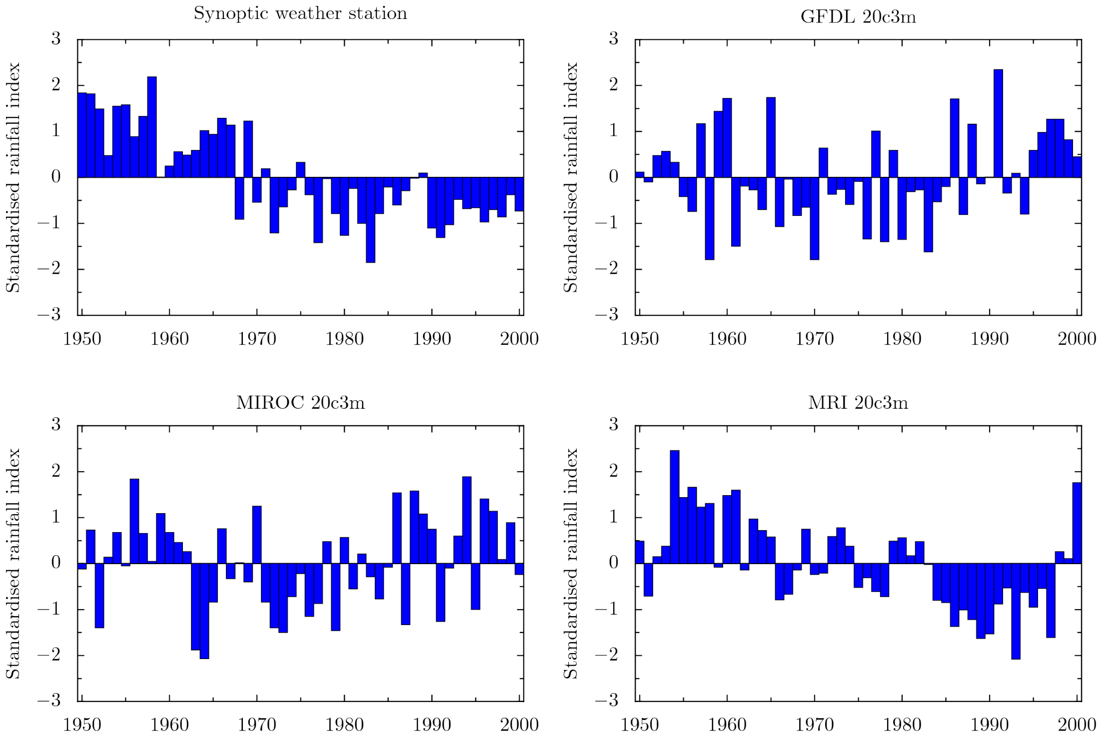

Figure 7.2: Standardised rainfall index for observed and IPCC model data in the period 1950–2000. Each value represents an average of the 11 synoptic weather stations in Senegal. The IPCC data, for three GCMs, were created using the methodology developed by this study.

remained constant. The mean event intensity would increase and crop yields might be adversely affected.

The methodology developed by this study to produce rainfall projections uses synoptic weather station observations from the past, so any change to the pattern and intensity of rainfall events in the future would not be represented in the data. The daily rainfall projections of the three GCMs were examined for evidence of changes to the rainfall regime in the future. The SRES A2 scenario was chosen as any changes in this scenario were likely to bound those of the other scenarios (see Section 7.1.2 for descriptions of the scenarios). Figure 7.3 compares the annual number of events and the mean event intensity against the annual rainfall for the observations and the GCM projections. The GCMs substantially overestimated the number of rainfall events while underestimating the mean event intensity (i.e.

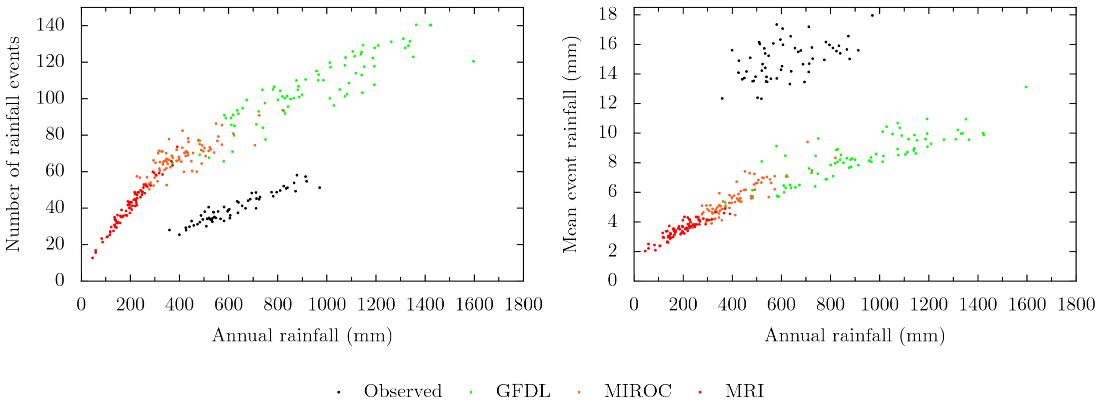

Figure 7.3: Analysis of rainfall events for observed and IPCC GCM data. The first graph shows the number of rainfall events per year and the second shows the mean event rainfall. The observed data are for the period 1950–2008 and the GCM data are for 1961–2000, 2046–2065 and 2081–2100. Each point is an annual average of the data at the eleven synoptic weather stations.

there were too many storms and the storms were too small). Table 7.2 shows that the observed rainfall was closely correlated to the number of rainfall events, while the observed mean rainfall intensity was less correlated (with the variations probably resulting from a small number of particularly intense events). The GCMs simulated the total rainfall as a function of both the number of events and the mean event intensity. The GCMs projected a small reduction in the number of events in the twenty-first century but, with the exception of the MIROC model, there was no concomitant increase in the mean event rainfall. It was concluded that there was no evidence that the rainfall projections of this study would be unsuitable for representing the twenty-first century climate. However, in view of the substantial discrepancies between the observations and the GCM simulations of the twentieth century rainfall, questions remain as to whether the GCM parameterisations of tropical convective rainfall can adequately simulate any changes to the rainfall regime in the future.

	1961–2000	2046–2065	2081–2100	R^2
Number of events				
Synoptic observations	38			0.90
GFDL	110	109	91	0.81
MIROC	69	69	66	0.60
MRI	42	39	39	0.95
Mean event rainfall (mm)				
Synoptic observations	14.7			0.27
GFDL	9.1	8.2	7.1	0.72
MIROC	5.1	6.1	5.9	0.78
MRI	3.5	3.5	3.5	0.79

Table 7.2: Comparison of the rainfall event statistics for the synoptic weather stations and the IPCC GCMs for Senegal. The mean number of events and the mean event rainfall are listed for three time periods. The data were derived from daily observations and daily IPCC data. The correlation in the final column is between either the number of events or the mean event rainfall for all available years and the total rainfall in those years.

7.1.2 Climate change in the twenty-first century

The IPCC has identified a range of potential future scenarios for climate modellers (IPCC, 2000). These scenarios were used in both the third and fourth assessment reports. Four groups of scenarios were produced (A1, A2, B1, B2), with the world population, economic growth rate and energy use varying between groups. Table 7.3 summarises the three scenarios used in this study. The B1 scenario has the lowest overall greenhouse gas emissions while the A2 scenario has the highest. The A1B scenario lies in the middle; the population is lower than that of the A2 scenario but the energy use per capita is very high.

Meteorological datasets were produced for these three scenarios from each GCM for the period 2000–2100. Separate twentieth-century data were also obtained for each model which covered the period 1900–2000. Figure 7.4 extends the observed interannual rainfall variations into the twenty-first century using

Scenario	Population (billions)	C emissions (GtC)	pCO_2 (ppmv)
B1	8.76	9.7	479
A1B	8.54	16.1	555
A2	11.67	17.3	559

Table 7.3: Overview of the three IPCC SRES scenarios used in this study. The figures are estimates for the year 2050. C is the annual carbon emissions from fossil fuel energy sources and pCO_2 is the atmospheric carbon dioxide concentration. The figures are taken from Hulme *et al.* (2001) and are based on the scenarios from the IPCC (2000).

projections from each GCM for the B1 and A2 scenarios. The projections from all three models suggest that the B1 scenario rainfall will be higher than that experienced during the last 40 years (while noting that none of the models accurately simulated the long Sahelian drought after 1970). In contrast, while higher rainfall is projected for the A2 scenario in the early part of the century, there is a drying trend in all three models towards the end of the century of similar length and magnitude to the 1970–2000 drought. The longest drought period of the B1 scenario is approximately 10 years while the A2 scenario has droughts lasting 20–50 years.

A climatology for each model for the years 2061–2100 is shown in Figure 7.5. These are compared with the observed climatology for 1961–2000 from Figure 7.1. Both the maximum and minimum temperatures rise substantially, particularly in the A2 scenario where the GFDL rainy-season temperature trend is different to that of the other two models. The rainfall in the B1 scenario is higher in all three models than that observed during the recent drought. However, higher A2 scenario emissions lead to lower rainfall and the recent drought becomes the climatic average by the end of the twenty-first century.

Time series of the temperature, VPD and ETo are shown in Figure 7.6 for the SRES A2 scenario at Kaolack. The temperature is projected to increase steadily over the twenty-first century by a total of 4 °C. The temperature increase is larger in the GFDL simulations. The VPD is also projected to increase overall but, with

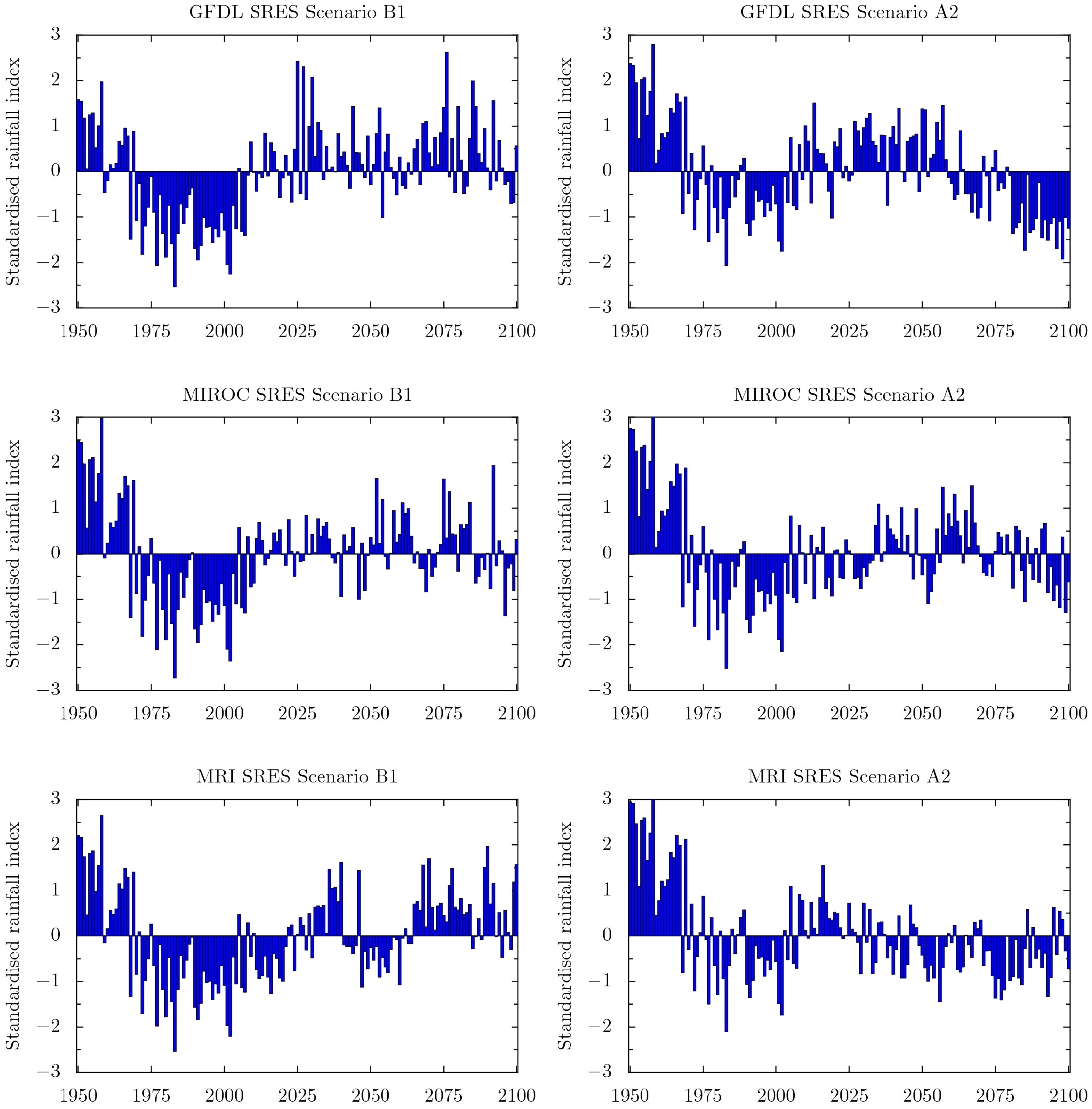

Figure 7.4: Standardised rainfall index for synoptic weather station and IPCC model data in the period 1950–2100. The graphs on the left-hand side show the SRES B1 scenario while the A2 scenario is shown on the right. Observed rainfall totals are used for the period 1950–2008 and GCM projections are used from 2009. Each value represents an average of the 11 synoptic weather stations in Senegal.

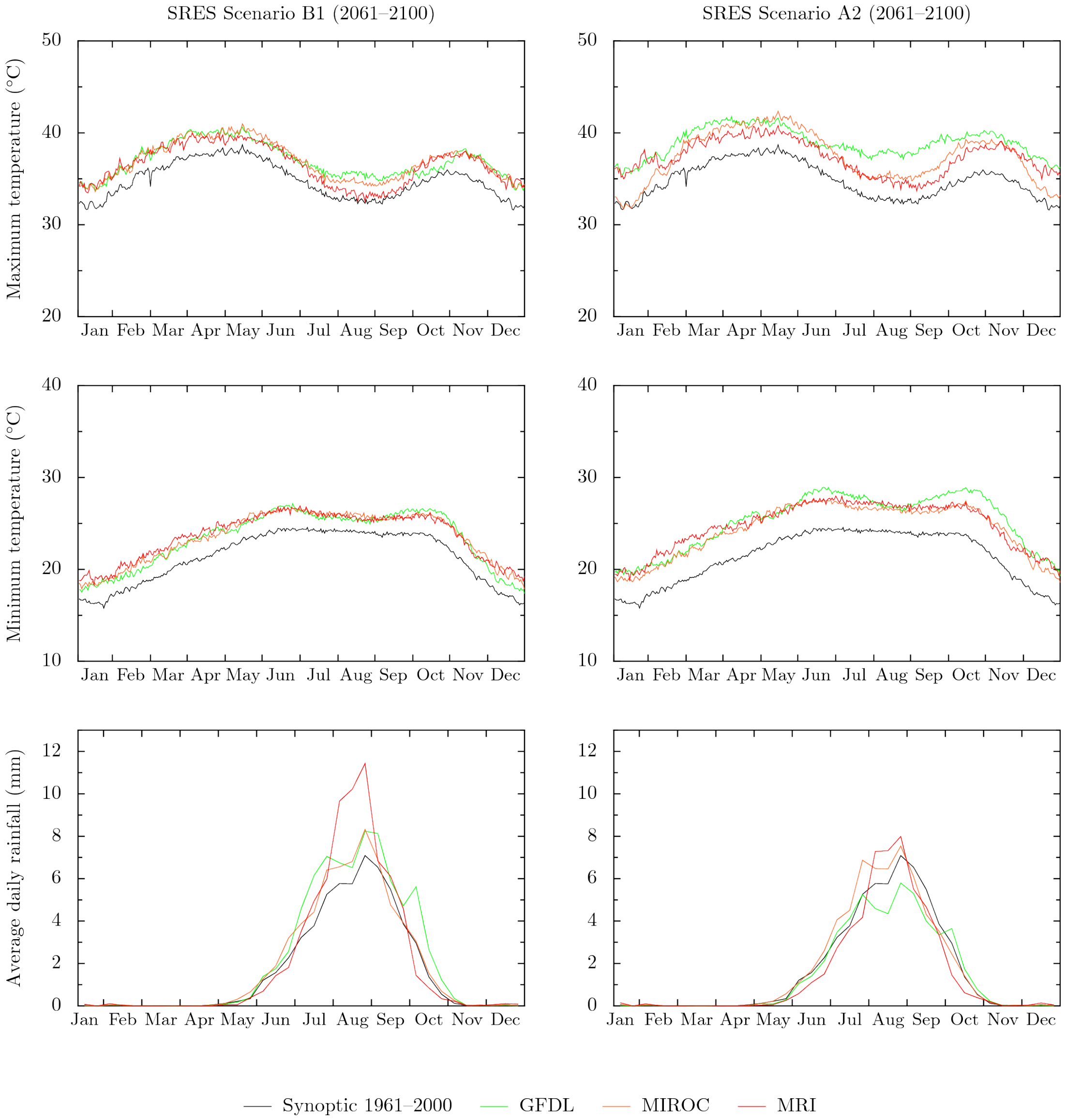

Figure 7.5: Comparison of IPCC model temperatures (daily maximum and minimum) and rainfall across Senegal for the years 2061–2100. The IPCC data, for three GCMs, were created using the methodology developed by this study. The graphs on the left-hand side show the daily averages for the SRES B1 scenario (or 10-day averages in the case of rainfall) while the A2 scenario is shown on the right.

the exception of the GFDL model, the change is small during the rainy season. Negligible changes to the ETo are simulated during the growing season.

7.2 Modelling climate change in CROMSAS

Climate change is projected to have a number of diverse impacts on crops (Easterling *et al.*, 2007; Porter and Semenov, 2005). Higher temperatures will increase the rate of phenological development, reducing the time for growth and the final yield, although this might be mitigated by adopting alternative varieties with longer developmental periods. Periods of unusually high temperatures could reduce the photosynthesis rate and could also reduce the final grain yield if they occur at critical growth stages such as flowering (Wheeler *et al.*, 2000).

Higher temperatures will also increase the reference evapotranspiration rate and hence the demand for water from the crop. The relative humidity will reduce, which will further increase the demand for water. Both the magnitude and the frequency of rainfall events could change (Meehl *et al.*, 2007), causing more droughts or floods.

Lobell and Burke (2008) conclude that changes in growing season temperatures represent a greater uncertainty for crop growth than changes in rainfall for most regions of the world. They used a statistical analysis of the relationships between mean temperature and rainfall and mean crop yields, so were unable to quantify any impact of an increase in the frequency of extreme events (e.g. severe drought, floods and periods of high temperatures).

Atmospheric CO_2 and ozone concentrations will also increase. Increasing CO_2, which will improve yields and reduce water use, is simulated in CROMSAS and the parameters are discussed below. Ozone is a pollutant that enters plants through the stomata and reduces photosynthesis by impairing Rubisco activity. The impact is greater on temperate than tropical crops (Mills *et al.*, 2007). The ozone concentration is projected to rise with climate change, perhaps substantially if no new international air quality legislation is enacted, which will reduce crop yields in the future (Ainsworth and McGrath, 2010). The impact of rising ozone is not simulated in CROMSAS.

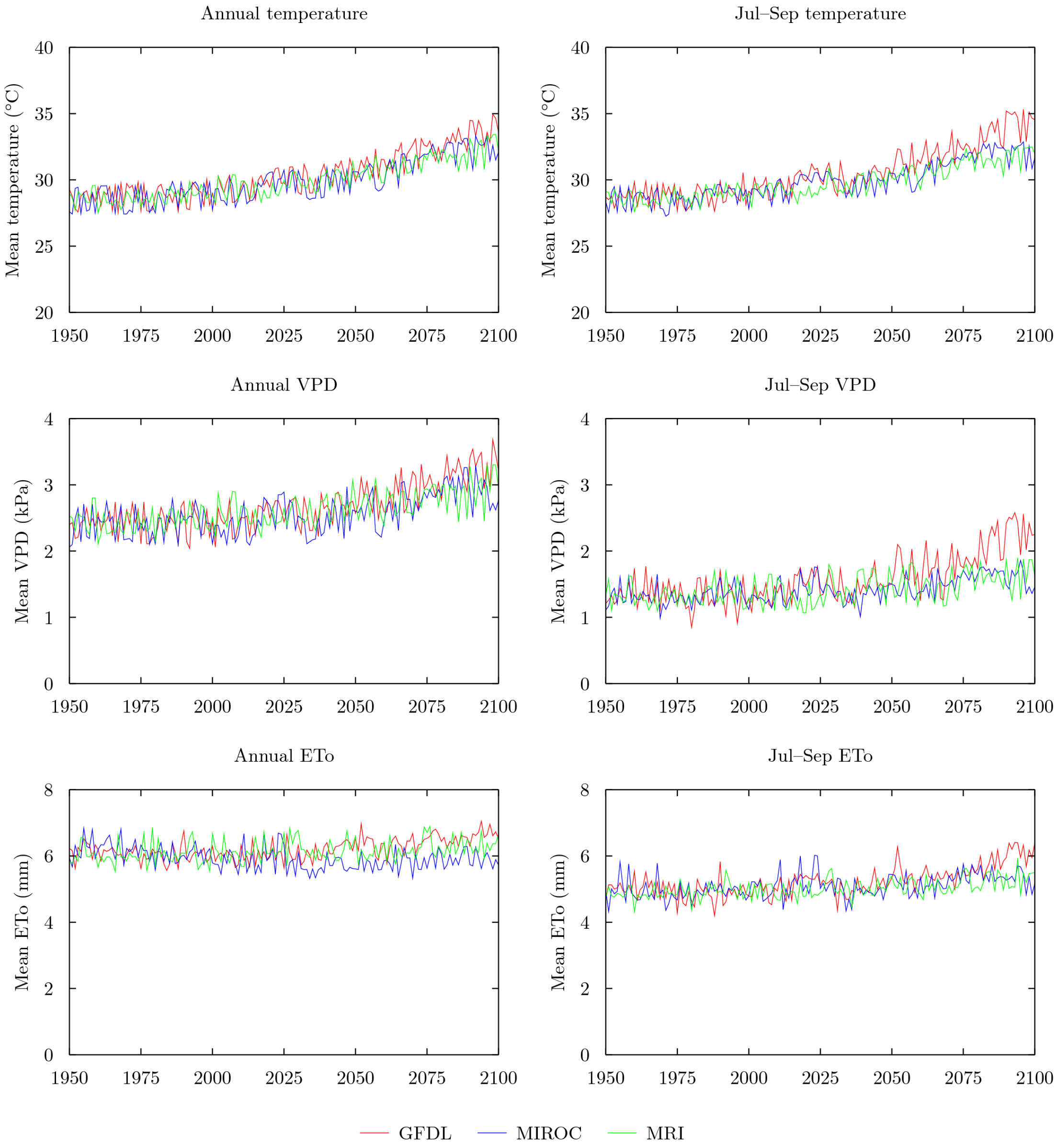

Figure 7.6: Time series of temperature, VPD and ETo projections for the SRES A2 scenario at Kaolack, Senegal. Mean values are presented for the whole year and for July to September (the peak growing season). The data were created using the methodology developed by this study. The ETo was estimated using the FAO56 method (Allen *et al.*, 1998).

7.2.1 Atmospheric carbon dioxide concentration

The atmospheric CO_2 concentration (denoted $[CO_2]$) has been artificially enriched in greenhouses for decades to increase the growth rate of plants (Kimball *et al.*, 1993), in a process called carbon fertilisation. It has long been postulated that the negative impacts of temperature and precipitation changes on crops that are forecast by climate change models will be offset by enhanced yields caused by rising $[CO_2]$ (Leakey *et al.*, 2006). Plants absorb CO_2 from the atmosphere through diffusion across leaf stomata, a process which also leads to the loss of water in the opposite direction through transpiration. Increasing the $[CO_2]$ causes the rate of leaf CO_2 absorption to increase, leading to enhanced growth for crops where the supply of CO_2 is the principle factor limiting growth. Where it is not the principle limiting factor, the crop still benefits from an increase in the leaf stomatal conductance and a corresponding decrease in the crop transpiration rate. This can indirectly boost the growth of water-stressed crops by increasing the soil moisture (Kimball and Idso, 1983).

Most of the experiments which have examined the response of crops to increased $[CO_2]$ have been performed for potted plants in sealed growth chambers, but there has been concern that these do not properly represent field conditions (Ainsworth *et al.*, 2008; Ainsworth and Long, 2005). More recently, open-top field experiments have been used, culminating in the use of Free-Air CO_2 Enrichment (FACE) experiments which raise the $[CO_2]$ within an open field. Although FACE experiments have been performed in a number of countries, the complexity of the injection system and the high running costs have limited studies to a small number of important crops. Most FACE studies have been performed in temperate countries and have not considered increased temperature, drought stress and tropospheric ozone concentration (Ainsworth and McGrath, 2010); no FACE experiments have been performed in Africa (Oak Ridge National Laboratory, 2010).

Pre-FACE studies showed that doubling $[CO_2]$ increased the growth of C_3 crops by approximately 30 % (Bowes, 1993; Kimball *et al.*, 1993). The growth of C_4 crops, which includes pearl millet, was expected to increase marginally at most at high [CO_2] because CO_2 is already concentrated by the C_4 photosynthesis pathway at ambient [CO_2] (Ainsworth and Long, 2005). Recent reviews have concluded that outdoor crops have a weaker response to increased [CO_2] than those grown in greenhouses (Leakey *et al.*, 2009) and that models tend to overestimate the fertilisation effect (Ainsworth *et al.*, 2008). The FACE experimental results have been re-analysed by several studies, with some arguing that the crop response may be lower than previously thought (Long *et al.*, 2005, 2006) and others concluding that the new analyses are consistent with the higher responses found previously (Tubiello *et al.*, 2007). Based on these analyses, the IPCC Fourth Assessment Report concluded that crop yields at 550 ppm [CO_2] would increase by 10 %–20 % for C_3 crops but by only 0 %–10 % for C_4 crops (Easterling *et al.*, 2007).

The growth of pearl millet has not been examined in FACE experiments (Oak Ridge National Laboratory, 2010). The growth and yield of irrigated sorghum in Arizona, USA was unchanged when the [CO_2] was increased from 360 ppm to 560 ppm but the grain yield increased by 15 % in drought conditions (Ottman *et al.*, 2001). Wand *et al.* (1999) also concluded that stressed C_4 grasses would respond better to increasing [CO_2] than unstressed plants. The growth rate and yield of maize in Illinois, USA was unchanged by increasing the [CO_2] to 550 ppm (Leakey *et al.*, 2006). A potential explanation for this lack of carbon fertilisation at Illinois is the low solar radiation relative to semi-arid zones in the tropics; Ghannoum *et al.* (1997) concluded that the growth of C_4 grasses would increase by 28 % at 700 ppm [CO_2] under high-light conditions but would be unchanged in low light. Crop growth at Illinois is likely to be limited by radiation availability, while the growth of millet in Senegal is more likely to be limited by the transpiration rate because the radiation intensity is higher further south. Studies have shown that the TUE of C_4 plants will increase as the stomatal conductance decreases; for example, Conley *et al.* (2001) measured a 16 % increase in the water use efficiency (WUE) of irrigated sorghum crop in a FACE experiment. It is therefore possible that the growth of C_4 crops, including millet, will increase in regions where TUE limits growth.

Crops must transpire a minimum amount of water during photosynthesis so the maximum TUE will eventually reach an upper threshold if the [CO_2] increases enough (Bierhuizen and Slatyer, 1965). The increase in the TUE can be represented using a curvilinear function with a upper threshold at 700–1000 ppm (Kimball *et al.*, 1993). The RUE can be represented using a similar curve with an upper threshold at the [CO_2] where the stomata are saturated with CO_2 and the maximum absorption rate has been achieved. In CROMSAS, the RUE curve is represented using a broken-linear function (Section 3.4.4). Following FACE and other experiments with C_4 crops, the threshold RUE is only 2 % above the current RUE. In the absence of data from the FACE experiments about sorghum growth in [CO_2] above 550 ppm, it is assumed that the TUE will increase linearly with [CO_2] until the daily threshold TE_{max} is reached. The TUE is assumed to increase by 16 % as the [CO_2] increases from 350 ppm to 550 ppm; this was the measured change in the WUE in the FACE sorgum experiments using dry plots where evaporation would have been limited (Conley *et al.*, 2001).

This approach increases the simulated growth rate of millet because growth is generally limited by TUE rather than RUE in the model simulations of Senegal. Since the FACE maize and sorghum studies concluded that the growth rate of C_4 crops will not be directly increased by carbon fertilisation, a sensitivity study was performed in which the increasing TUE causes the transpiration rate to reduce instead of increasing crop growth (Section 7.5).

7.2.2 Assessment of the accuracy of the climate model hindcasts

Before examining the crop yield projections for the twenty-first century, the simulations using observed meteorological data from the period 1950–2000 (from Chapter 6) were compared with simulations using the GCM datasets for the same period. Figure 7.7 shows the comparison of the yield distributions for high and low rainfall locations with the soil nitrogen set to 400 kg N ha^{-1}. The discrepancies between the GCM simulations and the observed simulations were mostly below 500 kg ha^{-1} and the yield distributions were similar from each dataset. The discrepancies are lower at lower soil nitrogen levels (not shown).

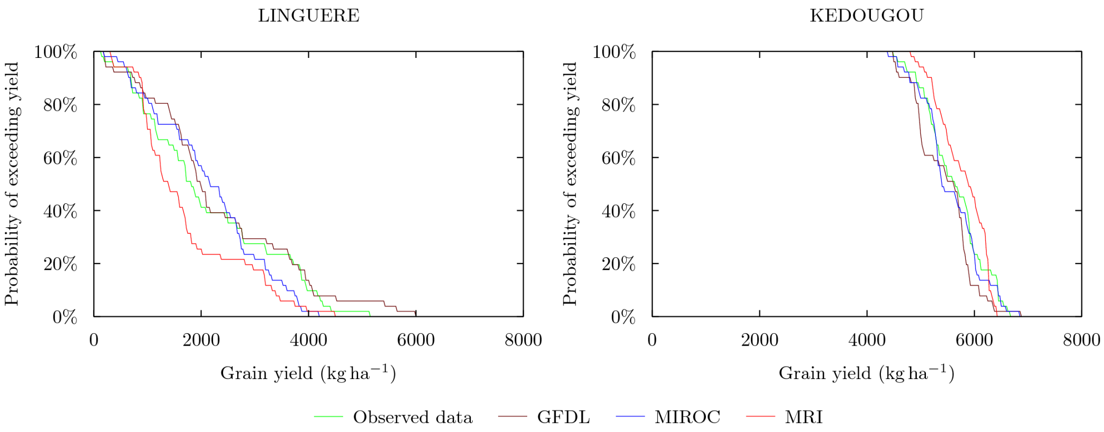

Figure 7.7: Comparison of CROMSAS simulations using observed and GCM climate data for the period 1950–2000.

7.3 Impact of climate change on smallholder farms

The analyses from Chapter 6 were repeated for each climate change scenario, using data from each GCM, with the aim of characterising how climate change might affect rainfed smallholder agriculture in the future. The analysis used meteorological data for the same six locations from three GCMs, for three SRES scenarios, so a large range of results were produced. The discussion in this section concentrates on the principal conclusions, with examples from the analyses used for illustrative purposes. The examples are taken from the SRES B1 and A2 scenarios as these were the lower and upper bounds for changes in the regional climate, with the SRES A1B scenario lying in-between.

7.3.1 Unstressed crops

The CROMSAS simulations suggest that the maximum achievable grain yield is likely to remain relatively unchanged at each location over the course of the twenty-first century. Figure 7.8 shows, for each GCM, the yield projections for unstressed crops under the SRES A2 scenario. Reductions in the yield are projected using GFDL data towards the end of the century as a result of the higher VPD (see Figure 7.6).

The GFDL and MRI simulations produce higher irrigated yields in the SRES

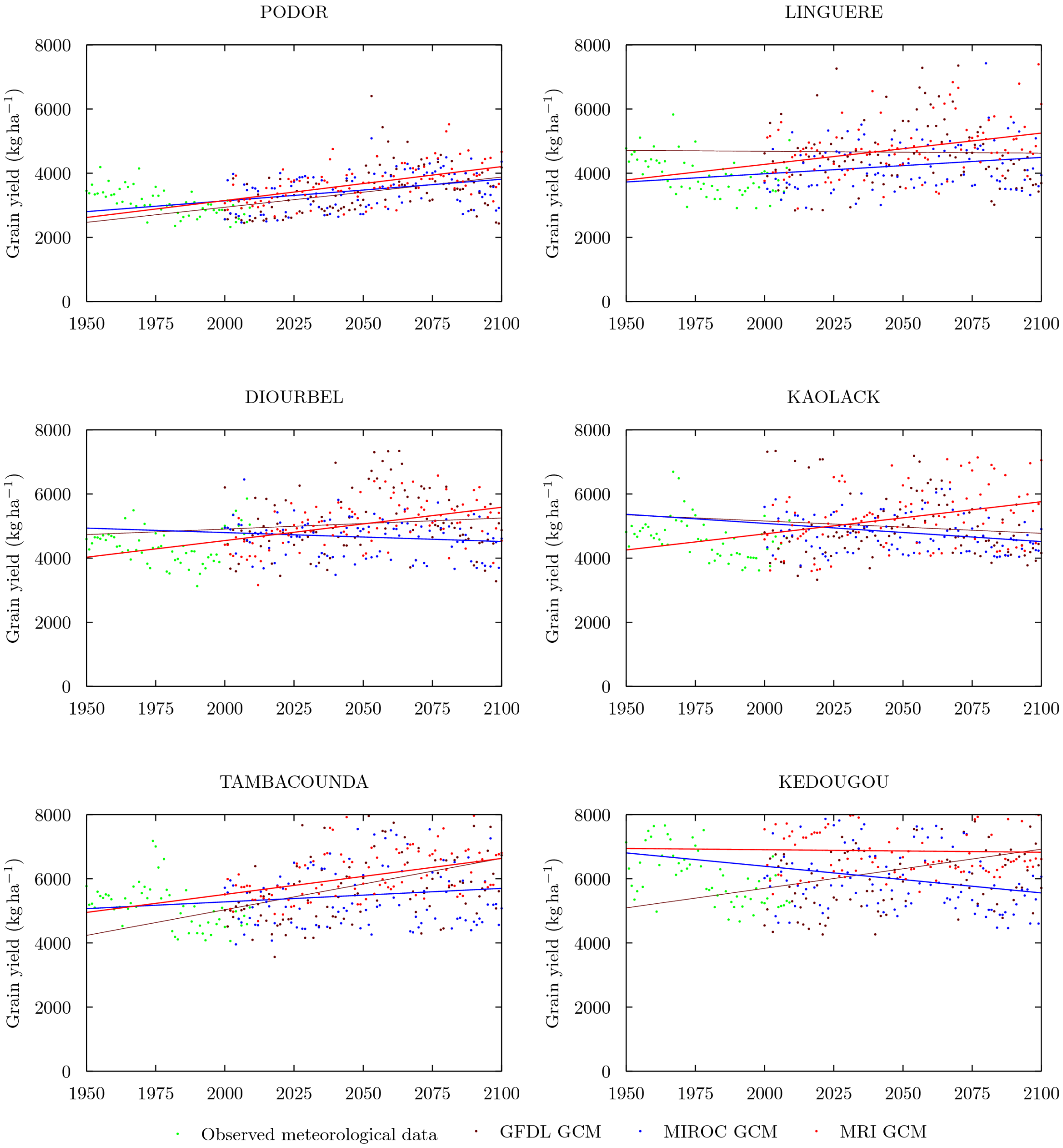

Figure 7.8: Simulated irrigated grain yields from three GCMs for the SRES A2 scenario in the period 2000–2100. The maximum yields are shown with neither evaporation nor nutrient stress affecting growth, and with the optimum planting date and planting density being used each year. The lines represent the linear regressions for each model over the period 2000–2100.

	Irrigated			Rainfed		
	GFDL	MIROC	MRI	GFDL	MIROC	MRI
SRES B1						
Podor	9	6	10	0	1	8
Linguere	0	5	9	−7	6	19
Diourbel	3	−2	10	0	3	15
Kaolack	−3	−5	10	−5	0	13
Tambacounda	16	4	11	17	5	11
Kedougou	12	−8	0	11	−8	0
SRES A2						
Podor	−17	11	13	−9	2	1
Linguere	−10	9	8	−29	8	−7
Diourbel	−8	0	5	−28	5	−1
Kaolack	−4	0	2	−18	5	−7
Tambacounda	−8	0	7	−21	0	4
Kedougou	−2	−10	−6	−4	−10	−6

Table 7.4: Annual mean change in the simulated grain yields for the SRES B1 and A2 scenarios in the period 2000–2100. Values were calculated using linear regression analysis for the three GCMs at the six study locations. There was no nutrient stress. The irrigated yields assumed no evaporation. The rainfed yields were at the optimum planting date and planting density each year. All figures have units $\mathrm{kg\,ha^{-1}\,y^{-1}}$.

B1 scenario than the A2 scenario but the MIROC data produces lower yields. Table 7.4 compares the mean annual changes, from linear regression analysis, at each location for the B1 and A2 scenarios. The variability is similar for both models. The maximum change is $17\,\mathrm{kg\,ha^{-1}\,y^{-1}}$ or $1700\,\mathrm{kg\,ha^{-1}}$ over the course of the century. Some large yield increases are projected for the SRES B1 scenario.

The largest reduction is simulated for GFDL data in the SRES A2 scenario because the VPD and the ETo are higher towards the end of the century than in the other models (Figure 7.6). Losses due to the higher VPD were balanced by an increase in the TUE from higher [CO_2] which boosted growth. An analysis showed that the growing duration tended to lengthen at Podor and Linguere because crops germinated later in the season when the temperatures had reduced from the peaks of the dry season. At the other locations, the growing duration was ≈ 85–90 days at both the start and the end of the century. The growing duration was static because the increase in the average rainy season air temperature from 29 ℃ to 34 ℃ (Figure 7.6) straddled the optimum temperature for phenological development of 31 ℃ to 33 ℃ in CROMSAS. Over the century, changes to the growing duration were masked by the larger interannual variability. Grain yields were little-affected by high temperature stress because the temperatures were too low on most days. It is possible that yields could be reduced by short periods of particularly high temperatures but this influence has not been studied in a controlled experiment for millet so is not simulated by CROMSAS.

7.3.2 Water-stressed crops

Different GCMs produce quite different rainfall projections for the Sahel region in the twenty-first century (Huntingford *et al.*, 2005). The standardised rainfall time series in Figure 7.4 compare the projections of the three GCMs used by this study.

The annual mean changes in the simulated 'perfect foresight' rainfed grain yields are shown in Table 7.4 for each scenario. It is interesting to compare these to the irrigated results, to see if the rainfed yield changes are being driven by the increasing temperature and VPD or by changes to the rainfall regime. The rainfed yield changes are similar to the irrigated yield changes for all three models in the B1 scenario. In the A2 scenario, GFDL rainfed yields at most locations are substantially lower while there is little change for the other scenarios. Overall, with the exception of the GFDL SRES A2 scenario, the changes to the crop yields over the century are primarily caused by increasing temperature and VPD.

A moving-average time series for the SRES A2 scenario is shown in Figure 7.9 for high and low nitrogen applications. Except at the driest locations, the variability between GCM datasets is very low for $50\,\mathrm{kg\,N\,ha^{-1}}$ and there is little variation over the century. The projected variability at $400\,\mathrm{kg\,N\,ha^{-1}}$ is much higher, particularly towards the end of the century when the GFDL dataset yields are particularly low at several stations. Similar trends were found for the SRES B1 scenario (Figure 7.10) except that the variability between models is generally lower for the high nitrogen application.

Changes in the distribution of good and bad seasons are important for smallholders. Figure 7.11 shows the distribution for the periods 2010–2039 and 2070–2099 in the SRES A2 scenarios. The distributions are very similar, even when there are differences in the mean yields between the two periods. These graphs indicate that the rainfall distributions across Senegal will continue to be predominantly a function of the mean rainfall (and hence the latitude) throughout the twenty-first century. The GCM data yield variability in the A2 scenario, which was highlighted above, has a similar magnitude in both good and bad years. Similar trends were found for the SRES B1 scenario (not shown).

7.3.3 Planting date and planting density

Dry planting is widely practiced in Senegal but Section 6.4.3 concluded that grain yields could be increased by delaying planting by around two weeks after the average dry-planting germination date. The same analysis was performed for the twenty-first century projections. The optimum delay was 2–4 weeks for all three models. The optimum delay depended on both latitude (Podor had the shortest delay) and the nitrogen application, with a shorter delay being optimum at high applications. At Tambacounda and Kedougou, dry planting caused mean annual losses of 0 to 700 $\mathrm{kg\,ha^{-1}}$ for high soil fertility levels, but only 100 $\mathrm{kg\,ha^{-1}}$ for fertility levels up to 100 $\mathrm{kg\,N\,ha^{-1}}$. At the other stations, dry planting was the best strategy in some years while later planning was better in others. The optimum planting date was not affected by the climate change scenario.

The optimum planting dates were compared for the periods 2000–2019 and 2080–2099 for the SRES A2 scenario, which was expected to have larger differences than other scenarios. Optimum planting dates were 2–3 weeks later at most locations for all three climate datasets. Dry planting germination was also delaying at most locations by up to 2 weeks. A feature of the projected reductions in the rainfall at the end of the twenty-first century is the delayed onset of the monsoon season.

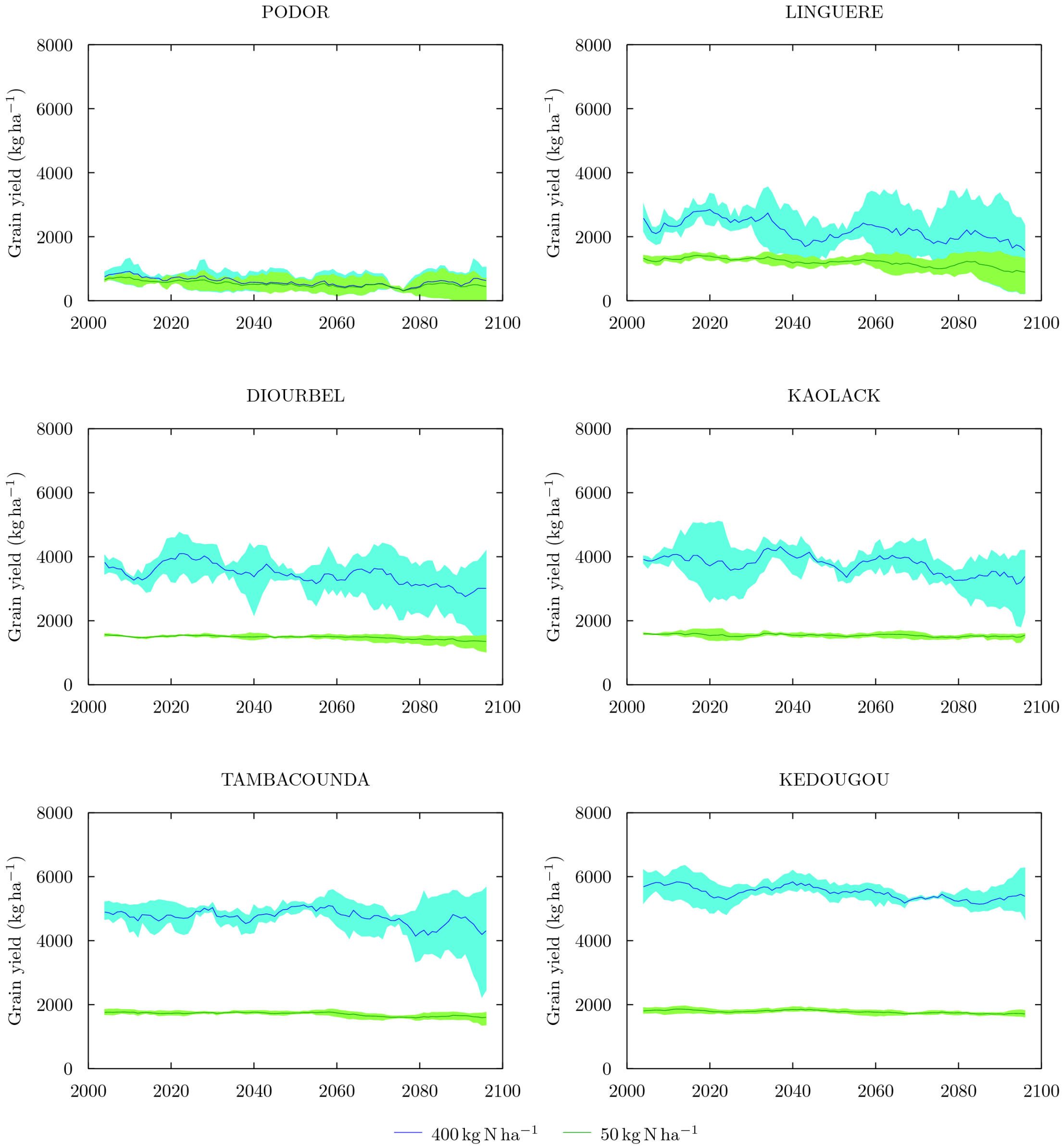

Figure 7.9: Rainfed grain yield time series from three GCMs for the SRES A2 scenario. A moving average with a 9-year period is used to smooth out short-term variability in the simulations. The solid lines show the average yield from the three GCM datasets while the shading shows the variability between datasets.

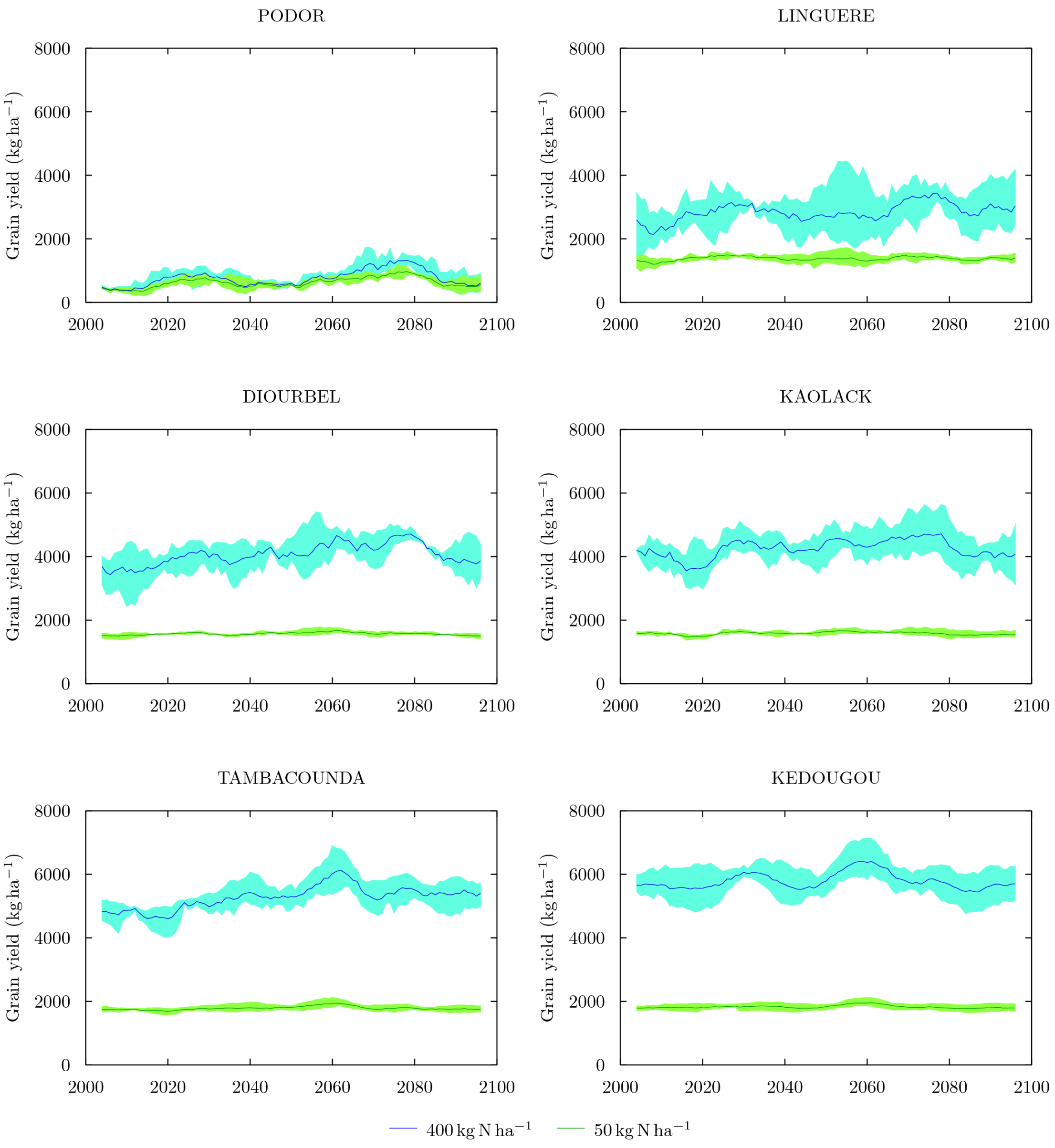

Figure 7.10: Rainfed grain yield time series from three GCMs for the SRES B1 scenario. A moving average with a 9-year period is used to smooth out short-term variability in the simulations. The solid lines show the average yield from the three GCM datasets while the shading shows the variability between datasets.

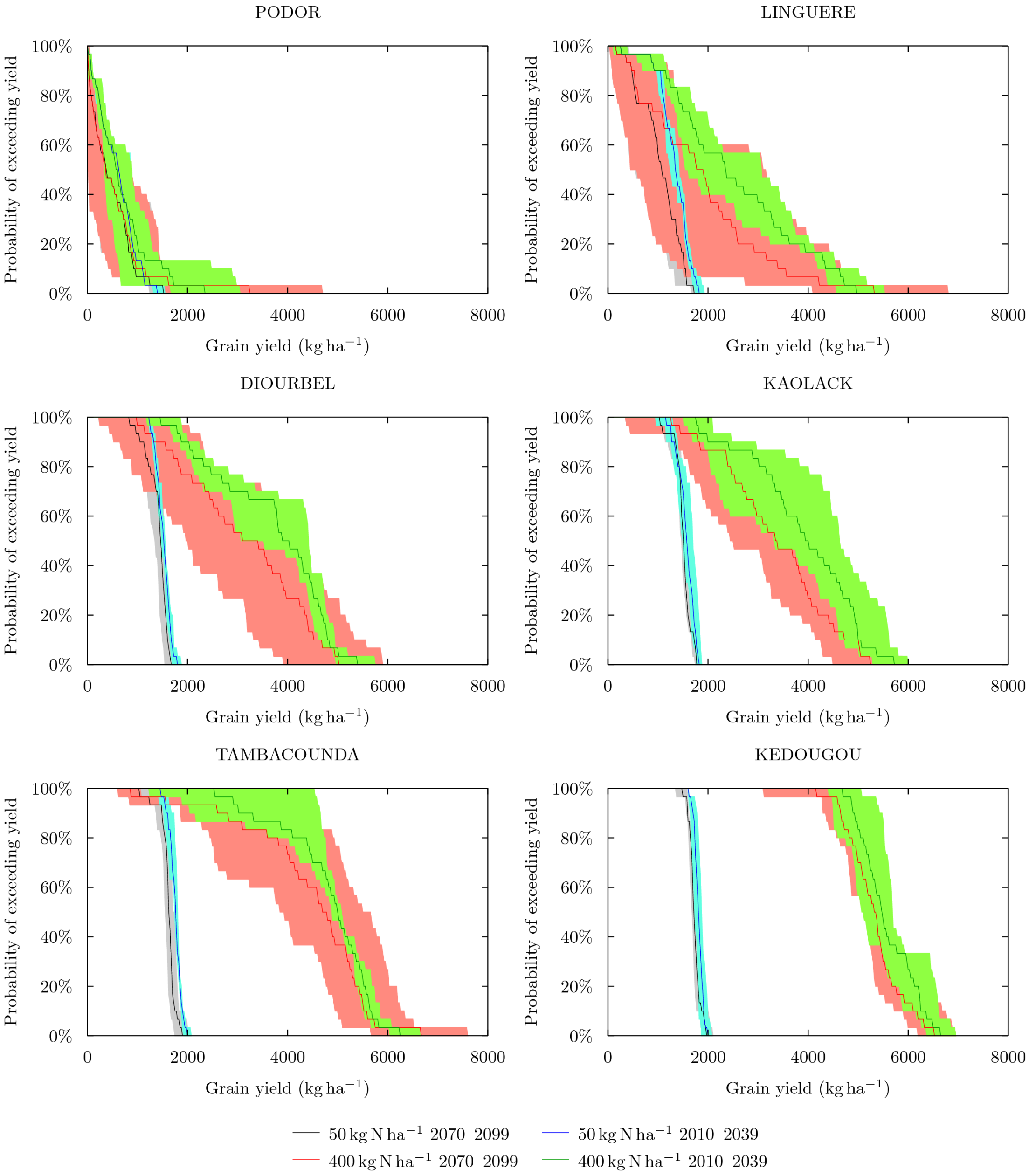

Figure 7.11: Interannual yield distributions for the SRES A2 scenario. Distributions are plotted for the periods 2010–2039 and 2070–2099. The solid lines show the average distributions from the three GCM datasets while the shading shows the variability between datasets.

The planting density analysis was repeated for the GCM data and the same conclusions were reached as for Section 6.4.4, with the optimum planting density depending on the nitrogen and soil water availability.

7.3.4 Financial impact

It is difficult to project how the profitability of farming will change over the next century because of the uncertainty in the long-term prices of grain and fertiliser. For example, the price of mineral fertiliser doubled in a few weeks in 2008. Nevertheless, if prices are assumed to stay constant, then the profitability of intensification is likely to be relatively unchanged throughout the century because yields are projected to be reasonably stagnant. The financial constraints on nitrogen application that were identified in Section 6.5 will remain unless the recovery rate can be improved.

7.4 Adaptation options

The optimum agricultural strategy for the last 60 years, identified in Section 6.6, was to fix the planting date, planting density and soil fertility (‘no adaptation’). This strategy continues to be the optimum in the twenty-first century under all of the scenarios because there are no sustained upward or downward trends during the century (Figures 7.9 and 7.10). A typical comparison of strategies is shown in Figure 7.12 for the MIROC SRES A2 dataset. No adaptation is a conservative strategy where less fertiliser is applied than in other strategies and crops are dry-planted. Profits are poorer in better years but large losses, which are a consequence of adapting to previous years at all locations, are avoided. Occasionally, adapting to the previous 10 years is more profitable than the fixed strategy.

If smallholders are assumed to be extremely risk-averse and unwilling to accept losses in some years then yields and profits are substantially reduced, by 80 % in some cases. It was occasionally possible to cultivate two fields using different planting dates or planting densities to raise profits while still avoiding losses but the benefit was small compared to the loss due to risk-avoidance. In fact, using

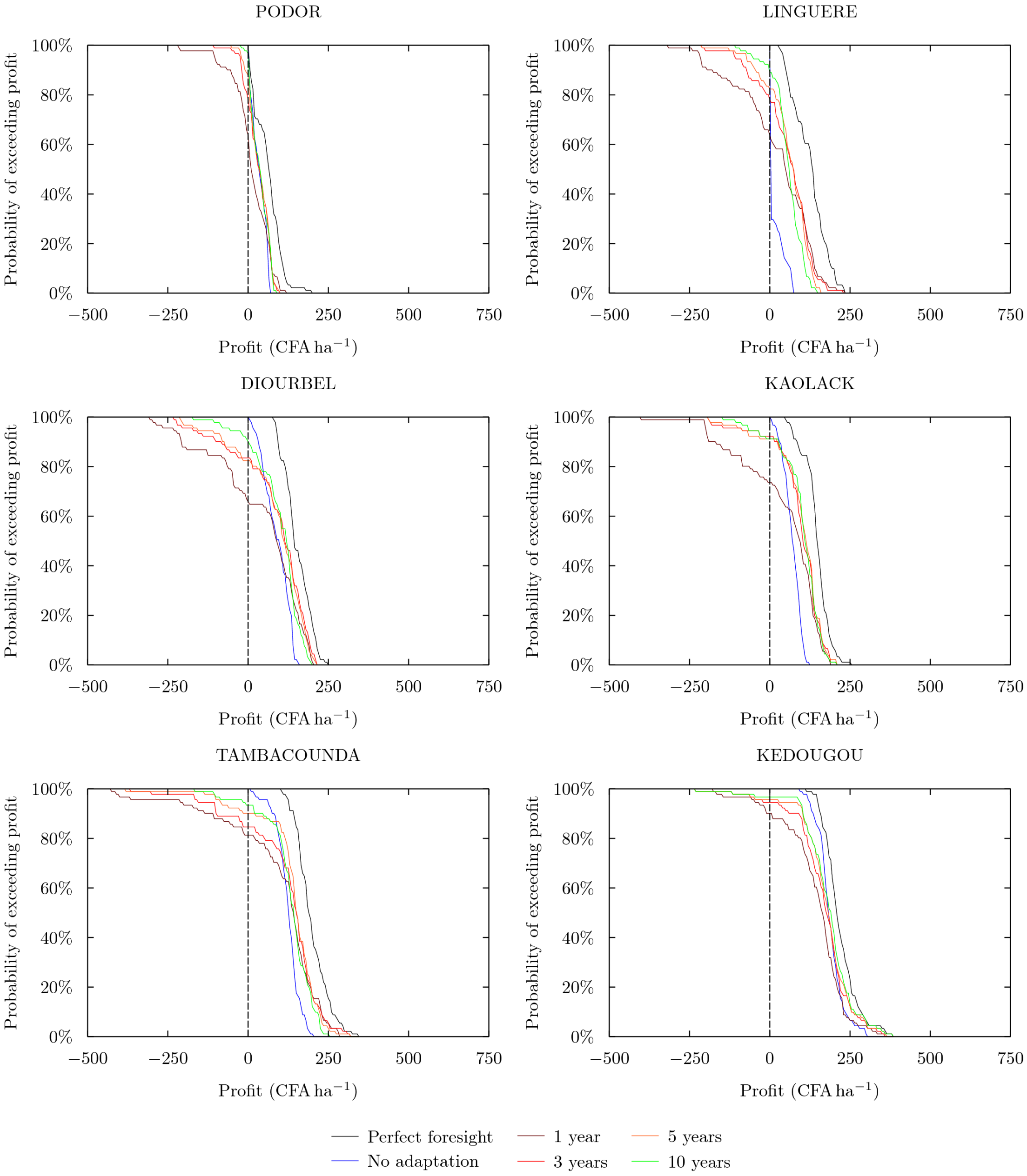

Figure 7.12: Long-term profits for a range of crop management adaptation options at the six locations. Simulations were performed for the period 2000–2100 using MIROC projections for the SRES A2 scenario. A nitrogen recovery rate of 50 % was assumed. The profit was calculated as the difference between the market price of fertiliser (150 CFA kg^{-1}) and the market price of millet (175 CFA). The costs of buying, transporting and applying fertiliser, and the additional costs of transporting millet to market, were not included in the calculation.

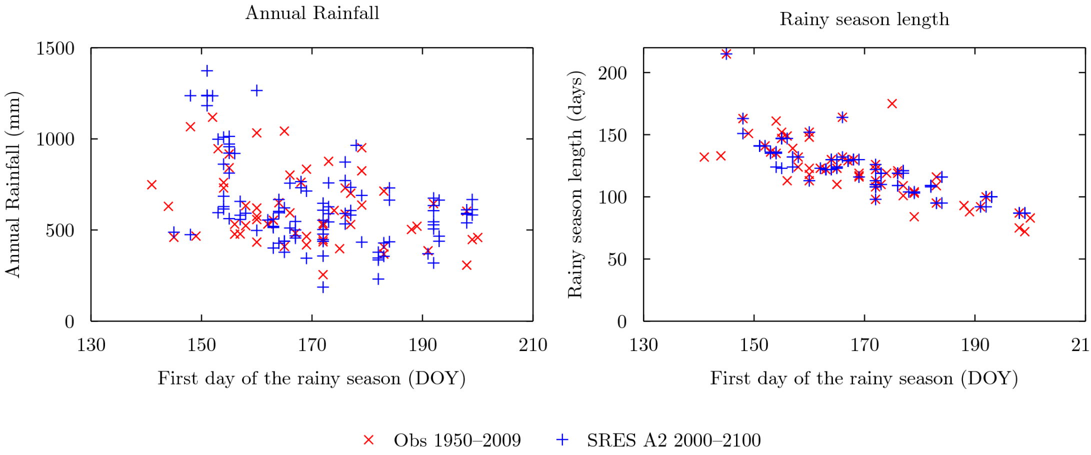

Figure 7.13: Total rainfall and the length of the rainy season at Kaolack as a function of the first day of rains, defined as the first day with rainfall exceeding 5 mm. The SRES A2 data were taken from the GFDL dataset.

a range of crops, planted at different times, is already a feature of agriculture in parts of the Sahel (Mortimore and Adams, 1999). Perhaps a more effective policy would be to offer insurance schemes to farmers in locations with higher rainfall to allow them to manage the large losses that occur in a small number of years.

The use of seasonal forecasts to guide adaptation strategies was discussed in Section 2.2.5. The start of the rainy season is very variable (Section 1.4) so it is interesting to see if the date of the first rains is a good indicator of seasonal conditions. This is important from a crop management adaptation perspective because the nitrogen application can be tailored to the rainfall expectations (Section 6.4.3). Figure 7.13 shows the total rainfall and the length of the rainy season at Kaolack as a function of the date of the first rains. The length of the rainy season is closely related to the first day of rains because the end of the season occurs around the same time every year. The total rainfall is much more variable, although the rainfall always exceeds 400 mm when the first rains occur before day 170 (16 June). The distribution of observed and projected future rainfall totals is similar. It might be possible for risk-averse smallholders to safely apply more fertiliser when the rainy season has an early start, but the onset date is not a reliable indicator of the total rainfall according to this evidence.

The other principle crop management decision in addition to the choice of planting strategy and fertiliser application is the choice of crop (Kurukulasuriya and Mendelsohn, 2007) and crop variety (Challinor, 2009; Dingkuhn *et al.*, 2006). Millet is the hardiest cereal crop so is the most suitable for the dryland regions of Senegal. The principle difference between varieties is the rate of phenological development (Section 3.1) and it was suggested in Section 4.2.4.1 that choosing different crop varieties could be a particularly useful strategy to reduce the impacts of rising temperature on the rate of development. However, the temperatures in Senegal over the twenty-first century are projected to straddle the optimum temperature for millet development so using alternative varieties will have little impact. It will be more important for smallholders to choose varieties appropriate to the length of the rainy season each year. If high temperatures are found to affect millet reproduction then using temperature-tolerant varieties might become an important adaptation strategy over the century (Dingkuhn *et al.*, 2006).

7.5 Sensitivity study: reduced growth

Two FACE experiments concluded that sorghum yields would not increase due to the direct influence of carbon fertilisation (Section 7.2.1). Grain yield projections in this chapter have assumed that crop growth benefits directly from increased [CO_2] through an increase in the TUE. A sensitivity study was performed to examine how crop yields would be affected if the increase in the TUE were to reduce water use instead of enhancing growth, as was observed in the FACE experiments.

Figure 7.14 shows that there is no difference in yields between the two methods except in optimum growing conditions. At Linguere, the direct and indirect influences of carbon fertilisation have a similar impact because the mean rainfall is so low. At Kedougou, only the high nitrogen application crops are affected, with a substantial reduction in the grain yield of $1500\,\mathrm{kg\,ha^{-1}}$ being projected at the end of the century because the absence of water stress means that there is no indirect fertilisation effect. This uncertainty has the potential to undermine high-input agricultural schemes in the future but is unlikely to affect smallholders who live in drier areas or use small amounts of fertiliser.

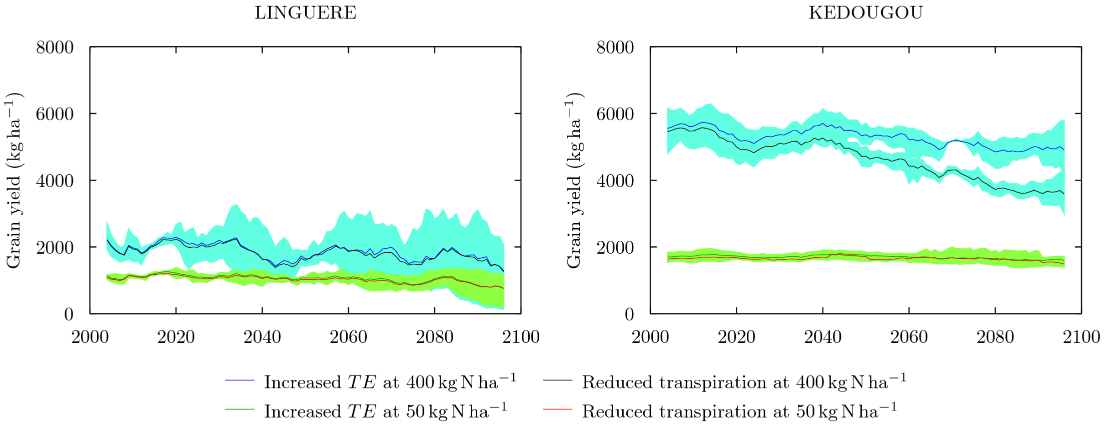

Figure 7.14: Influence of CO_2 fertilisation on grain yields for the SRES A2 scenario. A moving average with a 9-year period is used to smooth out short-term variability in the simulations. The solid lines show the average yields from the three GCM datasets while the shading shows the variability between datasets.

7.6 Discussion

The GCM climate data has similar inaccuracies to the NCEP/NCAR reanalysis data in Chapter 5. Three GCMs were chosen for this study, but a comparison of climate projections for the last 60 years showed that the simulated rainfall in particular was poorly represented, with none of the models simulating the long drought. Alternative datasets were produced for each GCM using 60 years of synoptic weather station data, with the assumption that GCMs simulate long-term changes in the climate better than the actual climate at any one time. This approach also ensured that the climate data variability would be similar to reality. In CROMSAS, the alternative GCM datasets produced grain yield trends similar to those from the synoptic weather station data.

A range of crop yield increases and decreases were projected using data from the three GCMs, with few discernible differences between the SRES A2 and B1 scenarios being apparent over the next century. It has been suggested that rising temperatures will have a greater impact than rainfall variability on agriculture (Adejuwon, 2006; Lobell and Burke, 2008) and the yield variations in this study were indeed primarily affected by changes to the temperature and the VPD. The suggestion of Washington *et al.* (2004) that the best strategy to manage climate change might be to focus on coping with climate variability is not supported by this analysis. The greatest changes were projected for fields with high nitrogen application, and the greatest variations between the GCM datasets were also found in these fields. For the SRES A2 scenario, the variations between models increased towards the end of the century which indicates increased uncertainty at that time. It is possible that the rainfall will reduce substantially and that the optimum planting date will be later in the season.

The projections of this study are inconsistent with the two previous studies reviewed in Section 2.3. Liu *et al.* (2008) forecast a millet yield increase of 25 % by 2030 in Senegal but this study projects little change in yield for either SRES scenario at that time. Adejuwon (2006) forecast increases in the first half of the century followed by decreases in the second half caused by high temperature stress. The magnitude of the changes in that study are much larger than the magnitude of the changes projected here. There is a need for a crop model intercomparison study using consistent datasets to identify the cause of the discrepancies between studies (Easterling *et al.*, 2007).

The no adaptation strategy continues to be the optimum approach for the twenty-first century as it was in the last 60 years (Section 6.6). This strategy is conservative and leads to smaller yields and profits in good years but avoids large losses in bad years. Those smallholders who are risk-averse will achieve very low yields and profits but this situation could be avoided by providing appropriate insurance for the worst years.

Rising temperatures are expected to have little impact on the crop duration throughout the century. There is limited knowledge about the susceptibility of millet to high temperatures but it is possible that using varieties that can tolerate high temperatures during the critical reproductive phases will be beneficial in the future (Dingkuhn *et al.*, 2006).

Porter and Semenov (2005) describe how temperature and rainfall distributions could change in the future, but analyses of the GCM projections suggest that the temperature and rainfall distributions will be similar to the past 60 years. Moreover, the adaptation sensitivity study in Section 6.6.2 showed that the yields and profitability of farming are determined primarily by the mean rainfall with rainfall and temperature distributions having a relatively small influence. A more important influence could be the absence of direct carbon fertilisation from rising [CO_2], which would lead to yields in high-input fields decreasing over the century (Section 7.5). There are other uncertainties about the response of millet growth and development to high temperatures and rising [CO_2] that will need to be addressed in CROMSAS in the future once suitable experimental data are available.

7.7 Summary

Anthropogenic climate change has been identified as a threat to smallholder farming in the Sahel, with some studies even forecasting the demise of rainfed Sahelian agriculture (e.g. Cline, 2007). The few crop model studies of climate change in West Africa have projected the difference between the yields at the present time and the yields at a point in the future (Section 2.3). This study has examined the long-term impact of climate change throughout the century at several locations in Senegal, using climate data from three GCMs. The opportunities for smallholders to adapt their crop management strategies to reduce the impact of climate change have also been assessed.

Crop yields are projected to be relatively constant throughout the century at all of the locations. The largest variations occur at high nitrogen levels and are the result of changes in the temperature and the VPD. The seasonal yield variability is not expected to change throughout the century. The projections of this study are inconsistent with those of previous studies of millet in Africa and a crop model intercomparison study is required to identify the causes of the discrepancies.

Chapter 8

Overall summary and future work

This chapter summarises the overall conclusions of the thesis in Section 8.1 and suggests some opportunities for further work in Section 8.2. The thesis concludes with a summary of the key findings in Section 8.3.

8.1 Overall Summary

The population of the Sahel region of West Africa has increased rapidly in recent decades but food production has lagged behind and the region has become heavily reliant on food imports (WFP, 2006). Rainfall variability and poor crop management practices have been identified as constraints on agricultural intensification in the region. This study developed a new crop model and used it to characterise the long-term impact of rainfall variability and crop management strategies on millet yields in Senegal. The potential impacts of climate change on millet cultivation, and the benefits of adapting crop management to reduce the impacts, were also assessed. This section summarises the findings of the study.

8.1.1 Agriculture in Senegal

Senegal was chosen for this study because it contains the full range of climatic zones, from sub-humid to arid, that are found in the Sahel. The total population of Senegal has quadrupled in recent decades but the cereal production per capita has reduced and the country now imports more than 50 % of its food requirements (FAO, 2009b). Millet is the most important subsistence cereal in Senegal, comprising more than 50 % of the total cereal production over the last 50 years. Millet yields have increased over the period, despite persistent droughts since 1970, but only average 650 kg ha^{-1} at present, which is much lower than the potential yield of 4000 kg ha^{-1} under optimal resources (Baron *et al.*, 2005). This study examined millet cultivation in Senegal.

Using nationwide statistics, Section 1.3 showed that the distribution of agriculture across Senegal is far from uniform. The rainfall gradient and the varying soil quality across the country have restricted agricultural development in most areas. The proximity of Dakar, coupled with average rainfall and soils, have led to sustained agricultural development in the groundnut basin, while other areas of the country are sparsely-populated with much empty land.

There are substantial spatial and temporal rainfall variations (Le Barbé *et al.*, 2002), particularly in the drier regions, which farmers must manage (Brooks, 2004). Using national production statistics, Section 1.4.4 showed that millet yields are lower and more variable in the drier north of the country. However, an analysis of the ESPACE project database (Affholder, 1992) showed that grain yields were far from uniform even within villages, with some much lower and others much higher than the regional averages. The differences within villages cannot be caused by rainfall variability and are most likely the result of different crop management strategies being used in different fields.

The ESPACE project, like all field surveys, was necessarily short-term and spatially-restricted, covering only a few years and a few locations. It is very unlikely that the weather during such an project will fully represent the long-term climate so it cannot be reliably used to identify the most appropriate crop management strategies for a particular location. Crop models, on the other hand, can simulate crop growth at large number of locations over many years so can be used to characterise the agro-meteorological characteristics of a region if the model simulations are accurate enough (Section 2.2). This study used a crop model to examine millet cultivation in Senegal over the long term.

8.1.2 Development and evaluation of the CROMSAS crop model

The strengths and weaknesses of current crop models were identified in a literature review (Section 2.1). It was concluded that the plant development and soil water balance are simulated with a similar level of complexity by all of the models but that the treatment of plant growth, grain yields and particularly leaf expansion differ substantially.

For this project, it was necessary for the chosen model to simulate varying planting dates and planting densities, varying amounts of nitrogen application, intercropping, and the impacts of climate change. The ideal model would also have few unnecessary parameterisations and would have a flexible design permitting alterations and ultimately coupling with other broader farming system models. APSIM was the only model that could simulate all of the required crop management options, but there was concern about the parameterisation of the leaf expansion and the root partitioning. The overall model design was far more complicated than was required for this study and, as a result of this complexity, it would have been difficult to alter the mechanisms of the model. It was decided that a new crop model should be developed.

8.1.2.1 The CROMSAS model

The CROMSAS model was designed to examine the impact of changing the planting date, the planting density and the nitrogen application on smallholder fields in Senegal. Together with the choice of crop and crop variety, these are the most important smallholder crop management decisions in the Sahel (Section 1.5). CROMSAS was designed with a similar structure to the existing crop models described in Section 2.1.1. Chapter 3 described the model. In common with the RESCAP model (Monteith *et al.*, 1989), resource flows are conserved and organs grow as a function of their mass so that the plant geometry is always realistic. A number of original features were introduced:

- a new leaf expansion sub-model simulates the growth of the leaves and the interaction between the leaf mass and the leaf area in a more realistic way than has been achieved in any of the existing models;

- a fixed-length juvenile stage has been introduced that is more consistent with experimental findings than the thermal time relationship used in other models;
- a comprehensive simulation of tillers has been designed which is more elegant than the approaches used elsewhere;
- the partitioning of assimilate to the roots and leaves is sensitive to water and nutrient stress;
- intercropping is simulated with any combination of crops and weeds;
- the soil evaporation, runoff and drainage have been redesigned; and,
- some of the potentially-important impacts of climate change (the impact of rising CO_2 on growth and the influence of temperature on leaf expansion and reproductive growth) are simulated.

Different varieties of millet can be simulated by changing model parameters. CROMSAS has been written in a structured, accessible way to facilitate the use of the model by other researchers. It would be relatively easy for other researchers to add new mechanisms, for example to simulate the impact of climate change on crop development. CROMSAS could also be integrated into larger farm system models in the future.

8.1.2.2 Calibration and evaluation of CROMSAS

Parameters for the model were taken from the literature, from other crop models or were calibrated using data from three smallholder fields in Senegal (Section 4.1). The leaf area and soil water distribution were accurately simulated throughout growth. A broad evaluation of the model was performed (Section 4.2). Grain yields from fields in the ESPACE database were accurately simulated. The skill of the model to simulate variations in the planting date, planting density and nitrogen management was examined. Variations in the planting density and nitrogen management were skilfully simulated but the simulations of the crop duration of local millet varieties as a function of the planting date were poor. The local varieties were found to have different development times and were probably more photoperiod-sensitive than the improved Souna variety that was simulated using CROMSAS, and it was concluded that the crop duration of the local varieties could be simulated accurately by re-calibrating the appropriate model parameters. Sensitivity studies were used to characterise the response of the model to rainfall and temperature variations. It was concluded that the simulations of CROMSAS were sufficiently accurate for the model to be used for agro-meteorological and crop management studies in Senegal.

8.1.3 Weather dataset production

The sensitivity studies in Chapter 4 showed that it was necessary to use accurate rainfall data and self-consistent meteorological data to produce accurate crop yield forecasts. A meteorological dataset was produced with daily data for 12 locations in Senegal for the years 1950–2009 (Section 5.1). The dataset was an amalgamation of an AGRHYMET database for 1950–1980 (Morel, 1992), rainfall data from CIRAD for 1950–1991 and the MIDAS database for 1985–2009 (UK Met Office, 2009). Gaps in the database were filled using hindcasts from the NCEP/NCAR reanalysis model. Although reanalysis models produce more accurate data than other GCMs (Section 2.5), the presence of systematic errors in the predictions means that it is necessary to compare observed and predicted data to identify appropriate coefficients to apply to the model data to avoid introducing biases into the observed dataset. The comparisons of observed and predicted data in Section 5.1.5 will be valuable for other researchers who wish to use reanalysis data with crop models in the future. The quality of the dataset was verified using a series of consistency checks.

Weather data were also required for the climate change simulations. From an ensemble of 18 GCMs, Cook and Vizy (2006) identified only four with moderately realistic rainfall variations in the Sahel region (Section 2.5.2). Three of these were chosen to produce climate change projections for this study (Section 7.1). A comparison of climate projections for the last 60 years against observed data showed that the simulated rainfall in particular was poorly represented by all three models, so the climate change datasets were produced for each GCM using observed weather data from 1950–2009 with perturbations to simulate long-term changes in the rainfall, temperature and humidity. This novel methodology, which was based on the assumption that GCMs simulate long-term changes in the climate more accurately than the actual climate at any one time, ensured that the climate data variability would be consistent with observations. Analysis of daily GCM projections for the end of the twenty-first century showed that the temperature and rainfall variability in Senegal in the future is likely to be similar to the current climatic variability.

8.1.3.1 Estimation of the reference evapotranspiration

The reference evapotranspiration rate (ETo) is an important determinant of the water use and growth rate of crops but no studies have identified the most appropriate method for calculating the ETo in the Sahel. An appraisal of several methods, which used a long time series of evaporation pan measurements and several time series of solar radiation measurements, concluded that the FAO56 Penman-Monteith equation was the most suitable for estimating the ETo in Senegal.

8.1.4 Influence of rainfall and crop management strategies on millet yields

Yield gap analyses are used to evaluate the difference between the attainable yield in a location and the actual yield (Section 2.2.1). A yield gap analysis was performed for the ESPACE fields using CROMSAS (Section 6.1). Achieved yields were estimated to be 51 % of the potential yields. Sub-optimal nitrogen application had the greatest impact on yields, followed by planting too early in the growing season. Using sub-optimal planting densities had a reasonably small impact.

The ESPACE observations only covered a 4-year period. CROMSAS was used to examine the long-term impact of variations in the rainfall on millet yields at six locations in Senegal (Section 6.3). The locations were chosen to represent all of the climatic zones of the Sahel. At the most northerly location, low rainfall prevented crop growth in many years. Agriculture was feasible in the groundnut basin but the simulated interannual grain yield variability was very high as a result of rainfall fluctuations. In more humid areas, where rainfall was more dependable, simulated yields were higher and fluctuations were smaller. Rainfall was not the only important climatic variable; the simulated grain yield at the most humid location in unstressed growing conditions was twice the unstressed yield at the driest location where the VPD was much higher.

8.1.4.1 Planting date

Field experiments with variable planting dates are particularly expensive to perform (Soler *et al.*, 2008) so several modelling studies have been used to identify how planting dates affect crop yields. They concluded that variations in the planting date primarily affect crops through the impact of extreme temperatures and water stress, and through changes to the crop development rate (Section 2.2.2).

Dry planting is widely practised in Senegal but a modelling study for Niger by Sultan *et al.* (2005) concluded that delaying planting until the monsoon onset would be more appropriate. Both the yield gap analysis and the long-term study using CROMSAS (Section 6.4.3) showed that higher average grain yields would be achieved at lower risk of crop failure if the planting date were delayed.

There was an assumption in the CROMSAS simulations that the crop would have exclusive access to all of the soil nitrogen irrespective of the planting date. In reality, numerous weeds germinate at the first rains which irreversibly use available nutrients if they are not controlled, so the optimum planting date is likely to be earlier than is simulated in CROMSAS. For smallholders, the increase in the grain yield resulting from a planting delay is also offset by the additional labour requirement for clearing the field of weeds prior to planting and, for those using photoperiod-sensitive crops, by a potential loss of animal feed from the extra biomass that would have been produced. Pests and disease might also have a greater impact if the planting date is delayed, as has been found in India (Hoogenboom *et al.*, 2001). It was concluded that yields could theoretically be increased by delaying planting, but that a holistic appraisal of the impact of this strategy on household livelihoods would be necessary before it could become the recommended management strategy.

8.1.4.2 Planting density

The planting density is varied by farmers according to the soil fertility and the expected rainfall (Mortimore and Adams, 1999). The use of unnecessarily low planting densities has been identified as a cause of low grain yields in the Sahel (Payne, 1997, 2000; Shapiro and Sanders, 1998). Comparatively few modelling studies have examined the influence of planting density on crop yields and none were found for West Africa (Section 2.2.3). An analysis of planting densities in the ESPACE database (Section 1.5.3) concluded that the planting density tended to be higher in locations with higher average rainfall or where fields were fertilised but that there were large variations.

It was concluded from the model simulations in Section 6.4.4 that a broad range of planting densities were optimal at each soil fertility level, and that the planting densities used by Senegalese smallholders were broadly optimised for millet and properly reflected variations in the soil fertility.

8.1.4.3 Nitrogen application

The majority of the crop modelling studies of dryland regions have examined how nitrogen application influences crop growth and interacts with rainfall (Section 2.2.4). Three broad conclusions have been identified: *a*) if nitrogen is limiting, the grain yield will rise proportionally with nitrogen application; *b*) if there is water stress then high nitrogen applications will have less influence on plant growth and could even reduce the grain yield; and, *c*) for smallholders in less developed countries, the most important limitation on nitrogen application in several studies is the cost of the fertiliser and the risk of large financial losses if there is poor rainfall.

In the CROMSAS simulations, the soil fertility was found to be the main yield-determining factor when there was sufficient rainfall, with very low yields being simulated in unfertilised fields (Section 6.4.2). Applying too much nitrogen occasionally reduced yields because the soil water was depleted too quickly but the loss of grain was generally small. The fractional grain yield losses and the yield variability increased as the soil fertility was increased, particularly in locations with lower average rainfall, which made nitrogen application more inefficient. This is important because fertiliser application is difficult and expensive.

Fields in the ESPACE study were categorised according to the distance between the field and the family compound. This distance is important from a financial perspective because of the time required to travel to the field and, more importantly, the time required to transport manure to the field, because several tonnes of manure is required to fertilise each hectare of land (Affholder, 1995). Section 1.5.2 showed that fields closer to the compound were more likely to receive manure than distant fields, where less bulky mineral fertiliser was more likely to be applied. The financial cost of fertilisation is an important constraint on agricultural intensification and was investigated by this study.

A simple economic analysis identified the mean long-term rainfall, the nitrogen recovery rate and the grain and fertiliser market prices as the four principal factors that determine the profitability of soil fertilisation (Section 6.5). In Senegal, the rainfall variability is very high, the recovery rate is often very low (Breman *et al.*, 2001; Fofana *et al.*, 2008), grain prices are depressed by the availability of imported rice and fertiliser is expensive in comparison with other continents (Gray, 2002). For low recovery rates, the most profitable strategy is to apply microdoses of fertiliser at high-rainfall locations, a strategy also identified by Cooper *et al.* (2008) for Zimbabwe. Intensification becomes financially viable at higher recovery rates or if the cost of fertiliser is reduced.

8.1.4.4 Adaptation to conditions in previous years

An investigation was performed to examine the opportunities for smallholders to improve grain yields by adapting their crop management decisions in light of the growth conditions in previous years. Adaptation has been identified as a key strategy to mitigate the impact of climate change in the future (Easterling *et al.*, 2007). It was concluded that the best strategy to maximise both grain yields and profits was in fact to use a fixed strategy for the whole period and to not adapt to the conditions in recent years. The long-term optimum nitrogen application for maximising profits in the fixed strategy depended on the recovery rate and the mean rainfall. The analysis was repeated using meteorological datasets with large variations in the rainfall and temperature distributions but the fixed strategy still produced the highest yields and profits. The optimal strategy is not sensitive to changes in these distributions and should be determined from the mean long-term rainfall at each location.

Another investigation was performed to examine the impact of risk-averse behaviour on crop management strategies. Yields and profits were substantially reduced because the optimal strategy to avoid financial losses while maximising profits was to dry-plant with little nitrogen application. However, cultivating two fields with different crop management strategies allowed farmers to greatly increased yields and profits while still avoiding financial losses because in poor years, profits in one field could make up for losses in the other. The principle difference between the strategies in the two fields was the use of different planting dates.

8.1.4.5 Pests and disease

Pests and disease were observed in many fields by the ESPACE project (Section 1.5.4) but the CROMSAS simulations in this study took no account of the ensuing damage. There is little information about the impact of pests and disease on grain yields and more field studies are required to facilitate a long-term modelling assessment.

8.1.5 Interpreting the conclusions in terms of smallholder livelihoods

Making the assumption that smallholders are risk-averse, the optimum simulated long-term strategy for them to minimise losses and maximise profits in the highest-rainfall region of the groundnut basin was to use little fertiliser. This strategy produced low overall yields but was the most successful at avoiding large losses in years when yields were severely affected by drought. Increasing the nitrogen application offers high yields but introduces great uncertainty to the household income streams, particularly if mineral fertiliser is involved. Smallholders will only be incentivised to greatly increase production if large losses in some years are acceptable or if there are no other opportunities for earning income.

But urban and rural areas are not independent, and the metropolis of Dakar and the many other towns in the groundnut basin offer numerous opportunities for smallholders to reduce their dependence on agriculture by pursuing business opportunities away from the farm. Diversification is an important measure to reduce the risk to the household, as has been observed by Mortimore and Adams (1999) in the highly-populated region around Kano, Nigeria, where smallholders sustain their livelihoods through a combination of agriculture, livestock and non-farm business opportunities.

One of the aims of this study was to understand how smallholders manage rainfall variability in the long-term. Rainfall is an important constraint in many parts of the Sahel which substantially reduces the grain yields in some years while having little impact in others. Imported food is sold at the many local markets across Senegal so smallholders have the option of growing food or earning income through other activities to buy food. Food insecurity in Senegal is caused by an inability to afford food, not an inability to grow food in years of poor rainfall. In these circumstances, farming is primarily an economic activity and the real effect of rainfall on smallholder livelihoods is to reduce the long-term effectiveness of fertiliser and hence to increase the cost of fertilising the fields to an uneconomical level. However, rainfall has a much lower impact on grain yields (and hence income) at low fertility levels, so the return on investment is much higher and the use of a limited amount of fertiliser is economically viable. The optimum strategy for smallholders to reduce the impact of rainfall variability is to farm at a low level of soil fertility, as efficiently as possible, and to earn income from other activities at other times of the year. Using copious amounts of mineral fertiliser could financially ruin a household in a year of poor rainfall, although this might change if the fertiliser recovery rate could be increased. Manuring, although limited by rainfall and labour costs, is a less risky strategy where possible.

Smallholders are characterised by their diversity (Mortimore and Adams, 1999; Scoones, 2001). Several cash and subsistence crops are often grown. Most rural smallholders own land and livestock but the amount of each varies widely, even within villages (Amerena, 1982; Gray, 2002). The wealth of households within a village also varies substantially. The majority of smallholders earn income from a range of non-farm activities and these can be more important than the farm, particularly for richer households. It is therefore not possible to assess the impact of rainfall variability on all smallholders in a simple way, because the vulnerability of households varies so widely. A useful extension to this study would be to assess the broader impact of rainfall variability on the vulnerability of a range of households. The characteristics of several representative households could be identified by field studies and the relative vulnerability of each to drought, and other stresses, could then be assessed. The findings could be used by aid agencies and governments to identify vulnerable households at an early stage and to optimise the provision of aid to those most in need.

Although this study concentrated on Senegal, the range of climatic regimes is typical of the Sahel as a whole. A range of constraints and opportunities exist across the Sahel, with variations in the climate, soil quality, crop varieties, infrastructure, access to urban areas, government policies and cultural norms all affecting smallholder agricultural systems. This combination of complexity and diversity makes the collection of representative socio-economic data to drive integrated models an extremely challenging task. In some places, smallholders will take advantage of local niches, for example where water can be accessed for irrigation. In many places, poor rainfall or poor soils will prevent agricultural development. In view of the inherent diversity, the conclusions reached in this study must be applied to other parts of the Sahel with care. Nevertheless, the principal constraints that have been identified here are likely to be equally important elsewhere in the Sahel, in places where similar crops are grown, in comparable soils, under a seasonal monsoon climate.

None of the conclusions of this study indicate that smallholder farming systems in Senegal are not optimised within the environmental and socio-economic constraints of the region. The aim of smallholders is not to increase crop production to feed the growing national population, but to pursue sustainable livelihood strategies. Food production is only likely to increase substantially when these two aims are indistinguishable.

8.1.6 The impact of climate change on millet cultivation

Anthropogenic climate change has been identified as a threat to smallholder farming in the Sahel, with some studies even forecasting the demise of rainfed Sahelian agriculture (e.g. Boko *et al.*, 2007; Cline, 2007). Crop models are increasingly being used to assess the potential impacts of climate change on crops (Section 2.3). However, few studies have examined the impacts of climate change on dryland agriculture using crop models. Most of these have examined large-scale global trends and have not considered pearl millet. Two studies recently examined the impact of climate change on millet cultivation in West Africa (Adejuwon, 2006; Liu *et al.*, 2008) but both probably overestimated the crop yields as a result of using averaged climate data. Neither examined how the interannual grain yield variability is likely to change and neither examined how the changes might have been mitigated through adaptation. It was concluded that a more comprehensive study was required to properly quantify the long-term impact of climate change on millet in West Africa using more realistic climate data.

There are a number of uncertainties about the response of crops to high temperatures and to an increased atmospheric CO_2 concentration (Section 2.1.2). There is further uncertainty about the ability of current crop models to simulate the effects of climate change because the models would be operating outside of the environment used for their evaluation and because a number of the potential influences of climate change are not simulated in current crop models. There are further concerns about the quality of climate projections from climate models since few models simulate an accurate rainfall distribution for West Africa (Section 7.1). The impact of variations in the climate model projections were examined in this study using data from three GCMs.

A range of crop yield increases and decreases were projected, with few discernible differences between the SRES A2 and B1 scenarios being apparent over the next century (Section 7.3). Yield variations were caused primarily by changes to the temperature and the VPD rather than the temperature, contrary to the general conclusions of Lobell and Burke (2008). The greatest changes were projected for fields with high nitrogen application, and the greatest variations between the GCM datasets were also found in these fields. For the SRES A2 scenario, the variations between models increased towards the end of the century which indicates increased uncertainty in the projections for that time.

The conclusions of this study are inconsistent with the two previous studies reviewed in Section 2.3. Liu *et al.* (2008) forecast a millet yield increase of 25 % by 2030 in Senegal but this study projects little change in yield for either SRES scenario at that time. Adejuwon (2006) forecast increases in the first half of the century followed by decreases in the second half caused by high temperature stress. The magnitude of the yield variation in that study is much larger than that projected here. There is a need for a crop model intercomparison study using consistent datasets to identify the cause of the discrepancies between studies (Easterling *et al.*, 2007).

The no adaptation strategy continues to be the optimum approach for the twenty-first century as it was in the last 60 years (Section 6.6). This strategy is conservative and leads to smaller yields and profits in good years but avoids large losses in bad years (Section 7.4). Those smallholders who are risk-averse will achieve very low yields and profits but it might be possible to manage the risks in the future by offering appropriate insurance to cover losses in the small number of poor years, although attempts to introduce similar schemes elsewhere have been largely unsuccessful (Hazell, 1992). The option of adaptation through the use of alternative varieties of millet was not examined in this study but is likely to have little impact because rising temperatures were not projected to substantially change the rate of phenological development throughout the century. There is limited knowledge about the susceptibility of millet to high temperatures but it is possible that using varieties that can tolerate high temperatures during the critical reproductive phases will be beneficial in the future (Dingkuhn *et al.*, 2006).

8.2 Future work

Several ideas for further work were identified during this study. They are presented here in two groups:

1. improvements to CROMSAS and field studies that could improve the accuracy of the model; and,
2. extensions of this study to improve our understanding of smallholder livelihoods in the Sahel.

8.2.1 CROMSAS improvements and agronomic field studies

The calibration of CROMSAS raised several issues. Water loss was underestimated in the early stages of crop growth, with runoff the most likely explanation. It is possible that the runoff rate changes through the season but there is little information about this in the literature. Water loss was also underestimated between 55 and 70 days in all three fields. It is possible that the crop was still developing green structures (stem and leaves) during this time as a result of the earlier drought; while the model alters assimilate partitioning in response to drought, the phenological timing of the end of leaf emergence and the start of leaf senescence are fixed and are not affected by water stress. This is an example of a more general shortcoming of CROMSAS (and other crop models) that the impact of water and nitrogen stress on crop growth is simulated but the impact on crop development is not. Another example is the rising atmospheric CO_2 concentration. Several models simulate the change in crop growth and water use but none consider the influence on crop development because it is not well understood (White and Hoogenboom, 2010).

The crops in the calibration fields appeared to extract a higher fraction of the soil water each day than observed by Dardanelli *et al.* (2004). It would be useful to measure the maximum water extraction rate in a field study to confirm the suitability of the approach and parameters used in CROMSAS.

The impact of temperatures exceeding 35 °C on crop development, leaf expansion, reproductive sinks and grain growth in millet has received little attention. Yet such temperatures will occur regularly in Senegal during the twenty-first century and controlled experiments are required to measure the impact of high temperatures on millet. In particular, the damage caused by short periods of very high temperatures is not represented in any model because of a lack of field data.

Challinor *et al.* (2005) simulates the impact of short periods of high temperatures on groundnut flowers and a similar routine could be developed for millet if suitable experimental data were collected.

FACE studies have concluded that rising CO_2 will not increase the yields of C_4 crops in non-stressed conditions (Ottman *et al.*, 2001). However, these studies were performed at higher latitudes than Senegal where the growth rate is more likely to be limited by solar radiation than the transpiration rate, and other studies have concluded that the growth of C_4 grasses would increase in high-light conditions (Ghannoum *et al.*, 1997). An experiment in Africa is required to find out if the growth of C_4 crops, including millet, will increase in regions where transpiration efficiency limits growth. While there would be logistical difficulties to build a full FACE experiment, it should be possible to perform an open-topped experiment at an agricultural research station to resolve this uncertainty.

A relatively simplistic representation of the nutrient balance was used in CROMSAS in comparison with the DSSAT and STICS models. Leaching can have a substantial impact on the nutrient balance under some conditions (Hafner *et al.*, 1993) but was not explicitly modelled in CROMSAS. The non-linear pattern of leaching is difficult to represent in models and some complex routines have been developed for this purpose (e.g. Brisson *et al.*, 1998). Since the frequency of large storms is unusually high in the Sahel, it is likely that a better representation of leaching would improve the simulations and allow a full nutrient cycling study to be performed. The loss of nitrogen to volatilisation could also be improved.

The decay rate of organic matter and manure into plant-accessible nutrients is poorly understood for dryland sandy soils. In CROMSAS, the manure was assumed to decay completely at the first rains but only 5 % of the natural plant-accessible soil nutrients were assumed to become available immediately. This ‘nutrient flush’ does occur but the magnitude is uncertain and the model would benefit from appropriate field studies.

The effectiveness of mineral fertiliser is linked to the concentration of soil organic carbon and the C:N ratio of soils but this relationship is not simulated in CROMSAS. It would be an essential addition if CROMSAS were to be used in a nutrient cycling study.

Finally, the damage caused to grain yields by pests and disease is not represented in CROMSAS because of a lack of field study information. More field studies are required to facilitate a long-term modelling assessment.

8.2.2 Future studies

The analysis presented here could be extended in a number of ways. Firstly, the cost of intensification, in terms of additional labour and the purchase of animals, fertiliser and other assets, is an important determinant of the agricultural strategy in the region. A simple economic analysis was used in this study which did not account for labour or other costs, and which did not examine the economics of manuring. An improved analysis would assess all of these costs, including labour, in order to properly understand the economic benefits of intensification.

Secondly, the meteorological observations could be mapped to a high-resolution grid and used to assess the impact of drought across Senegal or even the whole Sahel region. Using a spatial analysis would also improve the quality of the meteorological data because missing values were estimated in Chapter 5 using only temporal data from the same location, rather than including spatial relationships from other stations as well. Further extensions could add soil, socio-economic and other data to the grid. If meteorological data were not available or were highly variable (e.g. solar radiation and rainfall, respectively) then high-resolution satellite data could be integrated into the model.

Thirdly, it is difficult to assess the impact of rainfall variability on all smallholders in a simple way because of the diversity of households that exists even within a single village. A range of typical households could be defined from the literature, with a range of non-farm business opportunities, and the model could be used to assess the vulnerability of each group of households to rainfall variability and other stresses. CROMSAS could be integrated into one of the broader farm models in Section 2.4 to perform holistic simulations of households.

Fourthly, a common adaptation option that was not investigated in this study is the use of different crop varieties. Local varieties differ principally in the rate of crop development and information from the ESPACE database could be used to define a range of varieties as explained in Section 4.2.4.1. The model could then be used to identify the optimal variety according to the climatic conditions each year. Using alternative varieties is likely to be a particularly important adaptation option to reduce the impacts of higher temperatures resulting from climate change.

This study, in common with previous studies (e.g. Sultan *et al.*, 2005), concluded that yields could be increased if the planting date were delayed. The reasons for not delaying planting are not clear. It would be useful for a study to perform household surveys to identify the underlying drivers for early planting.

In the western Sahel, grain and leguminous crops are often intercropped in the same field (Craufurd, 2000; Gilbert *et al.*, 2003; Mortimore and Adams, 1999). By growing an early-maturing species with a late-maturing species, the farmer can sometimes utilise the available light and water more fully than if only one crop is planted in the field (Reddy and Willey, 1981). Intercropping is rarely practised in Senegal and so was not examined in this study. CROMSAS has been designed to simulate intercropping and an early evaluation with a field study (which is not presented in this thesis) produced promising results. It would be interesting to examine the potential benefits for Senegalese smallholders of intercropping millet and groundnut in the future.

Crop models have recently been developed to simulate large-area grain yields in order to assess the sensitivity of regional yields to climatic variations. For example, the precursor to CROMSAS, GLAM, was designed to examine the large-area yields of groundnut in India (Challinor *et al.*, 2004). Large-scale yields represent the average of a mosaic of many fields so simpler, less variable functions of leaf area development are used and nutrient stress is represented through a simple calibrated parameter. Nevertheless, the water balance is simulated in a similar way to other crop models. A study could examine the potential for using large-area models to estimate millet yields using seasonal forecasts in the Sahel. Such information would aid the planning processes of governments and aid agencies, as outlined in Section 2.2.5. A feasibility study was performed which compared CROMSAS simulations with regional grain yield data from the SVS project (2009) over the period 1986–2000. Correlations of $R^2 = 0.59$ were achieved for Diourbel, suggesting that large-area models could make a useful contribution in the Sahel. Correlations in the more humid regions were unsurprisingly poorer, although it was interesting to note that the dry-planting simulations had the highest correlations in drier regions while the delayed-planting simulations were better in more humid areas.

8.3 Final summary and key findings

1. The CROMSAS model was developed to examine the influence of climatic variability, climate change and crop management strategies on millet yields in Senegal. The model contains a number of original features including a new method of calculating leaf growth, changes to the millet phenology to allow temperature variations to be simulated more accurately, a comprehensive simulation of tillers, the influence of water and nutrient stresses on partitioning, intercropping, and new methods to calculate the soil water balance in sandy soils. It has been designed in a structured, accessible way to facilitate the use of the model by other researchers, and is expected to be a useful tool for assessing the potential impacts of climate change in the future.

2. A comprehensive evaluation examined the accuracy of the model in the sandy soils of Senegal and appraised the performance of the model for simulating a range of crop management strategies.

3. Meteorological data for twelve locations in Senegal were obtained from multiple sources for the period 1950–2009 and gaps in the data were filled using hindcasts from the NCEP/NCAR reanalysis model. The dataset is the most complete long-term weather record that is available for a region of the Sahel. The accuracy of the reanalysis model predictions was characterised for a range of Sahelian climatic zones. Long-term evaporation pan measurements were used to assess the accuracy of several evapotranspiration methodologies in the region for the first time.

4. A study of the impact of rainfall on crops was performed using 60 years of climate data at six sites in Senegal. Poor rainfall severely restricted yields in the north of the country in most years while having little impact

in the more humid south. Rainfall variability inhibits fertiliser use in the groundnut basin by reducing the effectiveness and hence the profitability of fertiliser application. The optimal planting date was found to be later than the current planting date at all but the driest locations. The reasons for not delaying planting are not well understood. A broad range of planting densities produce similar yields at each level of nitrogen application and current smallholder planting densities generally lie within this range.

5. Projections of the impact of climate change on millet cultivation have been produced for locations across Senegal. Crop yields are projected to be relatively constant throughout the century at all of the locations. The largest variations occur at high nitrogen levels and are the result of changes in the temperature and the VPD. The seasonal yield variability is not expected to change throughout the century. The projections of this study are inconsistent with those of previous studies of millet in Africa and an crop model intercomparison study is required to identify the causes of the discrepancies.

6. These conclusions were based on a study of several rainfall regimes in the sandy soils of Senegal. They should also be applicable to other parts of the Sahel with similar soils and climate, although care should be taken to identify the influence of any local factors that would affect the assumptions used by this study. Socio-economic constraints in particular are likely to vary across the Sahel, so the economic analysis, which is affected by both socio-economic factors and government policies, is unlikely to be applicable outside of Senegal.

Abbreviations

AGRHYMET	Centre Regional de Formation et d'Application en Agrométéorologie et Hydrologie Opérationnelle, Niamey, Niger
AMMA	African Monsoon Multidisciplinary Analyses (project)
APSIM	Agricultural Production Systems sIMulator (crop model)
CIRAD	Centre de coopération Internationale en Recherche Agronomique pour le Développement, Montpellier, France
CROMSAS	Crop Model for Sahelian Adaptation Studies (crop model)
DSSAT	Decision Support System for Agrotechnology Transfer (crop model)
ESPACE	Évaluation et Suivi de la Production Agricole en fonction du Climat et de l'Environnement (project)
ETo	Reference evapotranspiration rate
FACE	Free-Air Carbon dioxide Enrichment
FAO	Food and Agricultural Organization of the United Nations
FAO24	Penman-based method for estimating the reference evapotranspiration
FAO56	Penman-Monteith based method for estimating the reference evapotranspiration
GCM	Global Circulation Model (climate model)

GDP	Gross domestic product
GFDL	Geophysical Fluid Dynamics Laboratory, USA (climate model)
GLAM	General Large-Area Model (crop model)
H-S	HAPEX-Sahel
HAPEX	Hydrology-Atmosphere Pilot Experiment
IBSNAT	The International Benchmark Sites Network for Agrotechnology Transfer (crop model system)
IMF	International Monetary Fund
IPCC	Intergovernmental Panel on Climate Change
ITCZ	Intertropical Convergence Zone
LAI	Leaf Area Index
MIDAS	Land Surface Observation Stations Data (UK Met Office database)
MIROC	Model for Interdisciplinary Research on Climate (climate model)
MRI	Meteorological Research Institute, Japan (climate model)
NCAR	National Center for Atmospheric Research, USA
NCEP/NCAR	Reanalysis climate model
NNI	Nitrogen Nutrition Index
PAR	Photosynthetically-Active Radiation
RH	Relative Humidity
RLD	Root Length Density
RUE	Radiation Use Efficiency
SARRA	Systeme d'Analyse Regionale des Risques Agroclimatiques (crop model)
SLA	Specific Leaf Area

SRES	Special Report on Emissions Scenarios
SRL	Specific Root Length
SSH	Specific Stem Height
STICS	Simulateur mulTIdisciplinaire pour les Cultures Standard (crop model)
SVP	Saturated Vapour Pressure
TUE	Transpiration Use Efficiency
UKMO	UK Met Office
UNHDI	United Nations Human Development Index
VPD	Vapour Pressure Deficit
WFP	World Food Programme
WHO	World Health Organization
WMO	World Meteorological Organization
WUE	Water Use Efficiency

Bibliography

Adejuwon, J. O. (2006) Food crop production in Nigeria. II. Potential effects of climate change, *Climate Research*, **32**(3):229–245.

Affholder, F. (1992) Projet "Estimation et Suivi de la Production Agricole en fonction du Climat et de l'Environnement (E.S.P.A.C.E): Sénégal 1986-1991: Bilan Sommaire et Perspectives, Tech. rep., Institut Sénégalais de Recherches Agricoles.

Affholder, F. (1994) Influence de la fertilisation et du contrôle de l'enherbement sur la réponse des rendements du mil pluvial à un indice hydrique synthétique, in Reyniers, F. N. and Netoyo, L. (eds.) *Bilan hydrique et sécheresse en Afrique tropicale*, John Libbey Eurotext, Paris.

Affholder, F. (1995) Effect of Organic-Matter Input on the Water-Balance and Yield of Millet under Tropical Dryland Condition, *Field Crops Research*, **41**(2):109–121.

Affholder, F. (1997) Empirically modelling the interaction between intensification and climatic risk in semiarid regions, *Field Crops Research*, **52**(1-2):79–93.

Affholder, F. (2001) *Modélisation de culture et diagnostic agronomique régional*, Ph.D. thesis, Institut National Agronomique Paris-Grignon.

Ahuja, L. R. and Ma, L. (2002) *Agricultural System Models in Field Research and Technology Transfer*, chap. Parameterization of Agricultural System Models: Current Approaches and Future Needs, pp. 273–316, Lewis Publishers, Inc.

Ainsworth, E. A., Leakey, A. D. B., Ort, D. R. and Long, S. P. (2008) FACE-ing the facts: inconsistencies and interdependence among field, chamber and modeling studies of elevated CO_2 impacts on crop yield and food supply, *New Phytologist*, **179**(1):5–9.

Ainsworth, E. A. and Long, S. P. (2005) What have we learned from 15 years of free-air CO_2 enrichment (FACE)? A meta-analytic review of the responses of photosynthesis, canopy, *New Phytologist*, **165**(2):351–371.

Ainsworth, E. A. and McGrath, J. M. (2010) *Climate Change and Food Security*, chap. Direct Effects of Rising Atmospheric Carbon Dioxide and Ozone on Crop Yields, pp. 109–130, Springer.

Aliyu, B. S. and Emechebe, A. M. (2006) Effect of Intra- and inter-row mixing of sorghum with two varieties of cowpea on host crop yield in a Striga hermonthica infested field, *African Journal of Agricultural Research*, **1**(2):24–26.

Allen, R. G., Pereira, L. S., Raes, D. and Smith, M. (1998) Crop evapotranspiration. Guidelines for computing crop water requirements, Fao, FAO.

Allison, B. E., Fechter, J., Leucht, A. and Sivakumar, M. V. K. (1995) *Crop—Water—Simulation Models In Practice*, chap. Use of the CERES-Millet model for production strategy: Analysis in the Sudano-Sahelian Zone, pp. 175–188, Wageningen Academic Publishers.

Amerena, P. (1982) *Farmers' participation in the cash economy: case studies of two settlements in the Kano close-settled zone of Nigeria*, Ph.D. thesis, University of London.

Andrews, D. J. and Kumar, K. A. (2006) *Plant Resources of Tropical Africa 1: Cereals and Pulses*, chap. Pennisetum glaucum (L.) R.Br., pp. 128–133, Backhuys Publishers, Wageningen, Netherlands.

Arkebauer, T. J., Weiss, A., Sinclair, T. R. and Blum, A. (1994) In Defense of Radiation Use Efficiency – a Response, *Agricultural and Forest Meteorology*, **68**(3-4):221–227.

Ashraf, M. and Hafeez, M. (2004) Thermotolerance of pearl millet and maize at early growth stages: growth and nutrient relations, *Biologia Plantarum*, **48**(1):81–86.

Ashraf, M., Shabaz, M. and Ashraf, M. Y. (2001) Influence of nitrogen supply and water stress on growth and nitrogen, phosphorus, potassium and calcium contents in pearl millet, *Biologia Plantarum*, **44**(3):459–462.

Azam-Ali, S. N. (1984) Environmental and physiological control of transpiration by groundnut crops, *Agricultural and Forest Meteorology*, **33**(2-3):129–140.

Azam-Ali, S. N., Gregory, P. J. and Monteith, J. L. (1984a) Effects of Planting Density on Water Use and Productivity of Pearl Millet (*Pennisetum typhoides*) Grown on Stored Water: 1. Growth of Roots and Shoots, *Experimental Agriculture*, **20**(3):203–214.

Azam-Ali, S. N., Gregory, P. J. and Monteith, J. L. (1984b) Effects of Planting Density on Water-Use and Productivity of Pearl-Millet (*Pennisetum-Typhoides*) Grown on Stored Water: 2. Water-Use, Light Interception and Dry-Matter Production, *Experimental Agriculture*, **20**(3):215–224.

Azam-Ali, S. N., Simmonds, L. P., Rao, R. C. N. and Williams, J. H. (1989) Population, Growth and Water-Use of Groundnut Maintained on Stored Water: 3. Dry-Matter, Water-Use and Light Interception, *Experimental Agriculture*, **25**(1):77–86.

Azam-Ali, S. N. and Squire, G. R. (2001) *Principles of Tropical Agronomy*, CAB International.

Bacci, L., Cantini, C., Pierini, F., Maracchi, G. and Reyniers, F. N. (1999) Effects of sowing date and nitrogen fertilization on growth, development and yield of a short day cultivar of millet (*Pennisetum typhoides* L.) in Mali, *European Journal of Agronomy*, **10**(1):9–21.

Badini, O., Stockle, C. O. and Franz, E. H. (1997) Application of crop simulation modeling and GIS to agroclimatic assessment in Burkina Faso, *Agriculture, Ecosystems & Environment*, **64**(3):233–244.

Barbier, B. (1998) Induced innovation and land degradation: Results from a bioeconomic model of a village in west Africa, *Agricultural Economics*, **19**(1-2):15–25.

Barbier, B. and Carpentier, C. (2000) The conditions for sustainability of tropical agriculture. Bioeconomic models applied to five contrasting farming systems., in *International Association of Agricultural Economists conference*, Berlin.

Barnabás, B., Jager, K. and Fehér, A. (2008) The effect of drought and heat stress on reproductive processes in cereals, *Plant, Cell and Environment*, **31**(1):11–38.

Baron, C., Clopes, A., Perez, P., Muller, B. L. and Maraux, F. (1996) Sarramet: Gestion et Analyse de Series Climatiques, Tech. rep., CIRAD.

Baron, C., Sultan, B., Balme, M., Sarr, B., Traore, S., Lebel, T., Janicot, S. and Dingkuhn, M. (2005) From GCM grid cell to agricultural plot: scale issues affecting modelling of climate impact, *Philosophical Transactions of the Royal Society B-Biological Sciences*, **360**(1463):2095–2108.

Barrett, J. R. and Nearing, M. A. (1998) *Agricultural Systems Modeling and Simulation*, chap. Humanization of Decision Support Using Information from Simulations, pp. 1–18, Marcel Dekker, Inc.

Bationo, A. and Mokwunye, A. U. (1991) Role Of Manures And Crop Residue In Alleviating Soil Fertility Constraints To Crop Production – With Special Reference To The Sahelian And Sudanian Zones Of West Africa, *Fertilizer Research*, **29**(1):117–125.

Batterbury, S. and Warren, A. (2001) The African Sahel 25 years after the great drought: assessing progress and moving towards new agendas and approaches, *Global Environmental Change-Human and Policy Dimensions*, **11**(1):1–8.

Begg, J. E., Bierhuizen, J. F., Lemon, E. R., Misra, D. K., Slatyer, R. O. and Stern, W. R. (1964) Diurnal energy and water exchanges in bulrush millet in an area of high solar radiation, *Agricultural Meteorology*, **1**(4):294–312.

Begue, A., Desprat, J. F., Imbernon, J. and Baret, F. (1991) Radiation Use Efficiency of Pearl-Millet in the Sahelian Zone, *Agricultural and Forest Meteorology*, **56**(1-2):93–110.

Bidinger, F. R., Mahalakshmi, V., Talukdar, B. S. and Alagarswamy, G. (1982) Improvement Of Drought Resistance In Pearl Millet, in *Drought Resistance In Crops With Emphasis On Rice*, pp. 357–376, International Rice Research Institute.

Bieler, P., Fussell, L. K. and Bidinger, F. R. (1993) Grain growth of *Pennisetum glaucum* (L.) R.Br. under well-watered and drought-stressed conditions, *Field Crops Research*, **31**(1–2):41–54.

Bierhuizen, J. F. and Slatyer, R. O. (1965) Effect of atmospheric concentration of water vapour and CO_2 in determining transpiration-photosynthesis relationships of cotton leaves, *Agricultural Meteorology*, **2**(4):259–270.

Birch, C. J., Carberry, P. S., Muchow, R. C., McCown, R. L. and Hargreaves, J. N. G. (1990) Development and evaluation of a sorghum model based on CERES-Maize in a semi-arid tropical environment, *Field Crops Research*, **24**(1-2):87–104.

Black, C. and Ong, C. (2000) Utilisation of light and water in tropical agriculture, *Agricultural and Forest Meteorology*, **104**(1):25–47.

Blaha, M. and Rumbaugh, J. (2005) *Object-oriented modeling and design with UML*, Pearson Education, Inc., Upper Saddle River, NJ, USA.

Boko, M., Niang, I., Nyong, A., Vogel, C., Githeko, A., Medany, M., Osman-Elasha, B., R., T. and Yanda, P. (2007) *Climate Change 2007: Impacts, Adaptation and Vulnerability. Contribution of Working Group II to the Fourth Assessment Report of the Intergovernmental Panel on Climate Change*, chap. Africa, pp. 433–467, Cambridge University Press, Cambridge, UK and New York, NY, USA.

Bolton, D. (1980) The Computation of Equivalent Potential Temperature, *Monthly Weather Review*, **108**(7):1046–1053.

Boserup, E. (1965) *The Conditions of Agricultural Growth*, George Allen & Unwin Ltd, London.

Boulier, F. and Jouve, P. (1990) Evolution des systèmes de Production Sahéliens et Leur Adaptation à la Sécheresse, Tech. rep., CIRAD.

Bowen, I. S. (1926) The ratio of heat losses by conduction and by evaporation from any water surface, *Physical Review*, **27**(6):779–787.

Bowes, G. (1993) Facing the inevitable: Plants and increasing atmospheric CO_2, *Annual Review Of Plant Physiology And Plant Molecular Biology*, **44**:309–332.

Breman, H., Groot, J. J. R. and van Keulen, H. (2001) Resource limitations in Sahelian agriculture, *Global Environmental Change-Human and Policy Dimensions*, **11**(1):59–68.

Brisson, N., Bussiere, F., Ozier-Lafontaine, H., Tournebize, R. and Sinoquet, H. (2004) Adaptation of the crop model STICS to intercropping. Theoretical basis and parameterisation, *Agronomie*, **24**(6-7):409–421.

Brisson, N., Mary, B., Ripoche, D., Jeuffroy, M. H., Ruget, F., Nicoullaud, B., Gate, P., Devienne-Barret, F., Antonioletti, R., Durr, C., Richard, G., Beaudoin, N., Recous, S., Tayot, X., Plenet, D., Cellier, P., Machet, J. M., Meynard, J. M. and Delecolle, R. (1998) STICS: a generic model for the simulation of crops and their water and nitrogen balances. I. Theory and parameterization applied to wheat and corn, *Agronomie*, **18**(5-6):311–346.

Brooks, N. (2004) Drought in the African Sahel: long term perspectives and future prospects, Tech. Rep. Working Paper 61, Tyndall Centre for Climate Change Research.

Brooks, N., Adger, W. N. and Kelly, P. M. (2005) The determinants of vulnerability and adaptive capacity at the national level and the implications for adaptation, *Global Environmental Change Part A*, **15**(2):151–163.

Brouwer, R. (1983) Functional Equilibrium - Sense or Nonsense, *Netherlands Journal of Agricultural Science*, **31**(4):335–348.

Brown, M. E., Hintermann, B. and Higgins, N. (2009) Markets, Climate Change, and Food Security in West Africa, *Environmental Science & Technology*, **43**(21):8016–8020.

Bruck, H., Piro, B., Sattelmacher, B. and Payne, W. A. (2003a) Spatial distribution of roots of pearl millet on sandy soils of Niger, *Plant and Soil*, **256**(1):149–159.

Bruck, H., Sattelmacher, B. and Payne, W. A. (2003b) Varietal differences in shoot and rooting parameters of pearl millet on sandy soils in Niger, *Plant And Soil*, **251**(1):175–185.

Carberry, P. S. and Campbell, L. C. (1985) The growth and development of pearl millet as affected by photoperiod, *Field Crops Research*, **11**(2-3):207–217.

Carberry, P. S., Campbell, L. C. and Bidinger, F. R. (1985) The Growth and Development of Pearl Millet as Affected by Plant Population, *Field Crops Research*, **11**(2-3):193–205.

Casal, J. J., Sanchez, R. A. and Deregibus, V. A. (1986) The effect of plant density on tillering: The involvement of R/FR ratio and the proportion of radiation intercepted per plant, *Environmental and Experimental Botany*, **26**(4):365–371.

Challinor, A. (2009) Towards the development of adaptation options using climate and crop yield forecasting at seasonal to multi-decadal timescales, *Environmental Science & Policy*, **12**(4):453–465.

Challinor, A. J., Ewert, F., Arnold, S., Simelton, E. and Fraser, E. (2009) Crops and climate change: progress, trends, and challenges in simulating impacts and informing adaptation, *J. Exp. Bot.*, **60**(10):2775–2789.

Challinor, A. J., Slingo, J. M., Wheeler, T. R., Craufurd, P. Q. and Grimes, D. I. F. (2003) Toward a combined seasonal weather and crop productivity forecasting system: Determination of the working spatial scale, *Journal of Applied Meteorology*, **42**(2):175–192.

Challinor, A. J., Wheeler, T. R., Craufurd, P. Q., Ferro, C. A. T. and Stephenson, D. B. (2007) Adaptation of crops to climate change through genotypic responses to mean and extreme temperatures, *Agriculture Ecosystems & Environment*, **119**(1-2):190–204.

Challinor, A. J., Wheeler, T. R., Craufurd, P. Q. and Slingo, J. M. (2005) Simulation of the impact of high temperature stress on annual crop yields, *Agricultural and Forest Meteorology*, **135**(1-4):180–189.

Challinor, A. J., Wheeler, T. R., Craufurd, P. Q., Slingo, J. M. and Grimes, D. I. F. (2004) Design and optimisation of a large-area process-based model for annual crops, *Agricultural and Forest Meteorology*, **124**(1-2):99–120.

Choudhury, B. J., Idso, S. B. and Reginato, R. J. (1987) Analysis of an Empirical-Model for Soil Heat-Flux under a Growing Wheat Crop for Estimating Evaporation by an Infrared-Temperature Based Energy-Balance Equation, *Agricultural and Forest Meteorology*, **39**(4):283–297.

Christensen, J. H., Hewitson, B., Busuioc, A., Chen, A., Gao, X., Held, I., Jones, R., Kolli, R. K., Kwon, W.-T., Laprise, R., Magaa Rueda, V., Mearns, L., Menndez, C. G., Risnen, J., Rinke, A., Sarr, A. and Whetton, P. (2007) *Climate Change 2007: The Physical Science Basis. Contribution of Working Group I to the Fourth Assessment Report of the Intergovernmental Panel on Climate Change*, chap. Regional Climate Projections, pp. 847–940, Cambridge University Press, Cambridge, UK and New York, NY, USA.

Cisse, L. and Vachaud, G. (1988) Effect of Organic Amendment on Cultivation of Millet and Groundnut in a Degraded Sandy Soil in North Senegal. 1. Water-Consumption, Root Development and Crop Production, *Agronomie*, **8**(4):315–325.

Clerget, B. and Traore, S. (2009) Pearl millet and sorghum yield potential in West Africa, Tech. rep., CIRAD.

Cline, W. R. (2007) *Global Warming and Agriculture: Impact estimates by country*, Washington DC: Center for Global Development.

Conley, M. M., Kimball, B. A., Brooks, T. J., Pinter, P. J., Hunsaker, D. J., Wall, G. W., Adam, N. R., LaMorte, R. L., Matthias, A. D., Thompson, T. L., Leavitt, S. W., Ottman, M. J., Cousins, A. B. and Triggs, J. M. (2001) CO2 enrichment increases water-use efficiency in sorghum, *New Phytologist*, **151**(2):407–412.

Cook, K. H. and Vizy, E. K. (2006) Coupled model simulations of the west African monsoon system: Twentieth- and Twenty-First-century simulations, *Journal Of Climate*, **19**(15):3681–3703.

Cooper, P. J. M., Dimes, J., Rao, K. P. C., Shapiro, B., Shiferaw, B. and Twomlow, S. (2008) Coping better with current climatic variability in the rain-fed farming systems of sub-Saharan Africa: An essential first step in adapting to future climate change?, *Agriculture, Ecosystems & Environment*, **126**(1–2):24–35, international Agricultural Research and Climate Change: A Focus on Tropical Systems.

Cooper, P. J. M., Keatinge, J. D. H. and Hughes, G. (1983) Crop Evapotranspiration – a Technique for Calculation of Its Components by Field-Measurements, *Field Crops Research*, **7**(4):299–312.

Cour, J.-M. and Snrech, S. (eds.) (1998) *Preparing for the Future: A Vision of West Africa in the Year 2020*, West Africa Long-Term Perspective Study, OECD, Paris.

Craufurd, P. Q. (2000) Effect of plant density on the yield of sorghum-cowpea and pearl millet-cowpea intercrops in northern Nigeria, *Experimental Agriculture*, **36**(3):379–395.

Craufurd, P. Q. and Bidinger, F. R. (1988a) Effect of the duration of the vegetative phase on crop growth, development and yield in two contrasting pearl millet hybrids, *Journal Of Agricultural Science*, **110**:71–79.

Craufurd, P. Q. and Bidinger, F. R. (1988b) Effect of the Duration of the Vegetative Phase on Shoot Growth, Development and Yield in Pearl Millet (*Pennisetum americanum* (L.) Leeke), *Journal Of Experimental Botany*, **39**(198):124–139.

Cubasch, U., Meehl, G. A., Boer, G. J., Stouffer, R. J., Dix, M., Noda, A., Senior, C. A., Raper, S. and Yap, K. S. (2001) Projections of Future Climate Change, in Houghton, J. T., Ding, Y., Griggs, D. J., Noguer, M., van der Linden, P. J., Dai, X., Maskell, K. and Johnson, C. (eds.) *Climate Change 2001: The Scientific Basis. Contribution of Working Group I to the Third Assessment Report of the Intergovernmental Panel on Climate Change*, p. 881pp, Cambridge University Press, Cambridge, UK and New York, USA.

Dancette, C. (1976) Mesures d'évapotranspiration potentielle et d'évaporation d'une nappe d'eau libre au Sénégal, *Agronomie Tropicale*, **31**:321–338.

Dancette, C. (1983) Estimation des besoins en eau des principales cultures pluviales en zone soudano-sahélienne, *Agronomie Tropicale*, **38**:281–292.

Dardanelli, J. L., Ritchie, J. T., Calmon, M., Andriani, J. M. and Collino, D. J. (2004) An empirical model for root water uptake, *Field Crops Research*, **87**(1):59–71.

Davies, J. A. (1965) Estimation of Insolation for West Africa, *Quarterly Journal Of The Royal Meteorological Society*, **91**(389):359.

Demetriades-Shah, T. H., Fuchs, M., Kanemasu, E. T. and Flitcroft, I. (1992) A Note of Caution Concerning the Relationship between Cumulated Intercepted Solar-Radiation and Crop Growth, *Agricultural and Forest Meteorology*, **58**(3-4):193–207.

Dietz, A. J., Ruben, R. and Verhagen, A. (2004) *The Impact of Climate Change on Drylands*, vol. 39 of *Environment & Policy*, Kluwer Academic Publishers, Dordrecht, The Netherlands.

Dingkuhn, M., Singh, B. B., Clerget, B., Chantereau, J. and Sultan, B. (2006) Past, present and future criteria to breed crops for water-limited environments in West Africa, *Agricultural Water Management*, **80**(1-3):241–261.

Dingkuhn, M. and Sow, A. (1997) Potential yield of irrigated rice in African arid environments, in *Applications of Systems Approaches at The Field Level*

- *Proceedings of the Second International Symposium on Systems Approaches for Agricultural Development, Vol 2*, vol. 6, pp. 79–99, Kluwer Academic Publ.

Dodds, P. E., Meyer, W. S. and Barton, A. (2005) A Review of Methods to Estimate Irrigated Reference Crop Evapotranspiration across Australia, Tech. Rep. CRC for Irrigation Futures Technical Report No. 04/05, CRC for Irrigation Futures/CSIRO Land and Water.

Doorenbos, J. and Pruitt, W. (1977) Guidelines for predicting crop water requirements, Tech. Rep. Irrigation and Drainage Paper 24, Food and Agricultural Organisation of the United Nations.

d'Orgeval, T., Polcher, J. and Li, L. (2006) Uncertainties in modelling future hydrological change over West Africa, *Climate Dynamics*, **26**(1):93–108.

Dougill, A. J., Twyman, C., Thomas, D. S. G. and Sporton, D. (2002) Soil degradation assessment in mixed farming systems of southern Africa: use of nutrient balance studies for participatory degradation monitoring, *The Geographical Journal*, **168**:195–210.

Eagleman, J. R. (1971) An Experimentally Derived Model for Actual Evapotranspiration, *Agricultural Meteorology*, **8**(4-5):385–394.

Easterling, W. E., Aggarwal, P. K., Batima, P., Brander, K. M., Erda, L., Howden, S. M., Kirilenko, A., Morton, J., Soussana, J.-F., Schmidhuber, J. and Tubiello, F. N. (2007) *Climate Change 2007: Impacts, Adaptation and Vulnerability. Contribution of Working Group II to the Fourth Assessment Report of the Intergovernmental Panel on Climate Change*, chap. Food, fibre and forest products, pp. 273–313, Cambridge University Press, Cambridge, UK and New York, NY, USA.

Easterling, W. E., Rosenberg, N. J., McKenney, M. S., Jones, C. A., Dyke, P. T. and Williams, J. R. (1992) Preparing the erosion productivity impact calculator (EPIC) model to simulate crop response to climate change and the direct effects of CO_2, *Agricultural and Forest Meteorology*, **59**(1–2):17–34.

Edwards-Jones, G., Dent, J. B., Morgan, O. and McGregor, M. J. (1998) *Understanding options for agricultural production*, chap. Incorporating farm household decision-making within whole farm models, pp. 347–366, Systems approaches for sustainable agricultural development, Kluwer Academic Publishers, Boston, USA.

Ehlers, W. and Goss, M. J. (2003) *Water Dynamics in Plant Production*, CABI Publishing, Wallingford, UK.

FAO (2004) Desert Locusts cause severe crop damage in Mauritania, Food and Agricultural Organization of the United Nations, `http://www.fao.org/newsroom/en/news/2004/51403/index.html`.

FAO (2009a) FAOSTAT, `http://faostat.fao.org`.

FAO (2009b) Net trade in food, Food and Agricultural Organization of the United Nations, `http://faostat.fao.org/Portals/_Faostat/documents/pdf/map05.pdf`.

Fechter, J., Allison, B. E., Sivakumar, M. V. K., Vanderploeg, R. R. and Bley, J. (1991) An Evaluation Of The Swatrer And Ceres-Millet Models For Southwest Niger, in *Soil Water Balance In The Sudano-Sahelian Zone*, vol. 199, pp. 505–513.

Fischer, G., Shah, M., N. Tubiello, F. and van Velhuizen, H. (2005) Socio-economic and climate change impacts on agriculture: an integrated assessment, 1990 to 2080, *Phil. Trans. R. Soc. Lond. B*, **360**(1463):2067–2083.

Fischer, G., van Velthuizen, H., Shah, M. and Nachtergaele, F. O. (2002) Global agro-ecological assessment for agriculture in the 21st century: methodology and results, Tech. Rep. Research Report RR-02-02, International Institute for Applied Systems Analysis.

Fofana, B., Wopereis, M. C. S., Bationo, A., Breman, H. and Mando, A. (2008) Millet nutrient use efficiency as affected by natural soil fertility, mineral fertilizer use and rainfall in the West African Sahel, *Nutrient Cycling In Agroecosystems*, **81**(1):25–36.

Frissel, M. J. and van Veen, J. A. (eds.) (1981) *Simulation of nitrogen behaviour of soil-plant systems: papers of a workshop, Models for the behaviour of nitrogen in soil and uptake by plant, comparison between different approaches, Wageningen, the Netherlands, January 28 – February 1, 1980*, Centre for Agricultural Publishing and Documentation, Wageningen, Netherlands.

Fussell, L. K., Pearson, C. J. and Norman, M. J. T. (1980) Effect Of Temperature During Various Growth Stages On Grain Development And Yield Of *Pennisetum americanum*, *Journal Of Experimental Botany*, **31**(121):621–633.

Gastal, F. and Lemaire, G. (2002) N uptake and distribution in crops: an agronomical and ecophysiological perspective, *Journal of Experimental Botany*, **53**(370):789–799.

Ghannoum, O., Searson, M. J. and Conroy, J. P. (2007) *Agroecosystems in an Changing Climate*, chap. Nutrient and Water Demands of Plants under Global Climate Change, pp. 53–83, Taylor & Francis.

Ghannoum, O., vonCaemmerer, S., Barlow, E. W. R. and Conroy, J. P. (1997) The effect of CO2 enrichment and irradiance on the growth, morphology and gas exchange of a C-3 (*Panicum laxum*) and a C-4 (*Panicum antidotale*) grass, *Australian Journal Of Plant Physiology*, **24**(2):227–237.

Gilbert, R. A., Heilman, J. L. and Juo, A. S. R. (2003) Diurnal and seasonal light transmission to cowpea in sorghum-cowpea intercrops in Mali, *Journal of Agronomy and Crop Science*, **189**(1):21–29.

Gray, J. K. (2002) *The Groundnut Market in Senegal: Examination of Price and Policy Changes*, Ph.D. thesis, Faculty of the Virginia Polytechnic Institute and State University, USA.

Greenwood, D. J., Lemaire, G., Gosse, G., Cruz, P., Draycott, A. and Neeteson, J. J. (1990) Decline in Percentage N of C_3 and C_4 Crops with Increasing Plant Mass, *Annals of Botany*, **66**(4):425–436.

Gregory, P. J. (1982) Interaction of Shoot and Root Characteristics in the Response of Millet to Drought, in *Drought Resistance In Crops With Emphasis On Rice*, pp. 357–376, International Rice Research Institute.

Gregory, P. J. and Reddy, M. S. (1982) Root Growth in an Intercrop of Pearl Millet Groundnut, *Field Crops Research*, **5**(3):241–252.

Gregory, P. J. and Squire, G. R. (1979) Irrigation effects on roots and shoots of Pearl Millet (*Pennisetum typhoides*), *Experimental Agriculture*, **15**(2):161–168.

Gu, G. J. and Adler, R. F. (2004) Seasonal evolution and variability associated with the West African monsoon system, *Journal of Climate*, **17**(17):3364–3377.

Gueye, M. T. and Delobel, A. (1999) Relative susceptibility of stored pearl millet products and fonio to insect infestation, *Journal of Stored Products Research*, **35**(3):277–283.

Hafner, H., Bley, J., Bationo, A., Martin, P. and Marschner, H. (1993) Long-term nitrogen balance for pearl millet (*Pennisetum glaucum* L.) in an acid sandy soil of Niger, *Zeitschrift für Pflanzenernährung und Bodenkunde*, **156**(2):169–176.

Hammer, G. L., van Oosterom, E., McLean, G., Chapman, S. C., Broad, I., Harland, P. and Muchow, R. C. (2010) Adapting APSIM to model the physiology and genetics of complex adaptive traits in field crops, *Journal Of Experimental Botany*, **61**(8):2185–2202.

Hansen, J. (2005) Integrating seasonal climate prediction and agricultural models for insights into agricultural practice, *Phil. Trans. R. Soc. Lond. B*, **360**(1463):2037–2047.

Hansen, J., Sato, M., Ruedy, R., Lo, K., Lea, D. W. and Medina-Elizade, M. (2006) Global temperature change, *Proceedings Of The National Academy Of Sciences Of The United States Of America*, **103**(39):14288–14293.

Harris, F. (1995) *Nutrient dynamics of the farming system of the Kano Close-Settled Zone Nigeria*, Phd thesis, Department of Geography, University of Cambridge.

Harris, F. (2002) Management of manure in farming systems in semi-arid West Africa, *Experimental Agriculture*, **38**:131–148.

Hasegawa, H., Bryant, D. C. and Denison, R. F. (2000) Testing CERES model predictions of crop growth and N dynamics, in cropping systems with leguminous green manures in a Mediterranean climate, *Field Crops Research*, **67**(3):239–255.

Hasegawa, H., Labavitch, J. M., McGuire, A. M., Bryant, D. C. and Denison, R. F. (1999) Testing CERES model predictions of N release from legume cover crop residue, *Field Crops Research*, **63**(3):255–267.

Haussmann, B., Boubacar, A., Boureima, S. and Vigouroux, Y. (2006) Multiplication and preliminary characterization of west and central African pearl millet landraces, *Journal of SAT Agricultural Research*, **2**(1).

Hayward, D. F. and Oguntoyinbo, J. S. (1987) *The climatology of West Africa*, Hutchinson.

Hazell, P. B. R. (1992) The appropriate role of agricultural insurance in developing countries, *Journal of International Development*, **4**(6):567–581.

Hoogenboom, G., Gadgil, S., Singh, P., Reddy, T. Y., Seshagiri Rao, P. and Murthy, S. (2001) Peanut yield variability in rainfed production systems of the semi-arid tropics, in *Proceedings - Third International Symposium on Systems Approaches for Agricultural Development*, Lima, Peru.

Hulme, M. (2001) Climatic perspectives on Sahelian desiccation: 1973–1998, *Global Environmental Change-Human And Policy Dimensions*, **11**(1):19.

Hulme, M., Doherty, R., Ngara, T., New, M. and Lister, D. (2001) African climate change: 1900–2100, *Climate Research*, **17**(2):145–168.

Huntingford, C., Hugo Lambert, F., Gash, J., Taylor, C. and Challinor, A. (2005) Aspects of climate change prediction relevant to crop productivity, *Phil. Trans. R. Soc. Lond. B*, **360**(1463):1999–2009.

IBSNAT (1989) International Benchmark Sites Network for Agrotechnology Transfer (IBSNAT): Decision Support System for Agrotechnology Transfer (DSSAT) Version 2.1, Dept. Agron. & Soil Sci. College Trop. Agric. And Hum. Resources. Univ. Hawaii, Honolulu.

International Rice Research Institute (2010) World prices (US$ t^{-1} fob) of major fertilizer raw materials, `http://beta.irri.org/solutions/index.php?option=com_content&task=view%&id=250`, accessed Feb 2010.

IPCC (2000) Special report on emissions scenarios (SRES): a special report of Working Group III of the Intergovernmental Panel on Climate Change, Tech. rep., Cambridge University Press.

IPCC (2007) Climate Change 2007: Synthesis Report. Contribution of Working Groups I, II and III to the Fourth Assessment Report of the Intergovernmental Panel on Climate Change, Tech. rep., IPCC, Geneva, Switzerland.

IPCC (2010) Model output described in the 2007 IPCC Fourth Assessment Report (SRES scenarios), IPCC Data Distribution Centre, `http://www.ipcc-data.org/ar4/gcm_data.html`.

IRAT (1983) Valorisation Agricole Des Ressources Pluviométriques, Tech. rep., Division Économie et Valorisation de l'Eau, IRAT.

Irénikatché Akponikpè, P., Gérard, B., Michels, K. and Bielders, C. (2010) Use of the APSIM model in long term simulation to support decision making regarding nitrogen management for pearl millet in the Sahel, *European Journal of Agronomy*, **32**(2):144–154.

IRIN News (2009) SENEGAL: As protests swell "self sufficiency" plan is questioned, UN Office for the Coordination of Humanitarian Affairs, `http://www.irinnews.org/Report.aspx?ReportId=77961`, accessed 28 Apr 2008.

Jablonski, L. M., Wang, X. Z. and Curtis, P. S. (2002) Plant reproduction under elevated CO_2 conditions: a meta-analysis of reports on 79 crop and wild species, *New Phytologist*, **156**(1):9–26.

Jensen, M. E., Wright, J. L. and Pratt, B. J. (1971) Estimating Soil-Moisture Depletion from Climate, Crop and Soil Data, *Transactions of the ASAE*, **14**(5):954.

Jones, F. E. (1992) *Evaporation of water: with emphasis on applications and measurements*, Lewis Publishers, Inc., Chelsea, Michigan.

Jones, J. W., Hoogenboom, G., Boote, K. J. and Porter, C. H. (eds.) (2003) *DSSAT v4: Crop Model Documentation*, vol. Vol 4, University of Hawaii, Honolulu, USA.

Kalnay, E., Kanamitsu, M., Kistler, R., Collins, W., Deaven, D., Gandin, L., Iredell, M., Saha, S., White, G., Woollen, J., Zhu, Y., Leetmaa, A., Reynolds, B., Chelliah, M., Ebisuzaki, W., Higgins, W., Janowiak, J., Mo, K. C., Ropelewski, C., Wang, J., Jenne, R. and Joseph, D. (1996) The NCEP-NCAR 40-Year Reanalysis Project, *Bulletin of the American Meteorological Society*, **77**(3):437–471.

Kandji, S. T., Verchot, L. and Mackensen, J. (2006) Climate Change and Variability in the Sahel Region: Impacts and Adaptation Strategies in the Agricultural Sector, Tech. rep., Word Agroforestry Centre (ICRAF) and United Nations Environment Programme (UNEP), Nairobi, Kenya.

Keating, B. A., Carberry, P. S., Hammer, G. L., Probert, M. E., Robertson, M. J., Holzworth, D., Huth, N. I., Hargreaves, J. N. G., Meinke, H., Hochman, Z., McLean, G., Verburg, K., Snow, V., Dimes, J. P., Silburn, M., Wang, E., Brown, S., Bristow, K. L., Asseng, S., Chapman, S., McCown, R. L., Freebairn, D. M. and Smith, C. J. (2003) An overview of APSIM, a model designed for farming systems simulation, *European Journal Of Agronomy*, **18**(3–4):267–288.

Keating, B. A., Godwin, D. C. and Watiki, J. M. (1991) *Climatic Risk in Crop Production: Models for the Semiarid Tropics and Subtropics*, chap. Optimising nitrogen inputs in response to climatic risk, pp. 329–358, CAB International, Wallingford, UK.

Keating, B. A., Wafula, B. M. and McCown, R. L. (1988) Simulation of plant density effects on maize yield as influenced by water and nitrogen limitations, in Sinha, S. K., Shane, P., Bhargava, S. C. and Aggarwal, P. K. (eds.) *Proceedings of the International Congress of Plant Physiology*, New Delhi, India.

Kelly, V., Diagana, B., Reardon, T., Gaye, M. and Crawford, E. W. (1996) Cash Crop and Foodgrain Productivity in Senegal: Historical View, New Survey Evidence, and Policy Implications, Tech. Rep. MSU International Development Paper No. 20, Michigan State University.

Kennedy, C., Bell, P., Caldwell, D., Habetz, B., Rabb, J. and Alison, M. A. (2002) Nitrogen Application and Critical Shoot Nitrogen Concentration for Optimum Grain and Seed Protein Yield of Pearl Millet, *Crop Science*, **42**(6):1966–1973.

Kimball, B. A. and Idso, S. B. (1983) Increasing atmospheric CO2: effects on crop yield, water use and climate, *Agricultural Water Management*, **7**(1–3):55–72, plant production and management under drought conditions.

Kimball, B. A., Kobayashi, K. and Bindi, M. (2002) Responses of agricultural crops to free-air CO_2 enrichment, *Advances In Agronomy, Vol 77*, **77**:293–368.

Kimball, B. A., Mauney, J. R., Nakayama, F. S. and Idso, S. B. (1993) Effects Of elevated CO_2 and climate variables on plants, *Journal Of Soil And Water Conservation*, **48**(1):9–14.

Kurukulasuriya, P. and Mendelsohn, R. O. (2007) Crop Selection: Adapting to Climage Change in Africa, Policy Research Working Paper No. 4307, World Bank.

Lal, H. (1998) *Agricultural Systems Modeling and Simulation*, chap. Whole-Farm Simulation of Field Operations: An Object-Orientated Approach, pp. 567–595, Marcel Dekker, Inc.

Lal, R. (1995) Erosion-Crop Productivity Relationships For Soils Of Africa, *Soil Science Society Of America Journal*, **59**(3):661–667.

Le Barbé, L., Lebel, T. and Tapsoba, D. (2002) Rainfall variability in West Africa during the years 1950–90, *Journal of Climate*, **15**(2):187–202.

Le Houérou, H. N. (2009) *Bioclimatology and biogeography of Africa*, Springer, Berlin.

Leakey, A. D. B., Ainsworth, E. A., Bernacchi, C. J., Rogers, A., Long, S. P. and Ort, D. R. (2009) Elevated CO_2 effects on plant carbon, nitrogen, and water relations: six important lessons from FACE, *Journal Of Experimental Botany*, **60**(10):2859–2876.

Leakey, A. D. B., Uribelarrea, M., Ainsworth, E. A., Naidu, S. L., Rogers, A., Ort, D. R. and Long, S. P. (2006) Photosynthesis, productivity, and yield of maize are not affected by open-air elevation of CO2 concentration in the absence of drought, *Plant Physiology*, **140**(2):779–790.

Linacre, E. T. (1967) Climate and evaporation from crops, *J. Drain. Irri. Div.*, **93**:61–79.

Liu, J. G., Fritz, S., van Wesenbeeck, C. F. A., Fuchs, M., You, L. Z., Obersteiner, M. and Yang, H. (2008) A spatially explicit assessment of current and future hotspots of hunger in Sub-Saharan Africa in the context of global change, *Global And Planetary Change*, **64**(3–4):222–235.

Lloyd, C. R., Bessemoulin, P., Cropley, F. D., Culf, A. D., Dolman, A. J., Elbers, J., Heusinkveld, B., Moncrieff, J. B., Monteny, B. and Verhoef, A. (1997) A comparison of surface fluxes at the HAPEX-Sahel fallow bush sites, *Journal Of Hydrology*, **189**(1-4):400–425.

Lobell, D. B. and Burke, M. B. (2008) Why are agricultural impacts of climate change so uncertain? The importance of temperature relative to precipitation, *Environmental Research Letters*, **3**(3).

Lobell, D. B., Cassman, K. G. and Field, C. B. (2009) Crop Yield Gaps: Their Importance, Magnitudes, and Causes, *Annual Review Of Environment And Resources*, **34**:179–204.

Long, S., Ainsworth, E., Leakey, A. and Morgan, P. (2005) Global food insecurity. Treatment of major food crops with elevated carbon dioxide or ozone under large-scale fully open-air conditions suggests recent models may have overestimated future yields, *Phil. Trans. R. Soc. Lond. B*, **360**(1463):2011–2020.

Long, S. P., Ainsworth, E. A., Leakey, A. D. B., Nosberger, J. and Ort, D. R. (2006) Food for thought: Lower-than-expected crop yield stimulation with rising CO_2 concentrations, *Science*, **312**(5782):1918–1921.

Maman, N., Mason, S. C., Galusha, T. and Clegg, M. D. (1999) Hybrid and Nitrogen Influence on Pearl Millet Production in Nebraska: Yield, Growth, and Nitrogen Uptake, and Nitrogen Use Efficiency, *Agronomy Journal*, **91**(5):737–743.

Maracchi, G., Bacci, L., Cantini, C., Di Chiara, C., Martini, M., Montanelli, M., Prudenzano, M., Senni, B., Boulama, M., Daouda, M. and Labo, M. (1993) L'Agrométéorologie du Mil (*Pennisetum glaucum* (L) Leeke), Tech. Rep. Rapport CMAg No. 56, World Meteorological Organisation, Geneva.

Marshall, B. and Willey, R. W. (1983) Radiation Interception and Growth in an Intercrop of Pearl-Millet Groundnut, *Field Crops Research*, **7**(2):141–160.

Matthews, R. (2006) The People and Landscape Model (PALM): Towards full integration of human decision-making and biophysical simulation models, *Ecological Modelling*, **194**(4):329–343.

Matthews, R. B. (2002) *Crop-soil Simulation Models*, chap. Crop Management, pp. 29–54, CABI Publishing.

Matthews, R. B., Harris, D., Rao, R. C. N., Williams, J. H. and Wadia, K. D. R. (1988) The Physiological-Basis for Yield Differences between 4 Genotypes of Groundnut (*Arachis-Hypogaea*) in Response to Drought: 1. Dry-Matter Production and Water-Use, *Experimental Agriculture*, **24**(2):191–202.

Matthews, R. B., Reddy, D. M., Rani, A. U., Azamali, S. N. and Peacock, J. M. (1990) Response of 4 Sorghum Lines to Mid-Season Drought: 1. Growth, Water-Use and Yield, *Field Crops Research*, **25**(3-4):279–296.

McCown, R. L., Keating, B. A., Carberry, P. S., Hochman, Z. and Hargreaves, D. M. G. (2002) *Agricultural Systems Models in Field Research and Technology Transfer*, chap. The co-evolution of the Agricultural Production Systems Simulator (APSIM) and its use in Australian dryland cropping research and intervention, pp. 149–176, Lewis Publishers, Inc.

McDonagh, J. and Hillyer, A. (2000) *DFID Plant Sciences Research Programme Annual Report 1999*, chap. Soil fertility, legumes and livelihoods in northern Namibia, pp. 39–47, Centre for Arid Zone Studies, University of Bangor, UK.

McGregor, G. R. and Nieuwolt, S. (1988) *Tropical Climatology*, John Wiley & Sons Ltd, Chichester, UK, 2nd edn.

McPherson, H. G. and Slatyer, R. O. (1973) Mechanisms regulating photosynthesis in *Pennisetum typhoides*, *Australian Journal Of Biological Sciences*, **26**(2):329–339.

Meehl, G. A., Stocker, T. F., Collins, W. D., Friedlingstein, P., Gaye, A. T., Gregory, J. M., Kitoh, A., Knutti, R., Murphy, J. M., Noda, A., Raper, S. C. B., Watterson, I. G., Weaver, A. J. and Zhao, Z.-C. (2007) *Climate Change 2007: The Physical Science Basis. Contribution of Working Group I to the Fourth Assessment Report of the Intergovernmental Panel on Climate Change*, chap. Global Climate Projections, pp. 747–846, Cambridge University Press, Cambridge, UK and New York, NY, USA.

Meyer, W. S. (1988) Development of Management Strategies for Minimizing Salination due to Irrigation: Quantifying Components of the Water Balance under Irrigated Crops, Tech. rep., AWRAC Research Project.

Meyer, W. S. (1999) Standard Reference Evaporation Calculation for Inland, South Eastern Australia, Tech. Rep. Technical Report 35/98, CSIRO Land and Water.

Mills, G., Buse, A., Gimeno, B., Bermejo, V., Holland, M., Emberson, L. and Pleijel, H. (2007) A synthesis of AOT40-based response functions and critical levels of ozone for agricultural and horticultural crops, *Atmospheric Environment*, **41**(12):2630–2643.

Mishra, A., Hansen, J. W., Dingkuhn, M., Baron, C., Traoré, S. B., Ndiaye, O. and Ward, M. N. (2008) Sorghum yield prediction from seasonal rainfall forecasts in Burkina Faso, *Agricultural and Forest Meteorology*, **148**(11):1798–1814.

Monod, H., Naud, C. and Makowski, D. (2006) Uncertainty and sensitivity analysis for crop models, in Wallach, D., Makowski, D. and Jones, J. W. (eds.) *Working with Dynamic Crop Models: Evaluation, Analysis, Parameterization, and Applications*, Elsevier, Amsterdam.

Monteith, J. L. (1972) Solar-Radiation and Productivity in Tropical Ecosystems, *Journal of Applied Ecology*, **9**(3):747–766.

Monteith, J. L. (1977) Climate, in Alvim, P. d. T. and Kozlowski, T. T. (eds.) *Ecophysiology of Tropical Crops*, pp. 1–27, Academic Press, London.

Monteith, J. L. (1994) Validity of the Correlation between Intercepted Radiation and Biomass, *Agricultural and Forest Meteorology*, **68**(3-4):213–220.

Monteith, J. L. (1996) The Quest for Balance in Crop Modeling, *Agronomy*, **88**(5):695–697.

Monteith, J. L., Huda, A. K. S. and Midya, D. (1989) *Modelling the Growth and Development of Sorghum and Pearl Millet*, chap. RESCAP: A resource capture model for sorghum and pearl millet, pp. 30–34, ICRISAT Research Bulletin 12, Patancheru, India.

Monteny, B. A., Lhomme, J. P., Chehbouni, A., Troufleau, D., Amadou, M., Sicot, M., Verhoef, A., Galle, S., Said, F. and Lloyd, C. R. (1997) The role of the sahelian biosphere on the water and the CO_2 cycle during the HAPEX-Sahel experiment, *Journal Of Hydrology*, **189**(1-4):516–535.

Morel, R. (1992) Atlas Agroclimatique des Pays de la Zone du CILSS v1-11, Tech. rep., AGRHYMET.

Mortimore, M. J. and Adams, W. M. (1999) *Working the Sahel*, Routledge, London, UK.

Mortimore, M. J. and Adams, W. M. (2001) Farmer adaptation, change and 'crisis' in the Sahel, *Global Environmental Change-Human and Policy Dimensions*, **11**(1):49–57.

Muchow, R. C., Hammer, G. L. and Carberry, P. S. (1991) *Climatic Risk in Crop Production: Models for the Semiarid Tropics and Subtropics*, chap. Optimising crop and cultivar selection in response to climatic risk, pp. 235–262, CAB International, Wallingford, UK.

Muchow, R. C., Hammer, G. L. and Vanderlip, R. L. (1994) Assessing climatic risk to sorghum production in water-limited subtropical environments II. Effects of planting date, soil-water at planting, and cultivar phenology, *Field Crops Research*, **36**(3):235–246.

Netting, R. M. (1993) *Smallholders, householders. Farm families and the ecology of intensive, sustainable agriculture.*, Stanford University Press, CA.

Niangado, O. (2001) *Broadening the genetic base of crop production*, chap. The State of Millet Diversity and its Use in West Africa, pp. 147–157, CABI Publishing.

Niklas, K. J. and Enquist, B. J. (2001) Invariant scaling relationships for interspecific plant biomass production rates and body size, *Proceedings of the National Academy of Sciences of the United States of America*, **98**(5):2922–2927.

Norby, R. J., Sholtis, J. D., Gunderson, C. A. and Jawdy, S. S. (2003) Leaf dynamics of a deciduous forest canopy: no response to elevated CO_2, *Oecologia*, **136**(4):574–584.

Norman, M., Pearson, C. and Searle, P. G. E. (1995) *The Ecology of Tropical Food Crops*, Cambridge University Press, Cambridge, UK.

Nugent, P. (2007) Cyclical History in the Gambia/Casamance Borderlands: Refuge, Settlement and Islam from c. 1880 to the present, *Journal of African History*, **48**(2):221–243.

Oak Ridge National Laboratory (2010) FACE Data Management System, `http://public.ornl.gov/face/global_face.shtml`.

Omer, M. A., Saxton, K. E. and Bassett, D. L. (1988) Optimum Sorghum Planting Dates In Western Sudan By Simulated Water Budgets, *Agricultural Water Management*, **13**(1):33–48.

Ong, C. and Monteith, J. (1985) Response of pearl millet to light and temperature, *Field Crops Research*, **11**:141–160, pearl millet.

Ong, C. K. (1983a) Response to Temperature in a Stand of Pearl Millet (*Pennisetum typhoides* S. & H.): 1. Vegetative Development, *Journal of Experimental Botany*, **34**(140):322–336.

Ong, C. K. (1983b) Response to Temperature in a Stand of Pearl Millet (*Pennisetum typhoides* S. & H.): 2. Reproductive Development, *Journal of Experimental Botany*, **34**(140):337–348.

Ong, C. K. (1983c) Response to Temperature in a Stand of Pearl Millet (*Pennisetum typhoides* S. & H.): 4. Extension of Individual Leaves, *Journal Of Experimental Botany*, **34**(149):1731–1739.

Ong, C. K. and Everard, A. (1979) Short day induction of flowering in pearl millet (*Pennisetum typhoides*) and its effect on plant morphology, *Experimental Agriculture*, **15**(4):401.

Ong, C. K. and Squire, G. R. (1984) Response to Temperature in a Stand of Pearl Millet (*Pennisetum typhoides* S. & H.): 7. Final Number of Spikelets and Grains, *Journal Of Experimental Botany*, **35**(157):1233–1240.

Osborne, T. M., Lawrence, D. M., Challinor, A. J., Slingo, J. M. and Wheeler, T. R. (2007) Development and assessment of a coupled crop—climate model, *Global Change Biology*, **13**(1):169–183.

Ottman, M. J., Kimball, B. A., Pinter, P. J., Wall, G. W., Vanderlip, R. L., Leavitt, S. W., LaMorte, R. L., Matthias, A. D. and Brooks, T. J. (2001) Elevated CO_2 increases sorghum biomass under drought conditions, *New Phytologist*, **150**(2):261–273.

Page, J. K. (1961) The estimation of the monthly mean values of daily total short wave radiation on vertical and inclined surfaces from sunshine records for latitudes 40°N–40°S, in *UN Conference on new sources of energy*, vol. 4, p. 378–390.

Parker, D. C., Manson, S. M., Janssen, M. A., Hoffmann, M. J. and Deadman, P. (2003) Multi-agent systems for the simulation of land-use and land-cover change: A review, *Annals Of The Association Of American Geographers*, **93**(2):314–337.

Parker, D. J., Burton, R. R., Diongue-Niang, A., Ellis, R. J., Felton, M., Taylor, C. M., Thorncroft, C. D., Bessemoulin, P. and Tompkins, A. M. (2005) The diurnal cycle of the West African monsoon circulation, *Quarterly Journal of the Royal Meteorological Society*, **131**(611):2839–2860.

Parry, M., Rosenzweig, C., Iglesias, A., Fischer, G. and Livermore, M. (1999) Climate change and world food security: a new assessment, *Global Environmental Change – Human and Policy Dimensions*, **9**:S51–S67.

Parry, M., Rosenzweig, C. and Livermore, M. (2005) Climate change, global food supply and risk of hunger, *Phil. Trans. R. Soc. Lond. B*, **360**(1463):2125–2138.

Parry, M. L., Rosenzweig, C., Iglesias, A., Livermore, M. and Fischer, G. (2004) Effects of climate change on global food production under SRES emissions and socio-economic scenarios, *Global Environmental Change – Human and Policy Dimensions*, **14**(1):53–67.

Passioura, J. B. (1983) Roots and Drought Resistance, *Agricultural Water Management*, **7**(1-3):265–280.

Passioura, J. B. (1996) Simulation Models: Science, Snake Oil, Education, or Engineering?, *Agronomy*, **88**(5):690–694.

Payne, W. A. (1997) Managing yield and water use of pearl millet in the Sahel, *Agronomy Journal*, **89**(3):481–490.

Payne, W. A. (2000) Optimizing crop water use in sparse stands of pearl millet, *Agronomy Journal*, **92**(5):808–814.

Payne, W. A., Drew, M. C., Hossner, L. R. and Lascano, R. J. (1996) Measurement and modelling of photosynthetic response of pearl millet to soil phosphorus addition, *Plant And Soil*, **184**(1):67–73.

Payne, W. A., Hossner, L. R., Onken, A. B. and Wendt, C. W. (1995) Nitrogen and Phosphorus Uptake in Pearl-Millet and Its Relation to Nutrient and Transpiration Efficiency, *Agronomy Journal*, **87**(3):425–431.

Payne, W. A., Wendt, C. W., Hossner, L. R. and Gates, C. E. (1991) Estimating Pearl-Millet Leaf-Area and Specific Leaf-Area, *Agronomy Journal*, **83**(6):937–941.

Pearson, C. J. (1975) Thermal Adaptation Of *Pennisetum*: Seedling Development, *Australian Journal of Plant Physiology*, **2**(3):413–424.

Pearson, C. J. (1984) *The Physiology of Tropical Field Crops*, chap. Pennisetum millet, pp. 281–304, Wiley, Chichester, UK.

Pearson, C. J. and Derrick, G. A. (1977) Thermal Adaptation Of Pennisetum - Leaf Photosynthesis And Photosynthate Translocation, *Australian Journal Of Plant Physiology*, **4**(5):763–769.

Pelissier, P. (1966) *Les paysans du Sénégal. Les civilisations agraires du Cayor à la Casamance*, Imp. Fabrègues, Saint Yriex, France.

Penman, H. L. (1948) Natural Evaporation from Open Water, Bare Soil and Grass, *Proceedings of the Royal Society of London Series A*, **193**(1032):120–&.

Pingali, P. L., Bigot, Y. and Binswanger, H. P. (1987) *Agricultural mechanization and the evolution of farming systems in sub-Saharan Africa*, Published for the World Bank by Johns Hopkins University Press, Baltimore ; London.

Porter, J. and Semenov, M. (2005) Crop responses to climatic variation, *Phil. Trans. R. Soc. Lond. B*, **360**(1463):2021–2035.

Powell, J. M. and Williams, T. O. (1993) Livestock, Nutrient Cycling and Sustainable Agriculture in the West African Sahel, Tech. Rep. Gatekeeper Series No. 37, International Institute for Environment and Development.

Priestley, C. H. B. and Taylor, R. J. (1972) On the Assessment of Surface Heat Flux and Evaporation Using Large-Scale Parameters, *Monthly Weather Review*, **100**(2):81–92.

Randall, D. A., Wood, R. A., Bony, S., Colman, R., Fichefet, T., Fyfe, J., Kattsov, V., Pitman, A., Shukla, J., Srinivasan, J., Stouffer, R. J., Sumi, A. and E., T. K. (2007) *Climate Change 2007: The Physical Science Basis. Contribution of Working Group I to the Fourth Assessment Report of the Intergovernmental Panel on Climate Change*, chap. Cilmate Models and Their Evaluation, pp. 589–662, Cambridge University Press, Cambridge, UK and New York, NY, USA.

Raynaut, C. (2001) Societies and nature in the Sahel: ecological diversity and social dynamics, *Global Environmental Change-Human and Policy Dimensions*, **11**(1):9–18.

Raynaut, C., Grégoire, E., Janin, P., Koechlin, J. and Delville, P. L. (1997) *Societies and nature in the Sahel*, SEI global environment and development series, Routledge, London.

Reddy, M. S. and Willey, R. W. (1981) Growth and Resource Use Studies in an Intercrop of Pearl Millet—Groundnut, *Field Crops Research*, **4**(1):13–24.

Ritchie, J. T. and Alagarswamy, G. (1989a) *Modelling the Growth and Development of Sorghum and Pearl Millet*, chap. Simulation of sorghum and pearl millet phenology, pp. 24–26, ICRISAT Research Bulletin 12, Patancheru, India.

Ritchie, J. T. and Alagarswamy, G. (1989b) *Modelling the Growth and Development of Sorghum and Pearl Millet*, chap. Genetic coefficients for the CERES models, pp. 27–28, ICRISAT Research Bulletin 12, Patancheru, India.

Ritchie, J. T. and Alagarswamy, G. (1989c) *Modelling the Growth and Development of Sorghum and Pearl Millet*, chap. Simulation of growth and development in CERES models, pp. 34–38, ICRISAT Research Bulletin 12, Patancheru, India.

Ritchie, J. T. and Alagarswamy, G. (2002) *Effects of Climate Change and Variability on Agricultural Production Systems*, chap. Overview of Crop Models for Assessment of Crop Production, pp. 43–68, Kluwer Academic Publ.

Ritchie, J. T. and Godwin, D. G. (2000) CERES Wheat 2.0, `http://nowlin.css.msu.edu/wheat{_}book/`.

Ritchie, J. T., Singh, U., Godwin, D. C. and Bowen, W. T. (1998) *Understanding options for agricultural production*, chap. Cereal growth, development and yield, pp. 79–98, Systems approaches for sustainable agricultural development, Kluwer Academic Publishers, Boston, USA.

Rosenberg, N. J., Blad, B. L. and Verma, S. B. (1983) *Microclimate: the biological environment*, Wiley, New York, 2nd edn.

Rosenzweig, C. and Parry, M. L. (1994) Potential Impact Of Climate-Change On World Food-Supply, *Nature*, **367**(6459):133–138.

Russell, G. and van Gardingen, P. R. (1997) *Scaling-up: from cell to landscape*, chap. Problems with using models to predict regional crop production, pp. 273–294, Cambridge University Press.

Sadler, E. J., Bauer, P. J. and Busscher, W. J. (1995) Spatial Corn Yield During Drought in the SE Coastal Plain, in Robert, P. C., Rust, R. H. and Larson, W. E. (eds.) *Site-Specific Management for Agricultural Systems*, pp. 365–381, ASA, CSSA, and SSA, Madison, WI.

Sankhayan, P. L. and Hofstad, O. (2001) A village-level economic model of land clearing, grazing, and wood harvesting for sub-Saharan Africa: with a case study in southern Senegal, *Ecological Economics*, **38**(3):423–440.

Scoones, I. (2001) *Dynamics and Diversity*, chap. Transforming Soils: The Dynamics of Soil-fertility Management in Africa, pp. 1–44, Earthscan.

Shaffer, M. J., Bartling, P. N. S. and Ascough, J. C. (2000) Object-oriented simulation of integrated whole farms: GPFARM framework, *Computers and Electronics in Agriculture*, **28**(1):29–49.

Shapiro, B. I. and Sanders, J. H. (1998) Fertilizer use in semiarid West Africa: Profitability and supporting policy, *Agricultural Systems*, **56**(4):467–482.

Shepherd, K. D. and Soule, M. J. (1998) Soil fertility management in west Kenya: dynamic simulation of productivity, profitability and sustainability at different resource endowment levels, *Agriculture Ecosystems & Environment*, **71**(1-3):131–145.

Sinclair, T. R. and Seligman, N. G. (1996) Crop Modeling: From Infancy to Maturity, *Agronomy*, **88**(5):698–704.

Sinclair, T. R., Tanner, C. B. and Bennett, J. M. (1984) Water-Use Efficiency in Crop Production, *Bioscience*, **34**(1):36–40.

Singels, A. (1992) Evaluating Wheat Planting Strategies using a Growth-Model, *Agricultural Systems*, **38**(2):175–184.

Singh, U., Thornton, P. K., Saka, A. R. and Dent, J. B. (1993) *Systems Approaches for Agricultural Development*, chap. Maize modelling in Malawi: a tool for soil fertility research and development, pp. 253–273, Kluwer Academic, Dordrecht, The Netherlands.

Sivakumar, M. V. K. (1988) Predicting Rainy Season Potential From The Onset Of Rains In Southern Sahelian And Sudanian Climatic Zones Of West-Africa, *Agricultural And Forest Meteorology*, **42**(4):295–305.

Sivakumar, M. V. K. and Glinni, A. F. (2002) *Agricultural System Models in Field Research and Technology Transfer*, chap. Applications of Crop Growth Models in the Semiarid Regions, pp. 177–206, Lewis Publishers, Inc.

Slingo, J., Challinor, A., Hoskins, B. and Wheeler, T. (2005) Introduction: food crops in a changing climate, *Phil. Trans. R. Soc. Lond. B*, **360**(1463):1983–1989.

Soler, C. M. T., Maman, N., Zhang, X., Mason, S. C. and Hoogenboom, G. (2008) Determining optimum planting dates for pearl millet for two contrasting environments using a modelling approach, *Journal Of Agricultural Science*, **146**:445–459.

Soussana, J. F., Graux, A. I. and Tubiello, F. N. (2010) Improving the use of modelling for projections of climate change impacts on crops and pastures, *Journal Of Experimental Botany*, **61**(8):2217–2228.

Sowell, R. S. and Ward, R. C. (1998) *Agricultural Systems Modeling and Simulation*, chap. Modeling Processes and Operations with Linear Programming, pp. 113–156, Marcel Dekker, Inc.

Spitters, C. J. T. (1990) Crop Growth Models: Their Usefulness And Limitations, *Symposium On The Timing Of Field Production Of Vegetables*, **267**:349–368.

Squire, G. R. (1989) Response to Temperature in a Stand of Pearl-Millet: 10. Partition of Assimilate, *Journal of Experimental Botany*, **40**(221):1391–1398.

Squire, G. R. (1990) *The Physiology of Tropical Crop Production*, CABI Publishing, Wallingford.

Squire, G. R., Marshall, B., Terry, A. C. and Monteith, J. L. (1984) Response to Temperature in a Stand of Pearl-Millet: 6. Light Interception and Dry-Matter Production, *Journal of Experimental Botany*, **35**(153):599–610.

Steiner, J. L., Howell, T. A. and Schneider, A. D. (1991) Lysimetric Evaluation of Daily Potential Evapotranspiration Models for Grain-Sorghum, *Agronomy Journal*, **83**(1):240–247.

Stephens, W. and Hess, T. M. (1999) Modelling the benefits of soil water conservation using the PARCH model - a case study from a semi-arid region of Kenya, *Journal Of Arid Environments*, **41**(3):335–344.

Stewart, J. I. (1991) *Climatic Risk in Crop Production: Models for the Semiarid Tropics and Subtropics*, chap. Principles and performance of response farming, pp. 361–382, CAB International, Wallingford, UK.

Stisen, S., Jensen, K. H., Sandholt, I. and Grimes, D. I. F. (2008) A remote sensing driven distributed hydrological model of the Senegal River basin, *Journal Of Hydrology*, **354**(1-4):131–148.

Stöckle, C. O., Donatelli, M. and Nelson, R. (2003) CropSyst, a cropping systems simulation model, *European Journal of Agronomy*, **18**(3-4):289–307.

Stöckle, C. O., Martin, S. A. and Campbell, G. S. (1994) Cropsyst, a Cropping Systems Simulation-Model – Water Nitrogen Budgets and Crop Yield, *Agricultural Systems*, **46**(3):335–359.

Suleiman, A. A. and Ritchie, J. T. (2004) Modifications to the DSSAT vertical drainage model for more accurate soil water dynamics estimation, *Soil Science*, **169**(11):745–757.

Sultan, B., Baron, C., Dingkuhn, M., Sarr, B. and Janicot, S. (2005) Agricultural impacts of large-scale variability of the West African monsoon, *Agricultural and Forest Meteorology*, **128**(1-2):93–110.

Sultan, B. and Janicot, S. (2000) Abrupt shift of the ITCZ over West Africa and intra-seasonal variability, *Geophysical Research Letters*, **27**(20):3353–3356.

Sultan, B. and Janicot, S. (2003) The West African monsoon dynamics. Part II: The “preonset” and “onset” of the summer monsoon, *Journal of Climate*, **16**(21):3407–3427.

SVS project (2009) Suivi de la Vulnérabilité, `http://www.case.ibimet.cnr.it/SVS/page.php?page=history&type=N&country=ML`.

Syers, J. K. (1997) Managing soils for long-term productivity, *Philosophical Transactions Of The Royal Society B*, **352**(1356):1011–1021.

Tanner, C. B. and Sinclair, T. R. (1983) Efficient water use in crop production: Research or re-search?, in Taylor, H. M., Jordan, W. R. and Sinclair, T. R. (eds.) *Limitations to Efficient Water Use in Crop Production*, pp. 1–27, ASA, CSSA, and SSA, Madison, WI.

Tarhule, A. (2005) Damaging Rainfall and Flooding: The Other Sahel Hazards, *Climatic Change*, **72**(3):355–377.

Taylor, C. M. and Lebel, T. (1998) Observational evidence of persistent convective-scale rainfall patterns, *Monthly Weather Review*, **126**(6):1597–1607.

Taylor, C. M., Said, F. and Lebel, T. (1997) Interactions between the land surface and mesoscale rainfall variability during HAPEX-Sahel, *Monthly Weather Review*, **125**(9):2211–2227.

Teo, C.-K. and Grimes, D. I. F. (2007) Stochastic modelling of rainfall from satellite data, *Journal Of Hydrology*, **346**(1-2):33–50.

Thornton, P. K., Bowen, W. T., Ravelo, A. C., Wilkens, P. W., Farmer, G., Brock, J. and Brink, J. E. (1997) Estimating millet production for famine early warning: An application of crop simulation modelling using satellite and ground-based data in Burkina Faso, *Agricultural And Forest Meteorology*, **83**(1-2):95–112.

Thornton, P. K., Saka, A. R., Singh, U., Kumwenda, J. D. T., Brink, J. E. and Dent, J. B. (1995) Application of a Maize Crop Simulation-Model in the Central Region of Malawi, *Experimental Agriculture*, **31**(2):213–226.

Tiffen, M., Mortimore, M. and Gichuki, F. (1994) *More people, less erosion: environmental recovery in Kenya*, Wiley, Chichester.

Tompkins, A. M., Diongue-Niang, A., Parker, D. J. and Thorncroft, C. D. (2005) The African easterly jet in the ECMWF Integrated Forecast System: 4D-Var analysis, *Quarterly Journal Of The Royal Meteorological Society*, **131**(611):2861–2885.

Triggs, J. M., Kimball, B. A., Pinter, P. J., Wall, G. W., Conley, M. M., Brooks, T. J., LaMorte, R. L., Adam, N. R., Ottman, M. J., Matthias, A. D., Leavitt, S. W. and Cerveny, R. S. (2004) Free-air CO_2 enrichment effects on the energy balance and evapotranspiration of sorghum, *Agricultural And Forest Meteorology*, **124**(1-2):63–79.

Tsubo, M., Walker, S. and Ogindo, H. O. (2005) A simulation model of cereal-legume intercropping systems for semi-arid regions I. Model development, *Field Crops Research*, **93**(1):10–22.

Tubiello, F. N., Amthor, J. S., Boote, K. J., Donatelli, M., Easterling, W., Fischer, G., Gifford, R. M., Howden, M., Reilly, J. and Rosenzweig, C. (2007) Crop response to elevated CO_2 and world food supply – A comment on “Food for Thought...” by Long et al., Science 312:1918–1921, 2006, *European Journal of Agronomy*, **26**(3):215–223.

UK Met Office (2009) MIDAS Land Surface Stations data (1953–current).

UNDP (2005) Human Development Report 2005, Tech. rep., United Nations Development Programme.

University of Nottingham (1984) Microclimatology report 13: Response of groundnut to the distribution of rainfall or irrigation, Tech. Rep. R3208, Overseas Development Administration (Natural Resources and Environment Department), London, UK.

Uppala, S. M., Kallberg, P. W., Simmons, A. J., Andrae, U., Bechtold, V. D., Fiorino, M., Gibson, J. K., Haseler, J., Hernandez, A., Kelly, G. A., Li, X., Onogi, K., Saarinen, S., Sokka, N., Allan, R. P., Andersson, E., Arpe, K., Balmaseda, M. A., Beljaars, A. C. M., Van De Berg, L., Bidlot, J., Bormann, N., Caires, S., Chevallier, F., Dethof, A., Dragosavac, M., Fisher, M., Fuentes, M., Hagemann, S., Holm, E., Hoskins, B. J., Isaksen, L., Janssen, P., Jenne, R., McNally, A. P., Mahfouf, J. F., Morcrette, J. J., Rayner, N. A., Saunders, R. W., Simon, P., Sterl, A., Trenberth, K. E., Untch, A., Vasiljevic, D., Viterbo, P. and Woollen, J. (2005) The ERA-40 re-analysis, *Quarterly Journal of the Royal Meteorological Society*, **131**(612):2961–3012.

U.S. Census Bureau (2009) International Data Base, `http://www.census.gov/ipc/www/idb/ranks.php`.

USAID (2010) Senegal Disaster Assistance, U.S. Agency for International Development, `http://www.usaid.gov/our_work/humanitarian_assistance/disaster_assistance/countries/senegal/template/index.html`.

USDA-SCS (1964) National Engineering Handbook, US Department of Agriculture, Soil Conservation Service, Washington DC.

Vaksmann, M., Kouressy, M., Chantereau, J., Bazile, D., Sagnard, F., Toure, A., Sanogo, O., Diawara, G. and Dante, A. (2008) Use of genetic diversity of Malian local sorghums, *Cahiers Agricultures*, **17**(2):140–145.

van der Linden, P. (2009) *Climate Variability, Modeling Tools and Agricultural Decision-Making*, chap. The ENSEMBLES Climate Change Project, pp. 65–106, Nova Science Publishers, Inc.

van Duivenbooden, N. and Cissé, L. (1993) Fertilization of millet cv. Souna III in Senegal: dry matter production and nutrient uptake, *Fertilizer Research*, **35**(3):217–226.

van Keulen, H. (1975) *Simulation of water use and herbage growth in arid regions*, Ph.D. thesis, Wageningen.

van Keulen, H. and Veeneklaas, F. R. (1993) *Systems Approaches for Agricultural Development*, chap. Options for agricultural development: a case study for Mali's fifth Region, pp. 367–380, Kluwe, Dordrecht, The Netherlands.

van Oosterom, E. J. (2000) The APSIM Pearl Millet Module.

van Oosterom, E. J., Carberry, P. S., Hargreaves, J. N. G. and O'Leary, G. J. (2001a) Simulating growth, development, and yield of tillering pearl millet II. Simulation of canopy development, *Field Crops Research*, **72**(1):67–91.

van Oosterom, E. J., Carberry, P. S. and O'Leary, G. J. (2001b) Simulating growth, development, and yield of tillering pearl millet I. Leaf area profiles on main shoots and tillers, *Field Crops Research*, **72**(1):51–66.

van Oosterom, E. J., O'Leary, G. J., Carberry, P. S. and Craufurd, P. Q. (2002) Simulating growth, development, and yield of tillering pearl millet. III. Biomass accumulation and partitioning, *Field Crops Research*, **79**(2-3):85–106.

von Grebmer, K., Fritschel, H., Nestorova, B., Olofinbiyi, T., Pandya-Lorch, R. and Yohannes, Y. (2008) Global Hunger Index: The Challenge of Hunger 2008, Tech. rep., International Food Policy Research Institute.

Wade, L. K., Myers, R. J. K. and Foale, M. A. (1991) *Climatic Risk in Crop Production: Models for the Semiarid Tropics and Subtropics*, chap. Optimising plant stand in response to climatic risk, pp. 263–282, CAB International, Wallingford, UK.

Wallach, D. (2006a) *Working with Dynamic Crop Models: Evaluation, Analysis, Parameterization, and Applications*, chap. The two forms of crop models, pp. 3–10, Elsevier, Amsterdam.

Wallach, D. (2006b) *Working with Dynamic Crop Models: Evaluation, Analysis, Parameterization, and Applications*, chap. Evaluating Crop Models, pp. 11–53, Elsevier, Amsterdam.

Wand, S. J. E., Midgley, G. F., Jones, M. H. and Curtis, P. S. (1999) Responses of wild C4 and C3 grass (Poaceae) species to elevated atmospheric CO2 concentration: a meta-analytic test of current theories and perceptions, *Global Change Biology*, **5**(6):723–741.

Warren, A., Batterbury, S. and Osbahr, H. (2001) Soil erosion in the West African Sahel: a review and an application of a "local political ecology" approach in South West Niger, *Global Environmental Change-Human and Policy Dimensions*, **11**(1):79–95.

Washington, R., Harrison, M. and Conway, D. (2004) African Climate Report, Tech. rep., Department for International Development.

West-African Market Information Network (2010) Price statistics from the official West African Market Price Agencies, `http://www.resimao.org/html/en/region/home`, accessed Feb 2010.

WFP (2005) Analysis of Structural Vulnerability in Rural Areas in Senegal in the Framework of Preparation of the 20072011 Country Programme, Tech. rep., Dakar Regional Office, World Food Programme.

WFP (2006) Country Programme – Senegal 10451.0 (2007–2011), Tech. Rep. WFP/EB.1/2007/8/1, World Food Programme.

Wheeler, T. R., Craufurd, P. Q., Ellis, R. H., Porter, J. R. and Prasad, P. V. V. (2000) Temperature variability and the yield of annual crops, *Agriculture Ecosystems & Environment*, **82**(1-3):159–167.

White, J. W. and Hoogenboom, G. (2010) *Climate Change and Food Security*, chap. Crop Response to Climate: Ecophysiological Models, pp. 59–84, Springer.

Williams, J. R., DeLano, D. R., Heiniger, R. W., Vanderlip, R. L. and Llewelyn, R. V. (1999) Replanting strategies for grain sorghum under risk, *Agricultural Systems*, **60**(2):137–155.

Williams, J. R., Jones, C. A., Kiniry, J. R. and Spanel, D. A. (1989) The Epic Crop Growth-Model, *Transactions of the ASAE*, **32**(2):497–511.

World Bank (2004) Poverty in Senegal: from the 1994 Devaluation to 2001–2002, Tech. rep., Planning and Statistics Directorate.

World Bank (2006) World Development Indicators, Tech. rep.

World Food Summit (1996) Rome Declaration on World Food Security and World Food Summit Plan of Action, Tech. Rep. WFS 96/3, Food and Agricultural Organization of the United Nations.

Ziervogel, G., Cartwright, A., Tas, A., Adejuwon, J., Zermoglio, F., Shale, M. and Smith, B. (2008) Climate change and adaptation in African agriculture, Tech. rep., Stockholm Environment Institute.